



A Meteorological Investigation of the 'Springtime
Bump'

An Early Season Peak in the Fire Danger Experienced
in Tasmania

Paul Fox-Hughes

B. Sc. (Hons.) University of Tasmania

Submitted in fulfilment of the requirements

for the degree of Doctor of Philosophy

Institute for Marine and Antarctic Studies

University of Tasmania

December 2014

Declarations

Declaration of Originality

This thesis contains no material which has been accepted for a degree or diploma by the University or any other institution, except by way of background information and duly acknowledged in the thesis, and to the best of my knowledge and belief no material previously published or written by another person except where due acknowledgement is made in the text of the thesis, nor does the thesis contain any material that infringes copyright.

Signed:

Paul Fox-Hughes
30 September 2014

Statement regarding published work contained in thesis

The publishers of the papers comprising Chapters 2 to 6 hold the copyright for that content, and access to the material should be sought from the respective journals. The remaining non published content of the thesis may be made available for loan and limited copying and communication in accordance with the Copyright Act 1968.

Signed:

Paul Fox-Hughes
30 September 2014

Statement of Co-Authorship

The following people and institutions contributed to the publication of work undertaken as part of this thesis:

Paul Fox-Hughes, *Bureau of Meteorology, Institute for Marine and Antarctic Studies, ACE CRC = Candidate*
Rebecca Harris, *ACE CRC = Author 1*
Greg Lee, *ACE CRC = Author 2*
Michael Grose, *CSIRO Marine and Atmospheric Research = Author 3*
Nathan Bindoff, *Institute for Marine and Antarctic Studies, ACE CRC, CSIRO Marine and Atmospheric Research = Author 4*

Author details and their roles:

Paper 1, *A fire danger climatology for Tasmania:*

Located in chapter 2

Candidate was the sole author on this paper.

Paper 2, *Impact of more frequent observations on the understanding of Tasmanian fire danger:*

Located in chapter 3

Candidate was the sole author on this paper.

Paper 3, *Springtime Fire Weather in Tasmania, Australia: Two Case Studies:*

Located in chapter 4

Candidate was the sole author on this paper.

Paper 4, *Characteristics of some days involving abrupt increases in fire danger:*

Located in chapter 5

Candidate was the sole author on this paper.

Paper 5, *Future fire danger climatology for Tasmania, Australia, using a dynamically downscaled regional climate model:*

Located in chapter 6

Candidate was the primary author and generated the results reported (Percentage contribution estimate: 50%).

Author 1 contributed to the writing of the paper (20%).

Author 2 contributed the statistical analysis of some results (presented in Figs. 4, 7 and 8 and Tables 1 and 4) and presentation of Figs. 4 and 7 (15%).

All authors contributed to discussion of the results and editing of the paper drafts (Author 3 - 10%, author 4 - 5%).

Signed: _____



Kelvin Michael
Supervisor
IMAS UTAS
University of Tasmania

Date: _____

8-9-14



for
Craig Johnson
Head of School
IMAS UTAS
University of Tasmania

Date: _____

8-Sep-2014

Abstract

Datasets of Tasmanian fire weather observations are analysed to investigate the existence of an anecdotal “springtime bump”, an early fire weather peak in the Tasmanian fire season. Such a phenomenon is not well-documented in comparison to the usual summer to early autumn peak. The existence of a springtime fire danger peak is confirmed for eastern and southeastern Tasmania, approximately one year in two. It is also shown that there has been a substantial increase over recent decades in the number of springtime fire weather events in southeast Tasmania with peak McArthur Forest Fire Danger Index (FFDI) in excess of 40. Diurnal variations in fire danger between regions of Tasmania and between high- and low-elevation sites are examined, highlighting differences in typical diurnal fire danger behaviour in different regimes. For example, fire danger peaks are generally experienced during the morning at the (high-level, southeastern) summit of Mt Wellington, around noon on the west coast, and later in the day at low level southeastern sites. High temporal resolution observations illustrate that the peaks of fire danger can be quite short-lived and frequently occur at times other than mid-afternoon, however. Thus, 50% of daily fire danger peaks at Hobart Airport (in the southeast) occur at times other than 1500 Local Time (LT). This suggests that many climate studies which use widely available 1500 LT observations may substantially underestimate the level of fire danger in their areas of study. Case studies of two individual springtime fire weather events indicate that at least two mechanisms operate in the generation of severe fire weather. Hot, dry air can be advected from continental Australia and/or dry, high-momentum air can be transported from high in the troposphere to the surface through front/trough vertical circulations resulting in abrupt increases in fire danger during already severe events. In both cases, there is evidence of a foehn effect contributing to the warmth of the airmasses passing over the central Tasmanian topography. Further study of dangerous fire weather days throughout the fire season, using high temporal resolution fire weather observations, shows that the differences evident between the two case studies occur more generally and that there are distinct synoptic differences between the two

types of fire weather event. Abrupt fire danger increases are associated with the presence of jet streaks close to Tasmania and with negatively-tilted upper tropospheric troughs. Such features may be evident in numerical weather guidance some days in advance of events, allowing for early notice to fire and land managers. The seasonality of these events suggests that they have contributed to springtime fire danger over recent decades, but are not the sole cause of dangerous springtime fire weather. The short length of record of high temporal resolution observations does not permit an assessment of changes in frequency or seasonality. Investigation of projected future Tasmanian fire danger using regional climate modelling suggests that current trends are likely to continue, with a gradual increase in cumulative fire danger and in 99th percentile FFDI. Of particular note, the proportion of Tasmania subject to 99th percentile springtime fire danger in excess of FFDI 24 is projected to increase from 6% (1961-80) to 21% (2081-2100). This is a more rapid increase than is projected for summer, with very little change projected for autumn, trends which have been observed over recent decades.

Acknowledgements

I am indebted to my supervisory team: Graham Mills, Kelvin Michael and Mike Pook. While I had a fair, though general, idea of where I wanted to go when I started my research, they offered a great deal of very useful guidance on how to get there. My PhD took some eight years part-time, from start to finish, including a year of suspension while I travelled and worked overseas with my family, and I'm grateful to my supervisors for persevering with me – even after retirement, in two cases! Given the nature of the thesis topic, Graham bore the brunt of suggesting approaches to research questions, reviewing draft papers and proof-reading chapters. His far-sighted approach to framing questions of research interest made a great improvement to the final thesis, and his careful reading of often far-from-perfect drafts added considerable clarity and focus to papers and thesis chapters. Kelvin, as a Graduate Research Co-ordinator, was especially helpful in guiding me through the process of undertaking and completing the PhD, and provided a helpful overview of the various parts of the thesis, and Mike was very generous with his time and expertise in synoptic climatology.

The Bureau of Meteorology has given me the opportunity to study, and supported my attempts to say something useful about fire weather, in Tasmania and more generally. A Studybank bursary was available to me over several years to assist in the purchase of numerous texts and materials to further my research. In particular, the award of a Postgraduate Scholarship for the final six months of my PhD allowed me the time to focus on completing some research and draw together the various strands of my thesis into a coherent whole. I feel very fortunate to have worked for the Bureau for more than 25 years. The organisation places a great deal of emphasis on staff development on the one hand, and on the other is recognised nationally and globally for the quality of the service that it provides to the community.

Within the Bureau, a host of friends and colleagues have assisted with my work, whether that be providing helpful reviews of draft papers, pointing me to important data sources,

supplying useful scripts to plot or manipulate data, or just chatting enthusiastically about what we were all doing. In the Tasmania and Antarctica Regional Office in Hobart, the management team have been especially supportive of my various, often prolonged, absences from normal duties. Former Regional Director Steve Pendlebury and current RD John Bally have both, as former fire weather forecasters, been interested in what I was doing and prepared to allow me the time to do it. Steve Dixon, as manager of the Regional Forecast Centre and as acting RD for 12 months, arranged staffing to replace me, and was always willing to let me pursue promising research directions. David James and Melanie Webb, with numerous members of the Regional Forecast Centre, very ably carried the workload of the Severe Weather Section while I was offline. Kerri Budd gave me much help as I took my first faltering steps into the world of document processing with Lyx. Doug Shepherd (now retired) and Ian Barnes-Keoghan archived and made available much of the high frequency weather data that was to prove critical during the course of my research. Ian, in addition, cheerfully wrote and adapted virtuosic scripts to manipulate data that were immensely useful. Alan Wain, of the Centre for Atmospheric Weather and Climate Research and the Bureau's National Operations Centre, was always helpful with model data and coding.

The Tasmanian fire agencies: Tasmania Fire Service, Parks and Wildlife Service and Forestry Tasmania, have been very supportive of my research, part-funding the digitisation of the older Hobart observation record, through the Tasmanian Fire Research Fund. Individual agency staff have also been very helpful and supportive, Mark Chladil of the Tasmania Fire Service especially so. Mark reviewed a number of publications and other documents, was always ready to discuss technical matters (and anything else), and could be relied upon to unearth the most obscure references, as often as not from his personal library.

The Bushfire Co-Operative Research Centre very willingly took me onboard as a student early on, provided a receptive forum for results and funded the publication of one of the papers resulting from my research.

I spent a very productive and enjoyable twelve months working with the Climate Futures team at the Antarctic Climate and Ecosystems Co-operative Research Centre in the latter part of 2012 and through much of 2013. Professor Nathan Bindoff was unstinting in his support, not only of the work that I was doing at the ACE CRC, but of my PhD more generally. The other members of the Climate Futures team during the my time at ACE CRC, Bec Harris and Greg Lee, were tremendously helpful in getting me set up and productive in the early weeks and months, and were considered and enthusiastic collaborators.

Finally, I thank my family, my wife Purcelle and children Sam and Lexi, for their for-

bearance while I spent many hours on a computer, or just stared vaguely into the distance for far too long over the last few years, and my parents Anne and Lloyd Hughes for their interest and support over a lifetime.

Contents

1	Introduction	1
1.1	Overview	2
1.2	Discussion of approaches and review of literature	3
1.2.1	Fire danger meters and long-term fire danger climatology	4
1.2.2	Seasonal and regional variations in fire danger	5
1.2.3	Diurnal variations in fire danger	6
1.2.4	Case studies of fire weather events	6
1.2.5	Synoptic climatologies of fire weather	7
1.2.6	Future projections of fire danger and fire weather	12
1.3	Structure of this thesis	16
2	A Fire Danger Climatology for Tasmania	21
2.1	Introduction	23
2.2	Methods	24
2.3	Results	28
2.3.1	Hobart, Hobart City and Swansea	28
2.3.2	Launceston Airport and Strahan	34
2.3.3	Mt Wellington	35
2.3.4	Springtime fire danger	35
2.3.5	Springtime trends	38
2.3.6	Station Fire Danger Percentiles	39
2.4	Discussion	41
2.5	Acknowledgements	43
3	Impact of more frequent observations on the understanding of Tasmanian fire danger	45

3.1	Introduction	47
3.2	Data/Method	48
3.3	Results	53
3.3.1	Broad comparison of METAR and synoptic observation datasets	53
3.3.2	Duration of Events	55
3.3.3	Relationship between duration and severity of events	60
3.3.4	Time of Maximum FFDI	61
3.4	Discussion and Summary	62
3.5	Acknowledgements	65
4	Springtime Fire Weather in Tasmania, Australia: Two Case Studies	67
4.1	Introduction	69
4.2	Events and Data	71
4.2.1	7 November 2002	71
4.2.1.1	Surface weather and forest fire danger on 7 November 2002	71
4.2.1.2	Antecedent conditions	72
4.2.1.3	MSLP Progression	72
4.2.1.4	Upper level and satellite analysis	73
4.2.1.5	Airmass characteristics	76
4.2.1.6	Mesoscale features	78
4.2.2	12 October 2006	84
4.2.2.1	Surface Weather and Forest Fire Danger 11-12 October	84
4.2.2.2	Antecedent conditions	85
4.2.2.3	MSLP Progression	85
4.2.2.4	Upper Level Analysis	87
4.2.2.5	Airmass characteristics	87
4.2.2.6	Mesoscale features	89
4.3	Discussion	95
4.4	Acknowledgments	99
5	Characteristics of some days involving abrupt increases in fire danger	101
5.1	Introduction	103
5.2	Data and Methods	104
5.3	Results and Discussion	105
5.3.1	Synoptic Characteristics of Events	105

5.3.2	Satellite Imagery	111
5.3.3	Seasonal Distribution of spike and non-spike days	114
5.3.4	Applicability of results to other locations	115
5.4	Conclusion	117
5.5	Acknowledgements	118
5.6	Supplementary Figures	118
6	Future fire danger climatology for Tasmania, Australia, using a dynamically downscaled regional climate model	135
6.1	Introduction	137
6.2	Methods	140
6.2.1	Fire danger index (FFDI)	140
6.2.2	FFDI in the regional climate model	141
6.2.3	Validation of modelled FFDI	141
6.2.4	Change in future fire danger	142
6.2.5	Synoptic climatology	143
6.3	Results	144
6.3.1	Validation of modelled FFDI	144
6.3.2	Projected changes to accumulated fire danger	144
6.3.3	Projected changes to spatial extent and seasonality of fire danger	148
6.3.4	Surface pressure patterns associated with elevated fire danger	151
6.4	Discussion and Conclusion	155
6.5	Acknowledgements	157
7	Conclusion	159
7.1	Overview	160
7.2	Consideration of initial questions and application of results	165
7.3	Future Work	166
	Bibliography	169

List of Figures

2.1	Location of stations used to derive climatology.	27
2.2	Fire season activity 1919-2006 for Hobart City.	29
2.3	Monthly distribution of Very High FFDI at Swansea.	33
2.4	Decadal distribution 1947-2007 of spring and autumn occurrences of FFDI greater than or equal to 40 at Hobart.	39
2.5	Plot of percentile values for each fire season 1960-2006 at Hobart Airport. . .	41
3.1	Map of Tasmania, showing locations and topographic details mentioned in the text.	50
3.2	Stacked clustered column plots of 50 th , 90 th and 99 th percentiles of Forest Fire Danger Index.	54
3.3	Counts of FFDI ≥ 25 (Very High Fire Danger) by season.	56
3.4	Duration of fire danger.	58
3.5	Frequency analysis of times of Peak FFDI for various FFDI ranges.	63
4.1	Location of Tasmania and other places mentioned in this paper.	69
4.2	Plot of air temperature ($^{\circ}\text{C}$, brown), dewpoint temperature ($^{\circ}\text{C}$, green), wind- speed (km h^{-1} , blue) and FFDI (orange) at Hobart Airport on 7 November 2002.	72
4.3	Tasmanian rainfall deciles for the three-month period 1 August to 31 October 2002.	73
4.4	MSLP Australian Region charts for (a) 0000 UTC 5 November (b) 0000 UTC 6 November (c) 1800 UTC 6 November and (d) 0600 UTC 7 November 2002.	74
4.5	Charts of 300 hPa wind over and west of Tasmania, from the mesoLaps fore- cast initialized at 1200 UTC 6 November 2002.	74

4.6	Infrared satellite images over southeastern Australia at (a) 2030 UTC 6 November and (b) 0530 UTC 7 November, from the US NOAA GOES-9 satellite.	75
4.7	U.S. GOES WV image at 0426 UTC 7 November over southeastern Australia.	76
4.8	Radiosonde plots for (a) Hobart Airport at 2300 UTC 6 November 2002 (b) Eucla at 0000 UTC 05 November 2002, and (c) mesoLAPS 24 hour forecast sounding for 38 °S 136 °E, from model run initialised at 0000 UTC 05 November.	78
4.9	Modelled back trajectories of air parcels ending at 1500 m above ground level over Hobart at 0000 UTC 7 November.	79
4.10	Cross-sections through the line AB in Figure 4.5(b) at 0600 UTC 7 November	80
4.11	Pseudo-WV image generated from mesoLAPS model initialised at 1200 UTC 6 November, valid 0600 UTC 7 November.	81
4.12	MesoLAPS forecast cross-sections through the line CD in Figure 4.5(b), valid 0600 UTC 7 November.	82
4.13	Plot of air temperature (°C, brown), dewpoint temperature (°C, green), wind-speed (km h ⁻¹ , blue) and FFDI (orange) at Hobart Airport on 12 October 2006.	85
4.14	Tasmanian rainfall deciles for the three month period 1 June to 31 August 2006.	86
4.15	MSLP Analyses for 0000 UTC on (a) 9, (b) 10, (c) 11 and (d) 12 October 2006.	86
4.16	MesoLAPS 300 hPa chart, as per Figure 4.5, at 0300 UTC 12 October 2006. .	87
4.17	Routine radiosonde flights from Hobart Airport at 2300 UTC 10 October (grey) and 2300 UTC 11 October (black).	88
4.18	Model back trajectories ending at Hobart on 0000 UTC 12 October 2006, details as Figure 4.9.	90
4.19	Routine radiosonde trace for Woomera at 2300 UTC 10 October.	91
4.20	12 hour forecast cross-sections along the line EF in Figure 4.16, valid 0000 UTC 12 October.	92
4.21	Visible satellite image of Tasmania, valid 0330 UTC 12 October 2006.	93
4.22	MesoLAPS model cross-sections through the line GH in Figure 4.16 at 0300 UTC 12 October.	94
4.23	Peak McArthur FFDI values recorded on (a) 7 November 2002 and (b) 12 October 2006.	96

4.24	Scatterplot of Hobart Airport 850 hPa wind speed and dewpoint depression from routine morning radiosonde soundings between 1992 and 2010.	97
5.1	Map showing location of Hobart Airport, Tasmania.	104
5.2	Composite MSLP plots of (a) spike and (b) non-spike fire weather events from daily NCEP/NCAR reanalyses.	107
5.3	Composite plots of 250 hPa wind isotachs (in m s^{-1}) for (a) spike and (b) non-spike fire weather events from daily NCEP/NCAR reanalyses.	109
5.4	Composite plots at successive six hour intervals of NCEP/NCAR reanalysis 250 hPa windspeed.	110
5.5	Composite cross-sections through 43 °S from 100 to 160 °E of relative humid- ity (a) spike (b) non-spike and (c) non-event daily composite plots.	112
5.6	Composite plots of 0600 UTC vertical motion for (a) and (b) 500, (c) and (d) 700 and (e) and (f) 850 hPa for spike and nonspike events.	113
5.7	Proportional annual distribution of spike compared with non-spike events. . .	115
5.8	Geopotential height contours at 300 hPa, units m, for events documented as having abrupt increases in fire danger.	116
5S.1	0000 UTC MSLP charts for spike events.	119
5S.1	cont.	120
5S.1	cont.	121
5S.1	cont.	122
5S.1	cont.	123
5S.2	As for Fig. 5S1, but for nonspike events.	124
5S.2	cont.	125
5S.2	cont.	126
5S.2	cont.	127
5S.3	Satellite WV imagery of spike events. Imagery courtesy of NOAA and JMA.	128
5S.3	cont.	129
5S.3	cont.	130
5S.3	cont.	131
5S.4	Satellite WV imagery of nonspike events. Imagery courtesy of NOAA and JMA.	132
5S.4	cont.	133

6.1	Locations of Tasmania relative to the rest of Australia, and of Tasmanian weather forecast districts used in the analysis of changes to fire danger. . . .	143
6.2	Multi-model mean of annual 99 th percentile FFDI for each grid point over Tasmania between model times 2002-2012.	145
6.3	Multi-model mean \sum FFDI across Tasmania.	146
6.4	\sum FFDI for the six regional climate models used in this study.	147
6.5	Multi-model mean 95 th and 99 th percentile FFDI during the fire season (October-March).	149
6.6	Multi-model mean 99 th percentile FFDI for spring (SON), summer (DJF) and autumn (MAM), for the periods 1961-1980, 2041-2060 and 2081-2100.	150
6.7	99 th percentile FFDI for the six regional climate models used in this study, averaged by decade 1960-2090 and by BoM weather forecast district.	152
6.8	High resolution model domain, displaying composite surface pressure patterns for elevated FFDI.	154

List of Tables

2.1	Summary of the availability of synoptic observations from studied stations. . .	28
2.2	Crosstabulations month by hour of Very High forest fire danger index for Hobart City and Airport and Launceston Airport.	31
2.3	As for 2.2 for Strahan Airport and Mt Wellington.	32
2.4	Occasions when a springtime (Oct-Nov) peak in fire danger occurred.	37
2.5	Fire danger percentiles for each of the stations studied.	40
3.1	Occasions within the period October 1990 – June 2010 when FFDI at Hobart Airport reached 70.	61
5.1	Satellite Water Vapour features associated with spike and non-spike events. .	114
6.1	Parameter estimates for linear model representing change in \sum FFDI 1960- 2090 by weather forecast district.	148
6.2	Proportion of Tasmania exceeding FFDI percentile thresholds during the fire season (Oct-Mar).	149
6.3	Proportion of Tasmanian grid cells exceeding thresholds of 99 th percentile FFDI by season.	151
6.4	Parameter estimates for linear model representing change in 99 th percentile FFDI 1960-2090 by weather forecast district.	152
6.5	Frequency of occurrence of FFDI thresholds at the start (1961-1980) and end (2081-2100) of model simulations.	153

1: Introduction

1.1 Overview

Fire is a normal feature of the Tasmanian landscape during the warmer months of the year, depending on current and antecedent weather conditions. This thesis explores aspects of Tasmanian fire weather and fire danger, particularly during spring, where it is less commonly recognised that conditions can be conducive to the occurrence of fires in the landscape. The thesis is a response to the observation, from an operational weather forecasting perspective, that dangerous springtime fire weather seemed to be increasing in frequency and was increasingly severe in Tasmania during the early 2000's. A number of approaches were adopted to validate this observation and investigate meteorological factors behind it, to expand on the results and lead towards potential operational applications, and to assess projected future climate trends. By adopting a multi-faceted approach, the various strengths of available datasets were exploited, and their weaknesses mitigated.

The occurrence of fire in the landscape is a consequence of an ignition source together with the availability of flammable fuel and suitable weather conditions (Meyn et al., 2007). Both fuel flammability and weather vary with season, and the seasonality of fire occurrence, in turn, varies regionally (Carmona-Moreno et al., 2005), as discussed below.

Australia is one of the most fire-prone regions of the globe (Russell-Smith et al., 2007). Fire has shaped the Australian landscape, with many species requiring the occurrence of fire to propagate. There is evidence of fire activity in Australia since at least the Cretaceous (Macphail et al., 1993). It has been a regular part of the Australian environment since the late Miocene (Martin, 2006), around 10 million years ago, when polar ice sheets expanded, sea level fell and global climate cooled and dried. Rainforest vegetation in Australia contracted to generally coastal areas and was replaced by more open woodland including Eucalypt species. Charcoal evidence indicates fire activity started to become common from this time. Subsequently, burning has increased and decreased as climates changed (Mooney et al., 2011, Power, 2013), with some evidence that increased burning has occurred during periods of rapid change (Black and Mooney, 2006, Lynch et al., 2007), a feature also evident elsewhere (Marlon et al., 2009). Humans have contributed to the burning of the landscape since the arrival of Aboriginal people on the continent at least 45,000 years ago (Enright and Thomas, 2008), although it has been argued that there was no abrupt change in the amount of burning that occurred as a result of Aboriginal arrival (Mooney et al., 2011). There is, however, good evidence of an increase in burning in general with the arrival of Europeans in Australia (Lynch et al., 2007, Mooney et al., 2011).

While Tasmania has a cooler climate than much of the Australian continent, fire is still an important part of the landscape, but the interaction between climate, fire, vegetation and human activity is very complex (Bell, 1983, Ellis, 1985, Marsden-Smedley, 1998, Marsden-Smedley and Kirkpatrick, 2000, Von Platen et al., 2011), with humans having used fire in Tasmania for at least the past 23,000 years (Ellis, 1985). Part of the complexity noted above is that fire activity has varied regionally over time. In the southeast of the state, for example, there is evidence of an increase in fire occurrence in the past century (Von Platen et al., 2011). In the southwest, on the other hand, there has been a decrease in fire activity, in general, since European settlement and the cessation of Aboriginal burning (Marsden-Smedley, 1998, Macphail, 2010). The occurrence of fire weather and consequently fire danger, examined in this thesis, is one aspect of the complex set of interactions that define the Tasmanian environment, but it is the one that is most variable in the short term, and one for which there is a need on the part of meteorologists, emergency and land managers and the community in general for a greater degree of understanding.

1.2 Discussion of approaches and review of literature

The following sets the context for the topics discussed in the thesis, providing an introduction to the approaches adopted to investigate the central thesis problem, including:

- A climatology of fire danger derived from long-term synoptic weather observations;
- A shorter-term, but high temporal resolution, fire danger climatology with fewer stations available;
- Case studies of specific, extreme springtime fire weather events;
- A synoptic climatology of fire weather events, with relevance to springtime fire danger occurrence;
- And, a study of how Tasmanian fire danger is projected to change during the twenty-first century.

This section includes a survey of some of the key literature in the area – in some cases, the literature is quite extensive and a comprehensive survey would not be appropriate here, in others, the literature is minimal. The review is divided by chapter, as the specific topics are quite distinct.

1.2.1 Fire danger meters and long-term fire danger climatology

A variety of fire danger meters have been developed in different parts of the globe, applicable to the conditions and vegetation types for which they are intended. The meters integrate to differing degrees features of the topography, and antecedent and current weather conditions that affect characteristics of fires that may occur, such as the growth rate, intensity and rate of spread of fire.

The McArthur Mark V Forest fire danger index (FFDI) (McArthur, 1967) is widely used in Australia. It is the meter used currently in Tasmania for decisions on fire weather warnings, and implicitly for the imposition of Total Fire Bans by the Tasmania Fire Service. It was developed during the 1960's for conditions similar to the dry sclerophyll forests around Canberra where the research leading to its development occurred (McArthur, 1967). It includes a dependence on temperature, a stronger dependence on relative humidity and wind, and on a Drought Factor to incorporate the effects of antecedent rainfall. There is scope to vary fire behaviour aspects of the meter (including rate of spread and flame height) depending on slope and fuel load, but these are not considered here. In the calculations carried out in this thesis, the slope is assumed zero and fuel load a standard (for operational calculation) 12.5 tonnes/Ha of available fuel.

It is recognised, though, that there are a number of fuel types in Tasmania for which other fire danger meters are appropriate, including, broadly, buttongrass moorland and similar fuels and grasslands. Buttongrass moorlands are confined mostly to the west of Tasmania where approximately 1.1 million Ha are covered by this vegetation. During the 1990's, a series of experimental burns were carried out to develop a meter to safely manage fuel reduction burning in buttongrass (Marsden-Smedley and Catchpole, 1995a,b, 2001, Marsden-Smedley et al., 2001). The resulting meter is now used operationally. Due to the physical characteristics of the fuels and the environments in which they are typically found, the buttongrass moorland fire danger meter is quite different from the forest meter in its response to weather parameters. The moorland meter is very strongly dependent on wind, and less so on relative humidity and temperature. It is very strongly responsive to recent (last 48 hours or less) rainfall but insensitive to earlier rain.

Grasslands dominate the Tasmanian Midlands which are largely given over to agriculture. A grassland fire danger meter was developed, again by CSIRO's A.G. McArthur, in the 1960's (McArthur, 1966). Grassland fire danger is computed from temperature, relative humidity, windspeed and curing, an estimate of the degree of grass drying. The underlying topography

is assumed to be flat or undulating.

Several Australian fire and land management agencies have investigated the use of the Canadian Fire Weather Index (FWI) (van Wagner et al., 1992), which resolves fuel moisture and fire activity into more components than the FFDI or GFDI. Dowdy et al. (2009) compared the FFDI and FWI, noting that they are comparable but complementary indices, with, for example, the FWI more sensitive to windspeed than the FFDI, and less sensitive to temperature and relative humidity. While the FFDI is not the best meter for describing fire behaviour in all (or even most) vegetation types, it does offer an integration of the effects of meteorological parameters that highlights days that are genuinely dangerous, whichever vegetation type is present. In this thesis, the FFDI is used exclusively.

1.2.2 Seasonal and regional variations in fire danger

Fire weather and fire danger vary seasonally around the globe (Carmona-Moreno et al., 2005). In many regions, summer-autumn is the peak fire danger period, when heating and drying of fuels are at a maximum (Skinner et al., 1999, Pereira et al., 2005, Pitman et al., 2007, Salloum and Mitri, 2014) and dry lightning storms can be a prolific ignition source (Stocks et al., 2002, Dowdy and Mills, 2012, Kraaij et al., 2013). In other areas, the peak occurs in springtime, before fuels have experienced a flush of new, green growth (Valendik et al., 1998, Westerling et al., 2006, Drobyshv et al., 2012, Pollina et al., 2013) or weather conducive to fire is more common (Crimmins, 2006), and in some regions the dry, winter or winter-spring, season is active (Van Wilgen et al., 2000, Kraaij et al., 2013, Tian et al., 2014). A monsoonal period during the summer means that some areas experience elevated fire danger during spring and autumn, but not (or rarely) during summer (Lynch and Hessel, 2010). In addition, temperate and boreal areas of the globe are experiencing an increased length of fire season (Flannigan et al., 2009). Luke and McArthur (1978) broadly mapped areas of Australia subject to different fire seasons, and Russell-Smith et al. (2007) plotted satellite composite maps of fire hotspots by season, showing that different areas of the continent have active fires throughout the year. Fire was most active in southeastern Australia in summer-autumn in both analyses, but there was activity evident in Russell-Smith's composite map during mid-late spring and in this area only the period July through September was without some degree of fire activity. Chapter Two demonstrates that Tasmania does experience a typical primary fire danger peak during summer. In addition, however, a secondary peak occurs during spring in the east and southeast of the island, and, during some fire seasons, the highest fire dangers occur during the springtime peak.

1.2.3 Diurnal variations in fire danger

A more complete understanding of the variation of fire danger through the day is important meteorologically and for fire management (Beck and Trevitt, 1989, Beck et al., 2002). There is a widespread understanding that fire danger and fire activity generally peak mid-afternoon as, climatologically, that is the time of maximum heating, minimum relative humidity and fuel moisture and highest wind (e.g. Tolhurst and Cheney (1999), Whiteman (2000)). It is important to be aware of the possibility of activity at other times, however. Satellite remote sensing (Prins et al., 1998, Zhang and Kondragunta, 2008) has allowed a broadscale assessment of diurnal variability of fire activity, if not fire weather, confirming a mid-afternoon peak, but highlighting that other times may also be peaks of activity. Millán et al. (1998) note that a particularly dangerous situation occurs in Valencia, Spain, with the overnight combination of a dry land breezes and westerly winds driven by the passage of low pressure systems over the Iberian Peninsula, and Kepert and Fawcett (2013) document an early morning flare-up of a fuel reduction burn near Margaret River, Western Australia, that resulted in the destruction of 32 homes and damage to others. A further example occurred in one of the case studies considered in Chapter Four below, where fire danger over southeastern Tasmania abruptly increased during the early evening. Chapter Three highlights the fact that, for example, Hobart experiences only half of its diurnal fire danger peaks during the mid-afternoon.

1.2.4 Case studies of fire weather events

There is an abundance of studies of fire weather and fire events in the Australian and North American meteorological literature, although few from other regions. Case studies of fire weather events have in the past been important to document significant events that have occurred. In addition, they can provide an improved understanding of the mechanisms leading to the events, pointing the way to better forecasts, and also highlighting areas where additional research and understanding would be beneficial. For example, the manner in which cold fronts can surge along the southern Australian coastline was described by Mills (2002), and the formation and action of mesoscale low pressure systems over southeast Tasmania in Mills and Pendlebury (2003). Analysis of the Canberra fires of January 2003 (Mills, 2005a) and Wangary fire in South Australia in January 2005 (Mills, 2008a) led to an understanding of the mechanism by which abrupt fire danger increases occurred in fire weather events and of the utility of water vapour imagery in forecasting or nowcasting

such events. Documentation and examination of other occasions where abrupt increases in fire danger have occurred (e. g. Zimet et al. (2007), Huang et al. (2009), Charney and Keyser (2010)) have helped in formulating a better understanding of similar such events. An analysis of the Black Saturday fires in Victoria on 7 February 2009 (Engel et al., 2013, Thurston et al., 2014) highlighted the role of horizontal convective rolls in increasing wind variability at the surface and enhancing lofting of embers from fires. A recent analysis of the Margaret River in November 2011 (Kepert and Fawcett, 2013) demonstrated the role of small-scale topographic features in transporting dry air to the surface overnight, when fires are usually expected to be less active. Two case studies of dangerous springtime fire weather in Tasmania are included in Chapter Four, indicating different mechanisms for the source of extremely dry air observed in each event.

1.2.5 Synoptic climatologies of fire weather

Synoptic climatologies have been undertaken on a broad range of meteorological topics (see, for example Yarnal (1993), and the reviews in Yarnal et al. (2001) and Sheridan and Lee (2010)). However, relatively fewer such studies have considered the synoptic climatology of fire weather and/or wildfire. Flannigan and Wotton (2001) reviewed many of the North American studies, in particular noting the importance of both upper and lower atmospheric features to the occurrence of dangerous fire weather, and especially the presence (and persistence) of mid-tropospheric ridging. Potter (2012a) also reviewed a number of such studies, particularly from the first half of the twentieth century, noting that Beals (1914) was the earliest, and highlighted that that fire weather synoptic climatology studies tended to have been spread across a broad range of peer-reviewed literature, government reports and other documents. Beals (1914) documented the surface synoptic patterns across North America associated with several destructive fires for which at least some weather data was available, with the aim of providing advance notice of weather conditions that might lead to similar events in future. He did, however, note the importance of local effects on fire activity, particularly in mountainous areas, and also suggested that, in the cases of the large fires studied, the winds recorded were very likely generated by the interaction of the fires with the atmosphere.

By the mid-twentieth century, there was sufficient understanding of the area for some continental-scale studies to occur. Foley (1947) reviewed the meteorological situations associated with significant fire events that had occurred in each Australian state in previous decades, summarising characteristic synoptic features of their fire weather. Similarly,

Schroeder et al. (1964) documented typical surface or upper tropospheric patterns that were associated with elevated fire danger in the United States, considering 14 different climatic regions. In particular, Schroeder et al. (1964) noted that in some regions (specifically mountain or intermountain states) high fire danger occurred on the flanks of upper ridges beneath the jet stream. Schaefer (1957) also drew a connection between the jet stream and fire activity, highlighting 23 “blowup” fires (fires that rapidly increase in activity and/or scale) during 1955-56 in the United States that occurred within close proximity to the jet stream at the time. Schaefer suggested that the upper tropospheric strong winds might mix downward, resulting in higher fire danger through an increase in surface winds. Brotak and Reifsnyder (1977) identified synoptic features common to the occurrence of large wildfires in the United States in the decade 1963-1973. They noted that most fires occurred near a front, especially in the airmass following a dry cold front, and stressed the importance of the upper level pattern, pointing to the presence of an intense 500 hPa trough of limited latitudinal extent, associated with little or no precipitation but strong surface winds. Only a little earlier Newark (1975) noted, in the context of an analysis of the particularly severe Canadian fire season of 1974, that the persistence of a long-wave ridge at 500 hPa was an indicator of dangerous fire weather due to the long spell of fuel drying often associated with the pattern, but also the possibility of lightning occurrence without substantial precipitation. Nimchuk (1983), on the other hand, clearly identified the 500 hPa ridge breakdown as the most dangerous period for fire weather, agreeing, however, that the persistence of a ridge brings fuels to a critically dry state.

A large proportion of the synoptic climatology studies of fire weather in the last two decades is focussed on North America. Takle et al. (1994) used Yarnal’s 1993 synoptic classification scheme to partition West Virginian weather into eight types, three of which were associated with fire occurrence (pre-high, extended-high and back-of-high). The back-of high type was identified as being associated with the largest and most destructive fires of the dataset studied. Takle et al. (1994) highlighted that the wind direction in back-of-high conditions was conducive to the development of a foehn effect, but also noted that the weather type was comparable to the Schroeder et al. (1964) pre-frontal zone of elevated fire potential. The Yarnal (1993) classification scheme was modified slightly (with the addition of another pattern) by Pollina et al. (2013) in their examination of the influence of climatology and meteorology on wildfire occurrence in the northeast of the United States. Pollina et al. (2013) identified anticyclonic patterns (pre-high, extended high and back-of-high) as most associated with significant wildfire occurrence, whereas Takle et al. (1994) identified only

back-of-high systems as significant for fire weather. The pre-high and extended high patterns were, however, identified as the leading types present during wildfires in sub-regions of the study area. The pre-high was associated with large-scale atmospheric descent and a foehn effect in the lee of the Appalachian Mountains, and the extended high was accompanied by persistent lack of rain, allowing fuels to dry.

Building on the focus on mid-tropospheric systems and anomalies of systems documented earlier in e.g. Newark (1975), Skinner et al. (1999) examined the monthly to seasonal synoptic climatology of 500 hPa ridges over North America, and specifically Canada, stressing that anomalously persistent 500 hPa ridging generally occurred in proximity to areas that experienced more severe burning seasons.

Crimmins (2006) examined frequencies of synoptic types of 700 hPa height fields, obtained using Self Organising Map (SOM) classification techniques (Kohonen, 2001), noting that southwesterly flow types were most associated with critical fire weather in the southwest of the United States. The same technique of SOM was used in a different context by Trouet et al. (2009), who examined the relationship between large-scale circulation patterns, specifically the Pacific-North American (PNA) pattern and the Pacific Decadal Oscillation (PDO), and fire risk in the western United States. The authors noted that the favourable large scale conditions for fire risk (positive PNA and PDO) were generally associated with more frequent mid-tropospheric ridging in the area of study, as found with earlier studies.

There have been a number of European synoptic climatology studies in the last two decades that have focussed on fire weather, especially in the Mediterranean basin. The earliest of these was Millán et al. (1998), who noted the absence of previous studies, suggesting that there was a perception that fire had always been part of the Mediterranean landscape and not seen as worthy of study earlier. However, more dangerous fires were beginning to occur as a result, at least in part, of abandonment of traditional land management practices that limited fuel load. This trend highlighted the potential value of conducting synoptic climatological studies. Millán et al. (1998) studied the Valencia region of Spain, finding three situations most likely to be associated with dangerous fire weather: a local, diurnal land/sea breeze cycle; a “poniente” – a westerly Foehn effect as a low tracked across the Iberian peninsula; and, most dangerous, a combination of the previous two scenarios, acting in phase to reinforce the dry westerly winds descending from the interior of Spain, not dissimilar to the back-of-high scenario identified in Takle et al. (1994), where local-scale and synoptic scale effects reinforce to enhance fire danger.

On the other side of the Iberian Peninsula, in a study of fire activity in Portugal, Pereira

et al. (2005) identified, as in a high proportion of North American studies, the presence of a mid-tropospheric high being conducive to dangerous fire activity, together with an anomalously meridional surface flow, directing hot, dry North African air over the Iberian Peninsula. Hoinka et al. (2009) came to similar conclusions for central Portugal using a lagged covariances approach to the evolution of relevant meteorological fields in the lead up to critical fire weather days. Rasilla et al. (2010) also identified easterly or southeasterly flow regimes as contributing to the most extreme days in their study of 850 hPa geopotential height patterns related to wildfire risk in Spain. These fires generally occurred in the west of the country. A second set of patterns was also identified, however, that applied to the Mediterranean seaboard. As Millán et al. (1998) concluded, synoptic patterns resulting in westerly downslope winds off the Iberian highlands also contributed to the occurrence of damaging wildfires. Again, Rivas Soriano et al. (2013) identified surface easterly circulation patterns as contributing to the occurrence of large fires in western Spain and Portugal.

As did a number of the studies noted above, Papadopoulos et al. (2013) highlighted the role of anomalously high 500 hPa geopotential heights in the occurrence of large wildfires in Greece. They also, however, noted anomalously low surface pressures resulting in strong winds associated with the presence of low pressure systems. On the eastern Mediterranean seaboard, Levin and Saaroni (1999) noted that conditions conducive to wildfire in Israel were similar to those in Portugal (and many other continental margins), with synoptic systems advecting hot, dry winds closely linked to the largest and most dangerous fires. In this case, the occurrence of a North African cyclone, or “Sharav” and Red Sea trough during spring, after the climatological wet season had allowed the growth of abundant fuel, could facilitate the growth of dangerous fires. The return of the Red Sea trough in autumn caused a secondary peak in fire occurrence, with a large number of smaller fires occurring during the mild summer conditions under a common Persian Gulf trough.

Elsewhere, Geldenhuys (1994) briefly noted that fires occurring during foehn-like “berg-wind” episodes in the southern Cape of South Africa had been historically very significant. The bergwinds themselves occurred during the west-east passage along the South African coast of low pressure systems. Interestingly, the discussion of Geldenhuys (1994) follows similar lines to that of Moritz et al. (2010), both arguing that patterns of fire, and consequently vegetation, are likely to follow patterns of higher or more extreme winds forced by local topography. In the case of Moritz et al. (2010), the Santa Ana winds of southern coastal California drove fires through the chaparral ecosystems of the area.

There have been numerous fire weather publications over many decades in Australia,

most of which document the meteorology of specific events (e.g Whittingham (1964), Bond et al. (1967), Bureau of Meteorology (1985), Engel et al. (2013)). Relatively fewer studies of the synoptic climatology of fire weather have been attempted. Foley (1947) has already been mentioned as a pioneer in this context. Wallace and Gloe (1938) touched on synoptic structures, primarily focussing on wind direction as a key variable in the occurrence of dangerous fire weather, and Whittingham (1961) noted briefly that many of the worst Australian fire weather and fire events followed from rapid cyclogenesis over a limited area within a broad trough. Such a situation did indeed recur some six years later with the 7 February 1967 fires in southeast Tasmania that resulted in the destruction of over 1200 structures and the death of 62 people (Bond et al. (1967)). More broadly, Marsh (1987) documented the synoptic climatology of typical dangerous fire weather events in Tasmania, making reference to several significant fire and fire weather events, including 7 February 1967. He indicated that a Tasman Sea high pressure centre was common, with a 500 hPa trough to the west over the Great Australian Bight, with the possibility that one or more weak fronts with limited vertical extent might cross the state without displacing a reservoir of warm, dry air aloft before the passage of a more major change resulted in the most significant day of fire danger for the multi-day event. These situations resemble, again, the back-of-high synoptic pattern described in Takle et al. (1994), and earlier by Schroeder et al. (1964), in the United States and Nimchuk (1983) for Alberta.

In reviewing the 1983 “Ash Wednesday” devastating bushfires in Victoria, Australia, Mills (2005b) identified the 850 hPa temperature gradient as very unusual. He examined 40 years of reanalysis data to show that similar situations, in which a steep meridional 850 hPa atmospheric temperature gradient was present, often occurred with significant fire events. Mills (2005b) argued that such temperature gradients and their associated deep tropospheric troughs, through the thermal wind relationship, would result in strong northerly winds and probable high surface temperatures. The deep tropospheric troughs associated with these events relate closely to the back-of high events, again, of Takle et al. (1994) and Nimchuk (1983)’s 500 hPa high replacement situations, as indicators of the potential for large fire occurrence and severe fire weather. Long (2006) examined Victorian Extreme (FFDI greater than or equal to 50 at the time of the study) fire weather days, including “Ash Wednesday” 1983, assigning events at four long-term observation sites to a synoptic typing developed by Treloar and Stern (1993) based on wind direction and curvature over southeastern Australia. Consistent with the findings of Mills (2005b), most days of extreme fire danger were associated with synoptic types involving moderate to strong northwest to

northerly winds. Mills (2008b) took a different approach to the synoptic climatology of fire weather days, examining events characterised by abrupt increases in fire danger. He linked the occurrence of this type of event to upper tropospheric patterns conducive to deep descent, including typically anticyclonic curvature and the proximity of the anticyclonic shear side of jets. Less commonly, descent was inferred in some cyclonically sheared environments, including the cyclonic side of a jet entrance, and where curvature led to deceleration.

Synoptic climatology attempts to link the broad scale atmospheric structure to particular environmental impacts, whether that be the occurrence of smog in a city, rainfall over a cropping area or, in the cases described above, the development of dangerous fire weather conditions, whether by the examination of indices indicative of fire danger or of actual dangerous wildfires. In a substantial proportion of the studies considered above, the presence of persistent mid-tropospheric ridging was featured, to allow time for fuels to dry. Often, the most dangerous conditions were seen to accompany a change of pattern either explicitly, as in those studies that highlighted back-of high patterns, or implicitly, where the focus was on the presence of particular jet structures in the upper troposphere. The study conducted in Chapter Five falls into the latter category, with an emphasis on the structure of approaching upper troughs and extends the work particularly of Mills (2008b). It does, however, add to the body of literature highlighting the importance of mid- to upper-tropospheric processes in the occurrence of severe fire danger. In addition, much of the available literature noted mesoscale processes operating to focus the most extreme conditions on particular areas, with foehn effects often occurring, for example, as the result of wind flow in some larger scale atmospheric process. Peters et al. (2004) addresses this “cross-scale” interaction more broadly, noting its impact on dangerous fire weather events in the context of fire-atmosphere interaction. In the Tasmanian events studied in this thesis, such mesoscale focussing clearly also occurs. It is discussed explicitly in the case studies in Chapter Four, where a foehn effect is documented in both cases, but also occurs in the ageostrophic jet circulations that transport upper tropospheric air towards the surface.

1.2.6 Future projections of fire danger and fire weather

There is a large and growing literature examining climate effects and impacts, and many of these consider the likely effects of climate change on fire weather and fire occurrence. Thus, the following is intended to be indicative rather than comprehensive.

A number of studies have considered recent changes in fire activity on both global and local scales. Flannigan et al. (2009) highlighted that there has been a general global increase

in fire occurrence and area burnt since the Last Glacial Maximum, but there are local variations, including areas where fire activity has decreased. This trend suggests a strong temperature effect; however Pechony and Shindell (2009) argue that over much of the last millennium global fire activity has been most strongly influenced by precipitation, citing as examples the increased fire activity that occurred during the cold but dry 15th century Spörer Minimum and reduced fire activity in the cold, humid Maunder Minimum (17th-18th centuries). The latter authors argue that it is only since the Industrial Revolution that there has been a trend towards temperature-driven increases in fire activity, a trend which they – and many others - argue is very likely to continue. Flannigan et al. (2009) are in agreement with them in this regard, noting that fire seasons in temperate and boreal regions are lengthening and are likely to continue to do so. Using 16 Global Climate Models (GCM) Moritz et al. (2012) demonstrated that there is still not agreement between models over some 50% of global land area regarding the direction of change in fire probability in the near term (2010-2039), noting that the areas of greatest agreement regarding an increase are those already warm. There was greater agreement on the direction and magnitude of changes by the end of this century (2070-2099). Liu et al. (2010) also note a degree of divergence of model results but, in considering the end of the century (2070-2100), this divergence was less pronounced than the near-term results of Flannigan et al. (2009). Liu et al. (2010) note that increases in fire potential (as measured by the Byram-Keetch Drought Index) varied in their driver, with purely temperature-driven increases in some regions and a combination of temperature and drier conditions in others. Many studies noted that prediction of future fuels is a difficult problem, and considered only the future climate as an indicator of likely fire activity – the study in Chapter Six falls into this category. Hessler (2011) specifically considered the mechanisms by which future climate might affect fire regimes, identifying changes in fuel volume, fuel condition and ignition as critical. Flannigan et al. (2013) employed a metric of total fire season severity, the Cumulative Severity Rating (CSR), to demonstrate that three different climate models with three emissions scenarios all pointed to increases in the CSR by the middle of the 21st century (2041-2050) with further substantial and near-global increases by the end of the century (2091-2100).

Regionally, in addition to the results in Chapter Two, there have been several studies demonstrating an increase in recent decades in the level of fire danger and of fire activity e.g. Piñol et al. (1998) for Eastern Spain and Gillett et al. (2004) for Canada. The latter used GCM (Global Climate Model) output to demonstrate that the observed increases, which had varied with temperature, were likely a result of climate change. Many regional studies have

used a synoptic climatological approach, linking current or past fire activity or fire weather to broadscale weather features resolvable by numerical weather models, then inferring future fire danger and fire weather from an examination of the output of a single GCM or RCM (Regional Climate Model). Numerous studies consider North America, given the strength of the fire-related research effort in that region. Flannigan et al. (2000) calculated Seasonal Severity Rating (SSR), derived from two GCM values of FWI, to estimate likely fire activity and area burnt over North America by the middle of the 21st century, finding increases of up to 50% were likely over much of the continent, but that there were some areas where little change, or even a decrease, was possible.

Studies have also been carried out for Canada alone (Flannigan et al., 2005) and subregions (Podur and Wotton, 2010), and for regional areas of the United States (Brown et al., 2004, Fried et al., 2004, Yue et al., 2013). Miller and Schlegel (2006) specifically examined the projected occurrence of the Santa Ana wind, inferred from climate projections for Southern California. All of these studies found that a general increase in fire danger and fire risk was likely during the course of the current century.

Several studies have examined projected changes to fire danger in the Mediterranean basin. Moriondo et al. (2006) highlighted increases in FWI in European Union Mediterranean nations using a GCM assuming A2 and B2 emissions scenarios (Nakićenović, 2000). They found three mechanisms by which the fire danger increase occurred: an increase in the number of years experiencing fire risk, an increase in the length of the fire season and an increase in the number of extreme events. Carvalho et al. (2010) reported recent substantial increases in fire activity in Portugal and, using projected FWI values derived from an RCM at 12 and 25 km resolution, that a continuing increase was very likely. By the end of the 21st century (2071-2100), projected area burnt was modelled to be almost five times that currently burnt annually. Interestingly, Carvalho et al. (2010) found little difference in outcome between the 12 and 25 km projections. Using a different methodology and different RCM, at 10 km resolution, Carvalho et al. (2011) again found changes in meteorological variables during a future period (2041-2060) that would result in a longer fire season and greater fire danger in Portugal. Similar results were obtained for Spain for the end of the century (Vázquez de la Cueva et al., 2012).

In other regions of the globe, climate change studies have also shown increases in fire danger and fire risk. Malevsky-Malevich et al. (2008) examined projections for the Russian boreal forests, finding fire dangers were projected to increase in most, but not all, of the studied subregions during the 21st century. Shkolnik et al. (2008), using an RCM with 50 km

resolution, also demonstrated a projected increase in dangerous wildfire activity in several parts of Russia, with a greater increase in more extreme events. Tian et al. (2014) used a 50 km resolution RCM to diagnose projected increases in FWI in China during the century, with changes particularly in central and south-eastern China. They noted increases across a number of measures, similar to those found by Moriondo et al. (2006). Even in regions not usually associated with wildfire, studies suggest that fires may become a problem during the next several decades. Albertson et al. (2011) found that projected changes in climate and the moorland of the Peak District of northern England were likely to be conducive to more peat fires, with – as found in most other studies – an acceleration towards the end of the century.

There have been a number of studies of future fire danger specifically in Australia in recent decades (Beer and Williams, 1995, Williams et al., 2001, Hennessy et al., 2005) which indicate a general increase in fire danger across the continent during the 21st century (although Hennessy et al. (2005) suggest little change in Tasmania). Other studies have focussed on particular aspects of fire danger or the fire season. For example Pitman et al. (2007) used a regional climate model at 50 km resolution to examine January fire danger only, finding that, for a number of model runs and future emissions scenarios, across all regions, there were increases in fire danger, consistent with the earlier results using different methodologies (e.g Beer and Williams (1995), Williams et al. (2001)). In the same way that Miller and Schlegel (2006) examined a specific phenomenon associated with increased fire risk, Hasson et al. (2009) investigated the future modelled frequency of steep meridional temperature gradients at 850 hPa, following from the observation of Mills (2005b) that such features were often associated with destructive wildfires. They found, using 10 GCM calibrated against model performance over the 20th century, that there is likely to be a doubling in the number of steep gradient events by mid-21st century and a further increase by the end of the century, although there was some spread amongst the models. King et al. (2012) attempted to account for fuel load by modelling grass growth and curing using the GRAZPLAN pasture growth model fed with data from climate projections, then calculating McArthur GFDI. They found that, while fire danger and curing generally increased in the projections, fuel load decreased, with little net change in total fire danger through time.

1.3 Structure of this thesis

The thesis is comprised of a series of five papers, presented as chapters, which have been published in the peer-reviewed literature, with the exception of Chapter Five, currently in review. The remainder of this chapter will summarise the research papers and how they relate to each other.

Chapter Two is a climatology of fire danger in Tasmania, derived mostly from three-hourly synoptic weather observations and published in the *Australian Meteorological Magazine* (now *Australian Meteorological and Oceanographic Journal*) (Fox-Hughes, 2008). The paper employs the McArthur Mark V FFDI to examine regional and elevation-based differences in the typical fire danger regime around the island, to assess the seasonality of fire danger and to examine whether any changes have occurred over the period for which observations are available.

Chapter Two shows that eastern and southeastern Tasmania have experienced a rapid increase in the number of days of dangerous springtime fire weather over the last several decades, in addition to a gradual increase in the number of days of dangerous fire weather across the fire season. It shows that this part of the island is subject to a seasonal or sub-seasonal peak in fire danger approximately one season in every two, confirming the existence of a “springtime” bump perceived by operational fire weather forecasters and land managers. Further, it highlights clear differences in the diurnal pattern of fire danger between different regions of the island, and between high- and low-lying areas. Thus, for example, there is a clear tendency for fire danger to peak during the early morning at the elevated (1260 m) summit of Mt Wellington in southeast Tasmania, whereas in Hobart, less than 10 km distant but some 1200m lower, fire danger usually peaks some hours later during the afternoon.

Analysis of three-hourly observations in Chapter Two highlights the need for an examination of sub-daily weather data to understand the fire weather climatology of a region. This is the focus of Chapter Three, with an investigation of the diurnal variability of fire danger in Tasmania using half-hourly weather observations at three diverse sites for which approximately two decades’ data was available at the time the research was undertaken in 2009-2010. (Subsequently, the Australian Bureau of Meteorology has expended considerable effort to digitise selected earlier, hourly or half-hourly airport weather observations, providing a valuable resource for future study.) The study was published in the *American Meteorological Society (AMS) Journal of Applied Meteorology and Climatology* (Fox-Hughes, 2011).

Chapter Three demonstrates that up to 50% of fire danger peaks are missed by mid-

afternoon-only weather observations, despite this being the most common time for fire danger peaks. The information is important also to be able to adjust the results of future climate studies which often calibrate projected future fire danger and activity from past data, using once-per-day observations, as these are most widely available for an extended period. Chapter Three also highlights the considerable differences between the seasonal and diurnal patterns of fire danger between the study sites, and examines the relationship between event severity and duration, which is often not obvious but is nonetheless important to understand for forecasting and management purposes. Chapter Three and the data described within also form an important bridge to the improved ability to forecast abrupt fire danger increases discussed in Chapter Five.

The analyses in Chapters Two and Three provide a useful and important overview of fire danger behaviour in Tasmania. They also highlight that there is value in examining particular events, to better understand general mechanisms of fire danger and fire weather. Thus, two extreme springtime fire weather events are examined in Chapter Four (Fox-Hughes, 2012), published in the AMS journal *Weather and Forecasting*.

The springtime fire weather case studies presented in Chapter Four, those of 7 November 2002 and 12 October 2006, were both very significant events, with “Catastrophic” FFDI recorded in each case (although the term, referring to FFDI of 100 or more was not introduced until after the events). Using numerical weather prediction fields from the Bureau of Meteorology’s then- operational mesoLAPS model, it is demonstrated that the origin of the airmass is different in each case, with air descending into the boundary layer on 7 November 2002 from high in the troposphere, but similarly descending air on 12 October 2006 unable to affect the surface. The exceptionally dry air that was recorded in southeastern Tasmania on 12 October 2006 (and on the preceding days) is shown to originate over the drought-affected inland of continental Australia. The negatively-tilting structure and location of the upper-tropospheric trough near Tasmania on 7 November 2002 enhanced the vertical transport of dry, high momentum air whereas the more usual positive-tilting trough on 12 October was further from the island, both features reducing the capacity of air to descend to the surface.

Chapter Four shows that there were two separate atmospheric mechanisms generating elevated fire dangers in southeastern Tasmania in the cases examined: that of simple advection of hot, dry air ahead of an approaching front, and descent of dry, high momentum air from high in the troposphere associated with jet stream circulations, in addition to the local foehn effect that operated to enhance the warmth and dryness of the airmass reaching the

southeast. It is important for basic scientific understanding and for operational fire weather forecasting and land management to know whether the insights from Chapter Four can be generalised to other events. This was the motivation for the research documented in Chapter Five, in which a synoptic climatology is undertaken of events that clearly showed an abrupt increase in fire danger, when conditions were already dangerous, and of events that lacked any such “spike” in fire danger (submitted to the AMS Journal of Applied Meteorology and Climatology).

Chapter Five investigates the synoptic structures associated with two distinct classes of fire weather events. The types were defined by analogy with those of Chapter Four, as those for which a distinct “spike” in the fire danger occurred following a period when dangerous fire weather conditions already existed, and those events lacking such a spike. Necessarily, high temporal resolution fire dangers were required to distinguish the classes of events, and the dataset described in Chapter Three was used for this purpose.

Composites of NCEP/NCAR reanalyses for each event type showed that there were important differences between the types. There was a weak but distinct channel of reduced relative humidity evident in vertical cross sections through the troposphere in the spike composite, lacking in the “normal” composite. Both sets of events featured approaching cold fronts, but surface and upper troughs for the spike events were more advanced eastward than for normal events. Most significantly, jet streaks were located closer to Tasmania in the spike composite, structured so as to facilitate air mass descent through the troposphere, and the associated upper trough was negatively tilted (the trough axis increased in longitude from south to north), which is uncommon, and often associated with severe weather on account of the strong vertical motions accompanying such structures. An examination from reanalysis data of other apparent spike events cited in the introduction to the chapter revealed a similar upper tropospheric structure in those cases. This structure can be resolved by numerical weather prediction models and provides a very useful indicator well in advance of an event for the potential for fire danger spikes to occur, allowing fire and land managers to better prepare for these very dangerous events. In addition, there is a statistically significant peak in the occurrence of spike events in the late spring to early summer, which accounts for a proportion (but by no means all) of the “springtime bump” early season fire danger peaks documented in Chapter Two.

Chapters Two to Five examine the current and recent past of fire danger and fire weather in Tasmania. It is demonstrated in Chapter Two that there have been changes in extremes, in particular, even over the relatively short period for which instrumental data are available.

It is a very natural and important question to ask what the future is likely to hold. Chapter Six attempts to address this question, using dynamically downscaled regional climate model data for the twenty-first century, from the Climate Futures for Tasmania project (CFT) (Corney et al., 2013).

GCM projections generally do not resolve Tasmania, so cannot be expected to provide useful guidance at the scale of the island, or smaller scales. Even the modelling of Pitman et al. (2007), at 50 km resolution, would not resolve regional differences across Tasmania. Carvalho et al. (2010) noted similar difficulties in projections for Portugal (at 93, 000 km² area only 50% larger than Tasmania). The future fire danger projections from CFT were (and, at the time of writing, still are) the highest resolution future fire danger data available for Tasmania, at a scale (approximately 10 km) that could resolve useful regional detail across the island.

CFT modelling extended from 1961-2100, providing a substantial baseline period against which to validate future projections. Chapter Six (Fox-Hughes et al., 2014a), published in the *International Journal of Wildland Fire*, shows that recent patterns of fire danger are well-replicated by a multi-model mean fire danger. While 99th percentile values of model FFDI are lower than those observed using Automatic Weather Station data, they increase from the north and west of Tasmania towards the south and east in a similar fashion as the AWS data, and regional increases in the Derwent and Tamar Valleys are well-represented in the model. An increase in fire danger is modelled across the state during the present century, at a greater rate in those areas already subject to higher fire danger, and there is a greater increase again in 99th percentile fire danger in comparison to mean values. This feature has also been observed (as documented in Chapter Two), increasing confidence in the validity of the results. Surface pressure patterns associated with modelled high fire danger closely resembled those observed, with a characteristic lee mesoscale low over far southeastern Tasmania on days of elevated fire danger around Hobart, for example (as described in e.g. Mills and Pendlebury (2003)). The frequency of such days occurring with elevated fire danger increased by the end of the century in the models. The fire season was modelled to become longer, with the most rapid seasonal changes projected for springtime, but little change in autumn. This change in seasonality is consistent with the observations from Chapter Two of an increase in springtime dangerous fire weather in recent decades in eastern and southeastern Tasmania. In summary, while some broadscale GCM modelling does not suggest increasing fire danger for Tasmania through the 21st century, higher resolution regional climate modelling suggests the opposite: there is an increase in fire

danger across Tasmania, with an acceleration towards the end of the century. The projected increase is similar to that documented in Moriondo et al. (2006), with fire danger increasing across a number of measures: cumulative FFDI, season length and extremity of events.

Having presented each research paper in the body of the thesis, the Conclusion reviews its outputs, how they relate to each other and their value, both scientifically and in application to operational meteorology and land management. It then concludes with a brief discussion of areas of potentially useful future research.

2: A Fire Danger Climatology for Tasmania

Abstract

Forest fire danger indices are calculated for a number of Tasmanian locations over an extended period. Significant features of the resulting climatology include: the existence of a springtime peak in fire danger in eastern and southeastern Tasmania (although with substantial interannual variability), an apparent trend of increased severity of southeast Tasmanian springtime fire weather events, and differences in diurnal behaviour between the elevated location examined and those at lower levels.

2.1 Introduction

Fire danger indices integrate a number of weather parameters to estimate the effect on fire activity of ambient weather conditions. Climatologies of fire danger assist fire and land management agencies to plan effectively, and permit assessment of trends and variability in space and time. Tasmania is relatively small in area, but encompasses a diverse range of environments, and it is frequently the case that considerable differences in fire danger are evident across the state at any one time. There may also be substantial variability within fire seasons, and between successive fire seasons. In particular, there is the perception within the Tasmanian fire management community of a “springtime bump”, a peak of fire danger activity early in the fire season.

In order to characterise variability in fire season severity objectively and determine the existence of a springtime secondary fire danger peak, a fire danger climatology for Tasmania has recently been constructed using digitised weather data from a number of locations around the state. Where the data history is sufficiently long, the climatology has been examined to highlight any apparent trends. In particular, characteristics of springtime data are examined, as there appear to be a recent increase in the number of springtime days on which dangerous fire weather occurs. A more gradual increase over time of seasonal fire danger percentiles is also apparent. Substantial differences in fire weather behaviour are highlighted by the climatology, particularly between low-level eastern and southeastern stations and those in the north and west of Tasmania. Also substantial diurnal differences occur between the high and low level stations examined.

Foley (1947) provided a comprehensive overview of the state of fire weather forecasting and fire management across Australia at the time, together with a summary of significant fire events over the preceding few decades. Luke and McArthur (1978) discuss in broad terms the fire history and climatology of Australia, with sections on each State and Territory. They note that, up to that time at least, the peak fire danger period for Tasmania falls in summer and autumn.

Many other authors have developed fire danger climatologies from observational data for a variety of subject areas and purposes, both in Australia and overseas. Australian studies include that of Vines (1974), who investigated interdecadal variability in the long-term rainfall patterns of southeastern Australia, noting that significant drought occurred roughly every 13 years, and that dangerous fire seasons were associated with these droughts. He does point out, however, that rigorous statistical analysis had not been conducted on this work to

ensure that the variability discussed was not an artefact of the filters used in manipulating the data. Williams and Karoly (1999) examined the occurrence of extreme fire danger in Australia (including Hobart as a location) in connection with the El Niño phenomenon, noting patterns of increased fire danger during El Niño events. Verdon et al. (2004) examined long-term records of weather data in New South Wales, arguing that the effect of El Niño on the likelihood of dangerous fire weather is modulated by the influence of the Interdecadal Pacific Oscillation. Recently, Lucas (2010) has constructed a high-quality fire danger climatology for Australia for use as a reference dataset, again including Hobart in the dataset. Smith (1998) focused on the vulnerability to fire of Hobart specifically, and addresses a number of factors, including weather, influencing the likelihood of fire occurrence. Long (2006) constructed a climatology of extreme fire weather days for Victoria, using synoptic weather observations from four weather stations around the state, and briefly analysed two events, including Ash Wednesday 1983.

Overseas studies of fire danger climatology have focussed chiefly on North America. Flannigan and Harrington (1988) analysed the statistical relationship between raw meteorological variables with the area burned on a monthly basis in Canada, finding that long rain-free periods and days of low relative humidity were best (although only moderately) correlated with monthly area burnt. Taking a slightly different approach, Brotak and Reifsnnyder (1977) examined the synoptic weather patterns associated with 52 major wildfires in the eastern United States, finding that most occurred near surface cold-frontal zones. More significantly, major fires tended to be associated with the passage of a dry trough at 500 hPa. Crimmins and Comrie (2005) examined the relationship between wildfire occurrence and longer-term climate (up to several years) in the arid southwest of the United States, arguing that fuel accumulation is a function of greater than average rainfall up to three years before fire occurrence.

2.2 Methods

The McArthur Mark V forest fire danger meter (McArthur, 1967) is used operationally by fire agencies and the Bureau of Meteorology throughout much of Australia, particularly the southeast to estimate the Forest Fire Danger Index (FFDI). Using synoptic weather observations from a number of Tasmanian stations, FFDI time series are calculated to highlight times of year, and times of day, at different locations when fire danger tends to peak, and to note any trends in FFDI occurrence. This climatology also enables areas of potential future

research to be identified.

A number of fire danger rating categories are defined from ranges of FFDI values. “Low” fire danger rating is assigned to values 0-4, “Moderate” 5-11, “High” 12-23, “Very High” 24-49 and “Extreme” to FFDI of 50 or more. In Tasmania, forecast Very High (VH) fire danger (FFDI ≥ 24) is generally used as the trigger for the issue of a fire weather warning by the Bureau of Meteorology. At a higher level of alert, the Tasmania Fire Service will usually, depending on a number of factors, consider imposing a Total Fire Ban when forecast fire dangers exceed Very High 38.

The Mark V McArthur FFDI is calculated as a function of observed temperature, humidity and windspeed, as well as a “drought factor” that combines the effects of soil moisture deficit and recent rainfall on fuel moisture. The meter was adapted to allow computer calculation (Noble et al., 1980) and more recently modified to ensure a smooth transition between fuel moisture categories (Griffiths, 1998, 1999). In Tasmania, for many years the Mount Soil Dryness Index (Mount, 1972) has been used as a ground moisture input (or indicator of longer term drying) to modulate the drought factor input to the fire danger index.

In this study the FFDI values were calculated from synoptic observations, generally available at three-hourly intervals. A standard 12.5 tonnes/hectare of available fuel was assumed. Drought factors were calculated using the method of Griffiths (1998), and were updated with each synoptic observation (reflecting the practice used in the Tasmanian fire weather forecast service).

The selection of stations is constrained by the availability of homogeneous time series. Locations included in the study are Hobart, Hobart Airport, Swansea, Launceston Airport, Strahan and Mt Wellington, and, depending on the station history, observations are available at differing numbers of times per day and over differing lengths of record. Figure 2.1 indicates the location of all stations. Throughout this paper times of observations are presented in Local Clock Time (LCT) to avoid any problems arising from the transition to and from Daylight Saving Time (as Tasmanian synoptic observations are made according to Local Clock Time). Daylight Saving Time was introduced in Tasmania in 1972, and operates generally between October-March. During this period, Local Clock Time changes from 10 hours ahead of UTC to 11 hours ahead of UTC.

Recently, digitisation of synoptic data for Hobart has been completed back to 1920. Prior to the 1940’s, synoptic observations were made at 0900, 1500 and 2100 LCT. After a period of some years of variation during the mid-1940’s, in 1947 the observation schedule settled to include 0600, 1200, and 1800 in addition to the earlier times. Variations since then have

occurred only in the overnight observations (0000 and 0300 added in 1970). As has been the case with many sites, changes have occurred in the area of the Hobart City observation site since 1920. In particular, in 1967 a new Bureau of Meteorology Regional Office was constructed close to the observation enclosure, and in 1994 an Automatic Weather Station (AWS) was installed. At this time, the anemometer mast was moved further away from the Regional Office building, and elevated by three metres to increase the exposure to winds from the west and south previously somewhat sheltered by the 1967 building.

Digitised synoptic observations every three hours are available for Launceston and Hobart Airports from 1 January 1960. Twice daily observations at 0900 and 1500 LCT are stored for Swansea, on the central east coast, from the same start date. At these sites, there have been fewer disturbances from nearby construction than at the Hobart City site. However, instrumental changes have occurred on occasion, and at the airport sites AWS were installed in 1990 (Hobart) and 1992 (Launceston). At Swansea, wind was estimated using the Beaufort scale until 1992, when a Dwyer anemometer was installed. This in turn was removed in 1998, and estimation of wind speed recommenced.

Synoptic observations from the AWS sited on the summit of Mt Wellington, at 1260m above sea level, are available from April 1994, but are not reliable until 1995. The FFDI values calculated from this site are of interest for several reasons. They are the only observations from a significantly elevated site in the study, and provide a point of comparison to data from the remaining stations, despite a shorter period of record than those data. Proportionally, more of Tasmania lies above 1000m than is the case for any other Australian state, but little study has been made of different fire danger regimes pertaining to those elevated areas. Finally, the data might usefully supplement the HIGHFIRE¹ study of alpine fire occurrence being conducted as part of the work of the Australian Bushfire Co-Operative Research Centre, being from a more southerly location than any currently under consideration within that project.

Choosing a suitable site representative of the west coast of Tasmania is somewhat problematic. Synoptic observations are available at 0900 LCT and 1500 LCT for Strathgordon from 1957, but the site is quite sheltered from the dominant westerly quarter winds. Strahan Airport observation site was opened in 1976, but there are large gaps in the record prior to October 1987, so so data was examined from this time. There are still a number of minor gaps in the record used, however.

The limited time periods available for Strahan and Mt Wellington do not permit any

¹ <http://www.bushfirecrc.com/research/highfire/highfire.html>

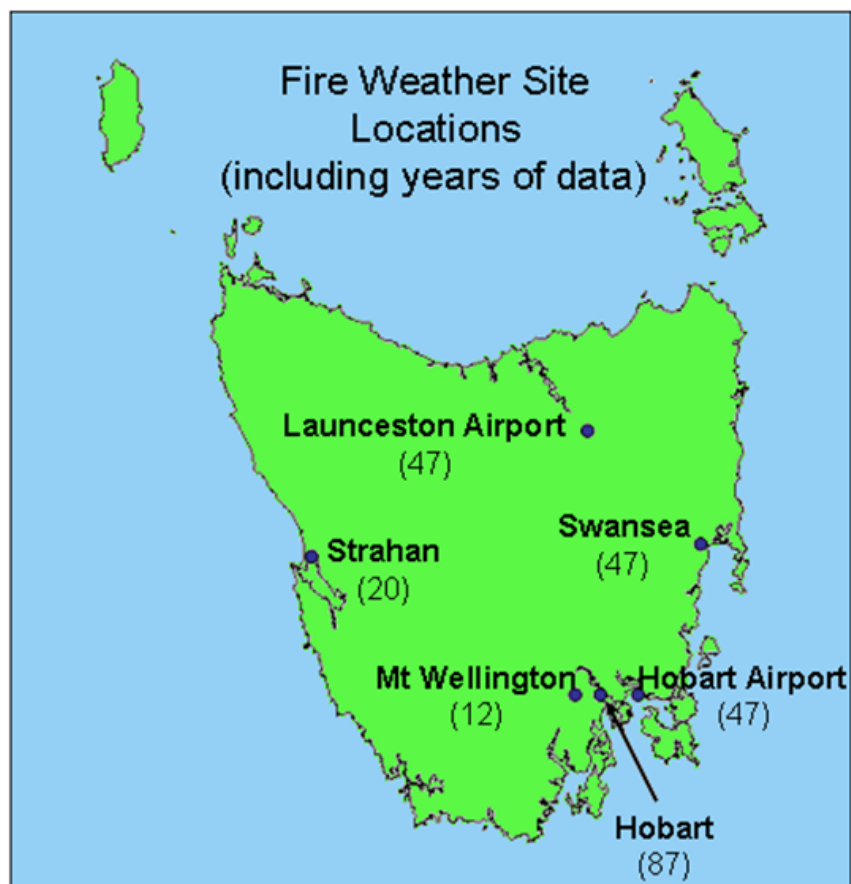


Figure 2.1: Location of stations used to derive climatology. Length in years of the data history used at each station is included in brackets.

Site	Dates available	Comment
Hobart City	1/1/1920- 20/4/1947	0900, 1500 and 2100, with additional observations from 1/1/1944
	21/4/1947 – 31/12/1969	0600 – 2100, 3 hourly
	1/1/1970 – 30/4/2007	Full 3 hourly synoptic programme
Hobart Airport	1/1/1960 – 30/4/2007	Full 3 hourly synoptic programme
Launceston Airport	1/1/1960 – 30/4/2007	Full 3 hourly synoptic programme
Swansea	1/1/1960 – 30/4/2007	0900 and 1500 synoptic observations
Strahan Airport	20/10/1987 – 30/4/2007	Full 3 hourly synoptic programme – but some observations missing
Mt Wellington	30/4/1995 – 30/4/2007	Full 3 hourly synoptic programme

Table 2.1: Summary of the availability of synoptic observations from studied stations.

consideration of trends in fire weather, but the longer records from the other stations do. Table 2.1 summarises the data availability for each station in this analysis. Occasional periods of observations from stations at non-standard synoptic times were not included in the dataset.

2.3 Results

Discussion of the fire danger characteristics of the study stations is grouped into low-level southeastern and eastern stations: Hobart (elevation 51 m above sea level), Hobart Airport (e. 4 m) and Swansea (el. 10.5 m), northern and western stations: Launceston Airport (el. 170 m) and Strahan (el. 20 m) and Mt Wellington (el. 1260 m), as broadly similar characteristics are evident within each such grouping.

2.3.1 Hobart, Hobart City and Swansea

Data for Hobart City are of particular interest given the long record available, despite changes during the record in both observation times and instrumentation. Figure 2.2 shows plots of the peak FFDI recorded and the number of VH FFDI recorded at 1500 LCT in a fire season, where a fire season is named by the first year of a period 1 July – 30 June of the following year. Only 1500 LCT observations were used in this presentation to avoid distortions resulting from changes in the number of observations made per day across the observing history. Very High fire danger is used here and throughout this study not only as a convenient indicator of potentially dangerous fire weather but also because it is, as noted above, the fire danger level at which a fire weather warning is usually issued in Tasmania, and so has substantial operational significance.

Considerable interannual variability is evident in the series of both peak FFDI and sea-

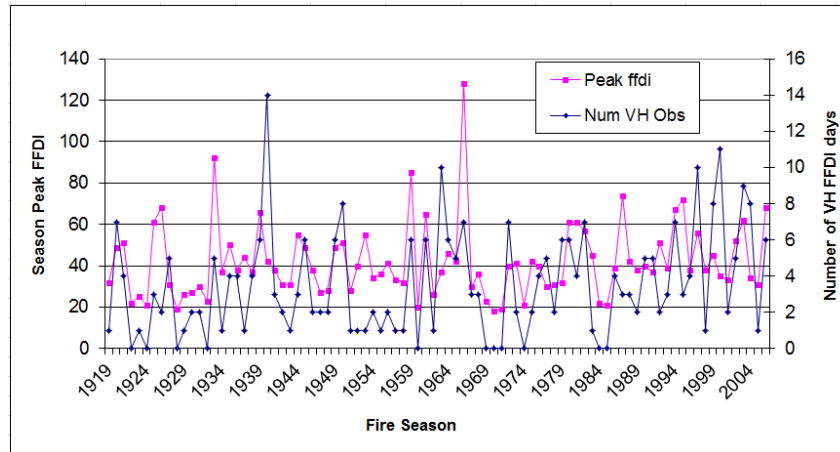


Figure 2.2: Plot of fire season activity 1919-2006 for Hobart City, based on 1500 LCT synoptic observations. Seasonal peak FFDI values are plotted in pink, the number of VH FFDI observations per season are plotted in blue.

sonal count of VH FFDI (Figure 2.2), and it is rare for there to be more than a few consecutive seasons of either low or high fire weather activity, as measured by either indicator shown.

There are notable differences between the two measures of seasonal severity. For example, the 1940-41 fire season was the worst of the series by a considerable margin in terms of the number (14) of days of VH FFDI (recalling that these are days when VH FFDI was observed at 1500 LCT), yet the peak seasonal FFDI was a relatively modest 42. On the other hand, the peak FFDI for the 1966-67 season and for the series as a whole was 128. This occurred on 7 February 1967, “Black Tuesday”, when 62 people were killed and 1,446 major buildings were destroyed (Bond et al. 1967). The number of VH FFDI days that season was 7, in the top quartile of seasons but not reflective of the extremity of the FFDI on 7 February 1967.

These differences are certainly at least partly a consequence of the fact that only 1500 LCT observations were used to construct this graph. As will be demonstrated later, significant fire danger peaks may occur at other times during the day. There are occasions when a sharp peak of fire danger occurs between synoptic observations, evident from an examination of more frequent observations (which are, however, only readily available since AWS have been introduced during the last 10-15 years).

The second most extreme outlier in the series of peak FFDI occurred during the 1933-34 season, with a value of 92. On 9 February 1934, “Black Friday”, fires in the Florentine and Derwent Valleys caused some life and property losses.

Of the top 8 seasons by number of VH FFDI days, when 8 or more days of VH FFDI were recorded, 5 have occurred since 1997. On the other hand, of the 26% of seasons with

peak FFDI > 50 , only 4 or 17% have occurred since 1997.

As noted above, observation times stabilised at three hourly intervals between 0600 and 2100 LCT by 19 April 1947. Observations at 0000 and 0300 were added from 1 January 1970 although, as might be expected, these latter times do not figure prominently in the record of VH FFDI observations. The additional observations permit at least a degree of resolution of the time of day at which peak FFDI occurs. A decomposition of VH FFDI occurrence by month and hour of the day is displayed in Table 2.2(a). Also displayed, in bold, are the number of occasions when the FFDI reached or exceeded 40, close to the level at which a Total Fire Ban is usually declared in Tasmania.

Table 2.2(a) indicates that VH FFDI has occurred in Hobart at all synoptic times, and during every month. It is, however, rare for Very High fire danger to occur between May – August inclusive, and unusual in September and April. Similarly it is rare between 0000 and 0600, and unusual at 0900 or 2100. Considering the smaller number of 0000 and 0300 observations compared to those at 0600, there is a suggestion that there is a higher frequency of VH FFDI at the earlier times than at 0600, although the numbers in each case a quite low. There is a rapid increase in the number of VH observations in October, a plateau in November then a further increase to a January peak. The number of observations falls to October-November levels in March, before a very substantial decline in April.

Peak time of the day for VH FFDI is 1500, as might be expected, but almost as many observations occur when 1200 and 1800 are combined. A separate database query indicates that there were 89 days in the 1947-2007 record where VH FFDI was recorded, but not at 1500, compared with 223 days during that period where VH FFDI was recorded at 1500. Thus, examination of the 1500 LCT record alone is likely to miss a substantial fraction (40%, in the Hobart data above) of the occurrences of VH FFDI in a 3-hourly time series, and it is highly likely some events would occur between the 3-hourly synoptic observations.

An illustrative example of such a day, and the one with the highest non-1500 FFDI, is 24 January 1990, which recorded a peak FFDI (based on synoptic observations) at Hobart of 60 at 1200. By 1500 a cool southeasterly change had pushed through the observation site, and the FFDI had fallen to 3.

Examination of the events where FFDI reached the more significantly dangerous level of 40 reveals that this has only occurred between October–March and, with two exceptions at 0900, between 1200 and 1800 LCT. It is perhaps noteworthy that there are as many 1200 LCT occurrences of VH40+ as 1500 occurrences during October- December, but significantly fewer during January-February.

Hour	Month											Total	
	7	8	9	10	11	12	1	2	3	4	5		6
0			1	1		2		1	1				6
300			1	1				2	1				5
600			1	2			2	1					6
900				3		6	5	1			2		17
				1		1							2
1200	1		8	11	13	28	30	18	8	2			119
				4	4	10	4	5					27
1500		1	9	26	27	33	45	40	33	9			223
				3	5	10	12	11	7				48
1800				9	12	11	19	26	9	1		2	89
				2	3	2	4	5					16
2100		1		1	1	3	2	3	3			1	15
Total	1	2	20	54	53	83	103	92	55	12	2	3	
				10	12	23	20	21	7				

(a) Hobart City VH FFDI month by hour 1947-2007.

Hour	Month											Total	
	7	8	9	10	11	12	1	2	3	4	5		6
0			1	1		1		3					6
300					1			1					2
600			1					1					2
900				4	1	3	1	2	1	1	1		14
								1					1
1200	1	1	6	14	21	34	38	18	13	6	1		153
			1	3	3	6	11	6	1				31
1500		1	6	28	31	39	51	46	31	7	1		241
			2	3	10	10	9	13	7				54
1800			1	8	16	21	29	30	9				114
				3	3	4	5	8					23
2100				1	3	1	2	1	1				9
Total	1	2	15	56	73	99	121	102	55	14	3		
			3	9	16	20	25	28	8				

(b) Hobart Airport VH FFDI month by hour 1960-2007.

Hour	Month						Total
	10	11	12	1	2	3	
1200			2	9	11	7	33
1500	1	4	25	52	36	11	129
			1	1	3	5	11
1800			1	10	27	4	55
Total	1	7	44	90	56	19	
			1	1	3	5	1

(c) Launceston Airport VH FFDI month by hour 1960-2007.

Table 2.2: Crosstabulations month by hour of Very High forest fire danger index for Hobart City and Airport and Launceston Airport. Because Swansea reported only at 0900 and 1500 LCT, its FFDI distribution is plotted separately. Data is presented July-June, to group peak months together in the centre of the table.

Hour	Month					Total
	11	12	1	2	3	
0				1		1
300				1		1
				1		1
600				1		1
900		1		1	1	3
1200	1	4	1	4	1	11
				1	1	2
1500	1	2	2	3	1	9
				1		1
1800		1	2			3
Total	2	8	5	11	3	
				3	1	

(a) Strahan Airport VH FFDI month by hour 1987-2007.

(e) Mt Wellington VH FFDI month by hour 1995-2007.

Hour	Month								Total	
	8	9	10	11	12	1	2	3		5
0			1							1
300	1		1			1	1		1	5
600			1	2	1	2	4	1	1	12
							1			1
900		1	1	1	2	1	2	2		10
			1				1			2
1200			1			1				2
			1							1
1500			1	3						4
			1							1
1800				1	1	1				3
2100	1		1							2
Total	2	1	7	7	4	6	7	3	2	
			3				2			

(b) Mt Wellington VH FFDI month by hour 1995-2007.

Table 2.3: As for 2.2 for Strahan Airport and Mt Wellington.

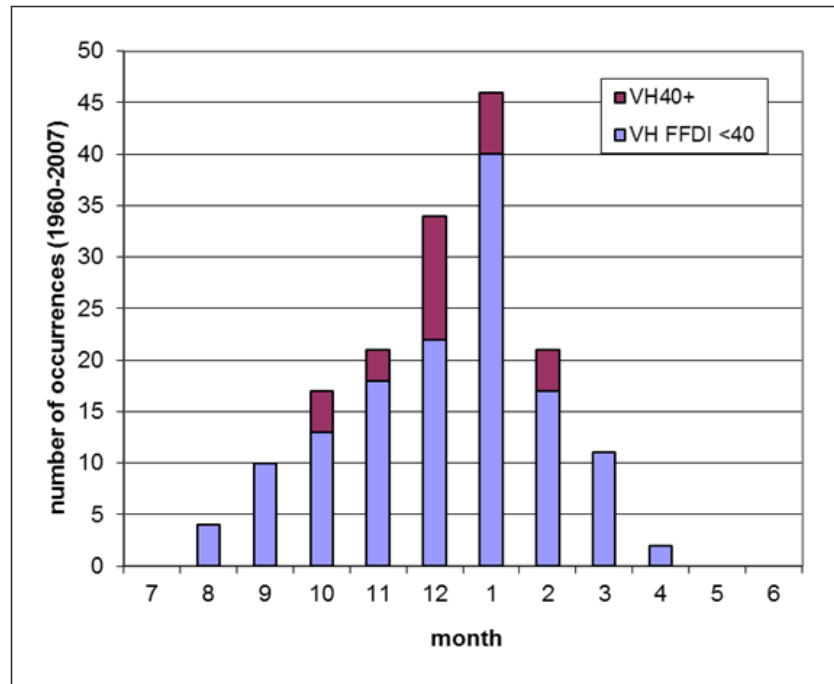


Figure 2.3: Monthly distribution of Very High FFDI at Swansea. Purple represents occurrences of fire danger index values between 24-39, while dark red indicates occurrences of index values of 40 or more.

Data for Hobart Airport are both more uniformly available (digitised observations at all synoptic hours from 1 Jan 1960) and less prone to the effects of changes in the local environment than is the case with the Hobart City record. The record does not, of course, extend back as far as that of Hobart City. While the two sites are quite close (approximately 20 km apart), it is useful to examine Hobart Airport data as a check on that of Hobart City, particularly in respect of trends in the data.

As with Hobart City, VH FFDI at Hobart Airport (Table 2.2(b)) has occurred at all synoptic times and every month (except, here, in June). The peak month, by the number of VH observations is January, and there is a steady increase over the previous months, without any evidence of the plateau seen in the Hobart City data. There is a rapid decline from March into April. A 1500 LCT peak is clear in the time of most frequent VH FFDI observation, but it is less marked relative to the times either side than is the case at Hobart City (representing slightly less than half of the 1200-1800 VH FFDI occurrences).

At the VH40+ level, there is a very slightly broader set of months and times than at Hobart City. Also, 1200 LCT VH40+ FFDI is as frequent as 1500 only during October. November and December have a clear 1500 LCT peak.

Data are available for Swansea from 1 January 1960, but include only 0900 and 1500 LCT observations. Nonetheless, it is possible to examine seasonal features and indications

of any possible trends over the period of available record. This is done in the form of a graph of seasonal variation, rather than in tabular format, as is the case with the other stations, because most VH observations at this station occurred at 1500. Figure 2.3 displays this monthly distribution of VH FFDI for Swansea. Purple bars indicate occurrences of Very High 24-39 and the dark red indicates those reaching or exceeding 40. No discrimination is made of the time of day of the observations, however only 13 occurred at 0900. Interestingly, 7 of these occurred during spring, a disproportionately high number. The highest FFDI value, 58, was recorded at 0900 on 12 October 2006 during an event which, as noted elsewhere will be the subject of further study.

Figure 2.3 indicates a steady increase in the number of VH FFDI events at Swansea into a strong January peak, then a more rapid decline into April. No events have occurred in May-August during the period of available observations. The distribution of VH 40+ events is limited to October-February, peaking in December. There is the suggestion of a plateau early in the season, with approximately the same number of observations in November as October. However, this represents at best a weak signal.

2.3.2 Launceston Airport and Strahan

The distribution of VH FFDI at Launceston Airport by month and synoptic hour is substantially different to the eastern and southeastern stations, as indicated in Table 2.2(c). VH FFDI is confined to the months of October-March (although only one October event has occurred in the record) and the afternoon hours of 1200-1800. There is a very steep increase from November to a pronounced January peak, with values falling away less abruptly through February-March. Only 1500 LCT observations between November-March have recorded VH 40+ FFDI, with a small February peak of only five occurrences.

The monthly distribution of FFDI for Strahan, on Tasmania's west coast, is similar to that for Launceston Airport, as evident in Table 2.3(a). Data for Strahan are available only from October 1987, less than half the period of record of Hobart and Launceston Airports. VH FFDI occurs only during the period November-March with a peak in February. The total number of such observations is very substantially lower than is the case for Launceston, even allowing for the longer record of that station. Peak time of day for VH FFDI is 1200. The observations of VH FFDI (including one of VH 40) between 0000 and 0600 LCT all occurred during one event, on 21 February 2001, ahead of the passage of a trough associated with a cool change. The majority of VH FFDI occurs either at 1200 or 1500. Only 4 VH 40+ events occurred in the record, three in February and one in March. Two of the VH 40+

events occurred at 1200, suggesting that a mid-afternoon fire danger peak is not as strongly favoured on the west coast as at other low-lying areas.

2.3.3 Mt Wellington

As indicated in Figure 2.1, Mt Wellington lies in southeast Tasmania. The AWS is located near the summit, at an elevation of 1260 m above sea level and represents a very different environment to any of the other stations examined.

Table 2.3(b) lists occurrences of VH FFDI and VH 40+ FFDI in the same format as earlier tables. VH FFDI has occurred during most months in spring through autumn, but only rarely in March through May and in September. While the length of record is only 12 years, there is the suggestion of peaks of VH FFDI in October-November and January-February.

VH FFDI has occurred at every synoptic hour, but with a peak at 0600 and 0900. This peak, in particular is substantially different to that observed at lower level stations. It is likely that the diurnal peak of fire danger occurs as an inversion develops or descends overnight to below the level of the AWS, allowing upper level dry air to reach the summit and upper slopes of Mt. Wellington (but not low elevations, in general). Windspeed above the inversion increases ahead of a cool change later in the day, and the FFDI increases also. As the inversion begins to erode as a result of the approaching change and thermal mixing during the day, the dewpoint temperature at the AWS increases (via mixing from lower levels) and the FFDI falls.

Five instances of VH 40+ FFDI are indicated in Table 2.2(e). These occurred in only two events: 21 February 2001 and 12 October 2006. It is worth noting also that all but one of the October instances of VH FFDI occurred between 2100 11 and 0600 12 October 2006.

2.3.4 Springtime fire danger

As noted above, there is a perception of a “spring bump” or peak in the fire danger during springtime within the fire management community in Tasmania. The above data do not seem to support this perception other than the plateau in the number of occurrences of VH FFDI in the statistics for October and November at Hobart. A closer examination of springtime FFDI data is useful to clarify the origin of this idea.

A springtime fire danger peak is defined here as a period in which the October peak monthly FFDI exceeded that of November by at least (arbitrarily) 10, or the November peak

exceeded that of December by the same amount. Identification of months satisfying either of these criteria is relatively simply automated, and the criteria quantify the intuitive idea of a “bump” as a period in which the FFDI is enhanced, followed by a quieter interval prior to the “main” fire season peak. Only observations after April 1947 are used. Examination of Table 2.4(a) reveals that of the 25 local peaks recorded, 10 occurred at either 1200 or 1800 LCT (and this excludes instances in 1993 and 1997 where the same peak value occurred at 1800 LCT, in addition to the documented 1500 LCT value). It was for this reason that data earlier than 1947 were excluded from the analysis, as the lack of non-1500 data was felt likely to distort the actual number of springtime season peaks recorded.

Of the 60 seasons’ data, 25 display an October or November peak monthly FFDI that exceeds (by at least 10) that of the following month. It can reasonably be said, then, that a “springtime bump” has occurred slightly less frequently than one in every two years at Hobart in the last 60 years. There is no obvious trend in the frequency, except that springtime peaks were relatively less frequent in the 1950’s, 1970’s and 1980’s, and more frequent in the 1960’s (every season between 1961-68) and since 2000. Seasonal peak FFDI values that occurred during spring are noted in Table 2.4 highlighted in bold (i.e. in addition to being local maxima, exceeding the peak FFDI of the following month, the highlighted observations are peak values for the entire season in which they occurred). There are 12 fire seasons in which the seasonal peak FFDI occurred during springtime, 20% of the total.

A similar analysis was conducted to test the occurrence of a springtime FFDI peak at Hobart Airport. Table 2.4(b) displays data in the same fashion as Table 2.4(a), but for Hobart Airport. Some 21 of the last 47 seasons (45%) show a springtime local VH FFDI peak (with a peak defined as before). Of the 21 occurrences listed, 10 represent the peak FFDI recorded during the corresponding season. Thus, 21% of seasons had a springtime FFDI peak as the season overall peak. These are very similar statistics to those noted at Hobart City, and increase confidence in the validity of the observations.

At Swansea, springtime peak VH FFDI have occurred in 10 of the 47 seasons 1960-2007. Table 2.4 indicates these, with the same derivation used as earlier. Again, seasonal peak FFDI are highlighted. Fewer seasons are listed or highlighted than was the case at either Hobart or Hobart Airport, suggesting a weaker “springtime bump” effect than is the case in southeast Tasmania. Approximately the same proportion of springtime peaks, however, one in two, was a seasonal peak as in the case of both Hobart sites.

There is no evidence of a significant springtime peak in FFDI either at Launceston Airport or Strahan, as can be seen from Table 2.2. Interestingly, however, the November

Season	Peak FFDI	Datetime (LCT)	Season	Peak FFDI	Datetime (LCT)
1951	25	02/11/1951 1800	1961	49	14/11/1961 1500
1959	52	21/11/1959 1200	1964	31	30/11/1964 1500
1961	65	14/11/1961 1500	1966	61	23/11/1966 1200
1962	50	17/11/1962 1200	1967	38	27/10/1967 1500
1963	43	18/10/1963 1200	1968	41	16/10/1968 1200
1964	33	30/11/1964 1500	1972	25	19/10/1972 1500
1965	37	13/10/1965 1500	1972	25	24/10/1972 1500
1966	45	23/11/1966 1200	1979	36	31/10/1979 1500
1967	30	27/10/1967 1500	1981	33	06/10/1981 1200
1968	24	16/10/1968 1200	1982	105	06/11/1982 1500
1972	39	19/10/1972 1500	1985	28	13/11/1985 1500
1978	31	02/10/1978 1500	1988	47	13/11/1988 1500
1982	43	06/11/1982 1500	1990	36	13/11/1990 1800
1986	29	04/11/1986 1500	1991	43	25/11/1991 1500
1987	40	02/11/1987 1800	1995	33	17/10/1995 1500
1990	35	13/11/1990 1500	1996	80	25/11/1996 1500
1991	37	25/11/1991 1500	2000	48	5/10/2000 1500
1993	33	26/11/1993 1500	2002	79	7/11/2002 1800
1995	72	17/10/1995 1500	2003	69	15/11/2003 1500
1997	46	22/11/1997 1500	2004	39	18/11/2004 1200
2000	35	05/10/2000 1500	2006	126	12/10/2006 1200
2002	72	07/11/2002 1800			
2003	51	15/11/2003 1500			
2004	46	18/11/2004 1200			
2006	74	12/10/2006 1200			

(a) Hobart City

(b) Hobart Airport

Season	Peak FFDI	Datetime (LCT)
1964	24	25/11/1964 1500
1965	33	24/10/1965 1500
1966	35	23/11/1966 1500
1968	88	28/10/1968 1500
1972	34	24/10/1972 1500
1977	40	9/11/1977 1500
1982	62	24/11/1982 1500
1990	31	13/11/1990 1500
2004	27	19/11/2004 1500
2006	82	12/10/2006 1500

(c) Swansea

Table 2.4: Occasions when a springtime (Oct-Nov) peak in fire danger occurred. Rows highlighted in bold are not only springtime peaks, but peak values of FFDI for the entire fire season.

VH 40+ event at Launceston Airport in Table 2.2(c) was the peak FFDI recorded in the 1982 season, with FFDI of 62 (the only Extreme FFDI in the Launceston Airport synoptic record), and the only springtime peak, as defined above.

The above analysis considered springtime peaks in terms of highest FFDI recorded, whether by month or season. Other metrics are possible, of course, including the number of VH FFDI observations recorded in any given month. A springtime peak is again evident when Hobart data is re-examined using this metric. While the details are not included here, the characteristics of the peak are very similar to those revealed using the definition applied in earlier paragraphs.

2.3.5 Springtime trends

While the frequency of springtime local peaks shows no obvious trend, there is a suggestion that springtime seasonal FFDI maxima are becoming more frequent in the case of both Hobart and Hobart Airport. Figure 2.4 displays the number of occasions, grouped by decade, since 1947 when VH FFDI in excess of 40 occurred during springtime at Hobart. There were 2 such occasions prior to 1947, both at 1500 LCT, but the lack of data at other synoptic times makes a direct comparison difficult.

Individual synoptic observations are used as the basis of the figure, so it is possible that more than one “event” was counted in any one day. As is evident from Table 2.2(a), there are no September events. The first month with more than one occurrence (not shown) is October 1995, with others in November of 1997 and 2002. Seven events occurred in October 2006, during 11-12 October, as noted above a period of exceptional fire weather.

Figure 2.4 indicates a strong increasing trend in the number of significant springtime fire weather events. As such, it is important to ensure that the trend is real, and not an artefact of instrumental changes at the site.

There have been a number of changes to the Hobart observation site during the course of its history. In particular, the installation of an AWS occurred in 1994, close to the time of rapid increase in the frequency of springtime VH40+ events. If the observed changes are driven solely by instrumental changes, a similar summer and autumn breakdown should reveal the same trend.

The autumn analysis is also displayed in Figure 2.4, and no obvious trend is evident. For the summer season (not shown), 32 of the 60 seasons since 1947 have at least one VH40+ event. Of these, 16 occur since 1980 (50% in the last 45% of the record), and 8 occur since 1995 (25% in the last 20% of the record). Thus, there is no significant trend evident in

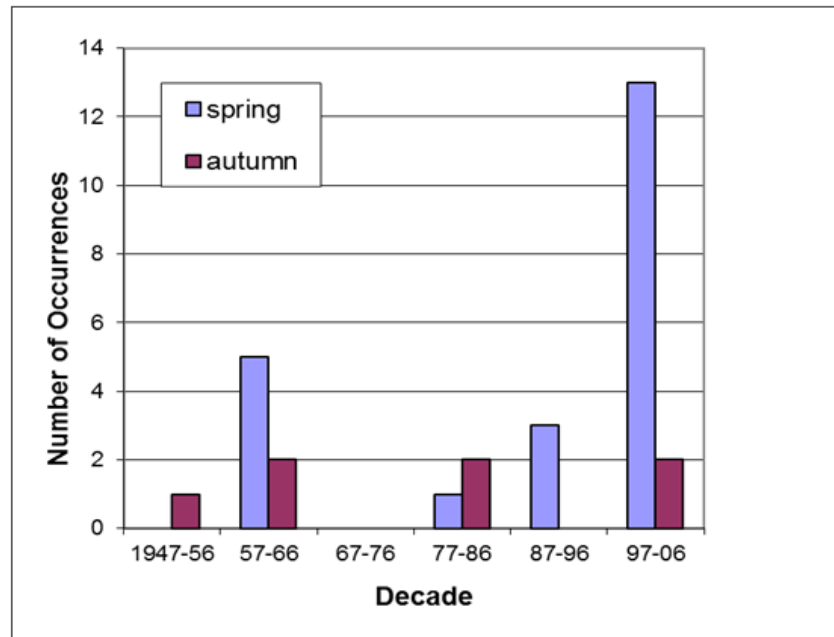


Figure 2.4: Decadal distribution 1947-2007 of spring and autumn occurrences of FFDI greater than or equal to 40 at Hobart.

the analysis of either the autumn or summer records, strongly suggesting that the observed trend on the springtime data is real, rather than being an artefact of the instrumental and environmental changes that have certainly occurred.

Springtime occurrences of VH40+ FFDI at Hobart Airport (not shown) reflect the trends evident at Hobart. Considering the data in terms of months during which at least one VH40+ event occurred (in order not to assign too much weight to the exceptional 11-12 October 2006 fire weather event which appears as six VH40+ occurrences at Hobart Airport), some 44% of such months have occurred in the last 26% (12 years) of the record, and a quarter have occurred since 2003 (last 9% of the record). Again, an examination of summer occurrences reveals no obvious trend in the data (not shown). There is, however, the suggestion of an increasing trend with the autumn data as all cases occur since 1991, although the small number of cases (6) limits the degree of confidence in this observation.

2.3.6 Station Fire Danger Percentiles

Determination of the relative frequencies of the highest FFDI values recorded at a location are important for characterising the nature of fire danger experienced there. For fire management purposes, it is also useful to have an indication of more routinely experienced fire danger levels. For this reason, Table 2.5, displaying fire danger percentiles, is included. The 50th, 75th, 90th, 95th and 99th percentiles for each of the stations examined above are calcu-

Site	Percentile				
	50	75	90	95	99
Hobart	4	7	11	14	26
Hobart Airport	5	9	13	18	31
Launceston Apt	4	8	12	15	23
Swansea	3	5	8	11	24
Strahan	1	3	5	7	15
Mt Wellington	1	2	4	6	15

Table 2.5: Fire danger percentiles for each of the stations studied. Percentiles evaluated from 0900-1800 LCT synoptic observations for the period October-March.

lated from the 0900-1800 synoptic observations for the period October-March, representing what is for most stations the most active times of the day during the most active time of the year. (Replacing 0900-1800 with 0300-1200 in the case of Mt. Wellington makes only a very slight difference to the outcome.) For Hobart City, the period over which the percentiles are calculated is April 1947 – April 2007. For the other stations, it is the entire record period as detailed in Table 2.1.

For Hobart, Hobart Airport and Launceston, the 50th percentile broadly represents the boundary between Low and Moderate FFDI, while for Swansea that occurs at the 75th percentile, and for Strahan and Mt Wellington around the 90th percentile. The 90th percentile at the first three stations is broadly the Moderate-High boundary of 11-12, which occurs at the 95th percentile for Swansea and (not shown) the 98th percentile for Strahan and Mt Wellington. The boundary between High and Very High FFDI (23-24) occurs around the 99th percentile for Hobart, Swansea and Launceston Airport, and (not shown) about the 98th percentile for Hobart Airport and at percentile 99.8 for both Strahan and Mt Wellington.

It is of interest to examine the possibility of trends in the fire danger observed at Tasmanian locations, in addition to the sharp trend in significant events evident in southeast Tasmania. Of the sites examined above, Hobart and Launceston Airports and Swansea have had relatively uniform site characteristics and observation schedules over an extended period, and their data were used to plot trends of fire danger over the periods of available record. The 3 plots have very similar characteristics so only Hobart Airport data are displayed, in Figure 2.5. The data used are the entire record of Hobart Airport, divided into fire seasons as discussed above, with percentiles of FFDI calculated for each season. Percentiles 95, 99 and 99.5 are plotted.

There does appear to be a slight increasing trend. Linear regression lines are superimposed on the each plot to indicate the trend. The slope of the regression line increases as the percentile examined increases: the slope of the 95th percentile regression line is 0.087, that

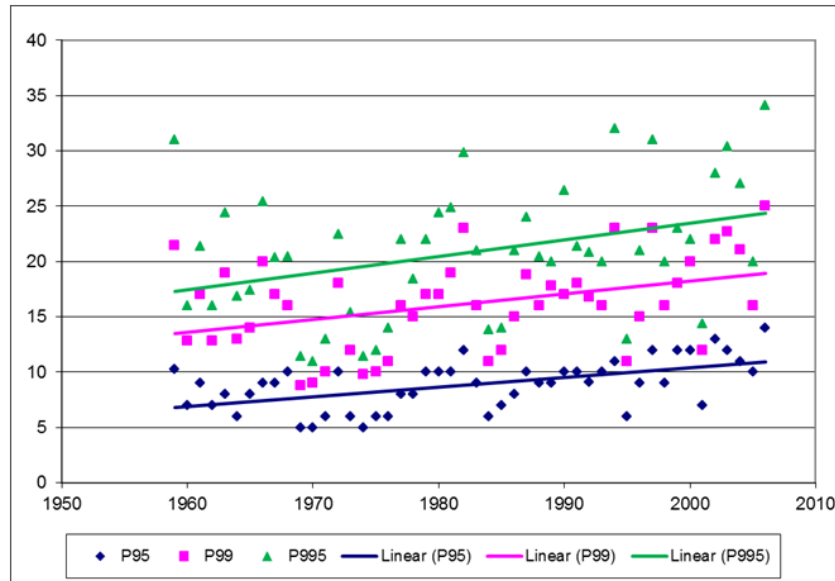


Figure 2.5: Plot of percentile values for each fire season 1960-2006 at Hobart Airport. The 95th percentile values are plotted in blue, 99th in pink and 99.5th in green. Linear regression lines are plotted in corresponding colours.

for the 99th percentile is 0.117 and for the 99.5th percentile is 0.151. As might be expected, the scatter of the plot also increases with increasing percentile. The correlation between year and 95th percentile FFDI is 0.544, while that for the 99.5th percentile decreases to 0.356. This suggests a steady slight increase in FFDI over time, and a greater increase in more extreme events. The data suggest a degree of interannual variability, increasing at the extremity of the distribution.

2.4 Discussion

The creation of a database of forest fire danger index values has enabled a useful ability to examine the variation in potential for fire activity in space and through time in Tasmania. Many of the results support anecdotal expectations, for example, the generally earlier onset during a fire season of potentially dangerous conditions in the south and east compared with the north and west of Tasmania.

The data also indicate the existence of a peak in fire danger during the spring in southeast Tasmania, and to a lesser extent on the east coast (but not in the north or west) in about one season in two. In about 20% of cases, this peak is the primary fire danger period of the season.

Differences in the diurnal behaviour of fire danger at low-lying and elevated sites are also evident in the data. The observed early morning peak in fire danger at high elevation has

important operational implications for fire managers, particularly in view of the relatively high proportion of Tasmania that lies in excess of 1000 metres above sea level. In such environments, the overnight and early morning period cannot necessarily be assumed to be a period of low activity, when fire crews can be stood down or rested ahead of an anticipated busier day.

It is possible that there is an element of diurnal forcing of summertime changes through southeast Tasmania, which is less strongly developed early in the fire season (see, e.g., the introduction to Mills (2002) for a discussion of models of the effect of the diurnal cycle on summertime cool changes). Thus, as noted above, there are as many 1200 LCT VH40+ peaks as 1500 LCT peaks at Hobart during the early part of the fire season. At this time, land-surface heating might be expected to play a less significant role in frontal development and movement. Conversely, there are fewer such 1200 peaks during January- February, when land-sea temperature contrast is greater. Similarly, the most common time of peak FFDI for Strahan is 1200 LCT.

The evidence for this argument is equivocal, however. There is no similar change in the peak time of FFDI for Hobart Airport during the course of a season, for example. This is an area which may repay additional study, potentially connecting historical data with recent advances in the understanding of the dynamics of summertime cool changes (e.g. Mills (2002)).

Available data suggest a broad increase in the fire dangers recorded in eastern Tasmania over the last several decades. In addition, there is evidence that the southeast in particular has seen an increase over the last decade in the number of dangerous springtime fire weather episodes. The events have occurred across a range of soil (and, by implication, fuel) moisture conditions, suggesting that it is the result not just of a general recent decline in springtime rainfall in southeast Tasmania, as indicated, for example, in Alexander et al. (2007). An examination of these events shows very low dewpoint temperatures to have occurred in many cases.

It is possible that changes in instrumentation and exposure over time could have some impact on these results. For example, Shepherd (1991) documented changes in the characteristics of the Hobart City observation site that would impact systematically on calculated fire dangers. Also, AWS were progressively installed in many locations over the last decade and a half. It is likely that the AWS sensors respond differently to very dry airmasses than do wet and dry bulb thermometers. Lucas et al. (2007) suggested that the inhomogeneities in measured humidity associated with the installation of an AWS are, however, relatively

small. On the other hand, changes in measured wind can be significant, particularly at higher wind speeds – generally, the range within which higher fire dangers occur.

Supporting the evidence for a real increase in the number of dangerous fire weather days in springtime is the fact that both Hobart and Hobart Airport show an increase during the mid-1990's despite the fact that an AWS was installed at Hobart Airport in 1990, and at Hobart City in 1994. Also, there has been no commensurate increase in the number of dangerous summer or autumn days, which might be expected if instrumental changes were responsible for the increased observation of very dry airmasses, or increased windiness. It is possible that these recent changes are the result of interdecadal variation rather than a broader climatic trend. From a fire management perspective, however, this is not as important as the fact that it represents a change from the experience of the relatively recent past, and may require a higher degree of preparedness earlier in the fire season than might otherwise be anticipated.

Again as noted in Alexander et al. (2007), the trends in percentile values are consistent with observations elsewhere, and with modelled global trends. In particular, the observed greater trend in more extreme values is consistent with those observed and modelled elsewhere.

Interestingly, Westerling et al. (2006) report a recent increase in western U.S. forest fire activity during spring, which they attribute to meteorological factors (rather than oft-cited land use changes). In the western U.S., however, the increase in fire activity is strongly correlated with increasing temperatures and earlier onset of spring snowmelt, factors which are not significant in southeast Tasmania.

Future research will examine several points noted above. The fire weather on and leading up to 12 October 2006 was exceptional and will be documented separately. More generally, the recent increase in springtime extreme fire danger will be examined, to highlight common features of the underlying weather and to identify any broadscale atmospheric features that might influence the changes.

2.5 Acknowledgements

Detailed reviews by Graham Mills, of the Bureau of Meteorology Research Centre, resulted in a considerable improvement in the clarity and focus of the paper.

A review by Steve Pendlebury, of the Tasmania and Antarctic Regional Office of the Bureau of Meteorology eliminated a number of remaining errors.

Ian Barnes-Keoghan, also of the Tasmania and Antarctic Regional Office of the Bureau of Meteorology, provided the script enabling calculation of data percentiles, and useful discussions on observational data integrity.

The Tasmanian Fire Research Fund partly underwrote the cost of completing the digitisation of the earlier Hobart City data included in this study.

3: Impact of more frequent observations on the understanding of Tasmanian fire danger

Abstract

Half-hourly airport weather observations have been used to construct high temporal resolution datasets of McArthur Mark V forest fire danger index (FFDI) values for three locations in Tasmania, enabling a more complete understanding of the range and diurnal variability of fire weather. Such an understanding is important for fire management and planning, to account for the possibility of weather-related fire flare-ups, in particular early in a day and during rapidly changing situations. In addition, climate studies have hitherto generally been able to access only daily or at best three-hourly weather data to generate fire weather index values. Comparison of FFDI values calculated from frequent (sub-hourly) observations with those derived from three-hourly synoptic observations suggests that large numbers of significant fire weather events are missed, even by a synoptic observation schedule, but particularly by observations made at 1500 local time only, suggesting that many climate studies may underestimate the frequencies of occurrence of fire weather events. At Hobart, in southeast Tasmania, only one half of diurnal FFDI peaks over a critical warning level occur at 1500 local time, with the remainder occurring across a broad range of times. The study reinforces a perception of pronounced differences in the character of fire weather across Tasmania, with differences in diurnal patterns of variability evident between locations, in addition to well-known differences in the ranges of peak values observed.

3.1 Introduction

Over much of the forested area of Australia, a forest fire danger index (FFDI) is calculated using the McArthur Mark V Forest Fire Danger meter (McArthur, 1967). McArthur noted that, depending on the density of forest cover, most eucalypt forests would achieve minimum fuel moisture (and therefore maximum capacity to sustain fire activity) during the early to mid-afternoon. In the case of many manual observation sites with records stretching over some decades, 0900 and 1500 Local Clock Time (LCT)¹ are the only times during the day at which readings were made. Of these, only the observations made at 1500 LCT generally provide observations representative of fire weather conditions during the day. McArthur (1967) indicated, and other researchers (Ryan, 1977, Tolhurst and Cheney, 1999, Beck et al., 2002) have felt, that, in most cases, surface heating has not been sufficient by 0900 LCT to allow mixing to the surface of air mass properties that will influence the day's fire weather conditions, in particular the moisture content of potential fuels.

While it is certainly useful for monitoring and fire weather warning purposes to indicate either forecast or observed conditions at a set time of the day, particularly when fire danger at that time is commonly high relative to other times, awareness of potential fire weather conditions at other times is critical for safe and effective fire control operations. When fire danger values are computed from all (eight 3-hourly) synoptic observations at sites for which a record is available throughout the day there is some evidence (Fox-Hughes, 2008) that peak fire danger frequently occurs at times of the day other than mid-afternoon.

A number of studies have examined the fire danger history at sites in Australia (Long, 2006, Fox-Hughes, 2008, Lucas, 2010, Santos et al., 2011), and some studies have linked fire weather behaviour to broadscale atmospheric and ocean processes such as ENSO (Williams and Karoly, 1999, Verdon et al., 2004). Many of these studies examine fire danger index values computed from weather parameters observed at 1500 LCT. It is widely recognised by these and other authors who have used 1500 LCT data, as the only available data, in fire weather climatological studies (Lucas, 2010) that FFDI may peak at times other than 1500 LCT. As a result, some potentially significant fire weather events are missed in such studies. Even when a full three-hourly synoptic dataset is considered, however, short-lived events may be missed (as discussed in Mills (2008b)). Here, "significant" is used for those

¹Times used throughout the analysis are Local Clock Time, to prevent any difficulties resulting from changeovers to and from Daylight Saving Time, which occurred in Tasmania every October and March during the period covered by this study. Local Clock Time is Australian Eastern Standard Time (ten hours ahead of UTC) outside of Daylight Saving Time, and eleven hours ahead of UTC during Daylight Saving Time.

events for which peak FFDI reaches at least 25 (Very High fire danger in the McArthur rating system), above which fire managers would not attempt a direct attack on a going fire.

With the increasing deployment of automatic weather stations (AWS) throughout Australia since the mid-1990's, hourly or half-hourly observations have become available from an increasing number of locations. This has demonstrated that, in certain conditions, short-period, large amplitude variations in FFDI can occur. The Climate Section, Tasmania and Antarctic Regional Office of the Australian Bureau of Meteorology, has digitised archived Tasmanian airport weather reports since October 1990. The length of the record is now such as to allow characteristics of these frequent observations to be determined, and to assess the impact of more frequent data on fire weather climates.

The current study aims to describe a more comprehensive fire danger climate at sites in Tasmania during periods of up to two decades, by computing fire danger indices from half-hourly airport AWS records. This task is of interest in its own right, allowing for example better planning by fire agencies. In addition, it can inform climate change studies that calculate future fire danger based on current and past levels of those quantities (e.g. Williams et al. (2001)). Many such studies make use of fire danger indices calculated from mid-afternoon weather observations. This is, of course, very reasonable as mid-afternoon is broadly regarded as the time of peak fire danger diurnally. In addition, many sites have very limited data available at other times, certainly over longer periods. This study aims to quantify the extent to which the assumption of a mid-afternoon fire peak is valid, at least in the Tasmanian context, and thereby to suggest the extent to which such climate studies have sampled the full range of fire weather behaviour of the studies' domains. Santos et al. (2011) are undertaking a similar study using Western Australian data.

3.2 Data/Method

FFDI values were calculated using observations of recent rainfall (in the form of a "drought factor"), temperature, dewpoint temperature and windspeed using the McArthur Mark V forest fire danger meter (McArthur, 1967), as encoded for numerical calculation by Noble et al. (1980). Drought factors were calculated using Soil Dryness Index values (Mount, 1972), using the modified drought factor calculation detailed in Griffiths (1999). The FFDI values resulting from these calculations are integers greater than or equal to zero. FFDI values have been grouped into categories for ease of public understanding and classification of fire risk, following McArthur (1967). The ratings used in Tasmania currently are: "Low-

Moderate” (LM, FFDI 0-11), “High” (H, 12-24), “Very High” (VH, 25-49), “Severe” (SEV 50-74), “Extreme” (EX, 75-99) and “Catastrophic” (CAT 100+).² In this paper, an additional distinction is made to highlight FFDI values that reach Very High 38, representing the upper extent of the Very High range, where fire weather warnings are issued by the Bureau of Meteorology in Tasmania and fire authorities declare a day of “Total Fire Ban”. A Total Fire Ban is a legally enforced prohibition by the Tasmania Fire Service (TFS) on the lighting of fires and restriction on other activities that might lead to an unintended fire ignition. Such a ban is generally imposed when the FFDI is forecast to exceed 38 at several locations. TFS reserves the right to declare a Total Fire Ban at other thresholds, however, depending on factors such as resource availability.

As noted above, digitised half-hourly or hourly AWS reports are available from a number of locations from October 1990 onward. Observations from Hobart, Launceston and Devonport Airports were chosen for examination in this study because all have a generally stable observation history with 24 hour observation coverage.

The locations of Hobart, Launceston and Devonport Airports are indicated in Figure 3.1. Devonport Airport is located on the central north coast of Tasmania, within approximately 500 metres of the coast, with Bass Strait to the north separating Tasmania from continental Australia. Launceston Airport lies at the southern end of the Tamar Valley, with Tasmania’s Central Plateau to the west and the northeast highlands to the east. Hobart Airport is in the southeast of the state, sheltered by the Wellington Range from the prevailing westerly winds that flow over Tasmania. To its immediate south lies Frederick Henry Bay, with Storm Bay and the Tasman Sea beyond.

Airport observations are recorded at routine intervals, in which case they are known for brevity in operations and in the remainder of this paper as “METARs”. Non-routine observations are recorded on the exceedence of criteria critical for aviation operations, in which case a “SPECT” is issued. Of the phenomena for which a METAR might be issued, only the occurrence of a wind gust is of relevance in this study. In particular, gusty winds are a feature of many days of dangerous fire weather. In the normal course of operations, the only occasions on which a scheduled METAR is not issued is when a SPECI has been issued within the preceding ten minutes. In addition, there are rules governing the frequency with which SPECI messages are issued.

The dates selected for analysis were those at each airport for which digitally archived

²Following the Victorian bushfire disaster of 7 February 2009, Australian fire authorities updated the classification of McArthur (1967) at the beginning of the 2009/10 fire season, largely to distinguish degrees of severity above FFDI 50.

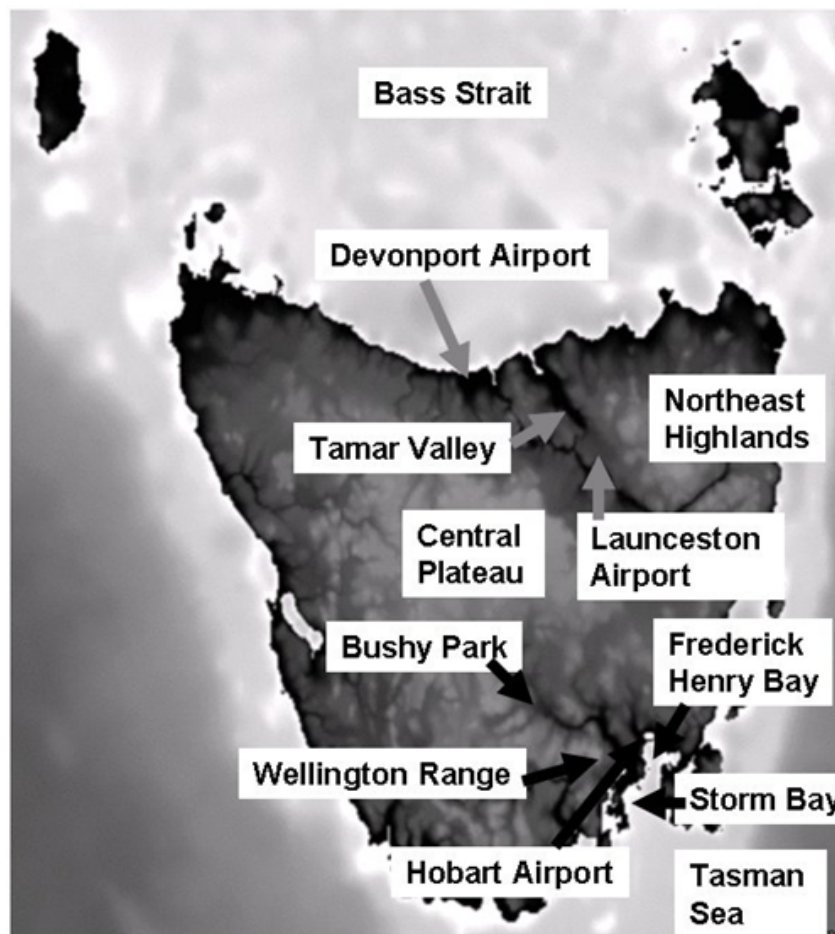


Figure 3.1: Map of Tasmania, showing locations and topographic details mentioned in the text. Lighter shading over land indicates higher topography.

routine half-hourly AWS observations were available. These are:

Hobart Airport: 2 October 1990 - 30 June 2010, uninterrupted for any prolonged period

Launceston Airport: 8 May 1992 – 29 July 2004 Devonport Airport: 21 July 1991 – 17 July

1998 and 19 October 2006 – 30 June 2010.

Thus, approximately 19 years of half-hourly data is available for Hobart Airport, and 12 years of data at the other two sites. Because the purpose of this paper is not a direct comparison between the three sites, it is not critical that the three sites have identical periods of data availability.

For the three airports, routine METARs are generated half-hourly, resulting in 48 METARs in a 24-hour period of normal operation. There may be many more SPECIs reported, particularly during windy days with frequent gusts. In order that such days are not over-represented in this analysis it is useful to employ at least one summary measure of the fire danger experienced during a day. For much of the following analysis, the peak FFDI reported between midnight and the following midnight is used as an indicator of the overall level of fire weather activity for a day. It is recognised that there are many other possibilities, and some of these alternatives are discussed later in the text. Briefly, alternatives to this measure include:

- Length of time that FFDI continuously exceeds a trigger value such as 24 or 50,
- Total time over a 24 hour period, or subset thereof, that FFDI exceeds a threshold value,
- An integration of the FFDI over 24 hours, or subset thereof.

Data were quality-controlled to remove occasional spurious observations that had slipped through the real-time quality checking. Observations which clearly exceeded climatological extremes or which were grossly inconsistent with those close in time were discarded. Thus, temperatures in the dataset that exceeded the record maximum temperature at each site were removed. Spikes in temperature or dewpoint that were clearly not associated with physical processes (such as frontal passages) were also removed, when detected. Such spikes and anomalous values frequently manifested as values 10 °Celsius or more different from those 30 minutes before or after. In addition, the count of observations per day was examined. It was deemed that there had been substantial problems with either the AWS itself or with communications on days for which fewer than 36 observations were stored. On this basis 145 days of observation were removed from the Hobart Airport dataset, 73 days' observations from Launceston Airport and 146 days' observations from Devonport Airport. Subsequent analysis was conducted on 349,421 observations on 7036 days for Hobart Airport, 212,332

observations on 4363 days for Launceston Airport and 183,195 observations on 3710 days for Devonport Airport.

Routine three-hourly synoptic reports from the same stations for the same time periods were also gathered. In most cases, these were a subset of the METAR/SPECI reports (except in events where a SPECI was reported within the ten minutes preceding a synoptic report and no routine METAR was then issued). In contrast to METAR/SPECI reports, only eight synoptic observations are made per day. Nonetheless, to allow as similar as possible a comparison between the two observation sets, maximum daily values of FFDI were also prepared for synoptic observations. It should be noted that maximum daily FFDI values computed from the (eight) synoptic observations are not the same quantity as FFDI computed solely from the 1500 LCT synoptic observation (as noted in the Introduction). To highlight this difference, and provide an indication of the degree to which studies using only 1500 LCT data may underestimate the true occurrence of fire weather events, the latter are included in this report. It is worth noting here that it is important to be aware of changes to and from Daylight Saving time when examining synoptic observations, hence the use of LCT in this report. It is less significant an issue for METAR reports, however, at hourly or half-hourly frequency.

While the three airports have enjoyed relative observational stability over the last two decades, some changes have occurred. An AWS was installed at Hobart Airport in April 1990. This was shortly prior to the period for which digitally archived data are available, and does not, therefore, affect the data examined here. Similarly, Devonport Airport AWS was installed in December 1990, prior to the commencement of half-hourly METAR reports.

An AWS was installed at Launceston Airport on 19 May 1992. In addition, the observation site at Launceston Airport was moved in July 2004, in response to increased security provisions, although the old site was maintained for several years at a reduced reporting frequency, for comparison purposes. The latter change at Launceston Airport is the more fundamental. Although the broad environment remained the same, the observation site was moved approximately 1350 metres to the south-southeast and half a metre higher in elevation, which affected the microclimate to some extent. A comparison of the available monthly summary data from the two sites reveals that the new station is slightly warmer during the day and colder at night than the old site (by fractions of a degree Celcius), and that it receives a little less rainfall – during 2007, for example, the old station received 541.2 mm compared to the new station's 471.8 mm. Both windspeed and dewpoint temperature are, on average, fractionally higher at the new site. It is acknowledged, however, that the period

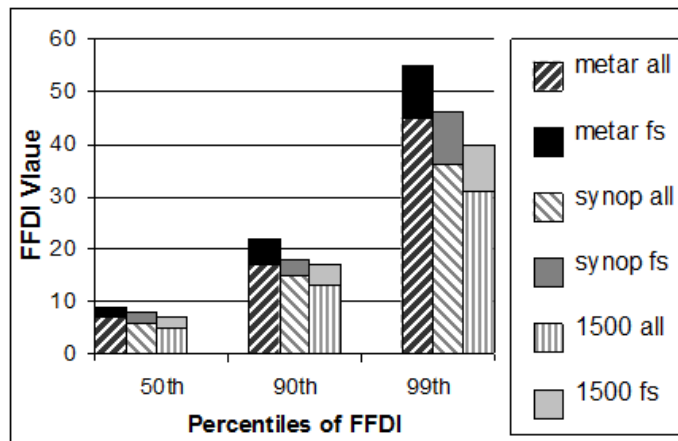
of overlap for the two Launceston Airport sites is relatively short, and any conclusions regarding differences between them are tentative. The dataset used in this study, however, has been restricted to the old site, for the period during which half-hourly reports are available, in order to rule out any possible effects of the site change on the results of this study.

3.3 Results

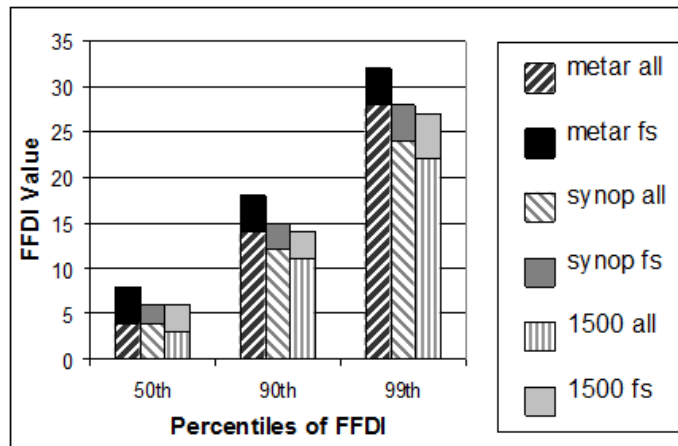
3.3.1 Broad comparison of METAR and synoptic observation datasets

Percentile values of FFDI are presented in Figure 3.2 for each station for both synoptic observations and METAR reports, based on maximum daily FFDI, in stacked, clustered columns. Several indicative percentiles (50th, 90th and 99th) are given in each case, using all data. Percentiles calculated for the period October-March within each dataset time period are indicated by an incremental increase on each column. Thus, for example, the 90th percentile of daily maximum FFDI computed for METAR observations at Hobart Airport throughout the year is 17, while the 90th percentile of METAR observations for the same site during October-March is 22. October through March is generally regarded as the peak fire weather period (the “fire season”), although occasional fire weather events do occur in September or April. In addition, percentile values of the FFDI measured at 1500 LCT values are included for comparison. A number of results are clear from Figure 3.2. For all stations, and for all percentile values, the METAR value for a percentile exceeds that for synoptic observations. Further, percentiles calculated from METAR and most synoptic observation values exceed those for 1500 LCT (synoptic) observations only. This is the case whether the whole year is considered or only the (nominally October-March) fire season. These summary statistics confirm that consideration of 1500 LCT data alone will underestimate the level of fire danger experienced at a site. Similarly, consideration of only synoptic observation data will also underestimate the true level of FFDI at a site. In particular, for higher percentile values the gap between METAR, all synoptic observations and solely 1500 LCT observations tends to widen, especially during the fire season. Thus, the more dangerous the fire weather, the more synoptic observations and 1500 LCT-only observations underestimate the true situation. However, the manner in which this difference increases with FFDI (or percentile of FFDI) has not been investigated.

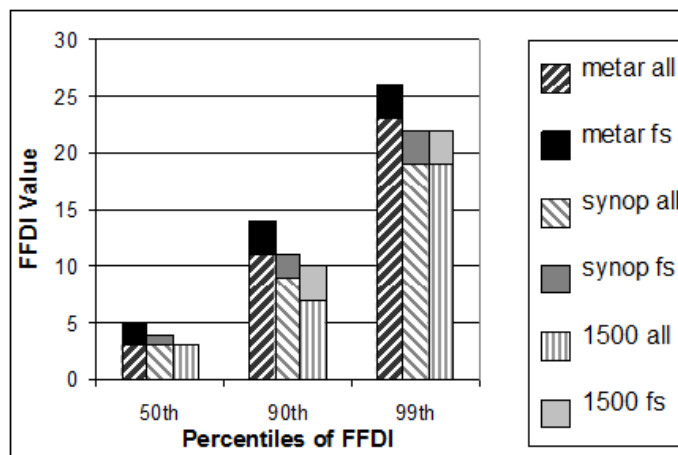
Figure 3.3 shows the number of days per year (July to the following June) on which the maximum FFDI was at least 25, for both METARs and synoptic observations at Hobart



(a)



(b)



(c)

Figure 3.2: Stacked clustered column plots of 50th, 90th and 99th percentiles of Forest Fire Danger Index values recorded at (a) Hobart Airport (b) Launceston Airport and (c) Devonport Airport of each of METAR reports, synoptic reports and 1500 LCT reports. Each column is split into the percentile obtained using all data for the year (“all” in the figure legend), capped with the increment obtained when the period considered is restricted to the usual fire season months of October through March of the following year (“fs” in the legend).

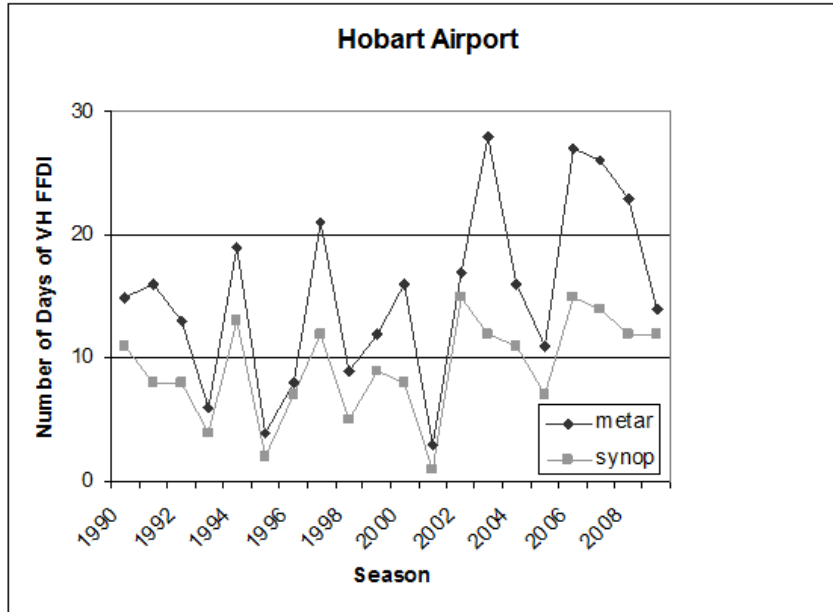
and Launceston Airports (Devonport Airport is similar, but with fewer counts of Very High FFDI). Years are labelled in the figure by their first calendar half-year, for example the 2006 year consists of the period 1 July 2006 to 30 June 2007. It is there will be at least as many days of VH FFDI when considering METARs compared to synoptic observations, since the latter are (in general) a subset of the former. Figure 3.3 demonstrates that for most seasons, there are between one and two times as many days of VH FFDI evident on METARs as synoptic observations, further illustrating that an assessment of fire danger levels based on synoptic (or less frequent) observations will under-represent the true levels of FFDI at a site.

There is a well-recognised, substantial interannual variability in the number of recorded Very High FFDI events. In the case of Hobart Airport, there is a range of 1 to 28 days per season on which VH FFDI was recorded over the study period. At Launceston Airport, the range is 0 to 14 days per season. There is also considerable variability in the ratio of events recorded as METARs to those recorded as synoptic observations. In general, active seasons result in a higher ratio of METAR events to those computed from synoptic observations. This is very likely a result of a higher number of SPECIs reported during the course of such seasons, noting that fire weather events are often characterised by gusty winds for which a SPECI is likely to be issued.

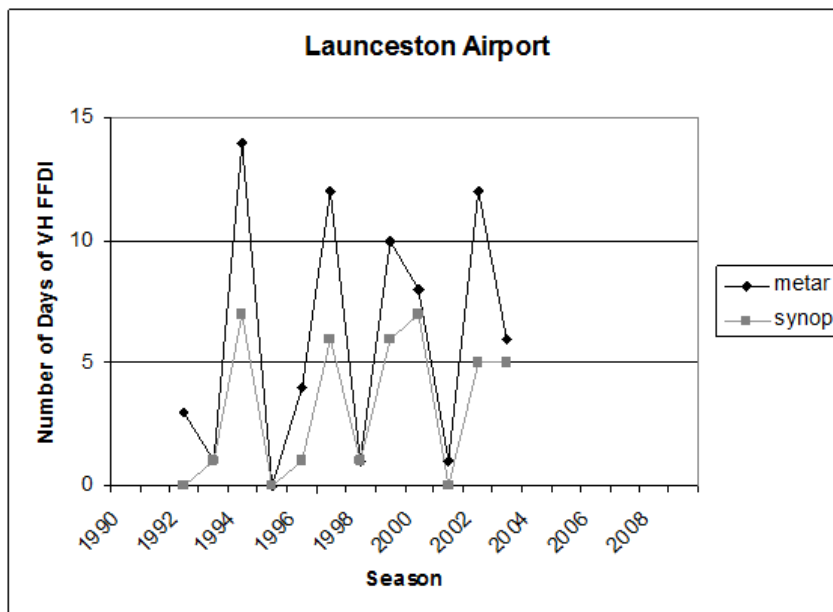
Further, a comparison of Figure 3.3(a) and (b) suggests that there is only a moderate correlation between the two plots. While some seasons are particularly active or inactive at both locations, there are other seasons in which there are very different levels of activity. For example, the 2002 (i.e. 2002-03) season was active at both locations, with 17 days on which VH FFDI occurred from METAR reports at Hobart Airport, and 12 at Launceston Airport. The following season, however, was relatively inactive at Launceston Airport, with 6 days of VH FFDI from METARs, but was the most active season in the dataset at Hobart Airport, with 28 METAR events. These differences are discernible from synoptic or even 1500-only observations, but are highlighted by the availability of more frequent observations, and are of some significance for studies of future climate, suggesting that single station data will be of use in projections for only quite limited regions.

3.3.2 Duration of Events

In many cases, episodes of VH FFDI are short-lived, and not resolved by synoptic observations (as suggested in Figure 3.2 and Figure 3.3). This assertion can be examined by checking the duration between the first and last observation of VH FFDI on days of Very



(a)



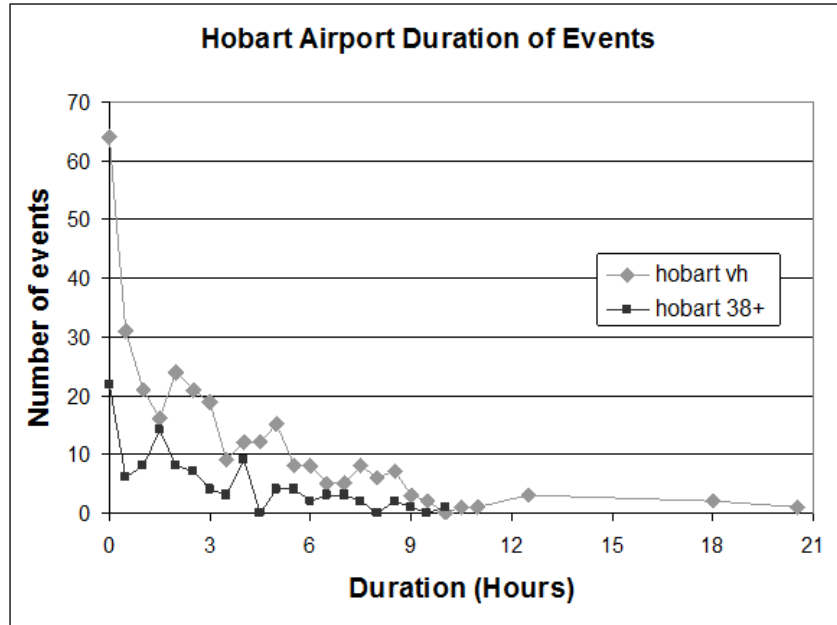
(b)

Figure 3.3: Counts of FFDI ≥ 25 (Very High Fire Danger) by season for (a) Hobart Airport and (b) Launceston Airport. Note different y-axis scales on the plots. The same x-scale is used on both plots, to better allow comparison of activity between the stations over different seasons.

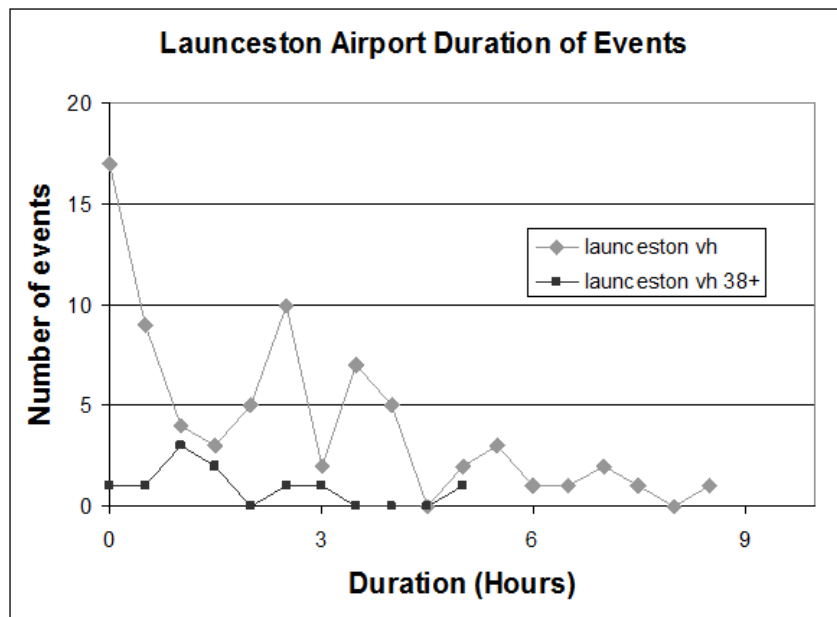
High fire danger. Particularly on marginal VH FFDI days, the FFDI can dip below VH rating for periods. Nonetheless, it is valid to define the VH event duration as the time interval between first and last VH FFDI observation, even if that period is not continuous. Of course, a number of different measures of event duration are possible, each of which may be informative in particular contexts. For example, the longest period of continuous VH FFDI, or the total time above VH FFDI are both reasonable indicators of the level of fire danger for a day. The time interval between first and last observation of VH FFDI, however, provides a stringent upper limit to event duration and therefore the likelihood of detection of the VH FFDI event by a synoptic or 1500-only observation schedule. Figure 3.4 plots the time interval between first and last VH FFDI observation for both Hobart (Figure 3.4(a)) and Launceston Airports (Figure 3.4(b)). VH FFDI events occurred very infrequently at Devonport Airport, and are not included here. Duration of events was binned into half-hourly categories. Those of duration less than one half-hour, most commonly single VH FFDI observations, were placed in the “0 hour” bin. Also plotted are the durations of events where the FFDI exceeds 38. Again, a single observation of VH 38+ was placed in a “0 hour” duration bin, together with, rarely, two or more such observations within a half-hour period (with no subsequent observation of FFDI greater than or equal to 38). In the case of both Hobart and Launceston Airports, there is a very rapid decrease in the number of VH FFDI events as duration increases, with a long tail of longer duration events, particularly at Hobart Airport. Interestingly, in both locations the decline in the number of VH 38+ events with increasing duration is much less abrupt.

Of considerable interest for both locations is the proportion of events lasting less than three hours, as these could potentially escape detection by a synoptic observing programme. For Hobart Airport, of the 301 VH FFDI events, 175 (58%) were of duration less than 3 hours and thus at risk of not being detected by a synoptic-only observation schedule. In the case of Launceston Airport 48 of a total 73 VH FFDI events (66%) lasted less than three hours.

Of the 100 cases of FFDI VH 38+ at Hobart Airport, 62 reached or exceeded FFDI 38 for less than three hours. When the criterion for FFDI was set at FFDI 70 (not displayed), some 17 events were detected in the METAR database for Hobart Airport, of which 15 (88%) were at or above FFDI 70 for less than three hours. At Launceston Airport, of the ten VH 38+ events, eight lasted less than three hours. The above suggests that the higher the value at which FFDI peaks, the less likely the peak is to be resolved by a synoptic observing network.



(a)



(b)

Figure 3.4: Duration of fire danger at (a) Hobart and (b) Launceston Airports. “Number of events” refers to the total number of events recorded at each station for the respective study periods, binned by half-hour. Axes are again scaled differently.

Further, of the 100 days where Hobart Airport FFDI equalled or exceeded 38, the first observation of $\text{FFDI} \geq 38$ occurred after 1500 LCT on 16 days, and on ten of those days, FFDI was still below 24 at 1500 LCT. Similarly, there are days in the Hobart Airport dataset on which the latest observation of $\text{FFDI} \geq 38$ occurred prior to 1500 LCT. Of the 100 days on which FFDI reached or exceeded 38, conditions had eased by 1500 LCT on 37 days. Of these 37 events, conditions had eased below FFDI 24 by 1500 LCT on 15 days.

As an example of the rapid variability of fire weather conditions around southeast Tasmania, the event of 22 January 2006 is examined. On this day, Hobart Airport recorded a peak FFDI value of 64 at 1825 LCT. This FFDI was the highest of the 16 days in the Hobart Airport dataset which recorded FFDI below 38 until after 1500 LCT. The FFDI was 13, barely in the “High” range, at that time and had been lower than that until 1430 LCT. A weak seabreeze was pushed offshore after 1630 LCT as northwesterlies strengthened. By 1700 LCT, the FFDI had climbed to 44, but by 1901 LCT a cooler, moist southeasterly change had moved through Hobart Airport and the FFDI fell to 15. The time that the FFDI spent above 38 was less than two hours, and the observation record indicates that FFDI was in the range above 24 for only a few minutes longer than that. On this occasion, the synoptic observation schedule captured the event, but not the peak value. Had the cold front traversed the Hobart Airport region an hour earlier, however, the event would not have been captured at all by the synoptic schedule. Furthermore, even in this scenario, the event would not have been registered by an examination of 1500 LCT-only observations.

It is worth noting that the brevity of this event was not simply a function of the microclimate of Hobart Airport, as a particular location in a complex coastal environment. Bushy Park, approximately 55 kilometres to the west-northwest of Hobart Airport in the inland Derwent Valley, also recorded elevated fire danger on this day. The FFDI at Bushy Park peaked at 52 and exceeded 38 for about 75 minutes, spending about three and a half hours with FFDI above 24. Thus, while the transition to and from elevated fire danger was not as abrupt at Bushy Park, it experienced comparable conditions to Hobart Airport. Other locations in southern Tasmania experienced broadly similar fire weather on this day, although Hobart Airport did record the highest FFDI. During this time, a number of fires were burning across a wide swathe of Tasmania, due to widespread lightning on 20 January. Most of these fires became more difficult to control as a result of the weather conditions on 22 January.

Some events have occurred with very pronounced peaks early in the day, for which the 1500 LCT observation was below the “High” range. A peak FFDI of 115 was recorded at

1200 LCT on 11 January 1991, yet the passage of a cool, moist southeasterly change resulted in a 1500 LCT FFDI value of 9. On the other hand, early onset of seabreeze conditions, as in 22 January 2006, or the persistence of a maritime boundary layer until well into the afternoon can mask the approach of a change and typically hot, dry north to northwesterlies are not then experienced until after a 1500 LCT reading has occurred.

These real and not atypical events indicate strongly that climatologies based solely on 1500 LCT observations will miss many such significant fire weather events. In order to resolve the full range of possible fire weather conditions, vital in an attempt to characterise current and future fire weather climatology, weather conditions throughout the day need to be considered.

3.3.3 Relationship between duration and severity of events

The event having the longest recorded period of FFDI in excess of 24, some 20.5 hours, occurred on 12 October 2006 at Hobart Airport. An accidental fire ignition occurred during this day, which resulted in an urban interface fire burning 800 Ha. This event also recorded one of the highest FFDI values in the entire Tasmanian fire weather database, and raises the question of whether long duration fire weather events are necessarily associated with unusually elevated FFDI, and vice versa.

An examination of events with FFDI at least 24 and lasting more than 10 hours (eight events at Hobart Airport during the study period) indicates that all but one had peak FFDI ratings greater than or equal to 50. The exception, 6 December 2006, had FFDI 25 at 0100 LCT, after a day on which FFDI exceeded 50 on 5 December. Late in the afternoon of 6 December, FFDI again increased above 24. This event, then, was of long duration only by virtue of a set of unusual conditions. (The definition of event duration was not amended at this point, however, as it affected only a very small proportion of the total number of events in the dataset.) Five of the remaining six events had peak FFDI of 69 or more.

To examine the possibility that significant events are necessarily, or usually, long-lived, days at Hobart Airport with a peak FFDI reaching at least 70 were identified, together with the duration of each event. The 17 resulting events (Table 3.1) had a surprisingly diverse range of durations, from 2 to 20.5 hours. These indicate that severity is usually, but certainly not always, associated with duration of at least 5 hours. Interestingly, two of the most dramatic counterexamples, on 11 January 1991 (peak FFDI 115, discussed above) and 21 January 1997 (peak FFDI 97), recorded $\text{FFDI} \geq 24$ for only 2.5 hours. Both events were associated with the development of small but intense mesoscale circulations over southeast

Date	Peak FFDI	Duration of Very High FFDI (hours)
11/01/1991	115	2.5
25/02/1991	79	7.5
07/03/1991	70	4
07/02/1993	74	4.5
06/12/1994	71	7.5
12/12/1994	71	11
22/12/1996	71	6.5
21/01/1997	97	2.5
07/11/2002	135	8.5
15/11/2003	92	6
04/03/2004	85	7
25/03/2004	87	2
11/10/2006	71	12.5
12/10/2006	126	20.5
11/01/2008	85	8.5
14/03/2008	101	18
22/01/2009	88	9

Table 3.1: Occasions within the period October 1990 – June 2010 when FFDI at Hobart Airport reached 70.

Tasmania. Mills and Pendlebury (2003) examined the latter event in detail.

3.3.4 Time of Maximum FFDI

The high temporal resolution of the METAR database allows an investigation of the time of greatest FFDI associated with fire weather events that may be of use for planning purposes by fire agencies, and in the design and interpretation of fire weather climate studies. The time of maximum FFDI of an event is defined here as the first occurrence during a day of the peak value. This is not a trivial definition, as the peak FFDI can occur on a number of occasions. For example, one event in the Launceston Airport METAR dataset recorded peak FFDI of at least 24 on six occasions. A reasonable definition of “peak time” might be the midpoint of the times of peak FFDI. The time of first occurrence of the peak FFDI, however, was chosen because it was felt that this would be of particular significance for fire managers.

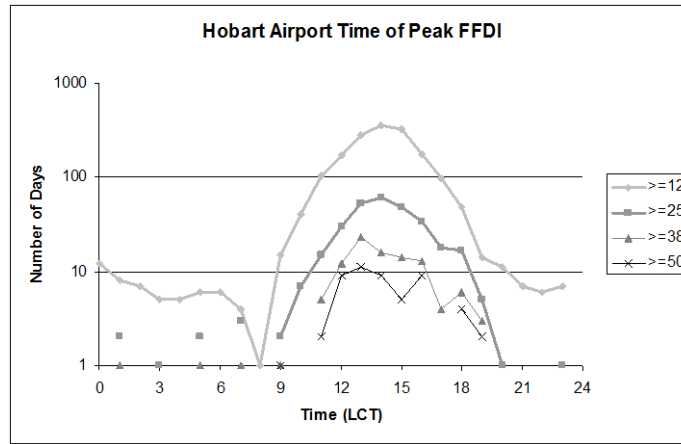
Ranges of values were examined for Hobart, Launceston and Devonport Airports. In the case of Hobart Airport (Figure 3.5 (a)), four sets were plotted. These were the range of times of peak FFDI for days with that peak ≥ 12 , 25, 38 and 50. Because Launceston Airport had fewer days of more severe fire weather (and no days of FFDI ≥ 50), only three ranges were plotted (Figure 3.5 (b)), these being days with peak FFDI greater than or equal to 12, 25 and 38. Similarly, two ranges were plotted for Devonport Airport, those days with peak FFDI ≥ 12 and ≥ 25 .

In all cases, peak FFDI occurred in the afternoon. At Launceston Airport, the most common time of peak FFDI of ≥ 12 , 25 and 38 was 1500 LCT in all cases, but with a tail skewed slightly towards earlier in the day, and no events with peak FFDI after 2000 LCT. Devonport Airport was quite similar to Launceston Airport, but with fewer days of “High” or “Very High” FFDI, experiencing a broad peak for both ranges between 1200 and 1600 LCT.

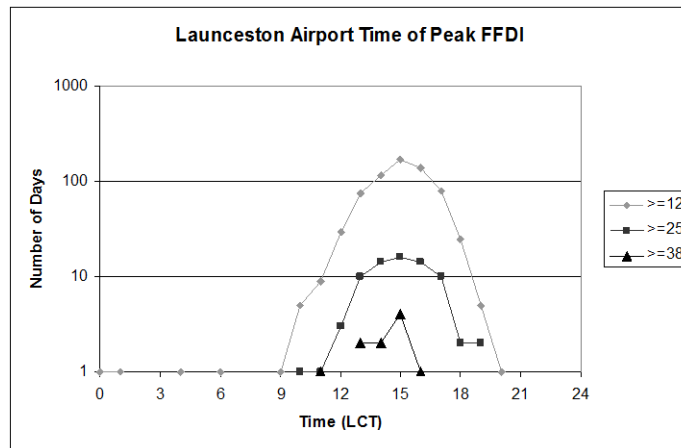
Hobart Airport experienced a much wider range of peak FFDI times in corresponding ranges of values, essentially at any time during the day, but with the most common time 1400 LCT for FFDI at least 12 and a slightly broader peak between 1300 and 1500 LCT for FFDI ≥ 25 . Of interest is the dip in the plot for FFDI ≥ 12 at 0800, for which there is no obvious solely meteorological reason. An examination of the raw data shows a decline from 0000 until 0800 in the number of days with peak FFDI during the early morning. It seems likely that this at least partly a consequence of the way peak daily FFDI is selected. As noted above, if there is more than one occurrence of the day’s highest FFDI, the earliest such occurrence is selected as the daily peak. During the early morning, in the absence of insolation and the resultant enhanced mixing and heating, it is less likely that a later time will record a higher FFDI. It is only after significant insolation has occurred that peak daily FFDI is likely to be recorded during any particular time period. A trend towards earlier maxima with higher FFDI is suggested by the set of days with peak FFDI at least 38, where time of peak FFDI was most commonly at 1300 LCT. A broad peak between 1200 and 1400 LCT, with a secondary peak at 1600 LCT, occurred for days with highest FFDI ≥ 50 , lending some support to the suggestion of earlier peak times for higher FFDI values.

3.4 Discussion and Summary

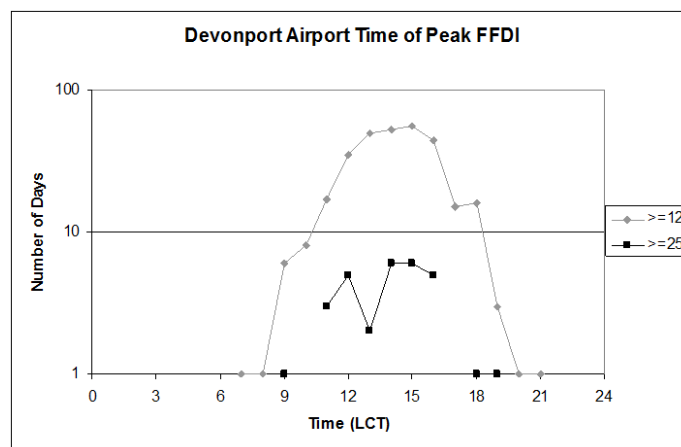
Operational meteorologists and their fire and land management colleagues have generally been aware of the variability of fire weather conditions during the course of a day, an awareness that this study goes some way to quantifying. On some occasions in the past, however, failures to control fire outbreaks have resulted from fire managers being faced with difficult weather conditions at “unusual” times of the day. The outcomes of this study have highlighted to fire and land managers the potential in particular for “early” starts to a day’s fire weather, an awareness which has been translated into both training and operations. Tasmanian fire agencies have ensured, as a result, an increased weight of response to incidents earlier in a day in recent seasons than was previously the case (M. Chladil, Tasmania Fire



(a)



(b)



(c)

Figure 3.5: Frequency analysis of times of Peak FFDI for various FFDI ranges at (a) Hobart (b) Launceston and (c) Devonport Airports, plotted with a logarithmic y-scale (to better resolve the plots displaying higher and lower ranges of FFDI).

Service, 2011, personal communication).

Information on the duration of fire weather events is valuable in an ongoing discussion about the appropriate length of time that conditions can persist above warning thresholds before a fire weather warning or alert is issued. Currently in Tasmania, any observation of FFDI above the warning threshold of 38 is considered justification for a warning. It is useful, though, to have an indication of the change in the number of warnings potentially issued should the warning criterion be amended to include a requirement for conditions to persist for a specified length of time.

This study raises the question of how, in forecasts for fire control purposes, to express fire weather variability most effectively. Traditionally, fire weather forecasts using the McArthur fire danger system in particular have provided details of the conditions at the time of maximum temperature, in the expectation that this will not be far from the period of peak FFDI. Alternatively, such forecasts have detailed explicitly the conditions at the time of peak fire danger. Clearly, both of these presentation methods offer a picture that is far from complete.

Hourly numerical weather model output can give a very detailed forecast of fire weather over an area of responsibility, but can present a very large amount of information for users to assimilate. One, or more usefully several, summary measures of forecast fire weather may still be the most realistic way of communicating forecast conditions for as broad an area as an Australian State or Territory for many users. Such summary measures can be computed easily from available hourly fields of fire weather from numerical weather prediction models. Perhaps the simplest such summary field is the peak FFDI over an area. Another field that the above discussion immediately suggests is that of time of peak fire danger index. It is clear that, while the most common time of occurrence of peak fire weather is mid-afternoon, there is a wide variability, depending on location and the meteorology of the day. A “time of maximum fire danger index” chart is very likely therefore to be of use to fire and land managers.

A potentially useful field that could be computed using hourly numerical weather prediction output is the integration of FFDI with time over an area. This is analogous to the Σ FFDI concept discussed by Beer et al. (1988), but with FFDI accumulated over 24 hours (or a subset thereof) rather than annually. The value of the measure lies in highlighting areas where the FFDI is forecast to be elevated for substantial periods of time, summarised in a single image. These summary data can be presented at individual sites, or, with full implementation of the Next Generation Forecasting System currently being deployed across Australia, as areal plots.

The availability of high resolution time series of fire weather observations has allowed examination of a number of characteristics of fire weather events, including duration and peak times, in addition to expanding on earlier climatologies. The calculation of forest fire weather conditions at high temporal resolution for three Tasmanian locations has also demonstrated that climatologies of fire weather using data solely at 1500 LCT, or even at all synoptic hours, are insufficient to resolve the true variability of fire weather at a location. At Hobart Airport, for example, examination of observations made at 1500 LCT alone will only resolve some 53% of days on which peak FFDI exceeded 38. This is important to bear in mind not only for safe fire management, but for interpretation of climate studies. While not the primary purpose of the study, the substantial and quite complex interannual variability of FFDI in Tasmania was also noted. This is an important issue in its own right for fire managers and forecasters, and will be the subject of future research.

3.5 Acknowledgements

Mark Chladil of the Tasmania Fire Service provided helpful feedback on early results of this study, and in the review process, particularly in regard to operational implications of the study for fire managers. Graham Mills of the Centre for Australian Weather and Climate Research and Kelvin Michael of the Institute for Marine and Antarctic Studies at the University of Tasmania insightfully reviewed drafts of the document. The editor and anonymous reviewers made a number of suggestions that helped clarify and improve the focus of the paper. Ian Barnes-Keoghan and Doug Shepherd (retired) of the then Climate and Consultative Services Section, Tasmania and Antarctic Regional Office of the Australian Bureau of Meteorology, commenced digital archival of Tasmanian airport weather reports in 1990, well before this activity was undertaken nationally in Australia. In doing this, they enabled this study to be undertaken. Figure 1 was generated using the Jules Map Server of UNAVCO, <http://jules.unavco.org/>.

4: Springtime Fire Weather in Tasmania, Australia: Two Case Studies

Abstract

A number of severe springtime fire weather events have occurred in Tasmania, Australia, in recent years. Two such events are examined here in some detail, in an attempt to understand the mechanisms involved in the events. Both events exhibit strong winds and very low surface dewpoint temperature. associated 850 hPa wind-dewpoint depression conditions are extreme in both cases, and evaluation of these quantities against a scale of past occurrences may provide a useful early indicator of future severe events. Both events also feature advection of air from drought-affected continental Australia ahead of cold fronts. This air reaches the surface in the lee of Tasmanian topography by the action of the Foehn effect. In one event, there is good evidence of an intrusion of stratospheric, high PV, air, supplementing the above mechanism and causing an additional peak in airmass dryness and wind speed.

4.1 Introduction

Tasmania, located south of the Australian continent (Figure 4.1), shares with other parts of southeastern Australia a history of frequent fire weather and fire events, including occasional fire disasters (Bond et al., 1967, Bureau of Meteorology, 1985, Mills, 2005b,a, Nairn et al., 2005). “Fire weather” refers to weather events resulting in higher than average temperatures, low relative humidity and strong wind, often following periods of low rainfall when vegetation will be particularly combustible.



Figure 4.1: Location of Tasmania and other places mentioned in this paper.

Episodes of low humidity and strong wind are a normal springtime feature of the Australian sub-tropics (Luke and McArthur, 1978), parts of North America (Westerling et al.,

2006) and of the Eurasian boreal forests (e.g. Stocks and Lynham (1996), Valendik et al. (1998)). Such regimes can have a significant impact on fire, marine, agricultural, aviation and public weather users. On the other hand, the season of peak fire weather in Tasmania has commonly been regarded as late summer into autumn (Luke and McArthur, 1978). Among fire managers and meteorologists, however, there has been discussion of a springtime “bump”, or early season peak in fire danger, subsiding before the primary seasonal peak occurred some months later. This springtime “bump” has been documented (Fox-Hughes, 2008) as occurring in October or November, roughly one year in two.

Over much of Australia, fire danger in forested areas is estimated using the McArthur Forest Fire Danger meter Mark V (McArthur, 1967). The resulting Forest Fire Danger Index (FFDI) is a function of temperature, relative humidity, (10 minute average) windspeed and fuel moisture, the latter encoded as a “drought factor” representing the fine forest fuel availability. Fox-Hughes (2008) examined FFDI values computed from synoptic observations at several Tasmanian sites, establishing that the springtime secondary peak is a feature of the east and south-east of the state.

Springtime fire weather is of concern for several reasons. Scientifically, it is of interest to know whether its recent increase in frequency is a response to a secular trend, or part of a long-term climatic cycle. Understanding the synoptic environments in which dangerous springtime fire weather occurs opens the possibility of linking such events to broader scale drivers, and seasonal prediction of “bad” springtimes. Operationally, it is important for fire managers to be aware of the potential for the occurrence of such events and prepare accordingly, during periods when resources are often still being allocated and planning undertaken for the fire season peak. Fire weather forecasters are therefore also particularly sensitive to the occurrence of these events, and need to be alert during the early fire weather season to indicators that a springtime fire weather event may develop. As part of a research effort to understand the nature and influences on the springtime peak, this study examines two events in some detail. The study forms a step between an observational station-based analysis establishing the existence of the springtime fire danger peak (Fox-Hughes, 2008) and future studies aimed at improving the predictability of both individual springtime fire weather events and, more broadly, seasons during which such events are more likely to occur. In the following sections, the selection of events for investigation will be discussed, and each event will be presented in its synoptic and mesoscale setting. Common characteristics will be examined and differences explored.

4.2 Events and Data

Both events examined here were very significant fire weather occurrences, characterized particularly by periods of surface dry air exceptional in the Tasmanian climate record. Thus, the immediate origin of the surface dry air pulses will be a focus of event descriptions.

On 7 November 2002, a late afternoon/early evening cool change was preceded by strong to gale force winds, with very warm, dry air. Approximately 40 wildfires were ignited in eastern Tasmania (Bureau of Meteorology, 2002). Fire danger was “Very High” (FFDI > 24) from early afternoon through mid-evening, peaking during the early evening as windspeed increased and dewpoint temperature fell immediately ahead of the front.

The week prior to 12 October 2006 was characterized by persistent very dry air over Tasmania. Successive frontal passages caused fire danger episodes on preceding days, and gale-strength prefrontal winds on 12 October resulted in exceptional fire weather. A 800 Ha fire on the outskirts of Tasmanian state capital city, Hobart, nearly destroyed many dwellings. In the event, a remarkable combination of preparedness and wind direction prevented significant structural damage.

Both cases are examined using archived data from the Australian Bureau of Meteorology mesoLAPS, a mesoscale version of the LAPS model (Puri et al., 1998). In 2002, the grid resolution of mesoLAPS was 12.5 km. By October 2006, a number of sub-domains existed with five km resolution, including one encompassing Tasmania.

4.2.1 7 November 2002

4.2.1.1 Surface weather and forest fire danger on 7 November 2002

Weather parameters and FFDI from Hobart Airport on 7 November are plotted in Figure 4.2. Data points are instantaneous values of temperature and dewpoint every minute, with 10-minute averaged windspeed, again available every minute. Drought factor throughout the day remained at 9 (indicating 90% of fine fuel available to burn). FFDI increased rapidly soon after midday (0100 UTC) as dewpoint fell to around -5°C and wind increased to $30\text{--}40\text{ km h}^{-1}$, mostly exceeding 50 km h^{-1} between 0530 and 0900 UTC. FFDI peaked over 100 at 0740 UTC as dewpoint temperature fell to -11°C and wind speed increased above 60 km h^{-1} . A secondary peak occurred at 0900 UTC, as dewpoint temperature briefly dropped again to -8°C . Subsequently, FFDI fell as windspeed and temperature decreased while dewpoint temperature rose. The event was unusual because of the magnitude of the peak FFDI and

because it occurred later than any other FFDI peak > 50 recorded at Hobart Airport.

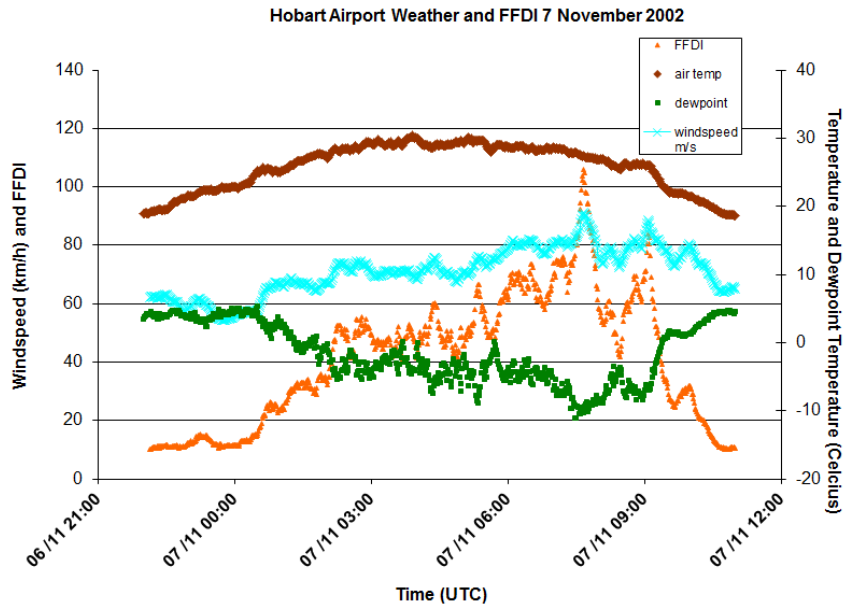


Figure 4.2: Plot of air temperature ($^{\circ}\text{C}$, brown), dewpoint temperature ($^{\circ}\text{C}$, green), windspeed (km h^{-1} , blue) and FFDI (orange) at Hobart Airport on 7 November 2002.

4.2.1.2 Antecedent conditions

Conditions prior to 7 November 2002 had been unexceptional. Tasmanian rainfall for October 2002 was close to average and, for the three months August-October, average in the east and largely above average in western and central areas (Figure 4.3). Consequently, fuel moisture levels were typical of mid-spring. It is worth noting, however, that much of Australia had experienced below or very much below average rainfall during August-October 2002. Persistent very dry conditions led to a prolonged period of bushfires in New South Wales in late 2002 (Attorney-General's Department, 2011, Taylor and Webb, 2004), and to devastating fires in Canberra (McLeod, 2003, Mills, 2005a) and in Alpine regions of Victoria in early 2003 (Bureau of Meteorology, 2003).

4.2.1.3 MSLP Progression

During early November 2002, several fronts crossed Tasmania as a high pressure system slowly moved eastward across the Great Australian Bight (Figure 4.4(a)). By 0000 UTC 6 November (Figure 4.4(b)), the high had moved over southeastern Australia, east of the Bight, and ridged southward over western Tasmania. Another front was progressing steadily eastward within a broad trough south of Western Australia, with a prefrontal trough de-

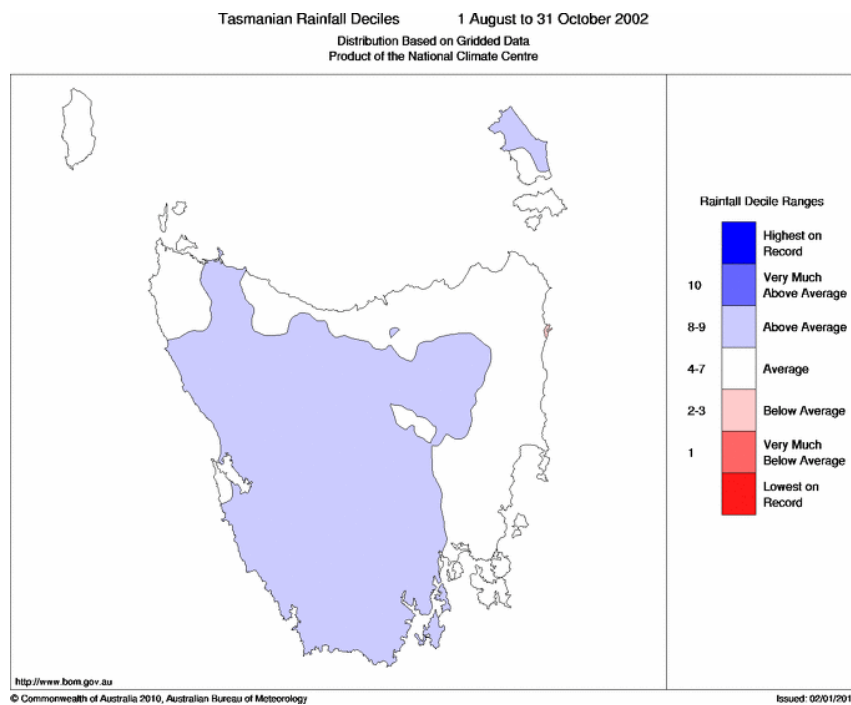


Figure 4.3: Tasmanian rainfall deciles for the three-month period 1 August to 31 October 2002. Shading indicates that much of Tasmania experienced above average (decile 8-9) late winter to early spring rainfall while the eastern and northern coastal fringes were close to average (decile 4-7). The image was generated with gridded data from the National Climate Center of the Australian Bureau of Meteorology.

veloping by 1800 UTC 6 November (Figure 4.4(c)), a common feature of Australian warm season frontal systems (Hanstrum et al., 1990). Frontogenesis occurred in the cold air behind the front as it moved east, and a low pressure system developed rapidly during 7 November in the trough in which the trailing front itself had formed (Figure 4.4(d)). The fronts crossed Tasmania during the early evening of 7 November, as the low pressure system moved to the east near 50 °S.

4.2.1.4 Upper level and satellite analysis

Figure 4.5(a) and (b) display mesoLAPS forecast winds initialized at 1200 UTC 6 November at 300 hPa around Tasmania. The upper level trough associated with the approaching frontal system can be seen in Figure 4.5 (a) at 1800 UTC 6 November near 125 °E. A broad jetstream lobe ahead of the trough is evident over waters west and south of Tasmania, while that to the rear of the trough is just visible on the far left of the figure.

Over the 12 hours to 0600 UTC 7 November (Fig. 5 (b)), the trough axis advanced to just east of 135 °E, and the trough became slightly negatively tilted, with the left entrance region of the leading jet streak immediately southwest of Tasmania. Subsequently (not shown), the 50 m s⁻¹ isotach extended through the apex of the trough at 0900 UTC, linking

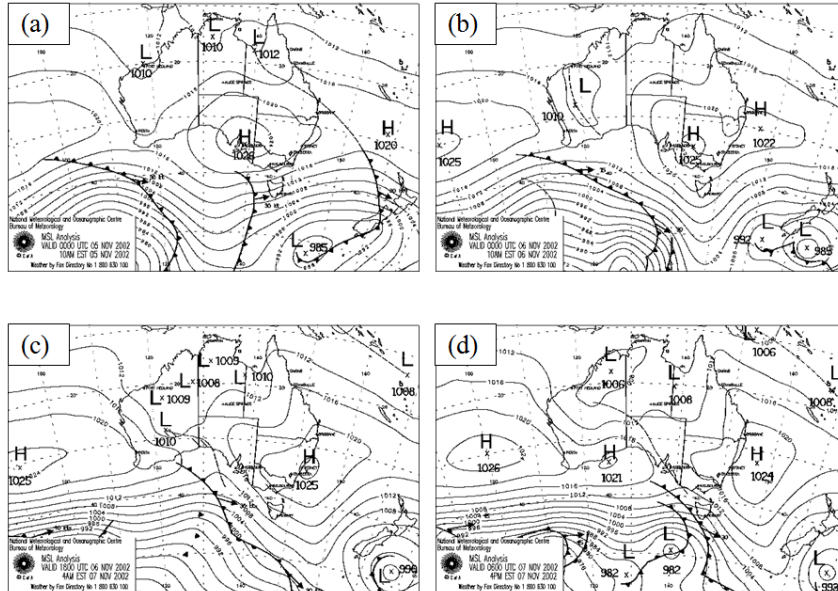


Figure 4.4: MSLP Australian Region charts for (a) 0000 UTC 5 November (b) 0000 UTC 6 November (c) 1800 UTC 6 November and (d) 0600 UTC 7 November 2002.

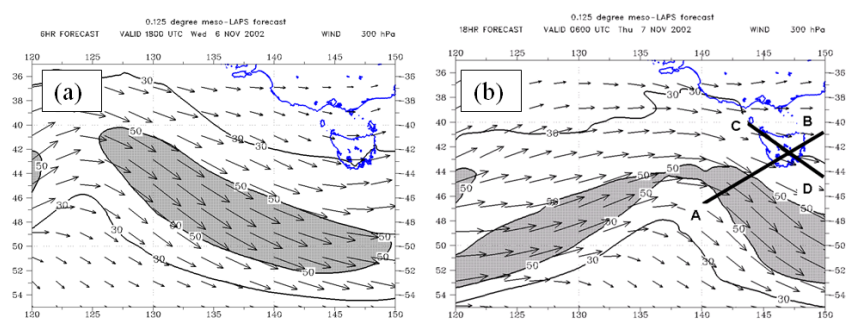


Figure 4.5: Charts of 300 hPa wind over and west of Tasmania, from the mesoLaps forecast initialized at 1200 UTC 6 November 2002, at (a) 1800 UTC 6 November (6 hour forecast) and (b) 0600 UTC 7 November 2002 (18 hour forecast). Windspeed in m s^{-1} , with areas greater than 50 m s^{-1} indicated in grey. Solid lines in (b) identify model cross-sections in Figures 10 and 12.

the jet streaks flanking the trough. The trough itself passed immediately south of Tasmania around 1200 UTC.

Rapid development of the secondary front and low to the south during 7 November is evident on US GOES-9 infrared imagery at 2030 UTC 6 November and 0530 UTC 7 November (Figure 4.6 (a) and (b) respectively). Frontal cloud is poorly organized at 2030 UTC west of Tasmania between 130 °E and 140 °E, with cloud corresponding to the prefrontal trough near the head of the Bight, around 35 °S 125 °E. The frontogenetic region west of the primary front is evident as a solid band of NW-SE oriented mid- to high-level cloud extending back from near 50 °S 123 °E. Over eastern Tasmania, a region of “banner” cloud had formed, moving offshore during the day as the fronts approached and allowing several hours of sunny conditions to enhance mixing of boundary layer air with higher momentum, drier air above.

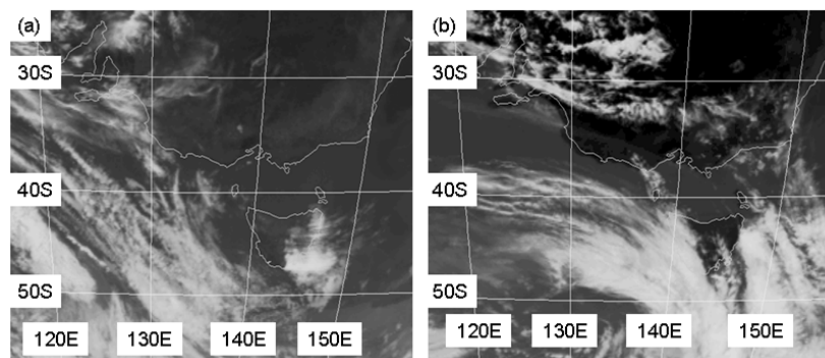


Figure 4.6: Infrared satellite images over southeastern Australia at (a) 2030 UTC 6 November and (b) 0530 UTC 7 November, from the US NOAA GOES-9 satellite.

By 0530 UTC, the fronts had moved rapidly towards Tasmania. The 0530 UTC IR image indicates an area of generally clearer sky over much of eastern Tasmania than had been the case earlier, with an area of cloud immediately east of Tasmania, likely banner cloud displaced somewhat eastward of its earlier position. In the west, however, incursion of mid- to high-level cloud associated with the approaching fronts had commenced. Their surface position was likely just off the west coast at the time. The second front displays a classic mid-upper conveyor belt above the surface feature, suggesting that it had matured rapidly during the day.

It is likely that the driest, high momentum air was associated with the passage across Tasmania of a “dry band” (Mills, 2008b) in the water vapour imagery. The 0426 UTC US GOES WV image (Figure 4.7) shows the main frontal cloud band clearly visible as an area of white, and the clear space over Tasmania evident on IR images is revealed as a significant,

though narrow, dry band extending back across western Victoria to a broad region of very dry air aloft over the Great Australian Bight. While the area of dry air over the Bight existed in previous images (not shown), the filament that crossed Tasmania during the afternoon only became visible during the day, as the frontal cloudband became more organised.

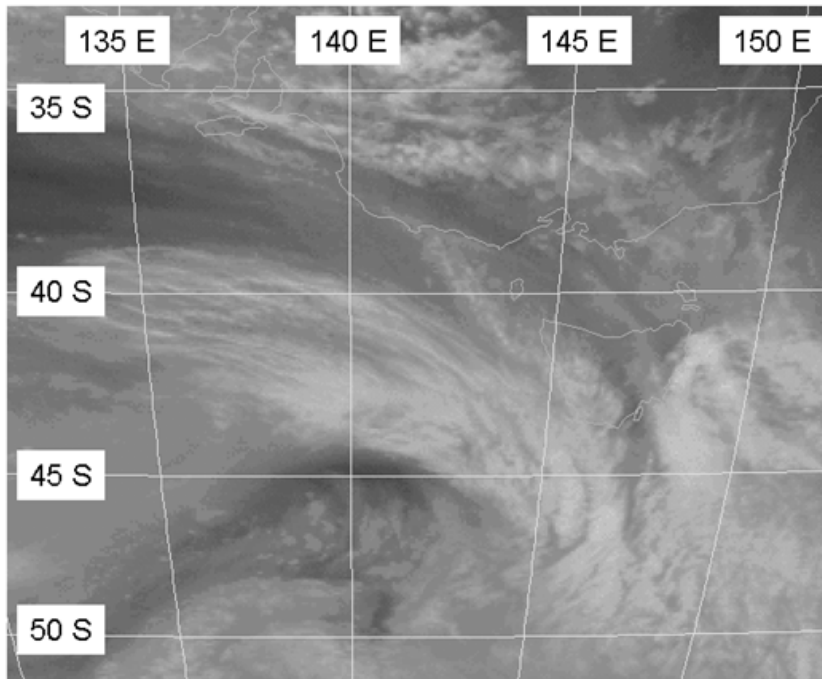


Figure 4.7: U.S. GOES WV image at 0426 UTC 7 November over southeastern Australia. White areas indicate high cloud, while dark areas indicate mid to high level dry air.

4.2.1.5 Airmass characteristics

Figure 4.8(a) shows the routine Hobart Airport radiosonde flight at 2300 UTC 6 November. The dewpoint temperature at 850 hPa was $-18\text{ }^{\circ}\text{C}$, in the lowest five percent of 850 hPa dewpoint temperature measurements since 1992. Further, the driest air in the troposphere occurred in a layer between about 930 hPa and 740 hPa. Once the surface temperature reached $29\text{--}30\text{ }^{\circ}\text{C}$, the lapse rate would have been close to dry adiabatic from the surface through this layer to almost 600 hPa. Indeed, as the temperature rose to $29\text{ }^{\circ}\text{C}$, the dewpoint temperature fell to $-4\text{ to }-5\text{ }^{\circ}\text{C}$. The Hobart Airport sounding suggests that the mean mixing ratio through the lowest third (or more) of the troposphere was about 2.6 g kg^{-1} , corresponding to a dewpoint temperature of $-5\text{ }^{\circ}\text{C}$ at the surface. It is clear, then, that mixing had occurred through the lower several hundred hPa of the atmosphere by early afternoon. Back trajectories for 120 hours ending 0000 UTC 7 November immediately around Hobart

are shown in 4.9, for parcels ending at a height of 1500 m above ground level. The back trajectories were calculated from mesoLAPS NWP model output, using the NOAA Hysplit model (Draxler and Hess, 1998). Trajectories were computed for 16 points on a square centered on Hobart, separated by 0.05° , approximately five km at the latitude of Hobart, allowing assessment of any divergence in the air parcel paths. As indicated in Figure 4.9, the 16 air parcels follow very similar trajectories out to 72 hours, increasing confidence that they represent the path followed by the airmass experienced at Hobart during the late morning. Between 0000 UTC on 2 November and 0000 UTC on 4 November, most parcels experienced sustained descent from above 5000 m over waters south of the Australian continent. (Corresponding back trajectories for 0300 UTC 7 November, not shown, reveal that all parcels originated high in the troposphere southwest of Australia.) By 0000 UTC on 4 November, the air parcels were located inland of the head of the Great Australian Bight, at an elevation of around 2000 m. At that time, this position was close to the center of the high that subsequently moved eastward. The elevation profile for the back trajectories indicate that air parcels subsided through the high, moving southward and into its western flank by 0000 UTC 5 November, before being entrained into the prefrontal northwesterly flow at an elevation of around 1500 m. During 6 November, parcels sank further to about 1000 m before beginning to rise, consistent with their poleward trajectory and ultimately in response to encountering Tasmanian orography, before sinking abruptly in the lee of the western Tasmanian range over Hobart. At 0000 UTC 5 November, the model parcels were near upper air station Eucla, Western Australia. The Eucla sounding at that time (Figure 4.8(b)) shows a dry airmass between 1000 and 2500 m elevation, with dewpoint temperature near -10°C , quite consistent with the air over Hobart 48 hours later. Modelled back trajectories of parcels ending at 1500 m above Hobart later in the day (not shown) indicate a broadly similar path. It is likely, then, that the 2300 UTC sounding is representative of the airmass over Hobart for much of the day.

The airmass over Hobart on 7 November experienced a long over-water trajectory, raising the possibility that its moisture content increased while it traversed the Great Australian Bight (and that the dry air observed was not of continental origin). A 24 hour forecast model vertical sounding from the mesoLAPS operational run of 0000 UTC 5 November is displayed in Figure 4.8(c), revealing the presence of a marine boundary layer below an inversion at about 900 hPa. There is a steep decline with height in dewpoint temperature within the boundary layer, and largely dry, continental, air above. The stability of the inversion layer likely prevented mixing between the two layers, with minimal transport of moisture into the

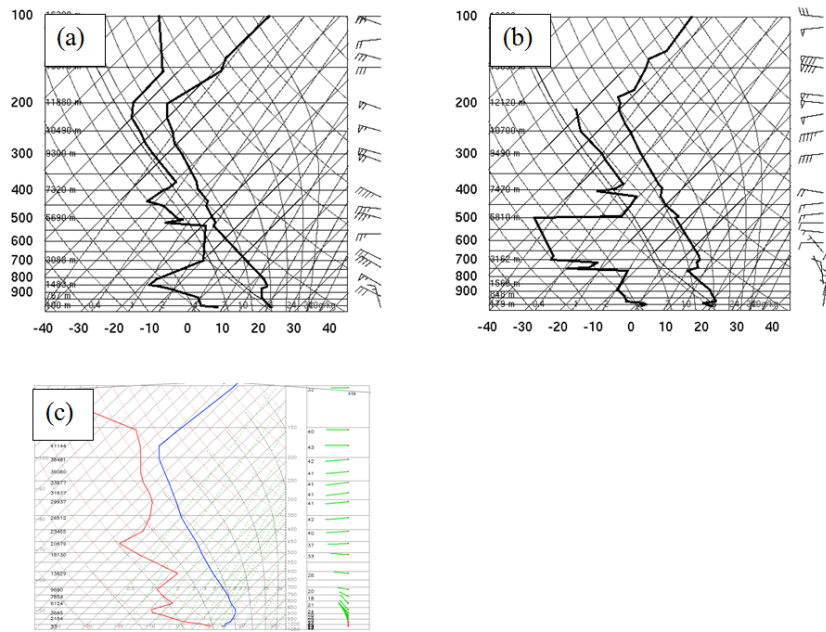


Figure 4.8: (a). Routine radiosonde trace released from Hobart Airport at 2300 UTC 6 November 2002. (b). Routine radiosonde flight at 0000 UTC 05 November 2002 from Eucla (Western Australia). Eucla is close to the position at 0000 UTC 05 November of the back trajectory shown in Figure 4.9, ending at Hobart at 0000 UTC 07 November. (c). Model vertical sounding near $38^{\circ}\text{S } 136^{\circ}\text{E}$, from 24 hour forecast of mesoLAPS, initialised at 0000 UTC 05 November.

overlying airmass.

4.2.1.6 Mesoscale features

Cross-sections from mesoLAPS run at 1200 UTC 6 November, along the line AB in Figure 4.5(b), are displayed in Figure 4.10, valid at 0600 UTC on 7 November. The left-hand extremity of the figure corresponds to the location of the center of the trough at that time. The tropopause height is depressed, as indicated by the cluster of PVU isopleths dropping from approximately 250 hPa over Tasmania to near 450 hPa, close to the trough axis. A region of relative humidity below 30% extends from immediately under this level to 700 hPa in the direction of Tasmania, approximately along the 300 K potential temperature isopleth (Figure 4.10(b)). Also evident in Figure 4.10(a) and extending along this axis is a well-defined region of anomalous PV, indicating a PV intrusion from the tropopause depression further west. In the center of Figure 4.10(a), above about 600 hPa, an area of high relative humidity is evident, corresponding to the frontal cloudband that can be seen in Figure 4.6 and Figure 4.7. Figure 4.11 is a pseudo-water vapour image generated from mesoLAPS for 0600 UTC 07 November, close to the time of the GOES WV image in Figure 4.7, presenting a different perspective of the mesoLAPS information. The frontal cloudband is clearly

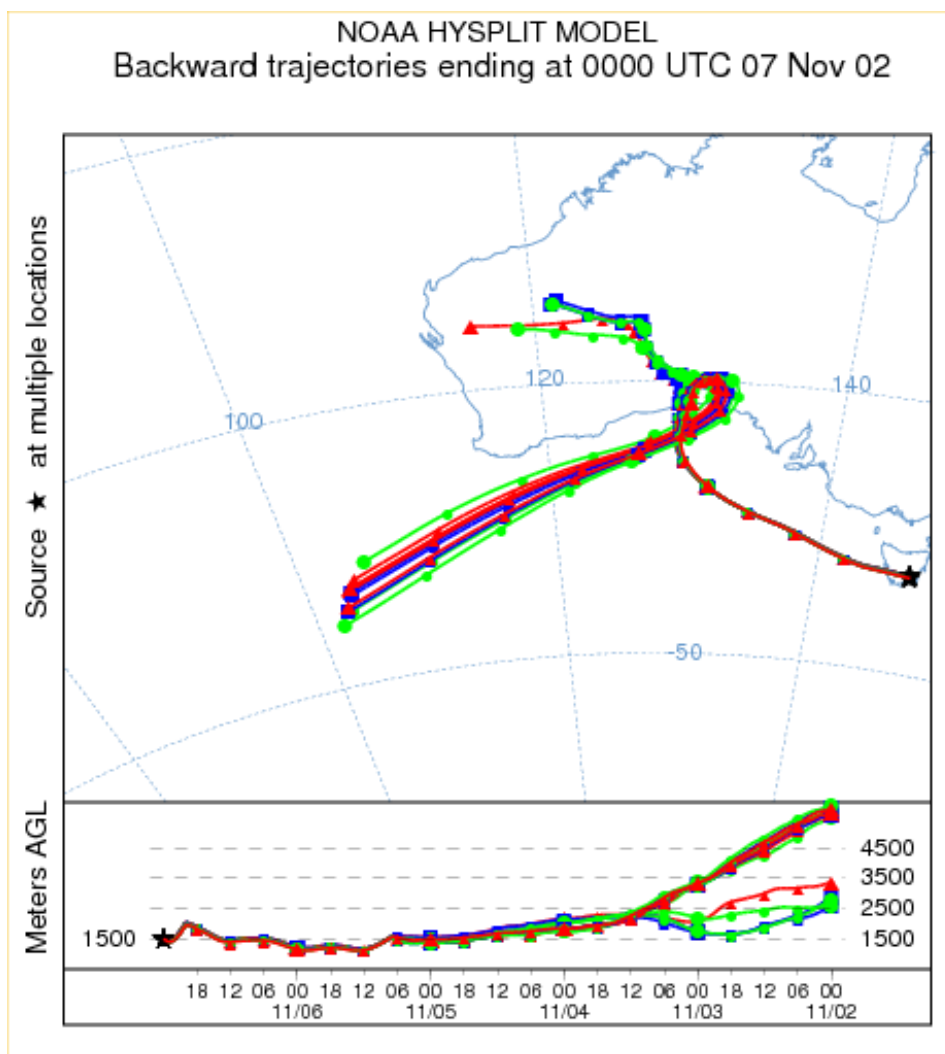


Figure 4.9: Modelled back trajectories of air parcels ending at 1500 m above ground level over Hobart at 0000 UTC 7 November. Top panel shows a plan view of parcel movement over a 72 hour period. Bottom panel shows a cross-section (height in metres) of the parcel trajectories. In both cases, a high degree of conformity is evident in the path taken by parcels to reach the cluster of endpoints around Hobart.

visible, as is the dry area immediately to its west and south associated with upper level descent. The pseudo-WV image provides a method of quickly assessing whether the model has resolved essential features of the atmospheric development, by comparison with actual WV imagery (see e.g. Georgiev and Martín (2001)). In this case, the correspondence between the two images of the frontal band, the tropopause descent near the trough axis and broad descent over the Great Australian Bight suggest that key aspects of the dynamics have been captured by mesoLAPS.

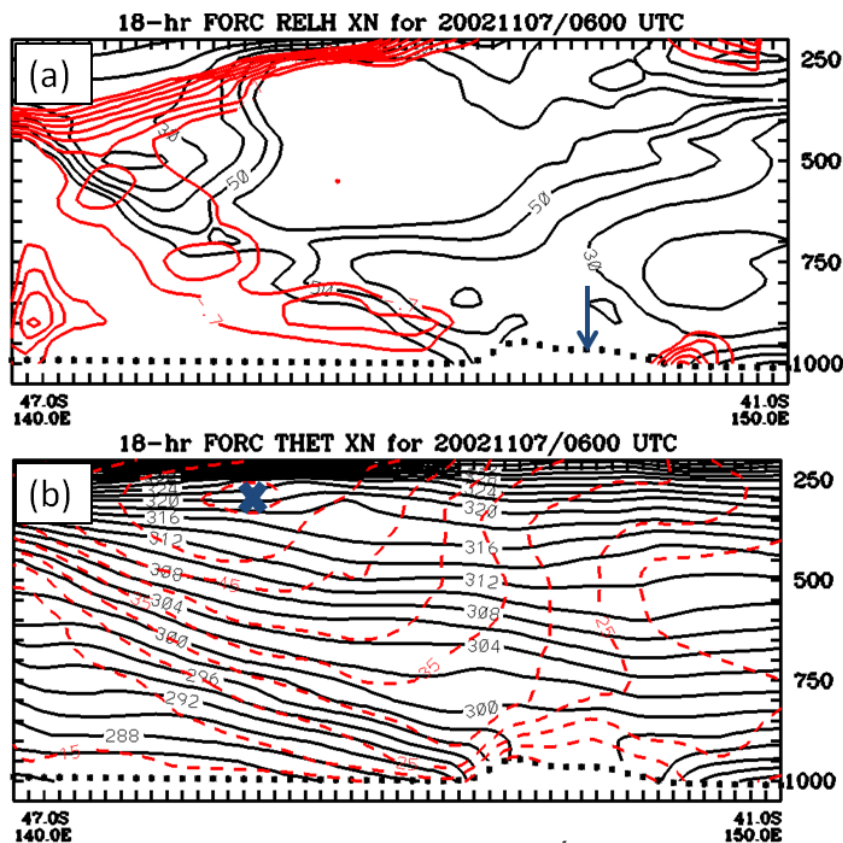


Figure 4.10: Cross-sections through the line AB in Figure 4.5(b) at 0600 UTC 7 November, from the 18 hour forecast of mesoLAPS initialized at 1200 UTC 6 November, showing: (a) relative humidity (black), at intervals of 10%, between 10 and 60%, and potential vorticity (red), at intervals of 0.2 PVU between -0.7 and -2.1 PVU. The approximate location of Hobart is indicated by an arrow. (b) potential temperature isentropes (black) at intervals of 2 K, and windspeed (red, dashed) isotachs at intervals of 5 m s^{-1} . Location of the jet core is indicated by a cross.

Figure 4.10(b) plots isentropes and isotachs along cross-section AB. The model atmosphere appears well-mixed to 850 hPa near Hobart, but substantially less so over waters either side of the Tasmanian landmass. The jet maximum of 50 m s^{-1} near 250 hPa is immediately below the tropopause. A lobe of increased windspeed descends from the jet towards Tasmania along the same axis as the relative humidity minimum. Within this lobe, the 30

m s^{-1} contour descends to 900 hPa, clearly within the boundary layer during the afternoon, and suggesting the possibility of gusts at the surface to around that value. The slantwise descent of this dry, high-momentum air in the frontal zone places it over southeast Tasmania within the upper part of the boundary layer, as judged from the Hobart sounding earlier in the day, allowing it then to mix to the surface to cause the observed evening FFDI peak.

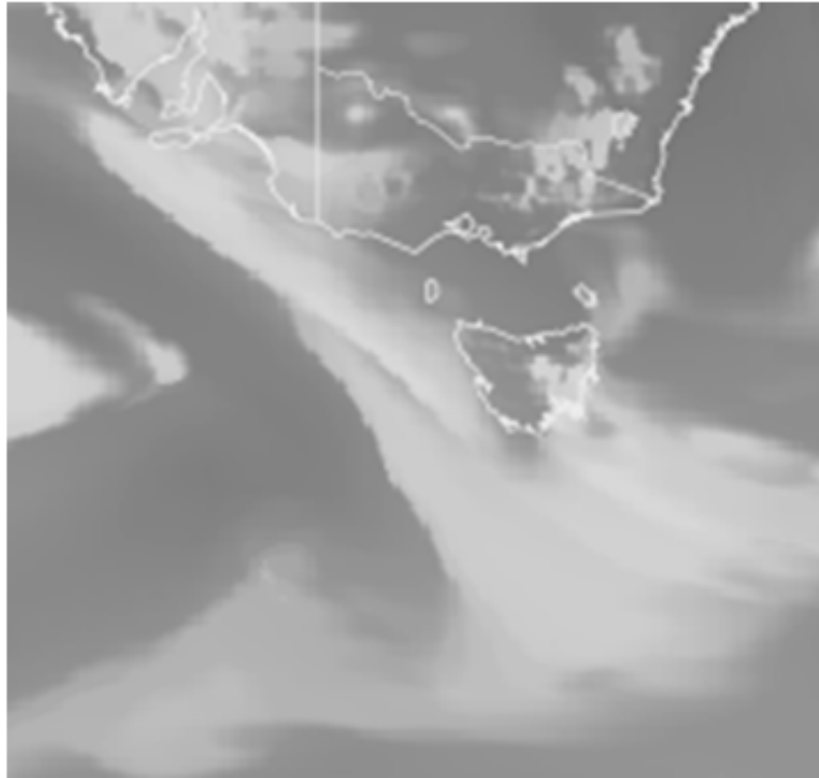


Figure 4.11: Pseudo-WV image generated from mesoLAPS model initialised at 1200 UTC 6 November, valid 0600 UTC 7 November.

Further, the 2300 UTC 6 November sounding from Hobart Airport shows that the top of the boundary layer during the afternoon of 7 November was at about 3000 m. Back trajectories to 120 hours ending at 3000 m above Hobart (not shown) at 0000 and 0600 UTC show an airmass origin over the waters south of Western Australia at a height of about 3000 m at 0000 UTC, rising to about 4000 m by 0600 UTC. Thus the air at the top of the boundary layer, capable of mixing to the surface by late afternoon, came from higher in the atmosphere during the afternoon than was the case during the morning. This can account for the increase in FFDI late in the day – the higher level air was drier and carried greater momentum than that lower in the atmospheric column.

The airmass over Hobart during much of the afternoon of 7 November was of northwesterly origin. Back trajectories of air parcels immediately above the surface at 0600 UTC 7

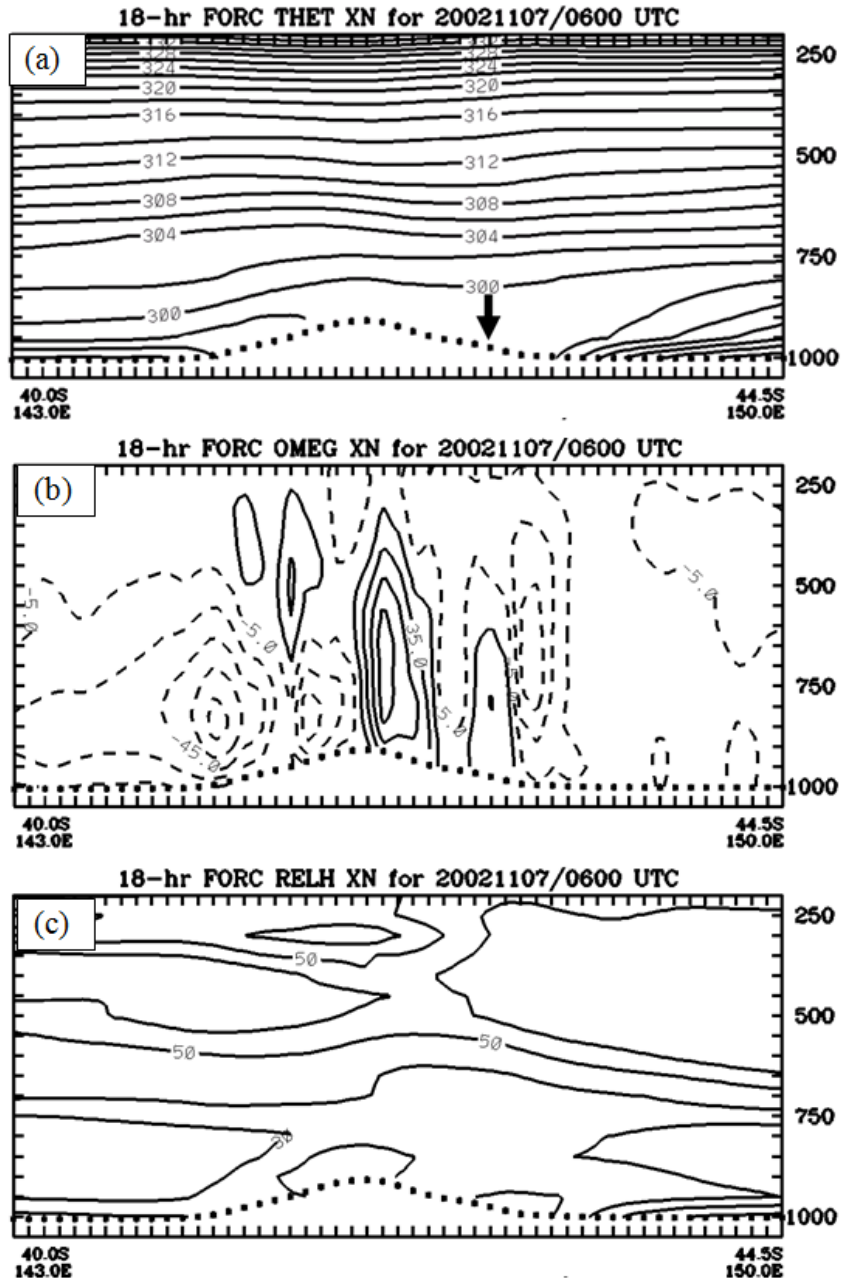


Figure 4.12: MesoLAPS forecast cross-sections through the line CD in Figure 4.5(b), initialised at 1200 UTC 6 November, valid 0600 UTC 7 November. The cross-sections show (a) potential temperature (K, interval 2 K), with the approximate location of Hobart indicated by an arrow (b) vertical motion, units hPa hr^{-1} , contoured every 20 hPa hr^{-1} , with negative (upward) values dashed, and (c) relative humidity, contoured every 10% between 10 and 60%.

November (not shown) indicated that, during the morning, parcels had been immediately west of Bass Strait, on a trajectory along the line CD in Figure 4.5(b). Vertical cross-sections of the model atmosphere along this line are shown in Figure 4.12. With respect to the northwesterly flow direction, Hobart lies in the lee of the central Tasmanian orography, much of which is over 1000 m above sea level. In Figure 4.12(a), over much of the land area a well-mixed lower atmosphere can be seen aloft, as discussed earlier. On the windward side of the island, however, there is strong evidence for a marine boundary layer in the lowest few hundred metres, with a rapid decrease in potential temperature up to the 300 K isentrope. In Figure 4.12(b), vertical motion along CD is shown, with contours every 20 hPa hr^{-1} , negative values dashed. Upward motion in excess of 85 hPa hr^{-1} is evident above the windward coast, while in the immediate lee of the highest orography air descending at more than 75 hPa hr^{-1} can be seen. Weaker descent (15 hPa hr^{-1} or more) occurs over Hobart. This pattern of features is characteristic of a foehn effect, which would have contributed to warming and drying of the air over Hobart during 7 November. The mountain wave aspect of the foehn effect would also have contributed to the descent of the anomalous PV air identified above. Sharples et al. (2010) discuss foehn winds in a context of southeast Australian fire weather, highlighting very similar structures of vertical motion over orography in other fire weather events. They also discuss the importance of orographic blocking of moist low level air upstream of the area subject to foehn winds, evidenced in Figure 4.12(a).

The alignment of upper and lower atmospheric processes sometimes occurs to allow advection of very dry air from near-stratospheric levels to the surface. Huang et al. (2009) diagnose the descent of upper tropospheric, exceptionally dry, air to the planetary boundary layer through the mechanism of the transverse ageostrophic circulation in the exit region of a jet streak moving southward over the western United States. Coupled with lower atmospheric conditions conducive to the development of severe downslope winds in the lee of southern Californian ranges, the dry air was conveyed to the surface to produce dangerous fire weather conditions. Zimet et al. (2007) described a similar occurrence contributing to dangerous fire weather conditions at Mack Lake, in the Great Lakes Region of North America. Charney and Keyser (2010) discuss the meteorological conditions contributing to the spread of a wildfire in the Double Trouble State Park in New Jersey. Again, downward transport of dry, high momentum mid-tropospheric air into a deep mixed boundary layer caused a rapid increase in fire danger during the day. Mills (2008b) investigates the association of WV dry bands with surface drying in Australia, hypothesising the descent of upper tropospheric air to the top of the boundary layer via dynamic processes, and its

further descent to the surface through deep boundary layer mixing. It is very likely that the same processes operated on and prior to 7 November 2002, in which a small scale feature developed over the course of several days and became evident in the satellite WV imagery and clear from its impact on surface weather parameters in southeast Tasmania, advected air from high levels to heights at which thermal and mechanical mixing could ensure the descent of that air to the surface.

4.2.2 12 October 2006

4.2.2.1 Surface Weather and Forest Fire Danger 11-12 October

FFDI values recorded on Thursday 12 October were comparable to those measured on 7 February 1967. On that date, FFDI peaked at 128, the highest calculated in a dataset of 3-hourly synoptic observations from 1960-2006. Devastating bushfires occurred in southeastern Tasmania, killing 62 people and destroying more than 1,400 major buildings. Bond et al. (1967) describe this event, while Fox-Hughes (2008) places it in a climatological context. On 12 October, FFDI calculated from the same set of synoptic observations peaked at 126 at Hobart Airport. FFDI calculated from data recorded every minute, as described in connection with the case of 7 November 2002, resulted in a peak FFDI of 133 (Figure 4.13). Hobart Airport's FFDI remained above 100 for at least 90 minutes in the late morning, and again during the afternoon. (It is worth noting that the peak FFDI on 7 February 1967 occurred over a single period of about an hour.) Further, four locations in southeast Tasmania reported FFDI of 100 or more during 12 October.

Individual weather parameters used to calculate FFDI were similarly extreme, as might be expected. The maximum temperature recorded at Hobart on 12 October was 33.1 °C, the third highest October maximum recorded at the site, and the warmest since a record of 34.6 °C was set on 31 October 1987. A number of sites recorded wind gusts in excess of 100 km h⁻¹, and Hobart recorded a gust to 93 100 km h⁻¹. The 10 minute mean wind at Hobart Airport during the period 0000 to 0800 UTC was generally between 50 and 60 100 km h⁻¹. Through much of southeast Tasmania relative humidity fell below 10% on both 11 and 12 October, and was as low as 4% during the afternoon of 12 October at Hobart Airport.

The final, very significant, feature of the event was its longevity. It has already been noted that Hobart Airport experienced an extended period of FFDI greater than 100. FFDI at Hobart city observation site, 15 km to the west, was "Very High" from 2239 UTC on 10 October until 0915 UTC the following day, when a cool change moved through. It is rare

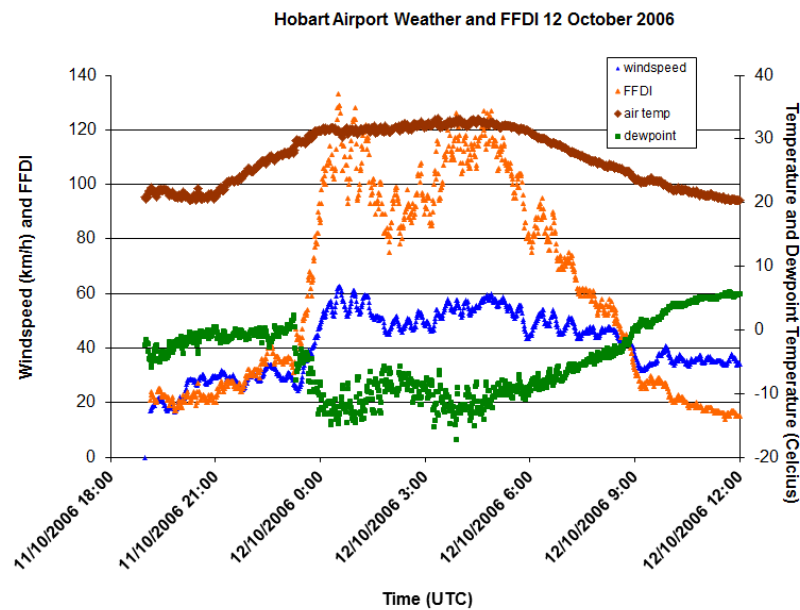


Figure 4.13: Plot of air temperature ($^{\circ}\text{C}$, brown), dewpoint temperature ($^{\circ}\text{C}$, green), windspeed (km h^{-1} , blue) and FFDI (orange) at Hobart Airport on 12 October 2006.

that two consecutive days record “Very High” fire danger in Tasmania, and unprecedented in the available record that FFDI in excess of 70 should be reported on consecutive days.

4.2.2.2 Antecedent conditions

Precursor conditions to 12 October were themselves exceptional. Southeastern Australia was in the grip of a decade-long drought (Trewin, 2006). Locally, parts of northern, central and southeastern Tasmania experienced driest-ever winter conditions (Figure 4.14). Despite some reasonable rainfall during September, record low year-to-date rainfalls to the end of September occurred at Hobart and a number of other locations. Finally, in the two weeks leading to 11 October, “Very High” FFDI occurred on five days, representing a very early, severe start to the 2006-07 fire season.

4.2.2.3 MSLP Progression

A 1038 hPa high pressure system located over the Bight on 9 October (Figure 4.15(a)) moved steadily eastward, weakening slightly to 1034 hPa, to be located over the southern New South Wales coast at 0000UTC 10 October (Figure 4.15(b)) as it began to direct a northwesterly airstream over Tasmania. A series of low pressure systems began to move well south of Tasmania from the evening of 10 October. At 0000 UTC on 11 October (Figure 4.15(c)), a broad area of low pressure lay from about 140°E to 160°E , south of

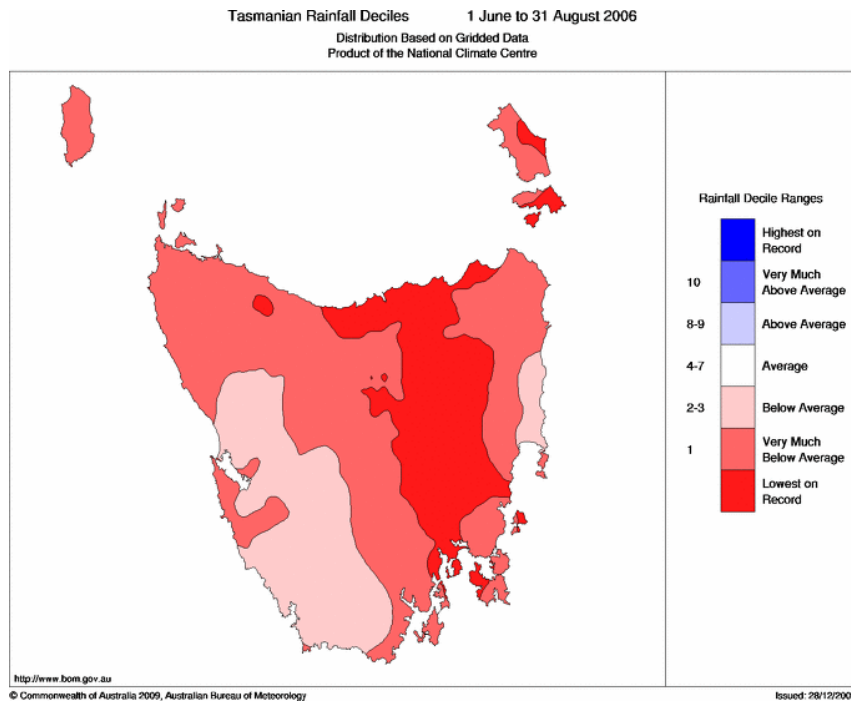


Figure 4.14: Tasmanian rainfall deciles for the three month period 1 June to 31 August 2006.

55 °S, with a cold front extending from a low center within the broader trough (outside the area of the Australian Region MSLP analysis) to a second low centered near 45 °S 115 °E.

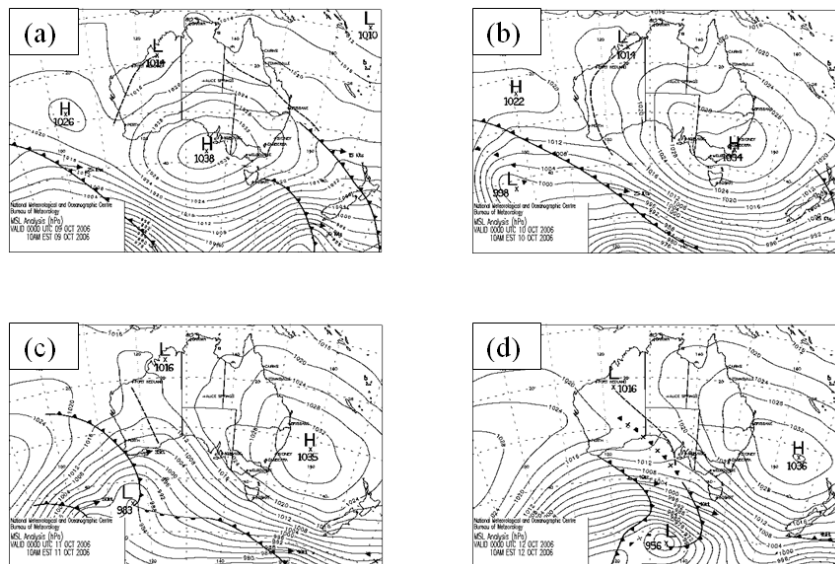


Figure 4.15: MSLP Analyses for 0000 UTC on (a) 9, (b) 10, (c) 11 and (d) 12 October 2006.

By 0000 UTC 12 October (Figure 4.15(d)), the northern portion of the cold front now approaching Tasmania had begun to weaken as most of the temperature contrast by which it had been defined became associated with a pre-frontal trough that had developed from the

Western Australian heat trough. At Tasmanian latitudes, however, the front maintained its structure and the pressure gradient over Tasmania tightened further as the front approached, before crossing the island in the late afternoon.

4.2.2.4 Upper Level Analysis

A mesoLAPS 300 hPa windspeed chart is presented in Figure 4.16, valid at 0300 UTC 12 October with the same boundaries as the case of 7 November 2002. A broad trough extended westward from the area of the figure, and a secondary trough was evident by slight curvature in the isotach field, particularly south of 50°S 138°E. A broad jet extended over waters south of Australia, with embedded maxima in excess of 70 m s⁻¹, on the flanks of the secondary trough, one immediately to the southwest of Tasmania with a second south of the Bight. The jet had been present in much the same location through the day, and persisted into the evening (not shown). Meanwhile the embedded maxima progressed steadily eastward within the broader area of enhanced flow.

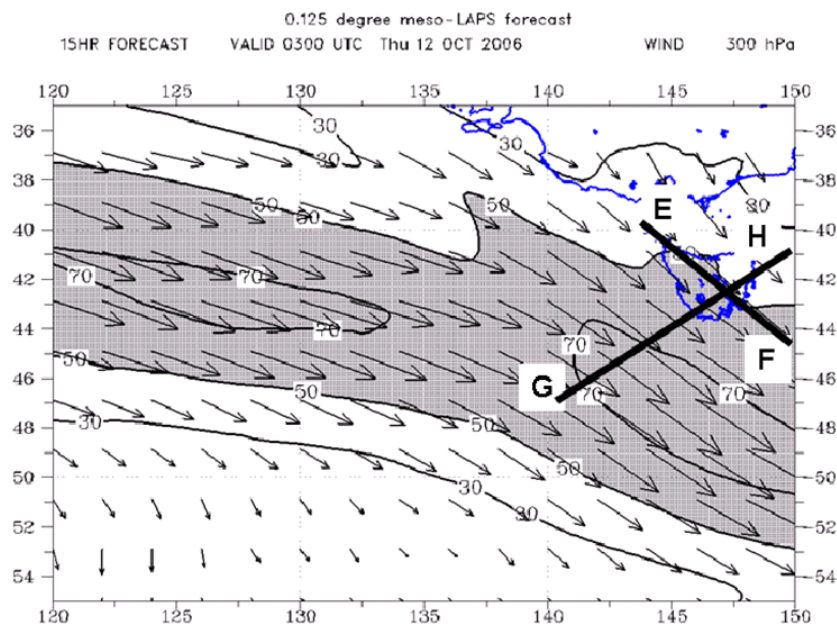


Figure 4.16: MesoLAPS 300 hPa chart, as per Figure 4.5, at 0300 UTC 12 October 2006.

4.2.2.5 Airmass characteristics

Low relative humidity was a particularly striking feature of early October 2006, with values below 15% (exceptional near sea-level in Tasmania) on several occasions, including 11 and 12 October. At 2300 UTC 10 October (Figure 4.17), a very dry layer was evident near

800 hPa. Dewpoint temperature was $-35\text{ }^{\circ}\text{C}$ at that level, and was in fact negative through almost the entire troposphere. Also at around 800 hPa was a temperature inversion of about $2\text{ }^{\circ}\text{C}$. By 2300 UTC 11 October the airmass below 800 hPa was almost completely mixed above a very shallow radiation inversion, with the dewpoint temperature approximately $-5\text{ }^{\circ}\text{C}$ through the layer. By 0100 UTC 12 October, the surface temperature at Hobart Airport was $32\text{ }^{\circ}\text{C}$, sufficient to substantially erode the isothermal layer between about 720 and 780 hPa evident on the morning sounding, permitting dry adiabatic mixing to at least 700 hPa, and very nearly to 600 hPa. Mixing the airmass below 700 hPa resulted in a surface dewpoint temperature around $-5\text{ }^{\circ}\text{C}$, similar to that experienced during the mid-morning of 12 October (Figure 4.13). For a period of several hours in the late morning and afternoon, however, the dewpoint temperature was substantially lower than that.

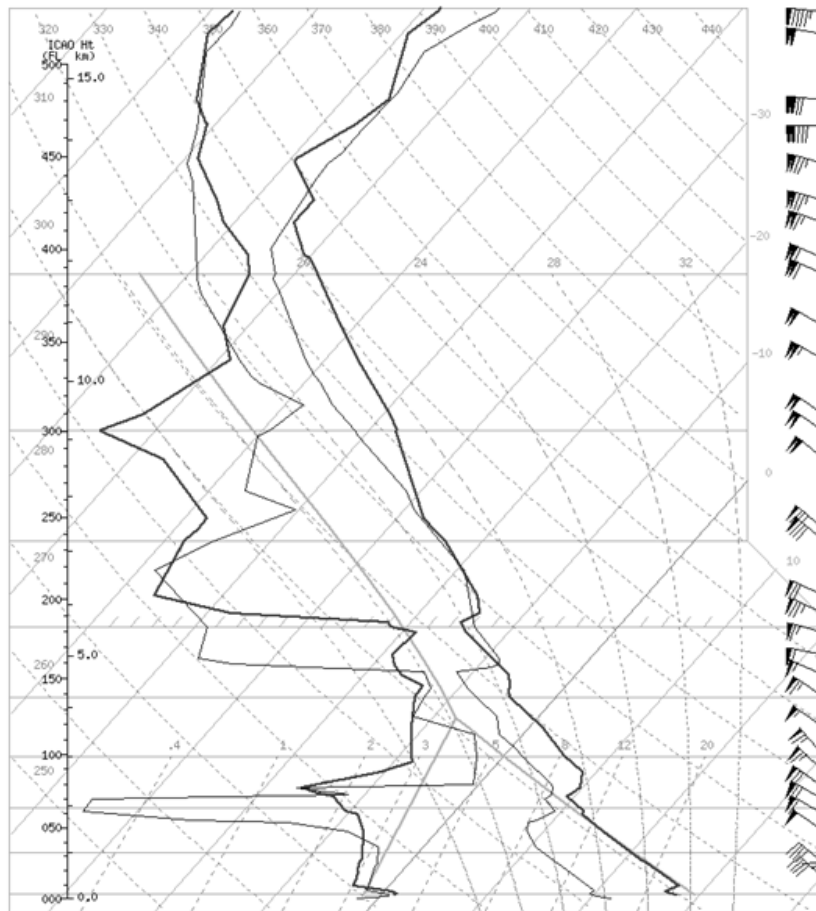


Figure 4.17: Routine radiosonde flights from Hobart Airport at 2300 UTC 10 October (grey) and 2300 UTC 11 October (black).

The source of the very dry air over Tasmania during this event was likely to have been the dry interior of continental Australia. Back trajectories from mesoLAPS were calculated

as for the previous case. The back trajectories indicate that the low level (250 m elevation) air mass over Hobart at 0000 UTC 12 October had been over western Victoria some twelve or more hours earlier, and just east of Woomera around 0000 UTC 11 October, where air parcels were modelled to have been at elevations between 500-1000 m. The atmospheric sounding for Woomera at 2300 UTC on 10 October (Figure 4.19) is extremely dry in the lower atmosphere. The surface dew point was -18°C , with a resulting relative humidity below 10%. While the dewpoint temperature increased (to -9°C) immediately above the surface, it again fell abruptly near 900 hPa and was below -40°C between about 850 and 700 hPa. In the layer from which the Hobart parcels were derived, dewpoint temperature was -10 to -11°C . Considering the moisture content of the air mass above and below this level, there was no opportunity for the admixture of more moist air into the layer. Advection of this air over Tasmania would certainly have been capable of resulting in the low relative humidity experienced during the late morning and early afternoon of 12 October, had it reached the surface.

A period of sustained descent over several days, increasing between 0000 and 1800 UTC on 10 October, is indicated by back trajectories (Figure 4.18) as air parcels followed an anticyclonically curved path. The location of the steepest descent, between about 28°S 145°E and 32°S 140°E , corresponds to the position of a northwest-oriented ridge extending from the high pressure center (Figure 4.15(b) and (c)), wherein such descent might be expected, despite the generally poleward trajectory of the air parcels. This period of descent would have contributed to the warming and drying of the air mass.

As the air crossed Bass Strait, there existed the possibility that it might have acquired additional moisture. Indeed, air parcels descended close to the surface near King Island while crossing Bass Strait (Figure 4.18). Measurements of the air mass over Tasmania do not, however, suggest that any significant amount of moisture was entrained at that time. The arguments presented in the discussion of the air mass trajectory leading to 7 November 2002, over the Great Australian Bight, are equally valid here. Hot continental air moving over the relatively cool waters of western Bass Strait would tend to reinforce a temperature inversion atop a shallow maritime boundary layer, inhibiting mixing into the dry layer above.

4.2.2.6 Mesoscale features

The operational mesoLAPS model, initialised at 1200 UTC 11 October, is used for additional diagnosis of the processes resulting in the weather experienced in southeast Tasmania on 12 October. Cross-sections through the path of the back trajectory between 40°S 144°E

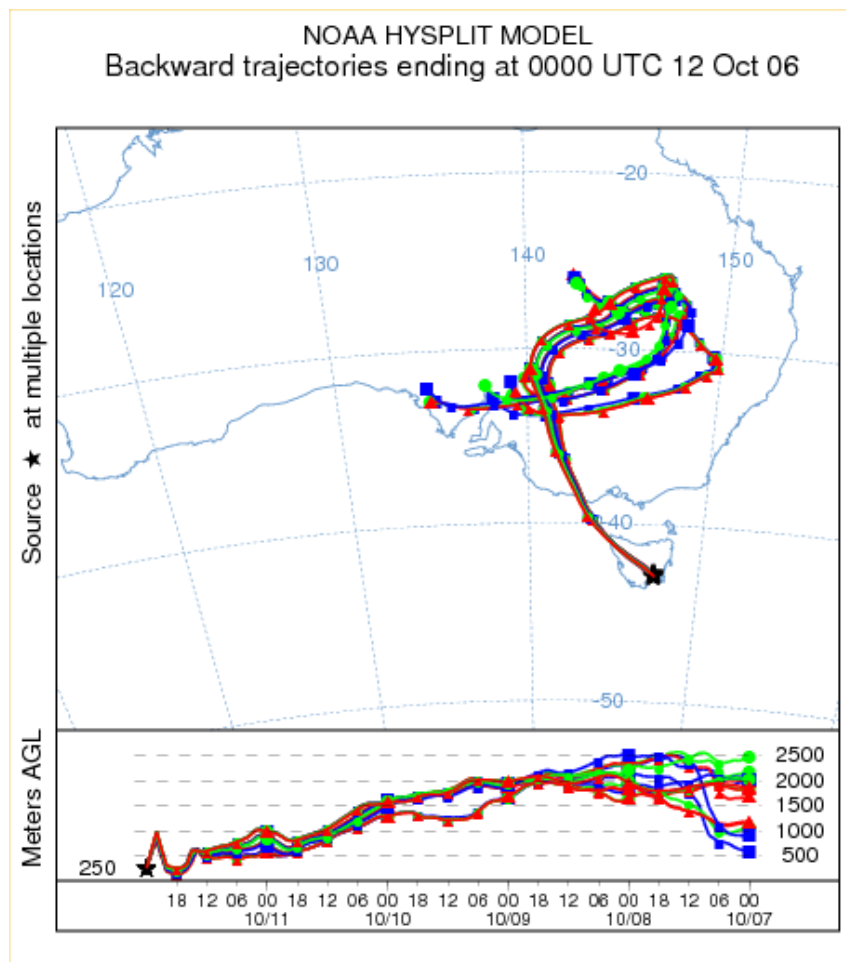


Figure 4.18: Model back trajectories ending at Hobart on 0000 UTC 12 October 2006, details as Figure 4.9.

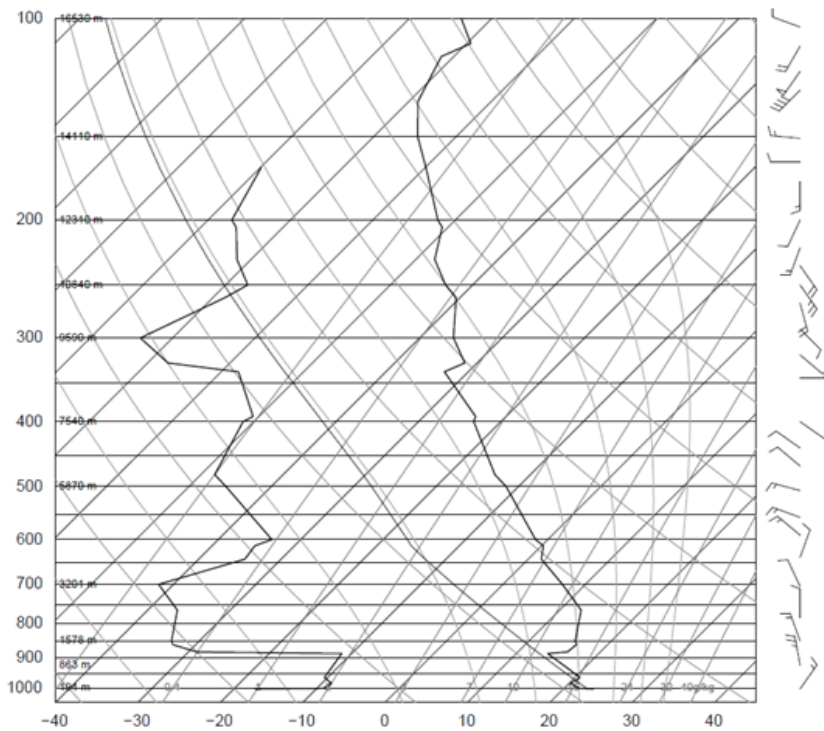


Figure 4.19: Routine radiosonde trace for Woomera at 2300 UTC 10 October.

and 45 °S 149 °E (line EF in Figure 4.16) reveal a pattern from early morning 12 October through the day consistent with a foehn wind.

Blocking of the low-level flow is evident both in observations from the north coast of Tasmania and in NWP output. Figure 4.20(a) displays potential temperature along the cross-section at 0000 UTC 12 October, with Hobart's approximate location indicated by an arrow. A well-mixed layer is evident between about 600 and 800 hPa across the breadth of the cross-section, with a generally well-mixed boundary layer in the lee of the Tasmanian Central Plateau on the right side of the figure. On the northwestern (left) side of the Tasmanian orography, potential temperature increases sharply with height, indicating a low-level maritime boundary layer, over which drier air from the Australian continent is able to flow. Observations from the north coast of Tasmania on 12 October support this conclusion. At coastal Devonport Airport the 0500 UTC temperature and dewpoint temperature were 20 °C and 10 °C. Some 23 km inland, at 295 m elevation, Sheffield recorded 23 °C and -3 °C. Clearly, the maritime boundary layer was quite shallow and limited to near-coastal locations.

The forecast cross-section of vertical motion, valid 0000 UTC 12 October, Figure 4.20(b), is representative of the sequence of vertical motion cross-sections from mesoLAPS during the day. Downward motion is indicated by solid lines, and upward vertical motion by dashed

lines, scaled every 20 hPa hr⁻¹. The model representation of the Tasmanian Central Plateau lies in the center of the cross-section, rising to approximately 900 hPa. Strong descent is clear immediately in the lee of significant orography, with peak descent rates over Hobart area exceeding 125 hPa hr⁻¹ near 850 hPa.

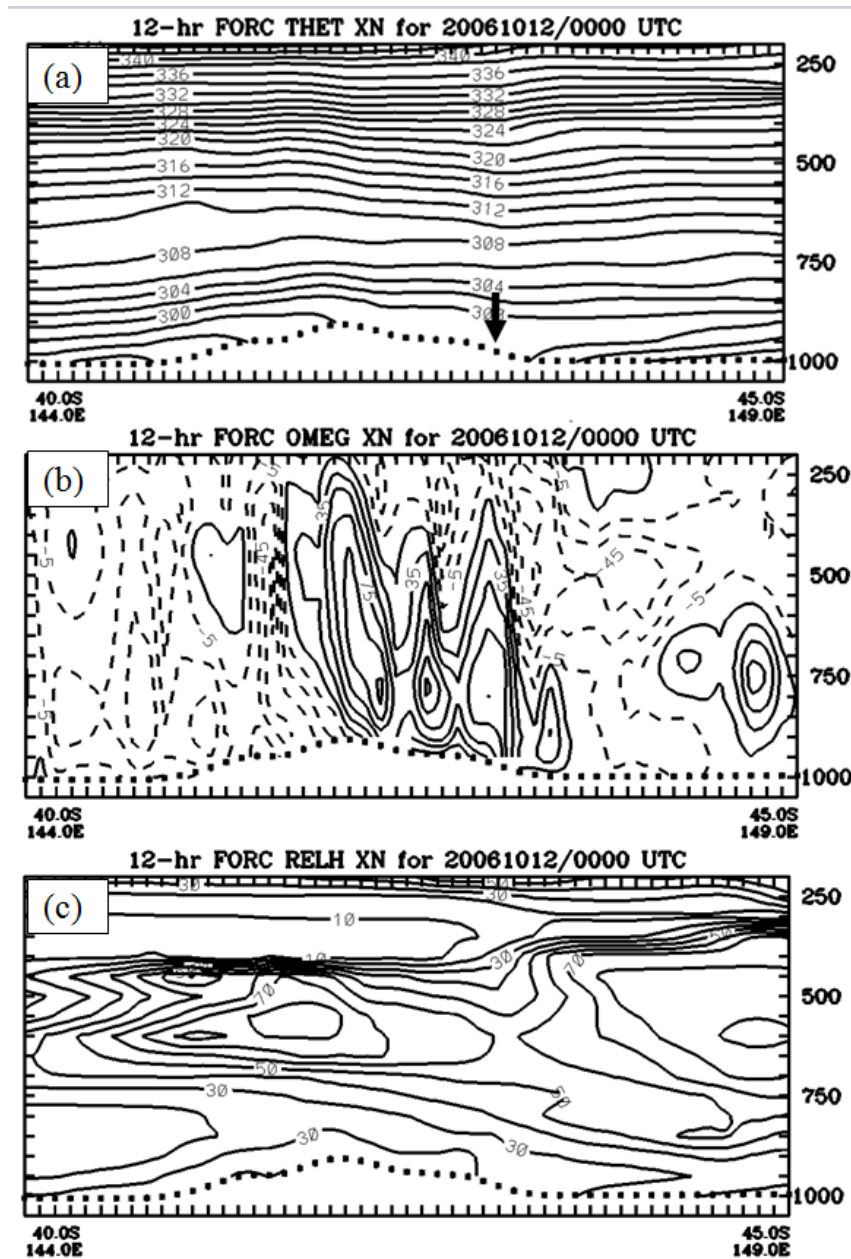


Figure 4.20: 12 hour forecast cross-sections along the line EF in Figure 4.16 (40.0 °S 144.0 °E to 45.0 °S 149.0 °E) from the 1200 UTC 11 October mesoLAPS numerical model run, valid 0000 UTC 12 October. Approximate location of Hobart is indicated by the arrow in the top panel. (a) Potential temperature isentropes, in K, at intervals of 2 K (b) Vertical motion, in hPa hr⁻¹, negative values dashed and contour interval 2 hPa hr⁻¹ (c) Relative humidity, at intervals of 10%.

Visible satellite imagery from mid-afternoon further suggests a foehn effect (Figure 4.21).

Sufficient cloud is visible to suggest the presence of a foehn wall extending from the far northwest of Tasmania over the western Central Plateau, with a foehn gap over southeast Tasmania. It is instructive to examine the model output relative humidity fields along the back trajectory path above from the same model run. At the three-hour forecast timestep (not shown), a layer of air with RH below 10% is evident north of the Tasmanian landmass at about 900 hPa, embedded in a broad low level layer of dry air (RH below 30%), extending up to about 800 hPa. However, the model does not advect the driest air over the Tasmanian orography, as surface observations indicate occurs, and seems to mix out the driest layer by the 12-hour forecast at 0000 UTC 12 October (Figure 4.20). It has been argued (Draper and Mills, 2008) that numerical models can have difficulty in representing accurately near-surface moisture fluxes. It seems likely in this case that the model is unable to correctly diagnose the moisture content of the airmass as it crossed the Tasmanian highlands.

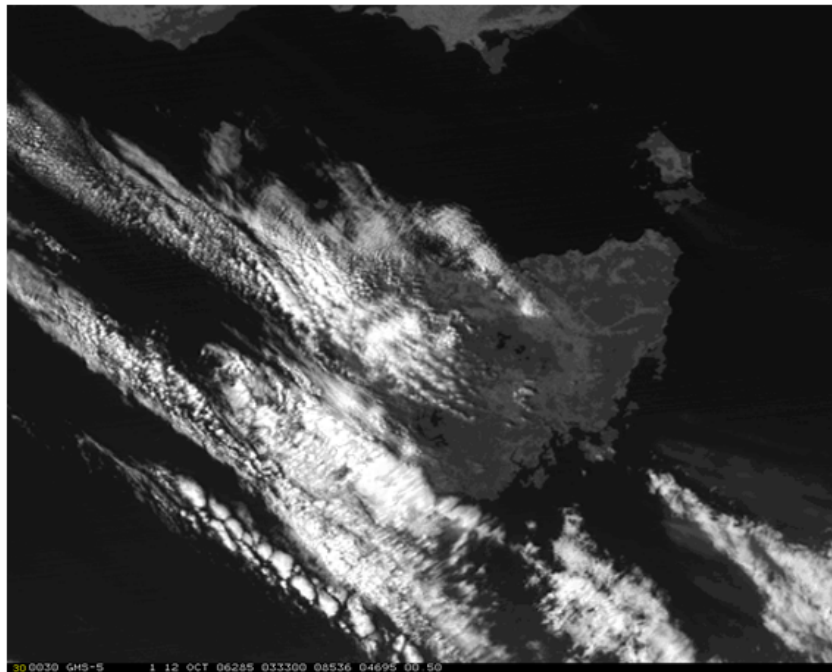


Figure 4.21: Japanese MTSAT-1 visible image of Tasmania, valid 0330 UTC 12 October. Frontal and prefrontal cloud is evident to the west of, and over western, Tasmania, and again to the southeast of the island. This pattern, and the absence of cloud over the southeast, is suggestive of the operation of a foehn effect at the time.

In this case, as in others cited by Sharples et al. (2010), the topographically generated downslope winds were sufficient to generate dangerous fire weather conditions. Adequate dry air pre-existed within the lower troposphere to permit the occurrence of the observed conditions, in contrast to the situation on 7 November 2002, where air was advected from higher in the atmosphere.

A 300 hPa jet streak lay to the southwest of Tasmania on 12 October 2006, in a similar location to that of 7 November 2002, yet there is no evidence from the observational record of dry air intrusions from high in the atmosphere. Certainly, the trough axis lay considerably further to the west in that event than in November 2002. It is, nonetheless, interesting to examine cross-sections of numerical model output to ascertain details of processes operating during the day. Fig. 22 represents a cross-section along the line GH in Fig. 16 of the 15 hour forecast mesoLAPS model atmosphere, initialised at 1200 UTC 11 October. As is the case on 7 November 2002, a tropopause depression is evident on the left of Figure 4.22(a), with a region of strong PVU gradient dropping from above 200 hPa to about 400 hPa, associated with the position of the jet streak (Figure 4.22(b)). A region of anomalous PV (-0.7 PVU) extends as low as 850 hPa, with a broad area of relative humidity below 30%.

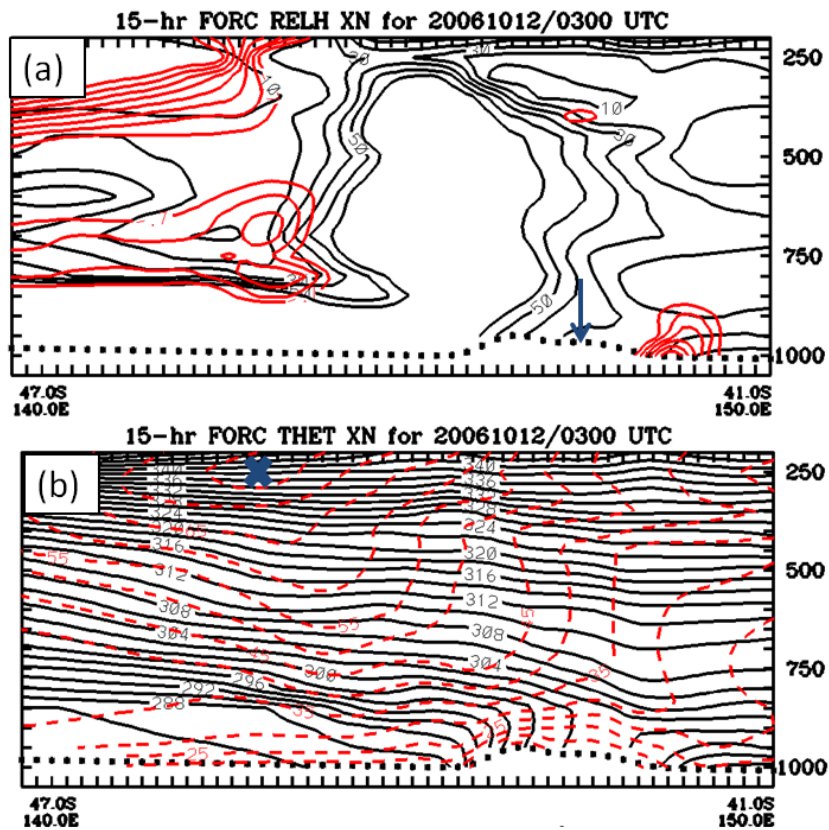


Figure 4.22: MesoLAPS model cross-sections through the line GH in Figure 4.16 at 0300 UTC 12 October, showing: (a) relative humidity (black), at intervals of 10%, between 10 and 60%, and potential vorticity (red), at intervals of 0.5 PVU between -1 and -2 PVU. The approximate location of Hobart is indicated by an arrow. (b) potential temperature isentropes (black) at intervals of 2 K, and windspeed (red, dashed) isotachs at intervals of 5 m s⁻¹. The jet streak location is indicated by a cross.

Examination of the isentropes, however, reveals an essentially horizontal orientation between approximately 700 and 850 hPa over waters west of Tasmania (left-hand side of the

figures), such as to inhibit the transport of upper level air any closer to the surface. This is in contrast to the situation on 7 November 2002, where isentropes slope markedly from the region of the jet streak towards the surface in the vicinity of Tasmania, enabling the progression of high momentum, high PV and low humidity air to the surface.

4.3 Discussion

The most dangerous fire weather experienced in Tasmania occurs with the passage of Southern Ocean cold fronts (Brotak and Reifsnnyder, 1977, Marsh, 1987). Springtime fire weather events follow this pattern, including the two events examined here. Further, the area experiencing heightened fire weather in each case was largely confined to eastern and particularly southeastern Tasmania, fitting the pattern of springtime fire danger discussed in Fox-Hughes (2008). In Figure 4.23 are plotted peak fire dangers experienced at stations in the Tasmanian observation network on (a) 07 November 2002 and (b) 12 October 2006. Most FFDI values plotted were obtained from routine reports recorded during the events, but, as discussed above, Hobart Airport values (arrowed) were recalculated using data recorded every minute. In addition, the two bracketed values in both plots are high-level southeastern stations, both above 800 m and less representative of fire weather conditions close to sea level. It is clear that elevated FFDI occurred predominantly in eastern and southern parts of Tasmania in both events, peaking in the southeast.

While strong winds and high temperatures contributed to the dangerous fire weather conditions observed, both of these springtime fire weather events were characterised particularly by extremely low dewpoint temperatures. The recording of -14°C dewpoint temperature at Hobart Airport on 12 October 2006 is lower than that on all but two other days (the latter including 11 October 2006). In a database of airport weather reports between 1990 and 2008, the observation ranks equal fifth lowest of the 322,000 observations. The lowest dewpoint temperature recorded on 7 November 2002 puts it at seventh in the same ranking scale, with only 16 observations of the same dataset recording lower dewpoint temperature. It is noteworthy that of the seven days recording such low dewpoints, six fall within the spring months of September to November, with five in October-November.

The documentation of each case study above indicates that there were a number of similarities in the mechanisms acting to cause surface drying. In both events studied, air was advected over Tasmania from the Australian continental interior ahead of approaching cold fronts, and slowly descended around the flanks of high pressure systems (Figure 4.4 and

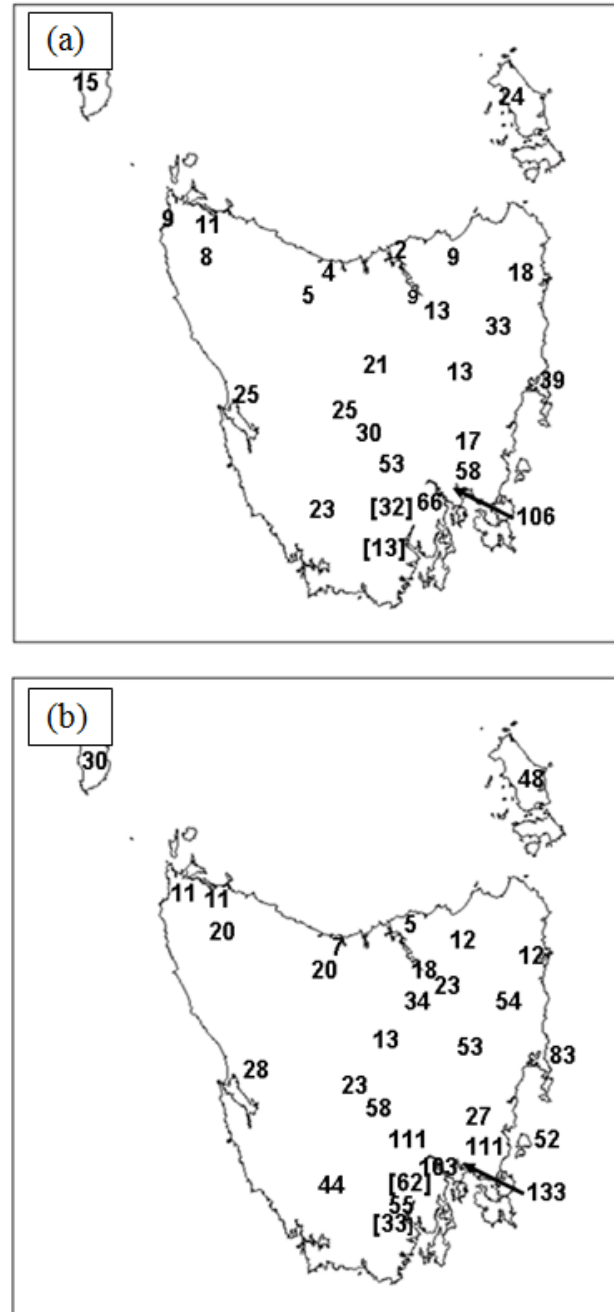


Figure 4.23: Peak McArthur FFDI values recorded on (a) 7 November 2002 and (b) 12 October 2006. In both diagrams, Hobart Airport values were computed from one minute data stream, as discussed in the text. Values for other locations were obtained from routine AWS reports during the days.

Figure 4.9, in the case of 07 November 2002, and Figure 4.15 and Figure 4.18 in the case of 12 October 2006). At these times, the regions from which air was advected over Tasmania were drought-affected and the air columns were consequently very dry (Figure 4.8(b) and Figure 4.19). Notably, the trajectories in each case originate over substantially different parts of continental Australia.

In both events, a foehn effect was evident and associated mountain wave activity, together with thermal mixing, acted to bring the advected dry air to the surface (Figure 4.12(a) and (b), and Figure 4.20(a) and (b)). This aspect of both cases is not uncommon in other documented fire weather events. Sharples et al. (2010) note the association between foehn winds and fire weather documented in a number of locations around the world, and document occurrences in southeastern Australia. Moritz et al. (2010) in particular point to the correlation between the preferred locations of modelled foehn-like Santa Ana of southern California and historical patterns of large wildfire activity. Mills (2008b) discusses the requirement for atmospheric processes to act in concert to produce surface drying – one process to supply dry air to mid- or low-levels, and a further process such as thermal or turbulent mixing over topography to occur to bring the dry air to the surface.

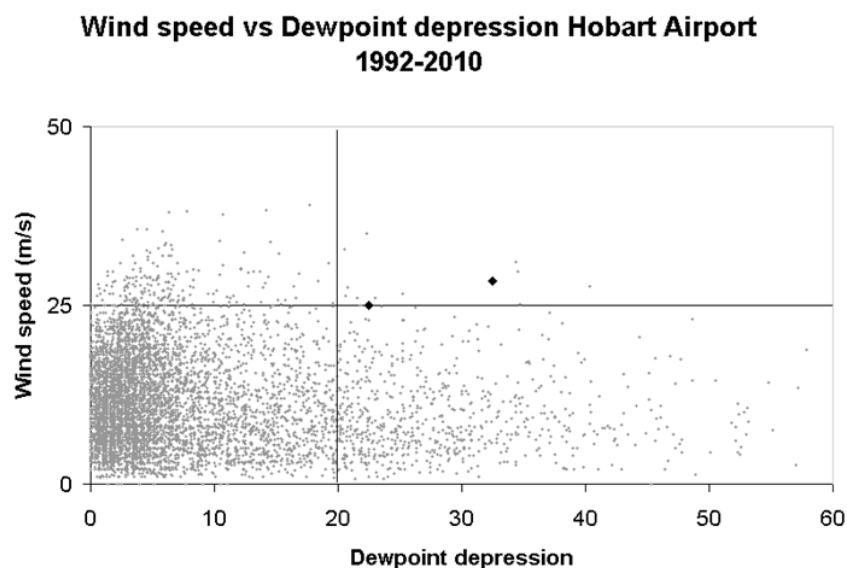


Figure 4.24: Scatterplot of Hobart Airport 850 hPa wind speed (m s^{-1}) and dewpoint depression ($^{\circ}\text{C}$) from routine 2200 or 2300 UTC (0900 local time) radiosonde soundings between 1992 and 2010. The two case study values are indicated by black diamonds. Threshold values of 25 m s^{-1} and $20 \text{ }^{\circ}\text{C}$, as discussed in the text, are represented by gridlines.

The coupling of such processes is suggested in Figure 4.24, a scatterplot of 850 hPa dewpoint depression (difference between dry-bulb and dewpoint temperatures) against wind speed at the same level, from routine morning radiosonde flights at Hobart Airport between

1992 and 2010. Here, it is assumed that higher windspeed at mountaintop height is likely to result in generation of mountain waves, with some degree of efficiency, resulting in dry air aloft mixing to the surface. Data points corresponding to the two case studies are represented by black diamonds. On 7 November 2002, windspeed was 28.4 m s^{-1} with a dewpoint depression of $32.5 \text{ }^{\circ}\text{C}$, while on 12 October 2006 corresponding values were 25 m s^{-1} and $22.5 \text{ }^{\circ}\text{C}$. The two cases lie at the upper right extreme of the plot. Most points lie in the lower left of the plot, corresponding to relatively light winds and small dewpoint depression. Some cases exhibit very large dewpoint depression ($> 50 \text{ }^{\circ}\text{C}$), but these generally are associated with light winds, and are hence likely to result from the presence of subsidence inversions associated with high pressure systems. It should be noted that extreme non-linearity of the dewpoint calculation at such low humidities makes exact values uncertain, however, it remains the case that the airmass is exceptionally dry on such occasions. MSLP analyses of the relatively few days corresponding to these parameter values confirm that they are largely days on which high pressure systems or ridges are close to Tasmania. Partitioning the plot at 25 m s^{-1} and $20 \text{ }^{\circ}\text{C}$ results in only 12 datapoints in the upper right quadrant. Of those during the October-March fire season (eight cases), five were days of significant fire danger while the others were affected by pre-frontal cloud. This analysis, abstracting common features of the springtime cases examined, may help alert forecasters to potential fire weather events some days ahead and provide a useful flag for fire weather events in climate change studies with large scale general circulation models.

In addition to the mechanism outlined above, it is very likely that additional processes operated on 7 November 2002. A pulse of exceptionally dry air is evident in the plot of weather data from Hobart Airport AWS (Figure 4.2) in the late afternoon, some hours after thermal mixing occurred to bring pre-existing dry air to the surface. There is good evidence from numerical weather guidance (Figure 4.10(a)) that an intrusion of stratospheric air occurred to below 900 hPa with the approach of a trough and associated cold front. The band of drier air associated with the intrusion can be seen in satellite imagery close to the time indicated in the numerical guidance (Figure 4.7). With thermal and/or turbulent mixing occurring to at least 3000 m (Figure 4.10(b)), the intrusion's dry, high-momentum air then mixed to the surface, resulting in the observed spike in weather parameters.

Investigation of these cases studies suggests techniques for forecasters to evaluate future events. Operational numerical weather prediction models are clearly capable of resolving the origins of environmental dry air in many cases. Visualizations, including vertical cross-sections, of model output displaying such fields as PV, relative humidity and potential

temperature may offer valuable clues to the likelihood of occurrence of rapidly escalating fire danger ahead of cold fronts. The 2002 case demonstrates that an awareness of a stratospheric intrusion can be important for fire weather forecasters and managers. Even after the atmosphere has become fully mixed during an already dangerous fire weather event, the movement into an area of such an intrusion can result in a substantial increase in observed fire danger levels. The analysis also confirms the value of water vapour imagery as an indicator of potential dry air descent in such situations.

In future, a synoptic climatology of Tasmanian springtime fire weather events will be undertaken, placing the occurrence of dangerous springtime events into broader context, to further improve understanding of these weather systems. This will result in improved forecasts of dangerous fire weather, and better outcomes for the community.

4.4 Acknowledgments

Several colleagues at the Australian Bureau of Meteorology assisted in the preparation of this paper. Graham Mills reviewed drafts and offered helpful suggestions, Alan Wain facilitated back trajectory figures, Lawrie Rikus prepared pseudo-WV imagery and Bert Berzins extracted archived satellite imagery. Kelvin Michael of the University of Tasmania's Institute for Marine and Antarctic Studies reviewed a draft of this paper. Figure 1 was prepared using the Jules map server at www.unavco.org, and the atmospheric soundings in Figures 4.8(a), 4.8(b) and 4.19 were generated from the University of Wyoming Department of Atmospheric Science server.

5: Characteristics of some days involving abrupt increases in fire danger

Abstract

A class of fire weather events has been identified recently in which the normal, often diurnal, rise and fall of fire danger is interrupted by abruptly worsening conditions, “spikes”, for which fire managers may be unprepared. Frequent observations from a site in Tasmania, Australia, show that spike events are associated with the passage of negatively-tilted upper tropospheric troughs, leading to descent into the atmospheric boundary layer of dry, high momentum air, a result supported by satellite water vapour imagery. Case studies from other major fire events, both in Australia and in the Northern Hemisphere, show similar characteristics. Statistically significant differences exist between the location and placement of trough and jet streak features during spike events and normal fire weather events, with differences in satellite water vapour imagery features also evident. The seasonality of spike events differs significantly from other fire weather events, with their occurrence peaking in late spring to early summer in Tasmania, in contrast to broad summer primary and mid-spring secondary peaks of non-spike events.

5.1 Introduction

Fire weather events are of concern to land managers and communities around the world. In most such events, fire danger increases following the erosion of an overnight inversion and will frequently reach a peak during the middle of the day or the afternoon, oscillating around the peak until a diurnal easing in the evening, or a cool change moves through (Millán et al., 1998, Mills, 2002). In some cases, however, following what appears to be the peak of an event, a further, abrupt, increase in fire danger occurs, with conditions becoming very substantially worse as a result of a rapid increase in wind, decrease in relative humidity, or both. Such events have been documented in numerous locations around the globe (Kaplan et al., 2008, Kondo and Kuwagata, 1992, Mills, 2008a,b, Zimet et al., 2007), including southeast Tasmania, Australia. Southeast Tasmania is subject to outbreaks of dangerous fire weather and occasional devastating wildfires (Bond et al., 1967, Foley, 1947), most recently on 4 January 2013 when over 200 structures were destroyed around the township of Dunalley.

Fox-Hughes (2012) (hereinafter referred to as FH2012) investigated two fire weather events occurring in this region, identifying characteristics of one event, which resulted in a “spike” of fire danger during the early evening, that were absent in the other “non-spike” (but still very dangerous) event. In the spike event, a lobe of high potential vorticity (PV) air extended from the tropopause to heights that were well below the top of the mixed surface layer of the atmosphere over southeast Tasmania at the time, allowing the passage to the surface of high momentum, low relative humidity air, resulting in the rapid increase in fire danger. In the non-spike event, such a lobe of high PV air also existed, but was clearly cut-off from the surface. A feature of many fire weather events in which rapid increases in fire danger have occurred is the presence of a “dry slot” or elongated dark band in satellite water vapor (WV) imagery (Mills, 2008b). Such a dry slot was evident during the spike event documented in FH2012. Both events above occurred during the Tasmanian springtime, September-November. During this season, there has been a marked increase in dangerous fire weather in eastern and especially southeast Tasmania over the last several decades (Fox-Hughes, 2008).

This paper aims to investigate whether the characteristics of the spike and non-spike fire weather events in FH2012 can be generalized, by

- Developing an objective means of identifying spike days
- Performing a composite analysis of spike and non-spike days;

- Comparing satellite WV imagery for spike and non-spike events; and,
- Identifying whether spike events have contributed to the increase in the number of dangerous springtime fire weather events in southeast Tasmania.

In Section 2, details of the selection of spike and non-spike days are discussed, together with the selection of a set of non-event days, and the generation of composite plots of atmospheric parameters. Results are presented and analysed in Section 3, and Section 4 presents concluding remarks and suggests implications of some of the findings of the paper.

5.2 Data and Methods

Half-hourly weather observations at Hobart Airport, in southeast Tasmania (Figure 5.1), were used to derive McArthur Forest Fire Danger Index (FFDI) values (McArthur, 1967) during the period 1990-2010. More details of the derivation of the FFDI values used are contained in Fox-Hughes (2011). North to northwesterly airstreams are associated with the most significant fire weather events in Tasmania, and Hobart Airport is well-placed to experience a well-mixed boundary layer in these events. A combination of thermal mixing, due to the site's position on the warmer leeside of the Tasmanian landmass, and mechanical turbulence, due to the presence of substantial orography upwind of Hobart, ensures that the boundary layer extends to at least 2,000 m on such days (FH2012 highlights boundary layer depth in the two cases examined).

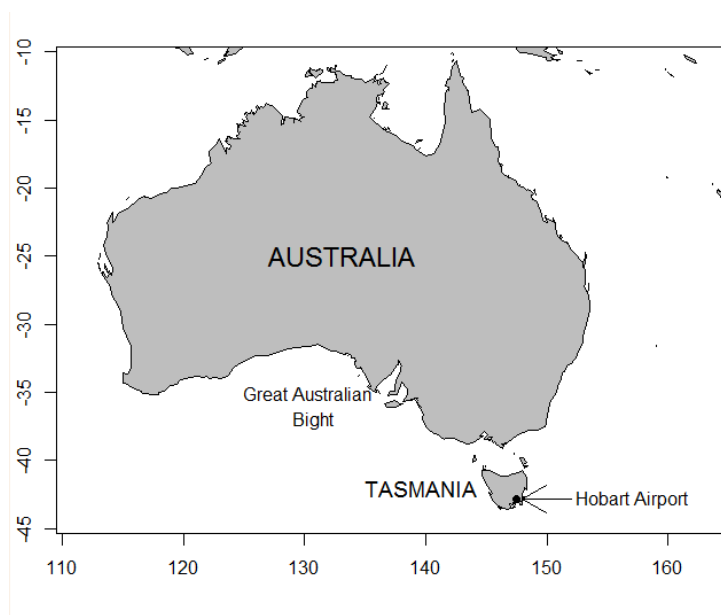


Figure 5.1: Map showing location of Hobart Airport, Tasmania.

Days with maximum FFDI values exceeding 24 (“Very High” fire danger) were selected, resulting in some 230 cases. Within that subset, the mean and standard deviation of the FFDI were calculated for those values exceeding 24, and the number of standard deviations (SD) of the maximum FFDI from the mean was calculated. Days on which the maximum FFDI was more than 2 SD from the mean were classed as fire weather spike days. The intent of this manipulation was to identify days on which fire weather conditions were already quite dangerous (the FFDI was already “Very High”) but conditions abruptly became substantially worse for a period. Some 37 days were classed as spike days on this basis.

To contrast spike days with days lacking this feature, events were selected where the maximum FFDI exceeded the mean of “Very High” observations by less than 1.5 SD. In this case, however, the maximum FFDI was required to be at least 38, the level of fire danger at which the Tasmania Fire Service generally considers the imposition of a Total Fire Ban to prevent the ignition of fires in the open. This criterion ensured that the non-spike data subset included days of very significant fire danger but, by definition, days that lacked an additional abrupt increase in the fire danger experienced during the course of the event. There were 25 days that satisfied these criteria.

Composites of atmospheric parameters were plotted for each type of event from NCEP/NCAR reanalysis data (Kalnay et al., 1996), using the facilities of the Physical Sciences Division of NOAA’s Earth System Research Laboratory (PSD/ESRL). In addition, 0000 UTC mean sea level pressure (MSLP) analyses prepared by the National Meteorological and Oceanographic Centre (NMOC) of the Australian Bureau of Meteorology corresponding to each type of fire weather event were manually examined. WV imagery for spike and non-spike events was examined for the presence of dark bands, or “dry slots” indicative of very dry air in the mid to upper troposphere (e.g. Mills (2008b)), which has potentially descended from near the tropopause.

5.3 Results and Discussion

5.3.1 Synoptic Characteristics of Events

Initially, MSLP charts at 0000 UTC (1100 local time during the months considered here) were examined for days in both fire weather sets. It has been well documented (Brotak, 1980, Marsh, 1987) that days of elevated fire danger in Tasmania, particularly in the southeast of the island, are generally associated with a frontal passage across the island. In each case of

spike days (Supplemental Figure 1, Fig. 5S1), a cold front was approaching Tasmania, or had very recently crossed the state. In the latter cases, Tasmania (in particular, the observation site of Hobart Airport) was subject to a vigorous post-frontal airstream. Equally, however, most days associated with non-spike events (Fig. 5S2) were also days of frontal or trough passages. In each of these cases, the fronts were embedded in a broader trough in the westerlies. In nonspike events, however, it was generally the case that fronts, and the broad troughs in which they were embedded, were located further westward than was the case with spike events, and consequently Tasmania was subject to a more well-defined northwesterly flow in nonspike events.

Daily composite MSLP images of (a) spike and (b) non-spike events are presented in Figure 5.2. In both composites, troughs are located close to Tasmania, with low pressure centres well south of the island, consistent with the NMOc analyses. The troughs extend from south of Australia through to heat lows over the northwest of the continent. High pressure centres are located in the Tasman Sea and in the Indian Ocean to the west of the Australian continent. Both plots correspond well to the observations noted above relating days of elevated fire danger to approaching frontal systems. The most pronounced difference between the two plots is that the trough axis is more advanced in the spike composite than in the non-spike case, with the eastern high centre located correspondingly further east. In Figure 5.2(b), stippled areas indicate where differences between the spike and non-spike MSLP patterns are significant at a 95% confidence level on a two-tailed t-test. The differences noted above are included in the stippled area, which extends over the eastern seaboard of Australia, including eastern Tasmania, the Tasman Sea to 160 °E and 60 °S (the edge of the domain considered) and areas at the head of the Great Australian Bight and waters immediately off the West Australian coast.

A similar, though more pronounced, difference in the position of the respective composite troughs is evident in a comparison of 250 hPa windspeed plots (Figure 5.3). Troughs are evident to the south of the Australian continent in both composite plots, and a wind maximum lies on the eastern flank of the trough, to the south of Tasmania. However, the spike composite trough (Figure 5.3(a)) is located 140 °E at 40 °S while the non-spike trough (Figure 5.3(b)) is well west, between 125-130 °E at the same latitude. While the non-spike 250 hPa wind maximum is stronger than that of the spike plot, with a larger core in excess of 45 ms⁻¹, the core axis lies near 50 °S. The spike wind maximum is weaker, but its axis runs over the south coast of Tasmania. Further, the composite jet at 250 hPa is cyclonically curved for the spike events but anticyclonically curved in the non-spike case. The

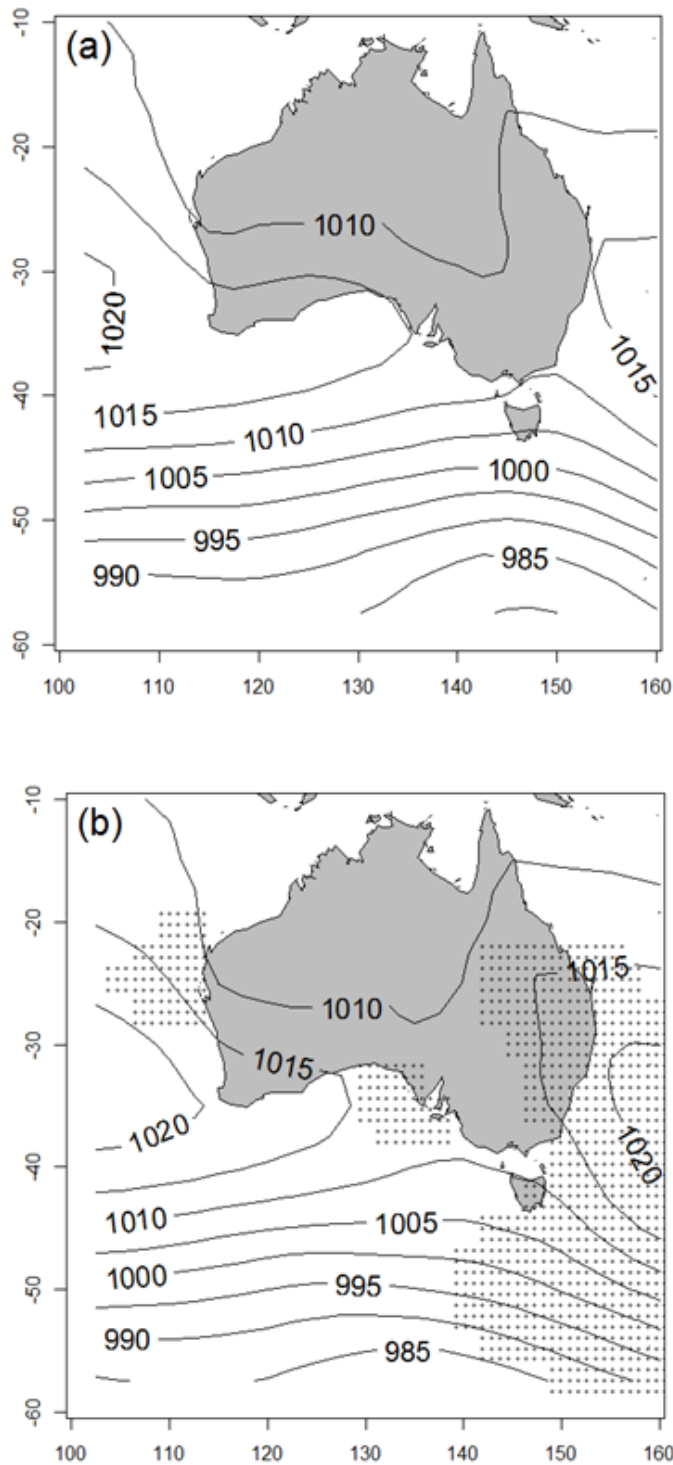


Figure 5.2: Composite MSLP plots of (a) spike and (b) non-spike fire weather events from daily NCEP/NCAR reanalyses. The stippled area in (b) indicates the region where the difference between spike and non-spike composites is significant at the 95% level.

entrance region of the cyclonically curved jet near Tasmania is a favourable location for convergence, and hence descent (Moore and Vanknowe, 1992). Vertical motion at 600 hPa for the composite spike case is superimposed on the windspeed field in Figure 5.3(a), with red tones indicating descent and blue ascent, illustrating a close alignment to the results of Moore and Vanknowe (1992). The 600 hPa vertical motion field in Figure 5.3(b) less closely approximates the anticyclonic curvature case of Moore and Vanknowe (1992), resembling more their straight line jet vertical motion field. Importantly, however, the maximum of upward vertical motion at that level lies over Tasmania, which is quite different to the spike case. Again, stippled regions represent regions where differences between the spike and non-spike 250 hPa wind fields are significant at the 95% confidence level on a two-tailed t-test. The stippled area encompasses the regions surrounding the jet streaks, including Tasmania, but excludes a strip immediately south and west of the island where the two composite jet streaks overlap.

It is worth investigating the evolution of the spike-event trough in a little more depth. A sequence of six-hour composite reanalysis plots at 1800, 0000 and 0600 UTC (corresponding to early morning, late morning and mid to late afternoon local time) on the days of spike events is displayed in Figure 5.4. They show a progressive increase in asymmetry of the trough, particularly at higher latitudes, as it advances eastward towards Tasmania, to assume a “negative” tilt (i.e. increasing longitude of the trough axis with proximity to the equator), suggesting rapid system development and potential for severe weather due to increasing vertical circulation. Atallah et al. (2007) note a similar structure in the extratropical transition of tropical cyclones, while Speer et al. (2000) have documented a number of negatively tilted troughs associated with heavy rainfall events. Macdonald (1976) and Glickman et al. (1977) describe such troughs in relation to the development of convective outbreaks. One such trough was observed, in particular, during the spike event documented in FH2012.

Composite cross-sections of relative humidity along 43 °S between 100 and 160 °E are displayed in Figure 5.5, for (a) spike, (b) non-spike and (c) non-event days from daily NCEP-NCAR reanalyses. Both spike and non-spike fire weather days suggest a well-mixed boundary layer in the vicinity of Tasmania, as expected during such events and in contrast to the non-event composite, where the boundary layer over Tasmania is indistinguishable from that over waters to the east or west. The non-spike composite has a well-defined area with relative humidity below 40% extending to below 500 hPa to the west of Tasmania, indicating the position of the upper level trough and a lower tropopause. In addition, immediately

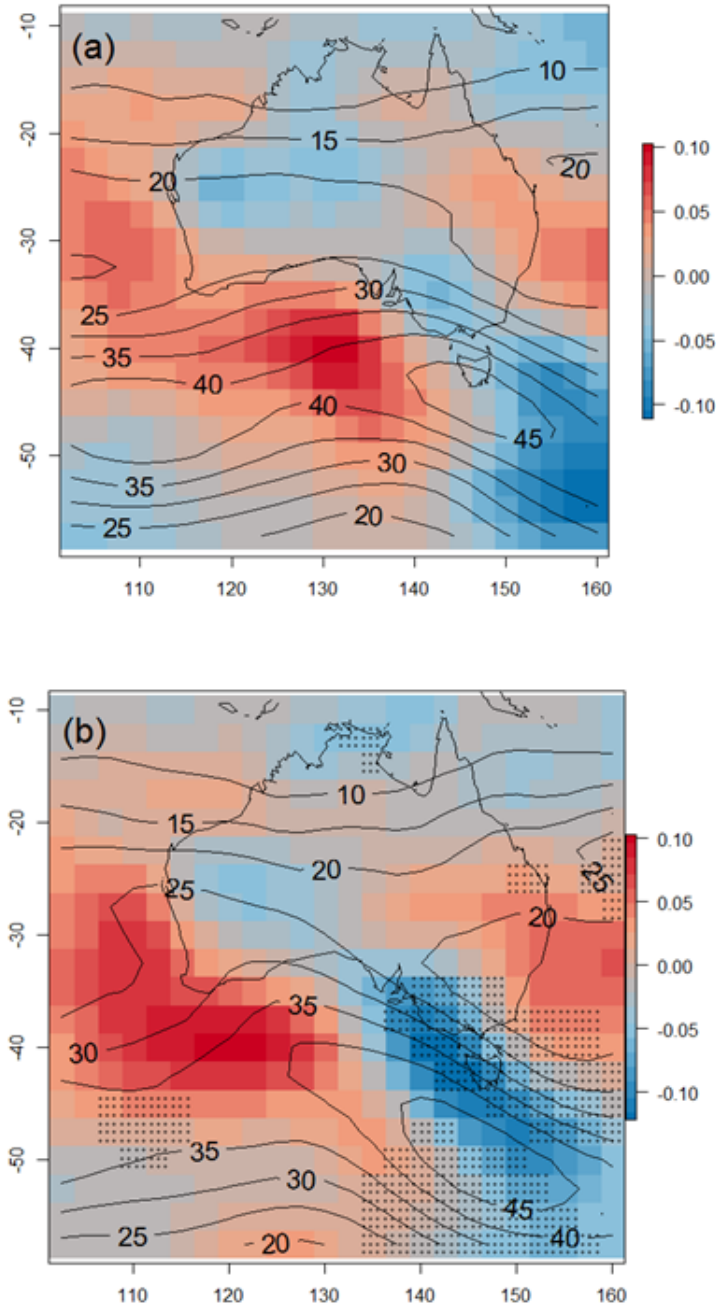


Figure 5.3: Composite plots of 250 hPa wind isotachs (in m s^{-1}) for (a) spike and (b) non-spike fire weather events from daily NCEP/NCAR reanalyses. Vertical motion at 600 hPa (Pa s^{-1}) is indicated in red (descent) and blue (ascent). The stippled area in (b) indicates the region where the difference between spike and non-spike composites is significant at the 95% level.

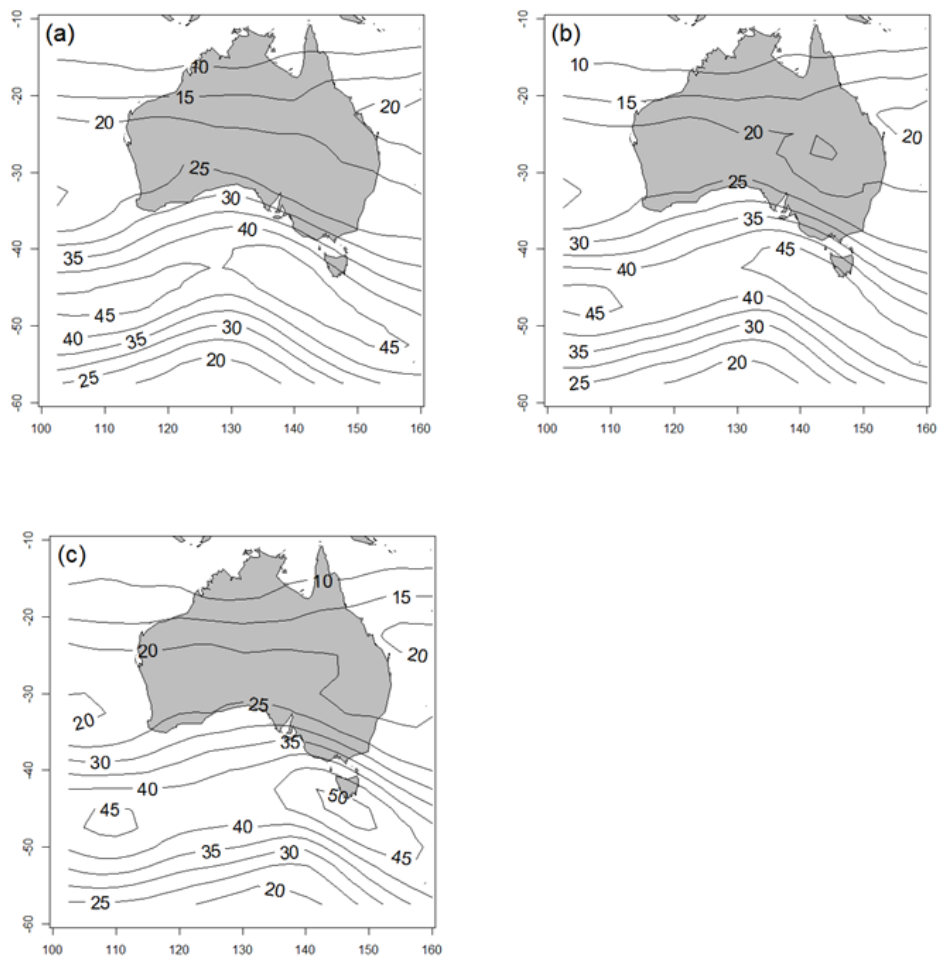


Figure 5.4: Composite plots at successive six hour intervals of NCEP/NCAR re-analysis 250 hPa windspeed (in m s^{-1}) at (a) 1800, (b) 0000 and (c) 0600 UTC.

east of Tasmanian longitudes, centred near 155 °E at about 850 hPa is a region of drier air between 40 and 45% relative humidity. Layers of dry air immediately above a pre-existing inversion typify the atmospheric profiles of days of dangerous fire weather in southeastern Australia. In these daily reanalysis composites, it is interesting that dry air associated with the upper trough in the spike composite (Figure 5.5 (a)) does not extend as strongly into the troposphere as occurs in the non-spike case. However, the trough (represented by the dry air) is centred closer to Tasmania, and there is a distinct (although weak) axis of lower relative humidity extending from the upper dry air reservoir to the well-mixed boundary layer. In the corresponding non-spike composite, while there is a similar, indeed better defined, axis extending downward to the top of the boundary layer to the west of Tasmanian longitudes, it is disconnected from the region of the well mixed boundary layer by a region of more moist air. These differences correspond remarkably well with the patterns of moist and dry air noted in the fire weather events examined in FH2012, in which one event was identified as a spike and the other as a non-spike front.

To further investigate the differences between the two types of event, composites of 0600 UTC vertical motion at 500, 700 and 850 hPa are presented in Figure 5.6 for spike and non-spike events. Clear differences are apparent: at 500 hPa, while both composites have upward vertical motion over Tasmania, it is weaker in the spike case, and the region of descent to the west (associated with the trailing flank of the trough) is much closer to the island. In the spike composite, the area of descent slopes to the east with lower elevation, so that descending air occurs over all of Tasmania at 850 hPa. The incursion of descending air in the non-spike case, if it exists at all, is much less clear, resulting in little or no descent over the state.

5.3.2 Satellite Imagery

Water vapour satellite imagery was available over the region of interest from 1995 onward, with imagery available for 31 (of 37) spike events and 15 (of 25) non-spike events (Supplementary Figures 5.S3 and 5.S4). The imagery in the hours leading to peak fire danger on spike and non-spike days was examined for features indicating dry conditions in the upper troposphere. Images were categorized as:

- having a dry slot within 5° of Tasmania;
- having an area of reduced WV within 5° of Tasmania;
- having a dry slot or area of reduced WV within 10° of Tasmania;

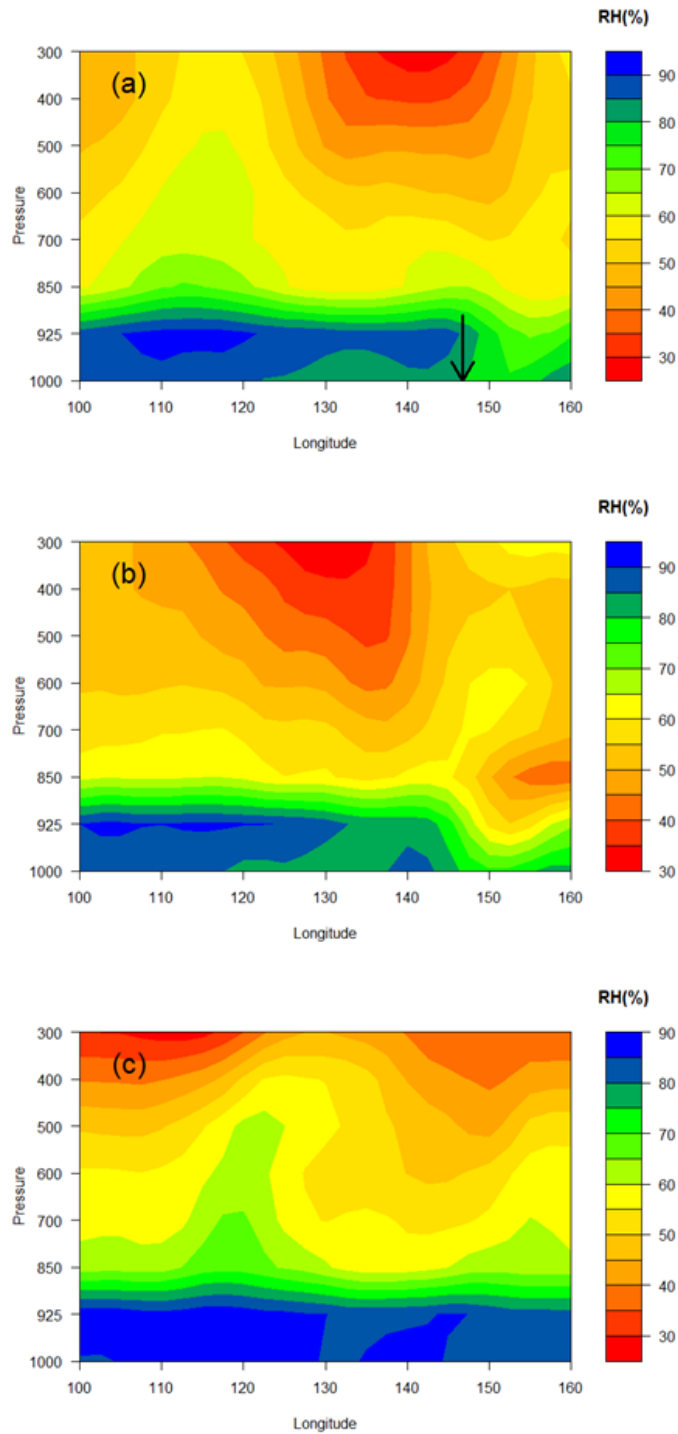


Figure 5.5: Composite cross-sections through 43°S from 100 to 160°E of relative humidity (a) spike (b) non-spike and (c) non-event daily composite plots (plots from PSL/ESRL website). The arrow in (a) denotes the position of Hobart Airport.

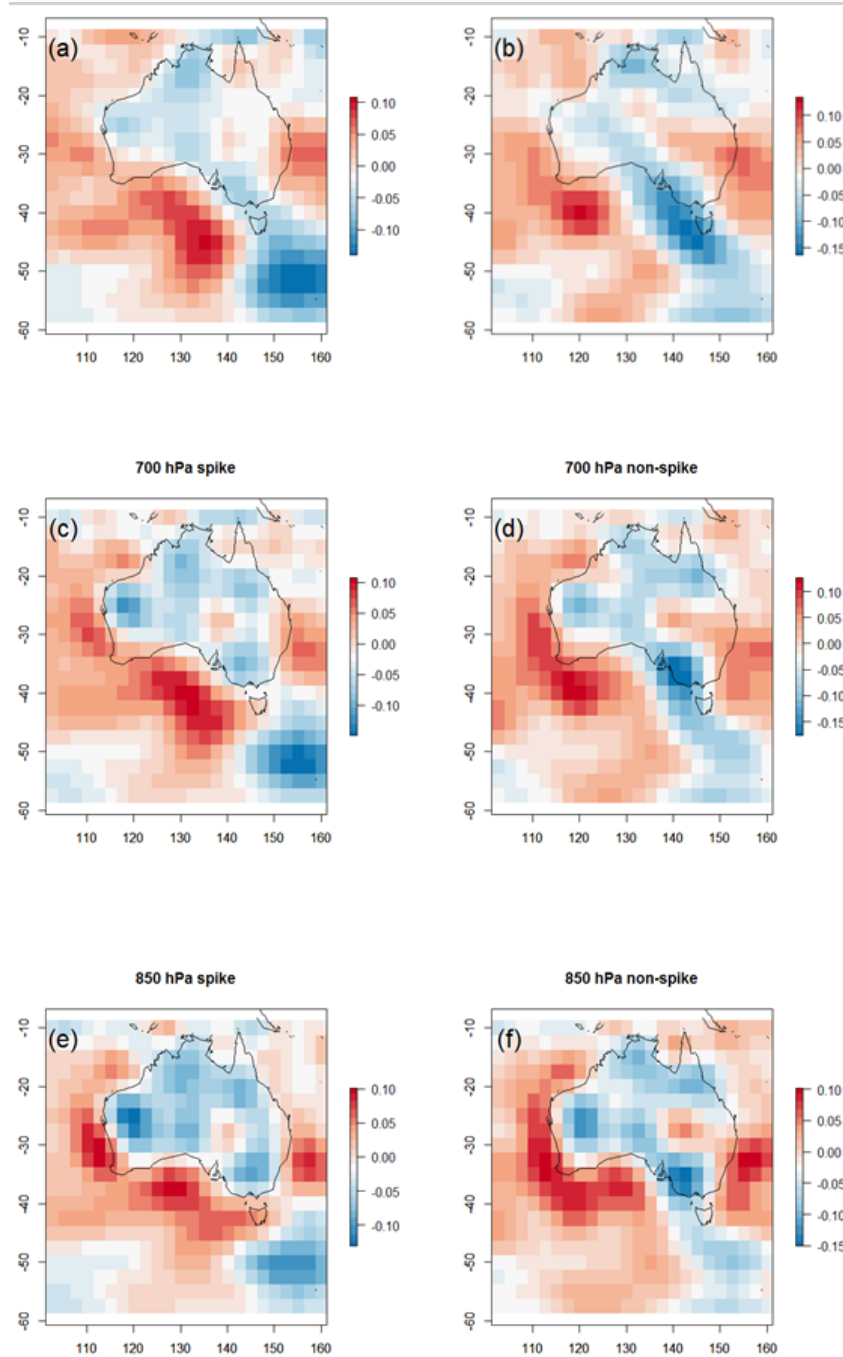


Figure 5.6: Composite plots of 0600 UTC vertical motion for (a) and (b) 500, (c) and (d) 700 and (e) and (f) 850 hPa for spike and nonspike events respectively. Red areas indicate descent and blue areas ascent. Units are Pas^{-1} .

- or having no evidence of reduced WV content within 10° of Tasmania.

Table 5.1 displays the categorisation: 22 spike events occurred with a dry slot within 5° of Tasmania, while images corresponding to the remaining 13 events indicated an area of reduced WV within 5° of Tasmania or a dry slot or area of reduced WV within 10° of Tasmania. No non-spike events had a dry slot within 5° of Tasmania. There were 12 non-spike events where WV imagery indicated an area of reduced WV within 5° of Tasmania or a dry slot or area of reduced WV within 10° of Tasmania, while three events showed no evidence of reduced WV content within 10° of Tasmania.

Nature of WV feature	Number of Spike Events	Number of Non-spike Events
Band within 5° of Tasmania	22	0
Area within 5° of Tasmania	3	8
Band/Area within 10° of Tasmania	6	4
No feature within 10° of Tasmania	0	3

Table 5.1: Satellite Water Vapour features associated with spike and non-spike events.

From the above, there is little evidence to link non-spike events with dry areas on satellite water vapour imagery, especially dry slots. On the other hand, the results strongly suggest a connection between spike events and WV features indicative of dry upper tropospheric conditions. In particular, most spike events (63%) were accompanied by a WV dry slot within 5° of Tasmania, indicative of pronounced descent of upper tropospheric or stratospheric air, and supporting the evidence presented in Section 5.3.1 that the structure of the composite trough and jet streak near Tasmania in the spike case were conducive to descent of upper-level air. Fire weather events are characterized by a deep, well-mixed boundary layer, increasing the likelihood that the upper-level air evident in a dry slot can reach the earth's surface and affect surface windspeed and moisture level, generating a spike in fire danger.

5.3.3 Seasonal Distribution of spike and non-spike days

Figure 5.7 displays a bar plot of the proportional occurrence of spike and non-spike events over the period 1990-2009 of the dataset. Non-spike events are approximately normally distributed about January, and occur during most months, with the exception of June. On the other hand, spike events are strongly clustered around late spring and early to mid-summer. A two-tailed χ^2 test indicates that the difference between the two distributions is significant at the $p=0.001$ level, strongly suggesting that there is an underlying real difference between the distributions.

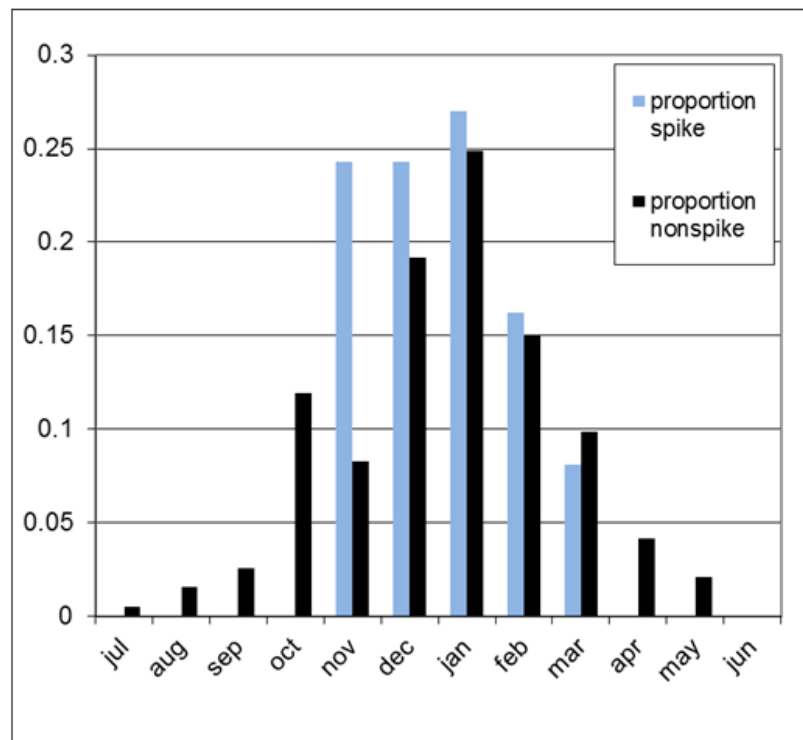


Figure 5.7: Proportional annual distribution of spike compared with non-spike events.

Spike events dominate the occurrence of dangerous fire weather days at the observation site in late spring-early summer. A secondary springtime peak in the seasonal occurrence of fire danger has been observed in recent decades in eastern and southeastern Tasmania (Fox-Hughes, 2008), and it is possible that spike events have contributed to this peak. Nine of the 37 spike events were recorded in November (the only Tasmanian springtime month which recorded spike events), and four of these events were the peak events for the corresponding fire season (7 November 2002 and 15 November 2003) or were secondary peaks for their season (13 November 1990 and 18 November 2004). Thus spike events have contributed to the occurrence of springtime fire dangers peaks in Tasmania during the two-decade period for which data is available, but they have not been the sole mechanism involved.

5.3.4 Applicability of results to other locations

The presence of negatively tilting upper tropospheric troughs on days already forecast to be dangerous fire weather days may be a useful indicator of the potential for abrupt increases in fire danger. It is of interest to assess whether this approach is applicable in other geographic locations. It is beyond the scope of this paper to perform this assessment in a rigorous

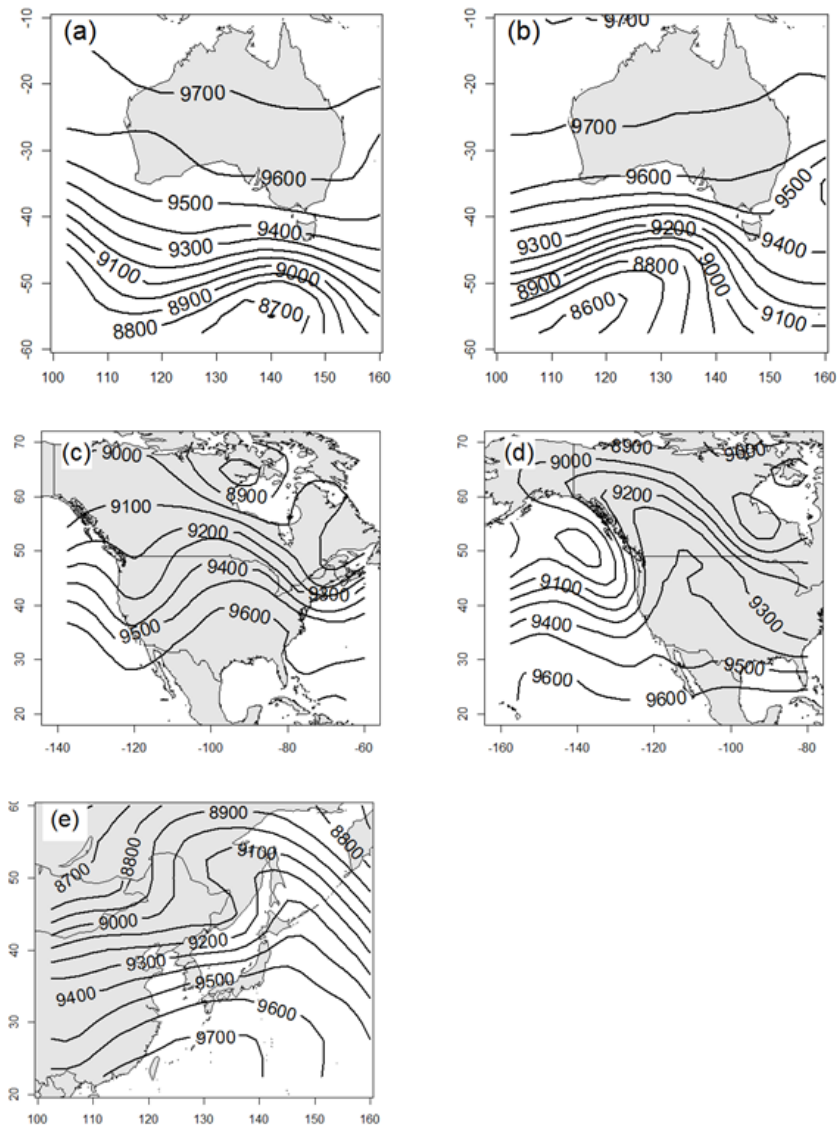


Figure 5.8: Geopotential height contours at 300 hPa, units m, for events documented as having abrupt increases in fire danger (a) Canberra, Australia, 18 Jan 2003, (b) Wangary, Australia, 11 Jan 2005, (c) Double Trouble State Park, United States, 02 June 2002 (d) Mack Lake, United States, 05 May 1980 and (e) Tohoku, Japan, 27 April 1983.

fashion; however a preliminary investigation of the upper trough structure in previously documented events is worthwhile. Figure 5.8 presents 300 hPa geopotential height plots for the dates and areas of events mentioned earlier in this article. In each case, there is a clearly defined negatively tilting trough present. In Figure 5.8(a), a negatively tilting trough is evident south of the Australian continent on 18 January 2003, the date of the devastating Canberra fires (McLeod, 2003, Mills, 2005a). A similar, but more pronounced trough can be seen in Figure 5.8(b), corresponding to the Wangary fire (Mills, 2008a). In the Northern Hemisphere, a negatively tilted trough extended from central northern Canada to the northeast United States (Figure 5.8(c)) on the date of the Double Trouble State Park fire (Kaplan et al., 2008, Charney and Keyser, 2010), in which erratic fire behaviour accompanied rapid surface drying and gusty winds. On the date of the Mack Lake fire (Zimet et al., 2007), another such trough lay just off the Pacific coast of the United States (Figure 5.8(d)). Finally, the rapid growth of forest fires in northeastern Japan on 27 April 1983 (Kondo and Kuwagata, 1992) was accompanied by a negatively tilted trough in the upper troposphere (Figure 5.8(e)). These examples strongly suggest that the results discussed above can be generalized to other locations.

5.4 Conclusion

On the basis of the above synoptic analysis, it is more likely in spike events than in non-spike events that air will be transported from the upper troposphere to the surface, via the ageostrophic circulations associated with jet stream cores coupled with turbulent mixing in a deep convective boundary layer (as described in e.g. Kaplan et al. (2008)). Further, the negative tilt of the upper level trough in spike events tends to more tightly focus vertical motions near to the trough (i.e. close to Tasmania) than is the case in positively or neutrally tilted troughs associated with non-spike events (Bluestein, 1993), at a time of the day (mid to late afternoon) when the mixed layer is likely to be deepest and most able to couple to overlaying layers of the troposphere. Available WV imagery reinforces this conclusion, with a majority of spike events being associated with WV dry slots, and reduced upper tropospheric WV content close to Tasmania evident at the time of all other spike events. A much weaker association exists between WV image features and non-spike events.

A marked difference in seasonality between spike and non-spike events is interesting and potentially useful for meteorologists and fire managers. The basis for the difference, however, is not currently clear. It may relate to the seasonality of negatively-tilting troughs in the

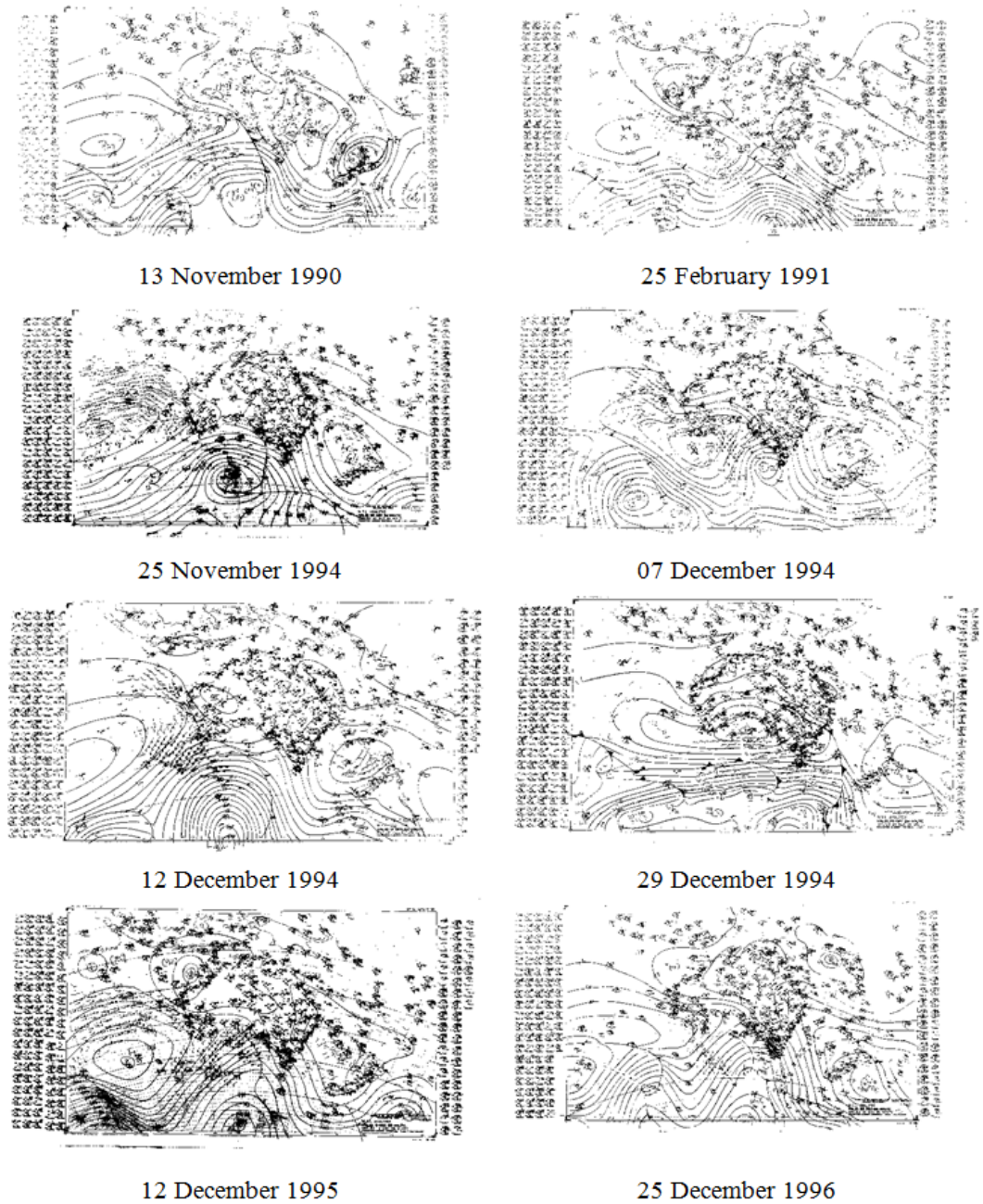
Australian region, but this awaits further exploration.

The differences evident between the synoptic patterns associated with fire weather events characterised by abrupt spikes in fire danger at Hobart Airport and those events lacking such features can be used by meteorologists to assist in the forecasting of fire danger spikes well in advance of the commencement of the events. A brief assessment of the nature of the upper trough associated with other documented cases of abrupt increase in fire danger is encouraging, but does not constitute confirmation of the generality of the technique. It will be necessary to ensure that these results can be robustly generalised to other locations, of course. If that is possible, the technique is likely to be a useful tool to highlight situations conducive to the occurrence of a dangerous phenomenon. Thus, the method provides an immediate tool for Tasmanian fire weather meteorologists, with the potential to extend its use to other parts of the globe.

5.5 Acknowledgements

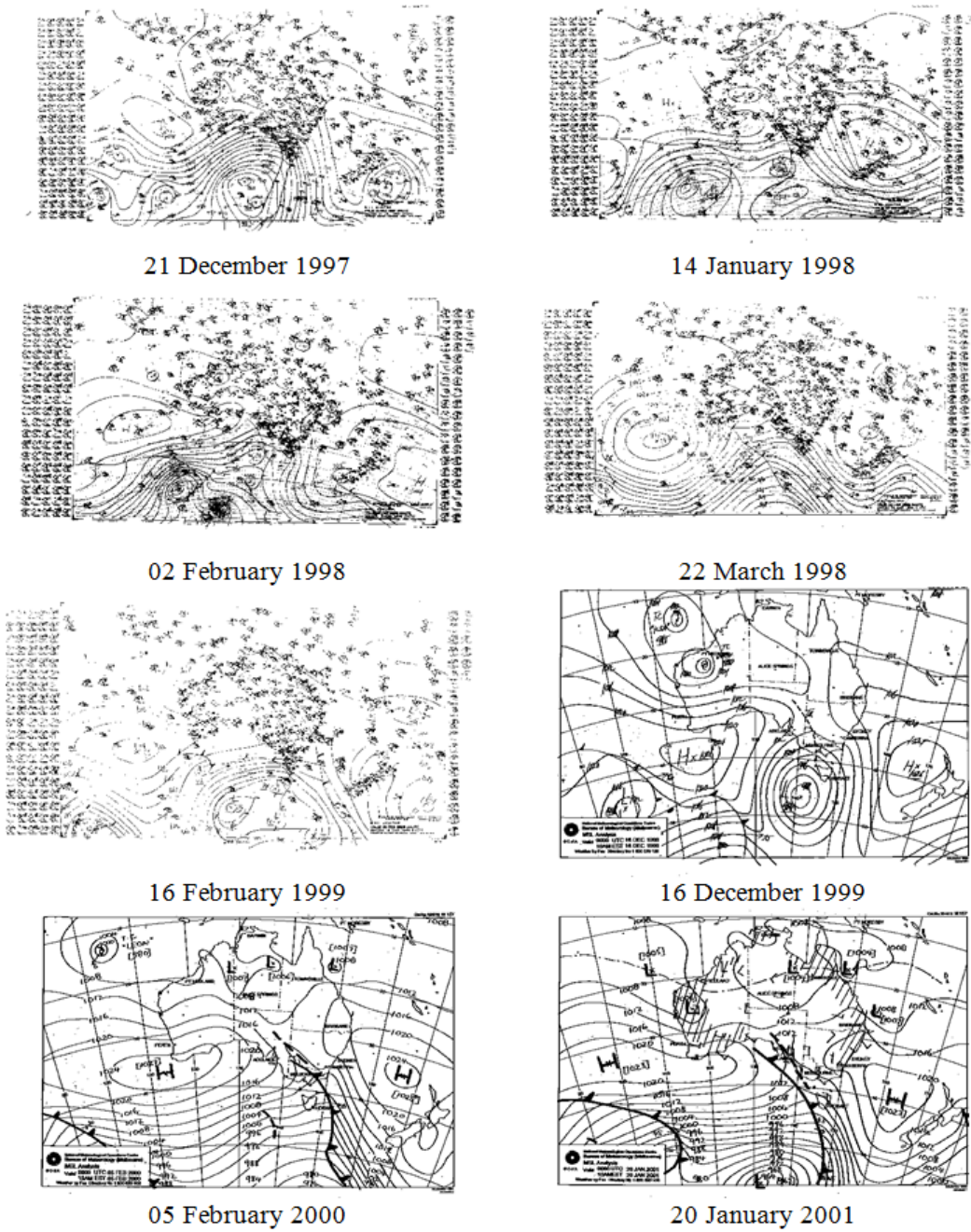
Reanalysis plots and data were provided by the NOAA/ESRL Physical Sciences Division, Boulder Colorado from their Web site at <http://www.esrl.noaa.gov/psd/>. Hobart Airport observations were obtained from the Australian Bureau of Meteorology's ADAM (Australian Data Archive for Meteorology) database, and MSLP analyses were obtained from the Bureau of Meteorology National Operations Centre (formerly National Meteorological and Oceanographic Centre). Helpful reviews and comments on the content of this paper were made by Graham Mills, Mike Pook and Kevin Tory of the Centre for Australian Weather and Climate Research.

5.6 Supplementary Figures



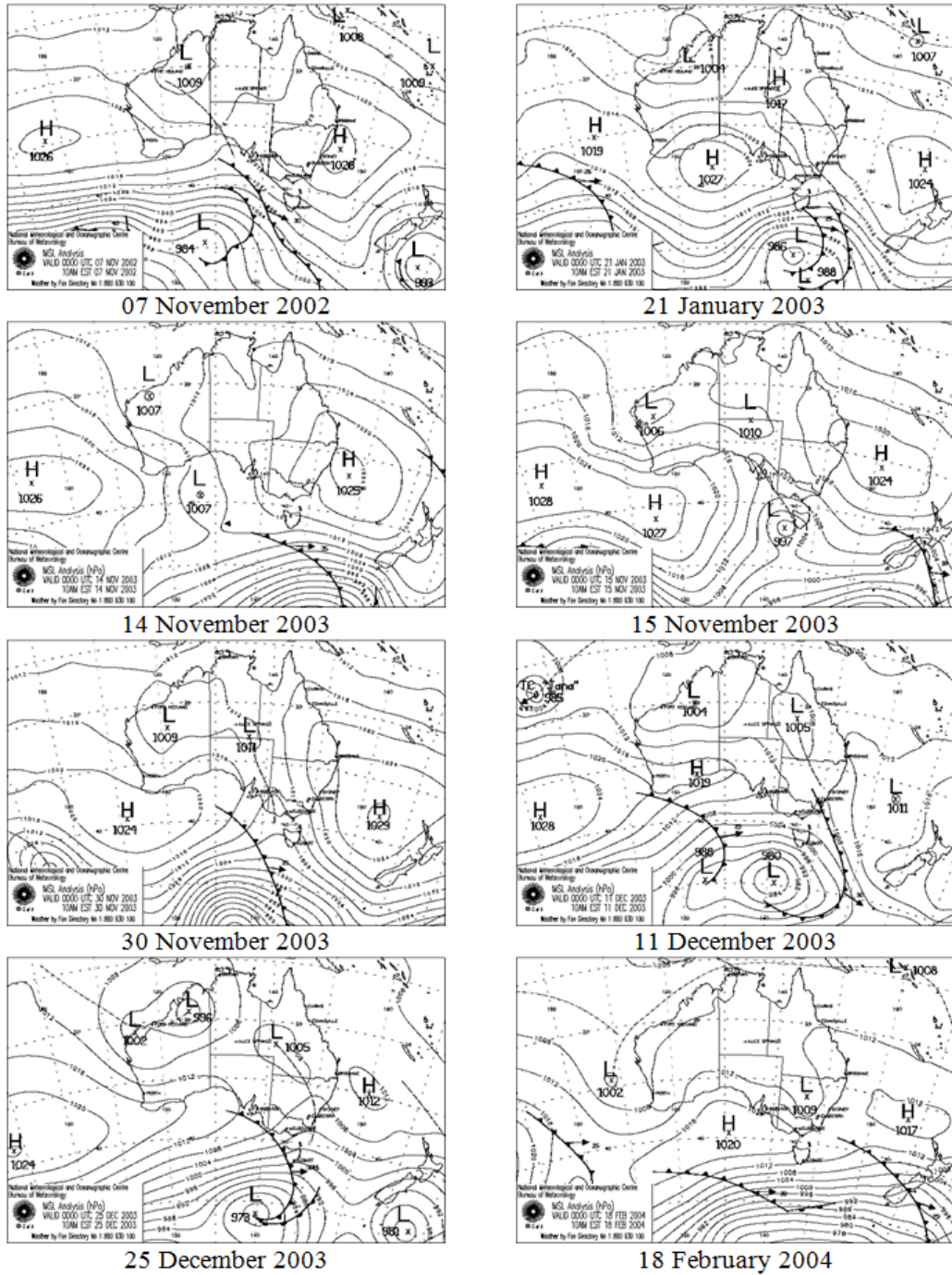
(a)

Figure 5S.1: 0000 UTC MSLP charts from the National Meteorological and Oceanographic Centre of the Australian Bureau of Meteorology for spike events. Note that the archiving method for charts changed in late 1999, to store cleaner machine-generated analyses.



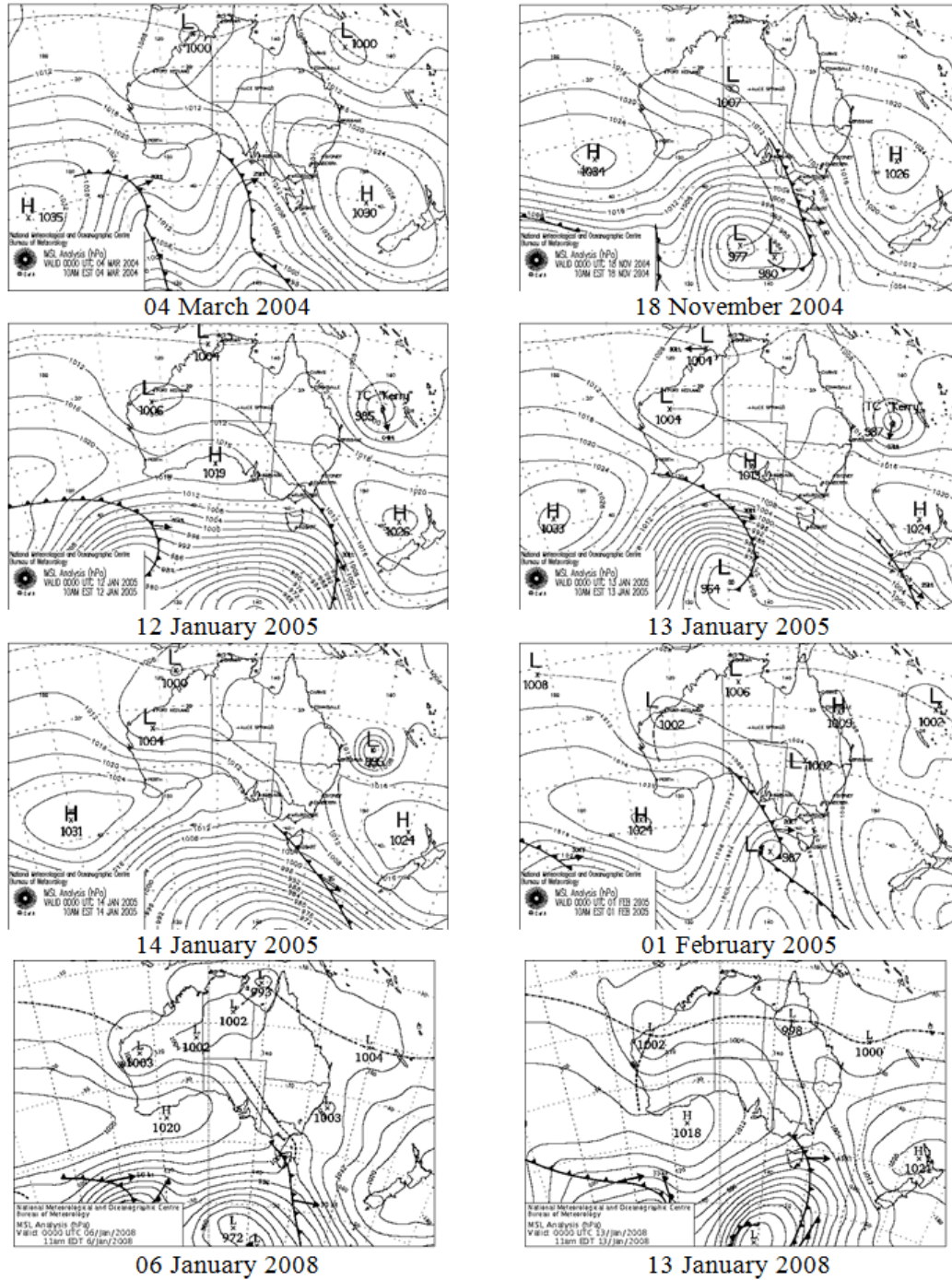
(b)

Figure 5S.1: cont.



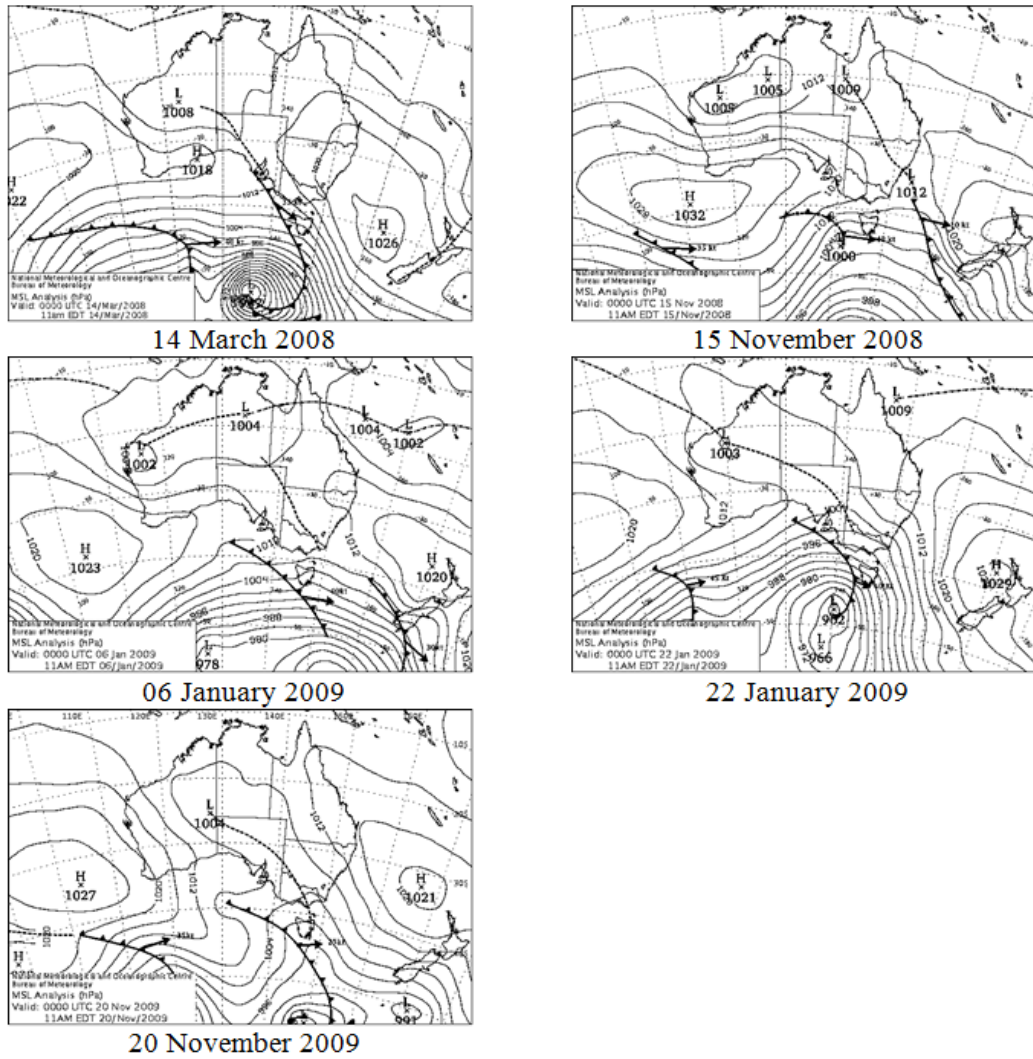
(c)

Figure 5S.1: cont.



(d)

Figure 5S.1: cont.



(e)

Figure 5S.1: cont.

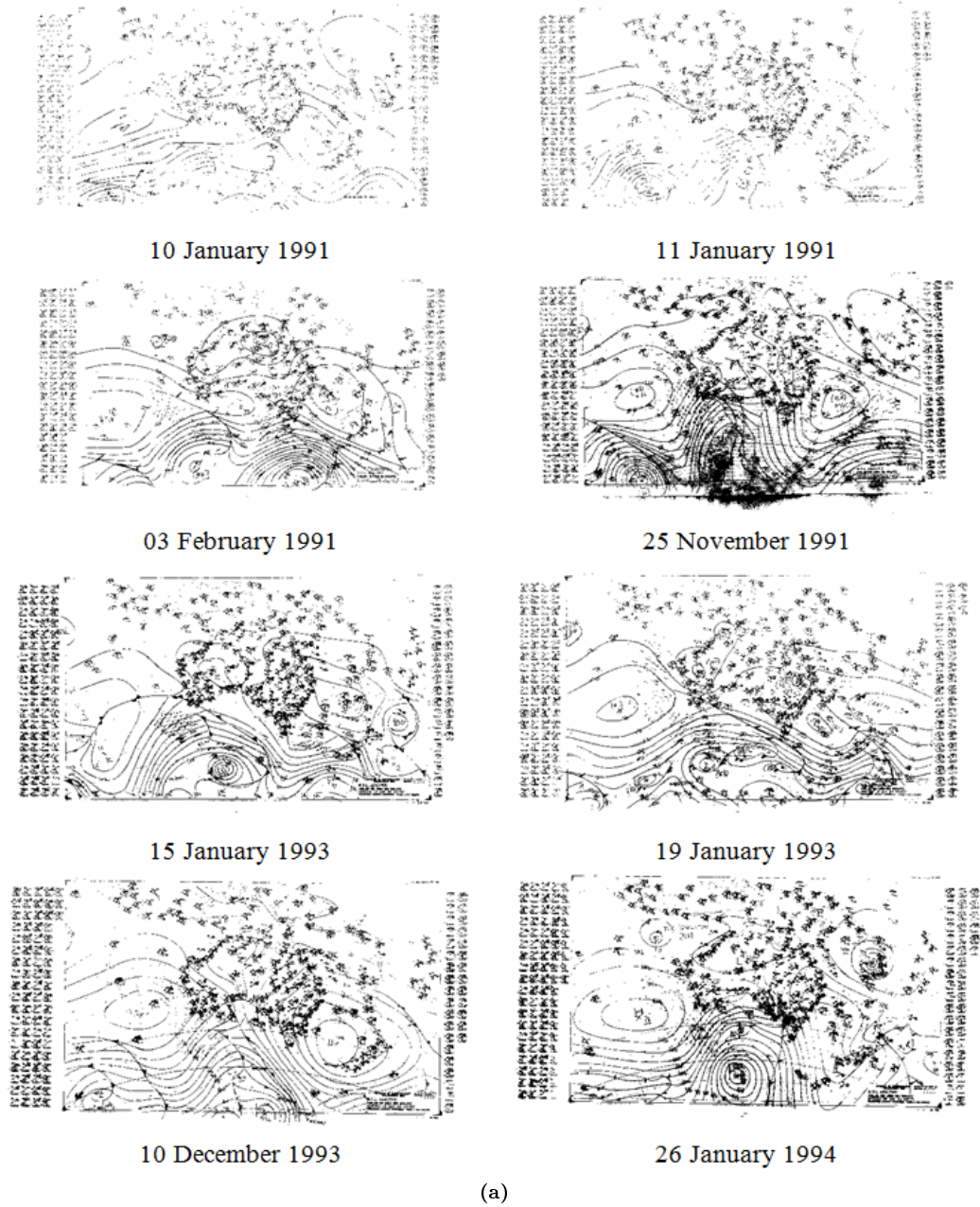
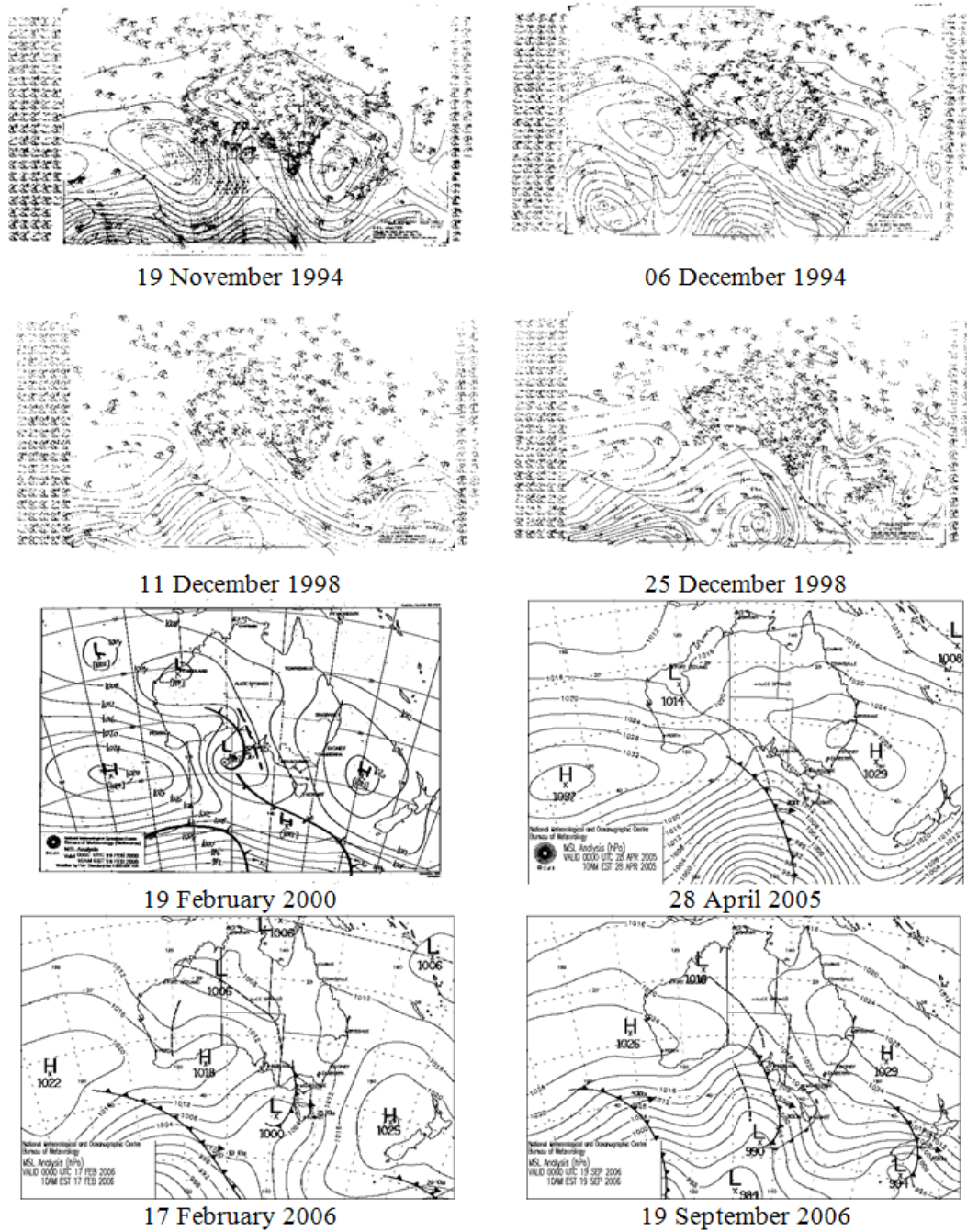
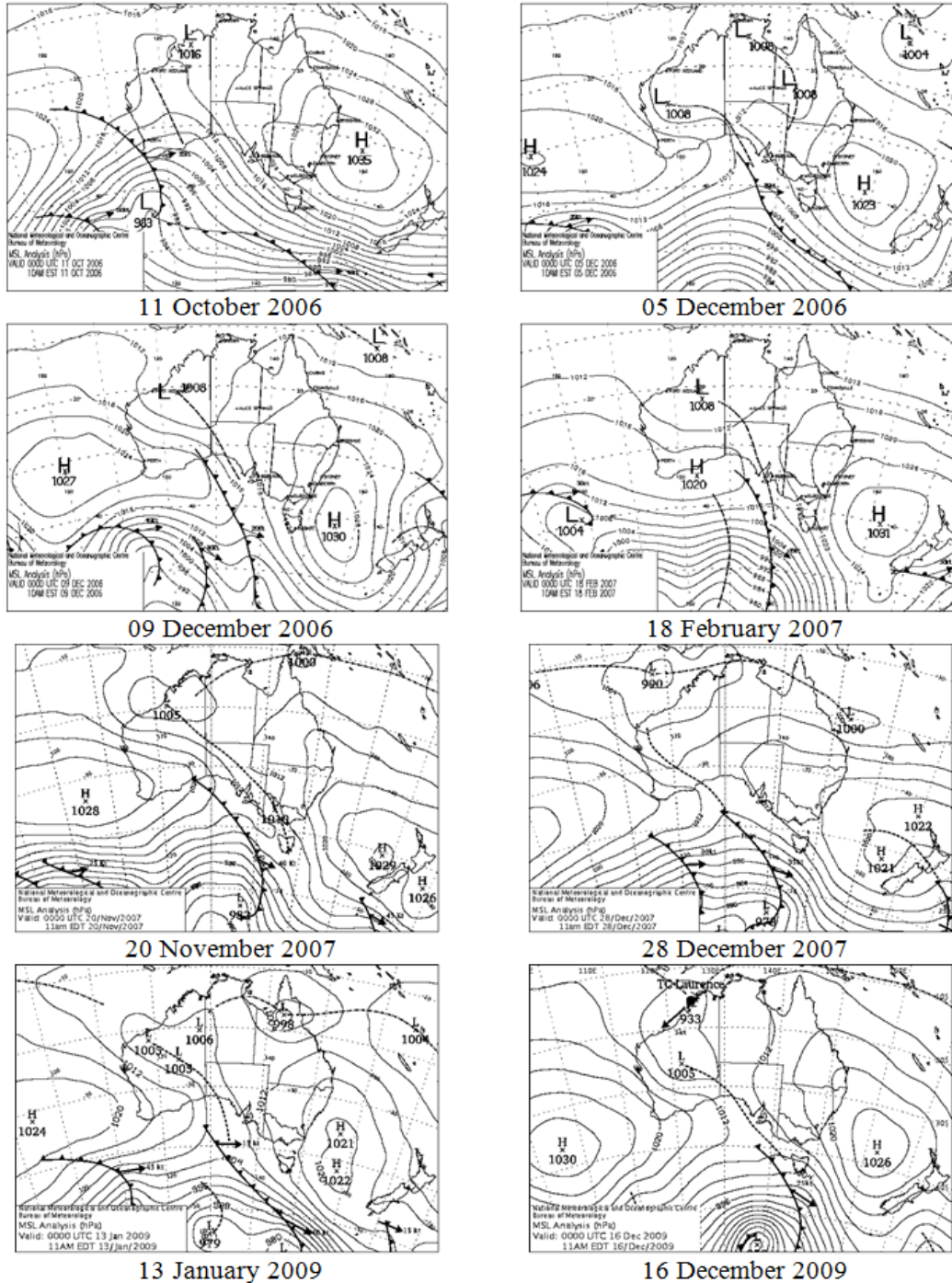


Figure 5S.2: As for Fig. 5S1, but for nonspike events.



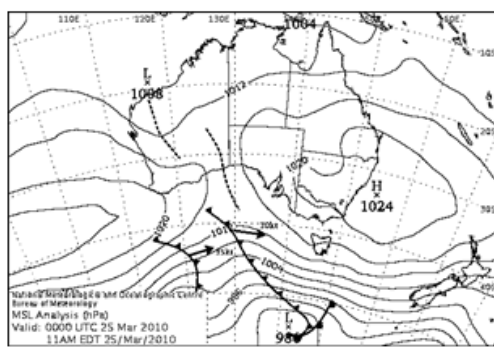
(b)

Figure 5S.2: cont.



(c)

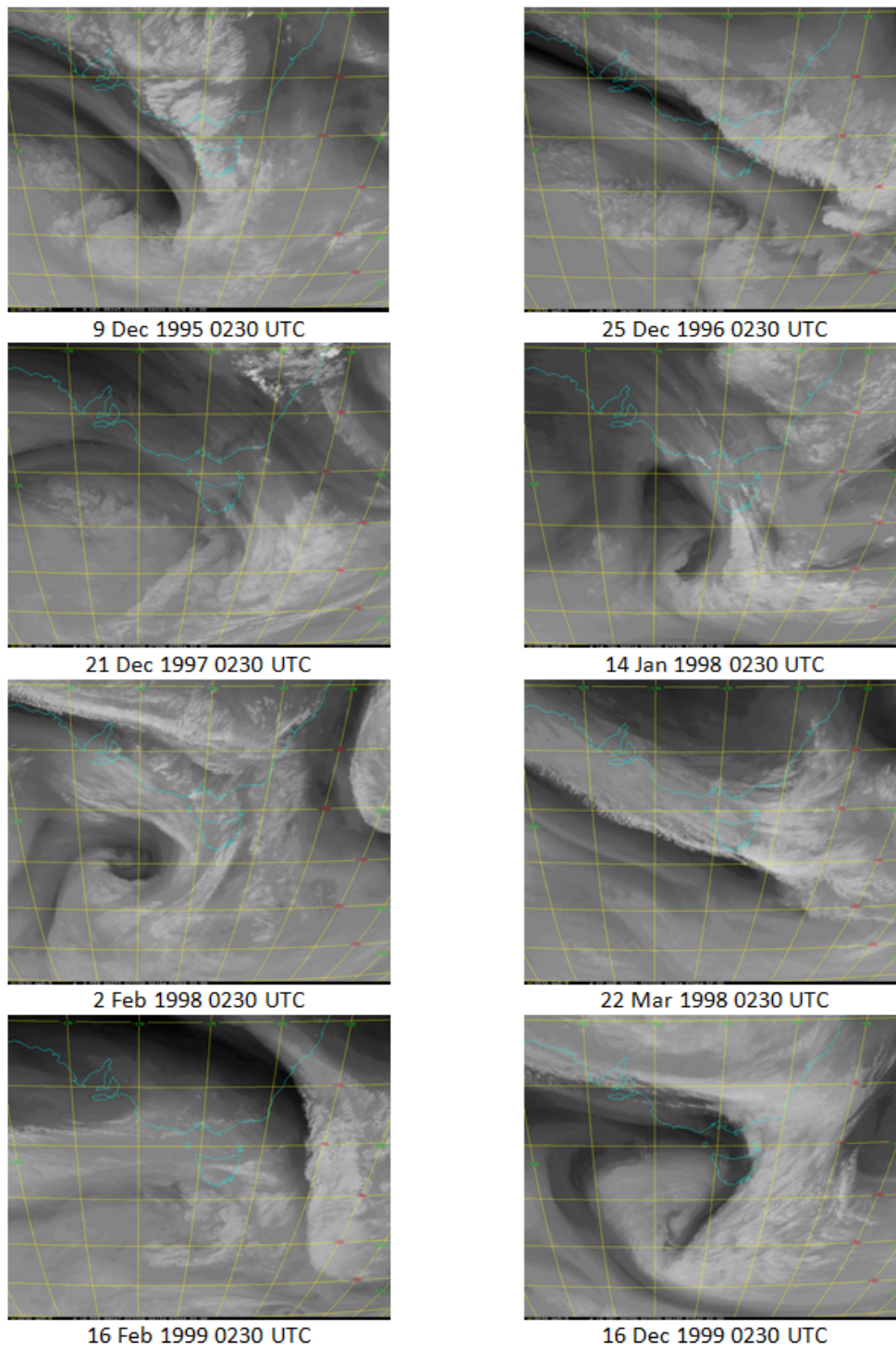
Figure 5S.2: cont.



25 March 2010

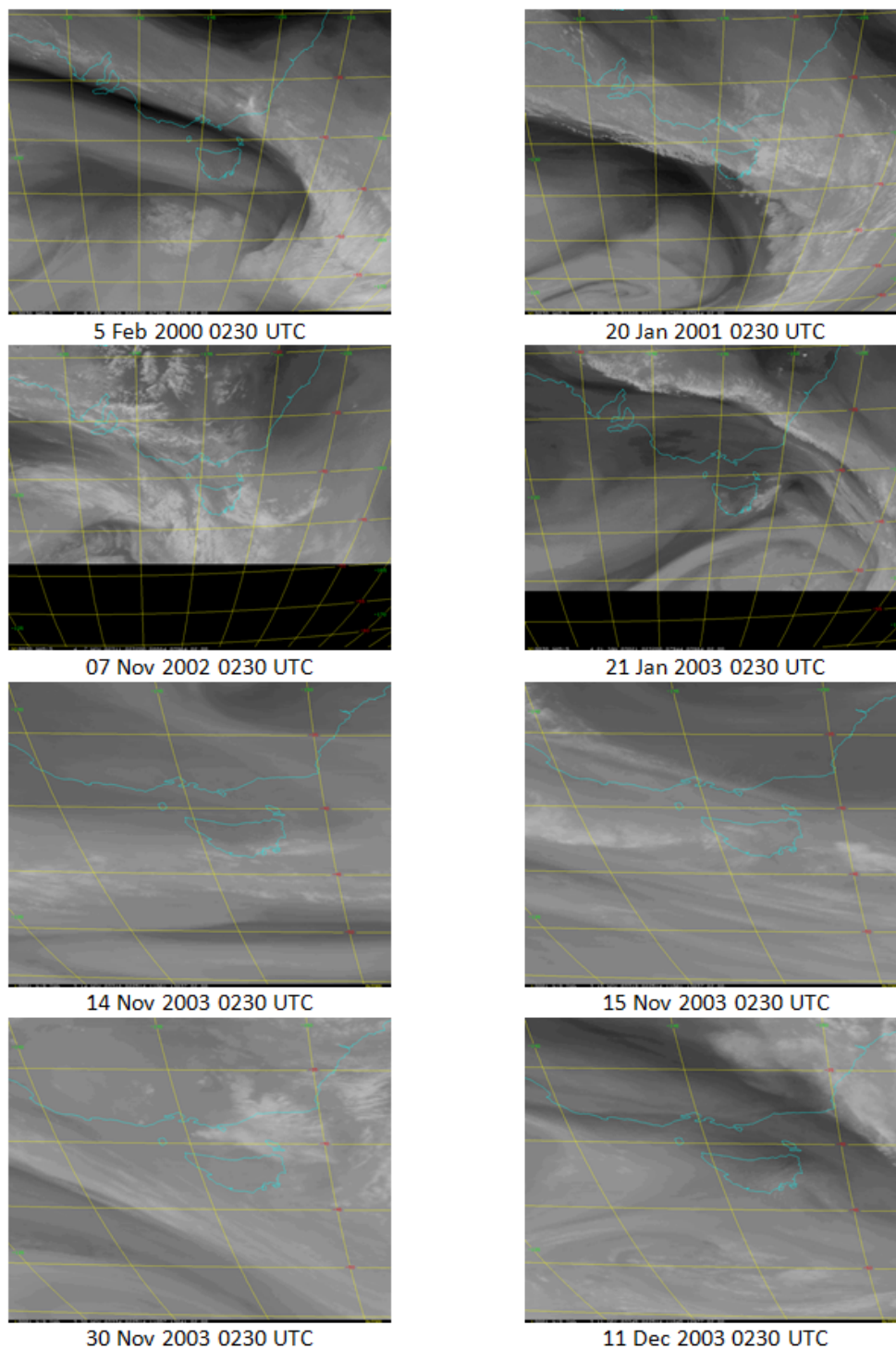
(d)

Figure 5S.2: cont.



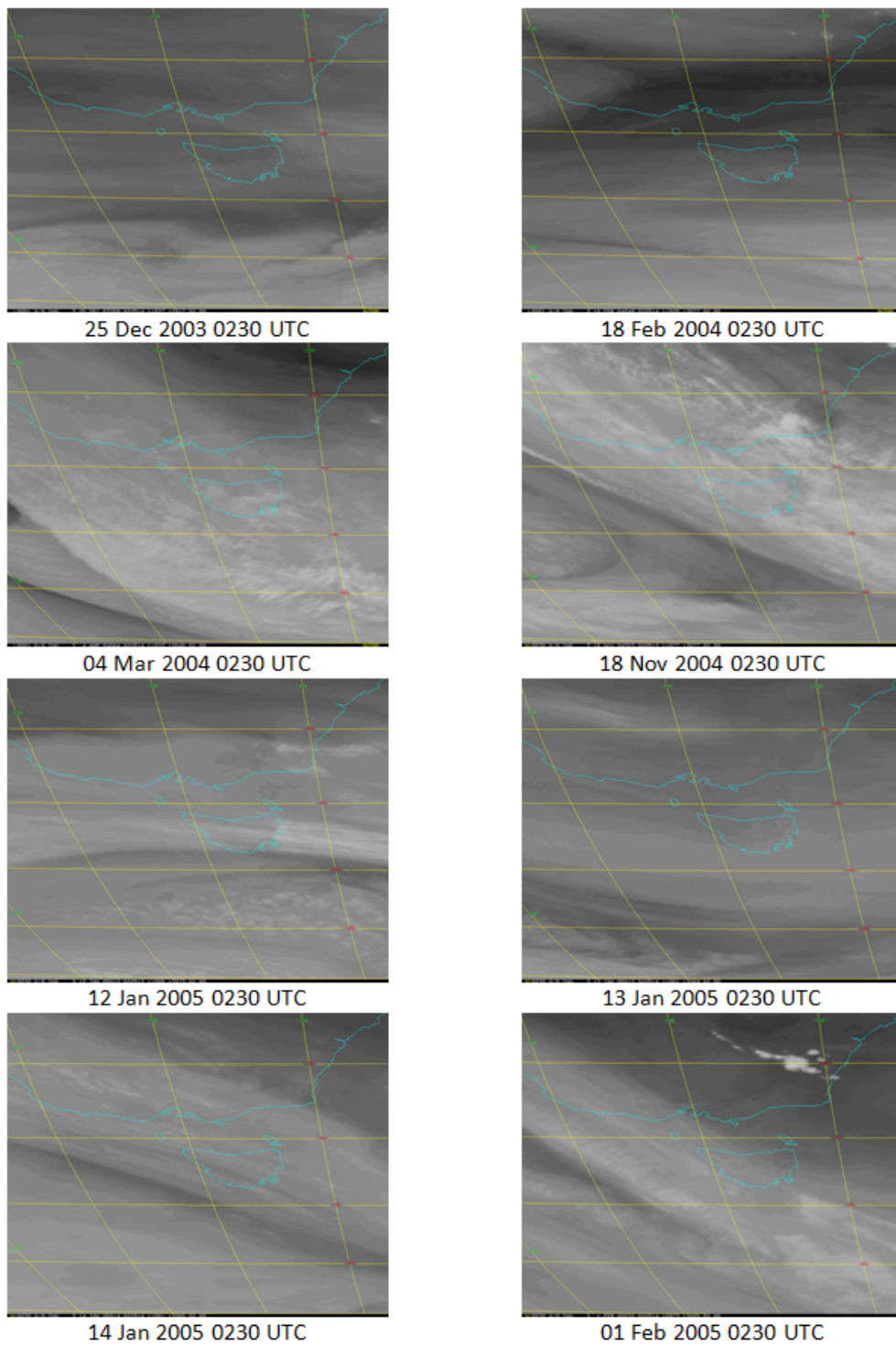
(a)

Figure 5S.3: Satellite WV imagery of spike events. Imagery courtesy of NOAA and JMA.



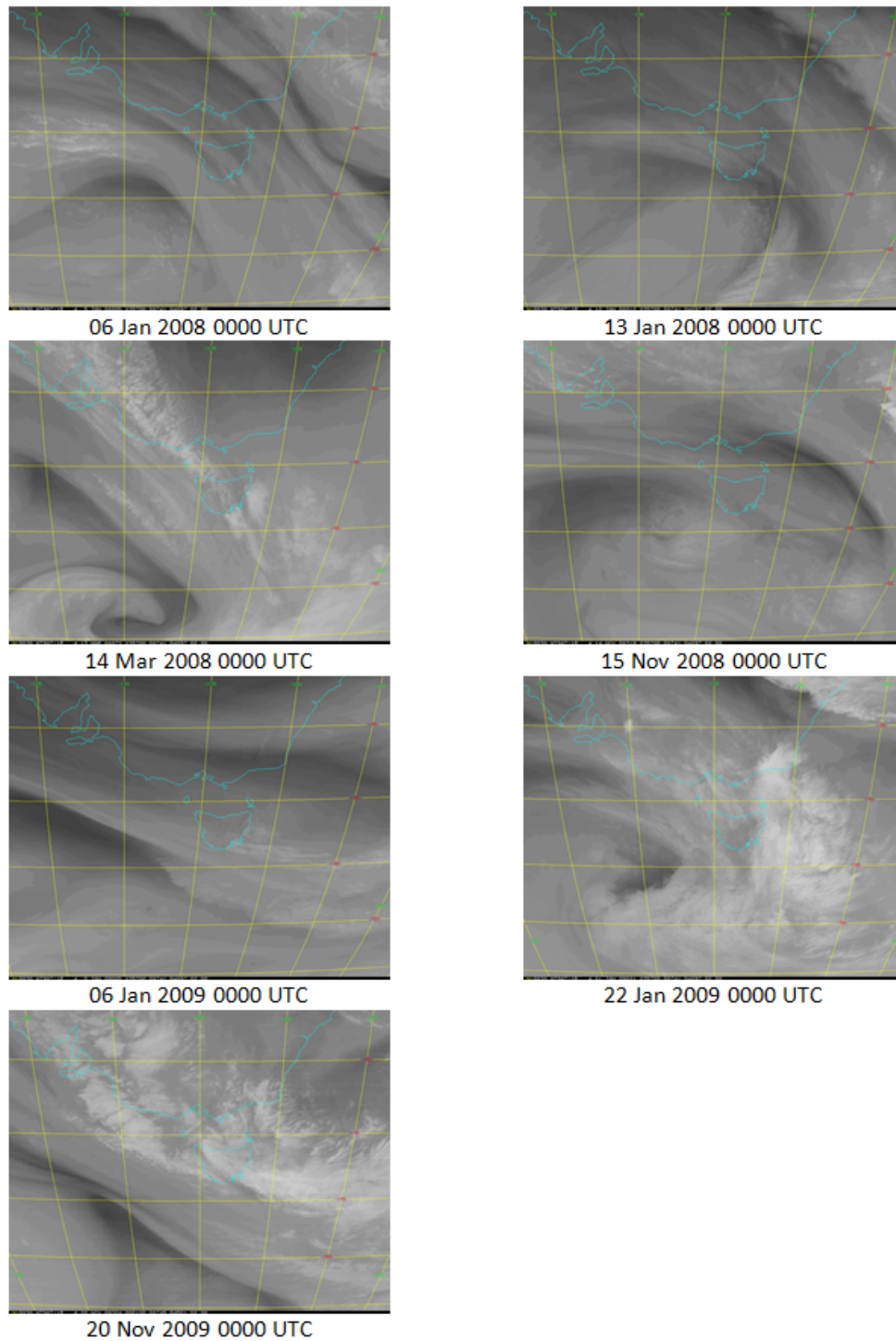
(b)

Figure 5S.3: cont.



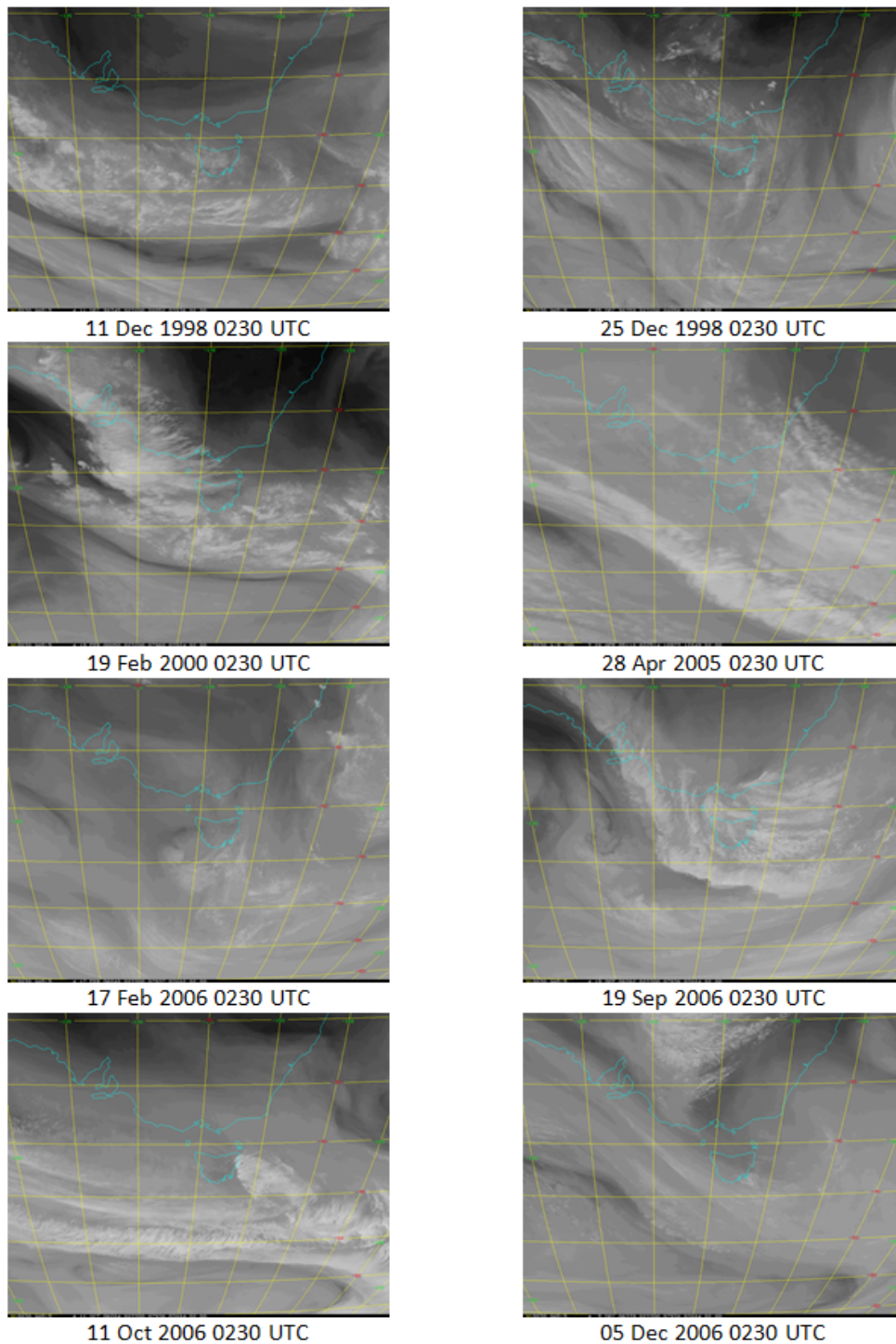
(c)

Figure 5S.3: cont.



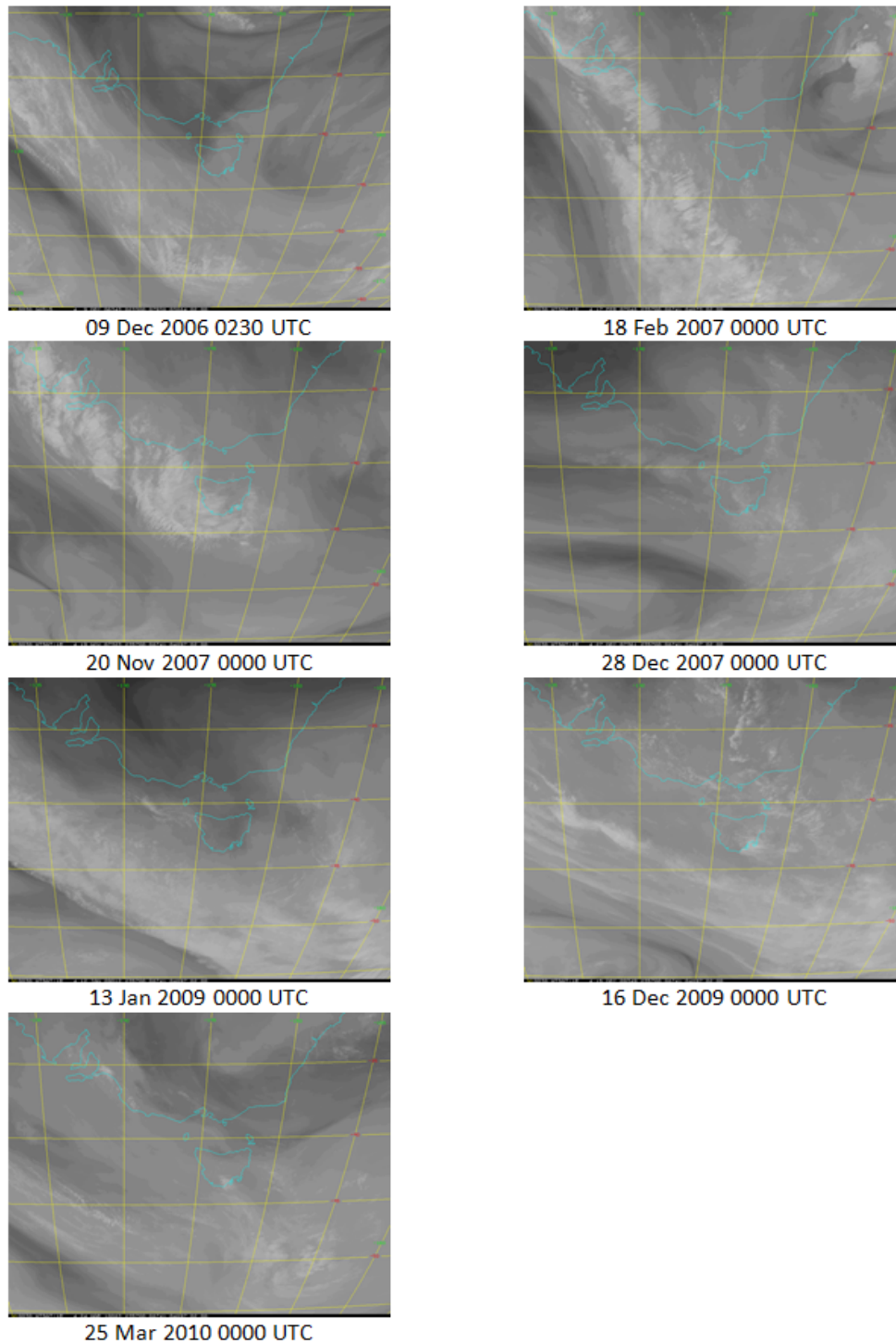
(d)

Figure 5S.3: cont.



(a)

Figure 5S.4: Satellite WV imagery of nonspike events. Imagery courtesy of NOAA and JMA.



(b)

Figure 5S.4: cont.

6: Future fire danger climatology for Tasmania, Australia, using a dynamically downscaled regional climate model

Paul Fox-Hughes^{A, C, D, F}, Rebecca Harris^A, Greg Lee^A, Michael Grose^B and Nathan Bindoff^{A, D, E}

^AAntarctic Climate and Ecosystems Cooperative Research Centre, Private Bag 80 Hobart TAS 7001, Australia

^BCSIRO Marine and Atmospheric Research, 107-121 Station St Aspendale VIC 3195, Australia

^CBureau of Meteorology, Level 5, 111 Macquarie St Hobart TAS 7001, Australia

^DInstitute of Marine and Antarctic Studies, University of Tasmania, Sandy Bay Hobart TAS 7001, Australia

^ECentre for Australian Weather and Climate Research (CAWCR), CSIRO Marine and Atmospheric Research, Castray Esplanade, Hobart TAS 7000 Australia

^FCorresponding author. Email: Paul.FoxHughes@acecrc.org.au

Abstract

Daily values of McArthur Forest Fire Danger Index were generated at approximately ten kilometre resolution over Tasmania, Australia, from six dynamically downscaled CMIP3 climate models for 1961-2100, using a high (A2) emissions scenario. Multi-model mean fire danger validated well against observations for 2002-2012, with 99th percentile fire dangers having the same distribution and largely similar values to those observed over the same time. Model projections showed a broad increase in fire danger across Tasmania, but with substantial regional variation – the increase was smaller in western Tasmania (district mean cumulative fire danger increasing at 1.07/year) compared to parts of the east (1.79/year), for example. There was also noticeable seasonal variation, with little change occurring in autumn, but a steady increase in area subject to springtime 99th percentile fire danger from 6% in 1961-1980 to 21% by 2081-2100, again consistent with observations. In general, annually accumulated fire danger behaved similarly. Regional mean sea level pressure patterns resembled observed patterns often associated with days of dangerous fire weather. Days of elevated fire danger displaying these patterns increased in frequency during the simulated twenty-first century: in southeast Tasmania, for example, the number of such events detected rose from 101 (across all models) in 1961-1980 to 169 by 2081-2100. Correspondence of model output with observations and the regional detail available suggest that these dynamically downscaled model data are useful projections of future fire danger for landscape managers and the community.

6.1 Introduction

South-eastern Australia has been identified as one of the three most fire-prone areas in the world (Hennessy et al., 2005). Fire danger has increased in recent decades (Clarke et al., 2013), and is projected to increase further with greenhouse warming (e.g. Pitman et al. (2007)). Bushfires already cause extensive damage and concern, and any increase in fire danger, or shifts in the frequency, intensity or timing of fires, will have widespread consequences for human communities and natural systems.

Both weather and climate influence fire danger. Average conditions of temperature, rainfall, evaporation, and radiation affect fuel growth and drying, while extremes of temperature, wind, and relative humidity drive fire weather and fire ignition potential. Weather parameters associated with high fire danger are all projected to change in future (Karl and Trenberth, 2003, Sherwood et al., 2010, Dai, 2011, McInnes et al., 2011, Trenberth, 2011).

The interaction between high fire danger and atmospheric conditions is relatively well studied (Brown et al., 2004, Bradstock, 2010, Potter, 2012a,b). Elevated fire danger in south-eastern Australia is associated with high temperatures and strong winds ahead of cold fronts. If a front extends for some depth through the troposphere, high wind speeds may be sustained following the frontal passage. Northwesterly winds will shift southwesterly, and any fires may spread across wide areas as the flank of the fire becomes the head (Mills, 2005b). Cross mountain flows and Foehn-like winds can also lead to locally high fire danger in mountainous regions such as Tasmania (Marsh, 1987, Sharples et al., 2010). However, future changes to synoptic weather patterns associated with high fire danger are less well studied (Hasson et al., 2009, Grose et al., 2014).

Fire danger is generally described using indices that incorporate surface air temperature, precipitation, relative humidity and wind speed. Numerous such indices exist, including the McArthur Mark 5 Forest Fire Danger Index (FFDI, (McArthur, 1967)), the Canadian Fire Weather Index (FWI, (van Wagner et al., 1992, Wotton et al., 2009)), and the United States National Fire Danger Ratings System (NFDRS, (Burgan et al., 1988)). Each index has limitations, but they are useful tools for summarising fire weather, and are commonly used in fire management. Comparisons of FFDI with the FWI show strong similarities between the two indices (Dowdy et al., 2010).

In eastern Australia the FFDI is widely used operationally by weather forecasters and fire services to determine fire hazard and safe conditions for controlled burning. Clarke et al. (2013) demonstrated significant increases in annual cumulative FFDI (\sum FFDI) since

the 1970s, particularly in southern Australia, and changes in the distribution and timing of the fire season. An increase in \sum FFDI of 6% between 1970 and 2007 was calculated for Hobart (Lucas et al., 2007), but fire danger did not increase uniformly through time, showing decadal variability, which is likely to continue into the future.

A number of studies have examined projected fire danger through the twenty-first century. Flannigan et al. (2013) highlight a projected increase in fire season severity and season length for most of the globe, using three GCM and three emissions scenarios, noting a high degree of model agreement with the A2 scenario for much of Australia, in particular Tasmania. References therein and others including Liu et al. (2010) have investigated implications of climate change on global wildfire potential using GCM, in this case by calculating Byram-Keetch Drought Indices. King et al. (2012) have applied a pasture growth model (GRAZPLAN) to the output of global climate models (GCM) to assess the impact of climate change in Australia on grassland fire danger calculations. Increasingly, downscaling of GCMs has been employed to produce regional projections of future fire danger. For example, Carvalho et al. (2010) describe increased future fire activity in Portugal under the A2 SRES scenario, using a downscaled climate model. Liu et al. (2013) find a generally increased fire risk in the United States using a suite of models also under the A2 scenario, although with substantial regional and inter-model variation.

Until recently, only GCM output was available to provide future climate projections for Tasmania. The resolution of these GCMs is insufficient to resolve regional climate processes over Tasmania, an island with a strong maritime influence, complex topography and several climatic zones. Even at broad regional resolution, discrimination of the diverse Tasmanian climate is poor. For example, Hennessy et al. (2005) were able to suggest only that Tasmania would become warmer and wetter, in contrast to the rest of south-eastern Australia, which was projected to become hotter and drier in future. Projected changes in fire weather/danger were consequently found to be low relative to the rest of the region (Hennessy et al. (2005), Lucas et al. (2007)). Pitman et al. (2007) demonstrated the benefits of using regional climate projections (at 56km resolution) in fire danger calculations at the continental scale, but coverage of Tasmania was incomplete. Bushfires are no less a concern in Tasmania than on mainland Australia, as recent events demonstrate. In early January 2013 forty bushfires burnt across the state. Of these, four burnt approximately 40, 000 hectares, causing widespread destruction of infrastructure, farms and homes, including 203 dwellings (Department of Premier and Cabinet, 2013). Area burnt each year averages approximately 29, 000 Ha, but can exceed 100, 000 Ha (Nicholls and Lucas, 2007). Further, while fires in the

wet sclerophyll forests that occur in higher rainfall areas of Tasmania are less frequent than in drier forest types (in some cases with return times >500 years), they can be extremely intense, especially in southern temperate areas (Wood et al., 2010).

In general, much of eastern Tasmania is dominated by dry eucalypt forest, while in parts of the west, north and far south wet eucalypt forest is common. In the inland east, in particular, agricultural grasslands are established (Russell-Smith et al., 2007). Moorlands occupy approximately 10% of the island's land area, mainly in the west (Marsden-Smedley and Kirkpatrick, 2000). All are fire-prone, under suitable conditions, with burning frequency a function of antecedent precipitation, but strongly influenced by human society (Marsden-Smedley and Kirkpatrick, 2000, Von Platen et al., 2011). As noted above, Tasmanian and, more generally, Australian fire danger and fire extent varies decadal, following variability in precipitation. The variability of Australian precipitation is an area of active research – it is somewhat dependent on the phase of the Interdecadal Pacific Oscillation (Verdon et al., 2004, Power et al., 2006), but also to the location of the subtropical ridge (Timbal and Drosowsky, 2013) and a number of other factors (Risbey et al., 2009).

Climate projections specific to Tasmania are now available, generated using a dynamically downscaled regional climate model (CSIRO's Conformal Cubic Atmospheric Model (CCAM)), detailed in Corney et al. (2010) and Corney et al. (2013). The fine-scale CCAM modelling produced projections at approximately 10 km resolution, enabling regional variation across Tasmania to be expressed. Modelling was undertaken for the Special Report on Emissions Scenarios (SRES) A2 emissions scenario (Nakićenović, 2000). Global emissions are currently tracking the A2 scenario quite closely (Peters et al., 2013), suggesting that A2 is a reasonable best case scenario under current foreseeable trends, and the appropriate benchmark for fire risk models in Australia under foreseeable conditions. The A2 scenario is broadly similar to the Representative Concentration Pathway (RCP) 8.5. The RCP structure has been introduced since the compilation of the CMIP3 archive (upon which our modelling was derived), to facilitate more detailed climate scenario building for modelling intercomparison (Van Vuuren et al., 2011) and is used in Phase 5 of the Coupled Model Intercomparison Project (CMIP5). It is worth noting, too, that initial comparisons of the CMIP3 and CMIP5 modelling indicate that they do not differ markedly over Australia (Irving et al., 2012).

Under the A2 scenario, average temperatures in Tasmania are projected to increase by 2.6 to 3.3 °C late this century. Temperature change is projected to be fairly uniform across Tasmania, and broadly similar across seasons. In contrast, total annual rainfall is not

projected to change, but there are significant changes in the spatial pattern and seasonality of rainfall. Annual rainfall is projected to increase over coastal regions, and decrease over central Tasmania and in parts of northwest Tasmania. After 2050, winter rainfall on the west coast is projected to increase significantly and summer rainfall to decrease. Rainfall in October to March is an important negative correlate with bushfires in Tasmania (Nicholls and Lucas, 2007), so this changing seasonality may lead to a shift in the timing of the bushfire season and a narrowing of the shoulder season in which prescribed burning can be conducted safely.

This paper aims to assess changes in future fire danger projected for Tasmania up to 2100 under the A2 emissions scenario, using regional climate model output and to investigate the synoptic climatology associated with fire weather in different regions of Tasmania under future climate conditions. Using a regional climate model provides information about relevant processes at an appropriate temporal and spatial scale for the size of Tasmania, enabling assessment of seasonal changes as well as changes in cumulative annual FFDI. A companion paper, Grose et al. (2014), focuses on southeast Tasmania, examining broad-scale drivers of fire weather, as well as specific geographic and topographic features making that region particularly vulnerable to elevated fire danger.

6.2 Methods

In this section, we discuss the calculation of FFDI, and methods used to verify the calculations against observations. We then document the measures used to characterise change in fire danger over time. We performed all calculations using the R statistical language R Development Core Team (2012).

6.2.1 Fire danger index (FFDI)

The McArthur FFDI is based on temperature (T , °C), wind speed (v , km h⁻¹), and relative humidity (RH, %), combined with an estimated fuel dryness (hence availability to burn), the Drought Factor (DF), a number between 0 and 10. DF is calculated by combining estimates of the effects of (a) direct wetting from recent ‘significant’ rainfall (> 2 mm); and (b) wetting from below, dependent on soil moisture content. The latter is calculated as a soil moisture deficit, using Mount’s Soil Dryness Index (SDI) Mount (1972), widely used in Tasmania.

6.2.2 FFDI in the regional climate model

Output from CCAM was used to provide the input variables for FFDI calculations. Six Global Climate Models from the Coupled Model Inter-comparison Project Phase 3 (CMIP3) archive (Meehl et al., 2007) were downscaled using CCAM: ECHAM5/MPI-OM, GFDL-CM2.0, GFDL-CM2.1, MIROC3.2(medres), UKMO-HadCM3 and CSIRO-Mk3.5. These models were chosen because of their ability to model current south-east Australian climate means and variability to an acceptable standard (Smith and Chandler, 2010), and to represent a spread of projected rainfall change in southeast Australia present in the CMIP3 set of models. GCM projections were downscaled in two stages: first, to approximately 60 km resolution over Australia with sea surface temperature and ice cover forcing from the GCMs, then the fine scale simulations were generated using spectral nudging from the intermediate model (Corney et al., 2010). When nesting a fine-scale model within a larger domain, spectral nudging (or scale-selective downscaling) is an alternative to specification of lateral boundary values by the host model. Spectral features from the host are filtered, with longer wavelength features passed to the nested model, and small-scale features permitted to evolve freely in the nested model (Thatcher and McGregor, 2009).

We generated FFDI grids at daily resolution from rainfall accumulated to midnight (Universal Time), and daily maximum temperature, minimum relative humidity and maximum wind-speed at each model grid cell. Rainfall and temperature were bias-adjusted against gridded observational data (Corney et al., 2010). FFDI values generated in this way provide an envelope of maximum possible values, because the extremes of these parameters do not necessarily occur at the same time. On days of dangerous fire weather, however, it is common for maximum temperature, minimum RH and maximum wind speed to approximately coincide (e.g. the events in Fox-Hughes (2012)), so the values calculated for dangerous days are likely to lie close to the envelope of maximum possible FFDI. We then computed a multi-model mean of the FFDI from individual models.

6.2.3 Validation of modelled FFDI

We calculated maximum daily FFDI on all observations from Tasmanian Bureau of Meteorology Automatic Weather Stations (AWS) between 2002 and 2012. During the fire season (generally October-March in Tasmania), these AWS reported half-hourly. Prior to 2010, most AWS reported at synoptic (three-hourly) intervals outside of the fire season to save communications costs. It is unlikely that significant fire danger peaks were missed by coarser

cool-season reporting frequencies, however, as only low FFDI values generally occur in the cooler months. The most recent decade was chosen for verification to incorporate data from as many AWS as possible, as AWS coverage in Tasmania has increased substantially in recent years. The ability of CCAM to reproduce realistic FFDI distributions was tested by comparing both the spatial distribution and absolute values of multi-model mean 99th percentile FFDI for the period 2002-2012 with the observed values. Further, modelled synoptic patterns associated with high fire danger were compared to those observed, to assess the realism of model scenarios of high fire danger.

6.2.4 Change in future fire danger

To assess the changes in future fire danger that are projected to occur in Tasmania up to 2100 under the A2 emissions scenario, we employed a number of complementary measures: For each grid cell, we calculated annual \sum FFDI from July to June, to reflect the southern Australian fire season. There is a wide variation of \sum FFDI across Tasmania, so we examined values averaged across Australian Bureau of Meteorology weather forecast districts (the area within each such district having a broadly similar climate). We further averaged these values over one decade periods, to reduce the impact of inter-annual variability (acknowledging, however, the possibility of decadal-scale or longer cycles), and to highlight longer-term climate trends. We considered districts in a roughly east-west transect of Tasmania (Figure 6.1), analysing \sum FFDI in each district using generalised least squares regression with a model of the form

$$y = \beta_{i0} + \beta_{i1}x_1 + \beta_{i2}\varepsilon$$

where y is \sum FFDI, x_1 is time (decade between 1960 and 2090), β_{ij} , $i = 1, 2, \dots, 6$, $j = 0, 1, 2$ are per-district linear intercept, slope and variance ratio coefficients estimated by the model and ε is a normally distributed error term (Pinheiro and Bates, 2000, Pinheiro et al., 2013). We centred data on the midpoint of the temporal scale (2025) to remove correlation between slope and intercept estimates.

We employed high percentiles of FFDI to describe changing spatial and seasonal patterns of dangerous fire weather over time. For each grid cell, and each model, we calculated 95th and 99th percentile of FFDI within contiguous two-decade slices, and then averaged this value across the models to obtain a multi-model mean percentile dataset. We considered changes during the fire season (October-March for this analysis), in the first instance, then examined changes to spring (SON), summer (DJF) and autumn (MAM) fire danger sepa-

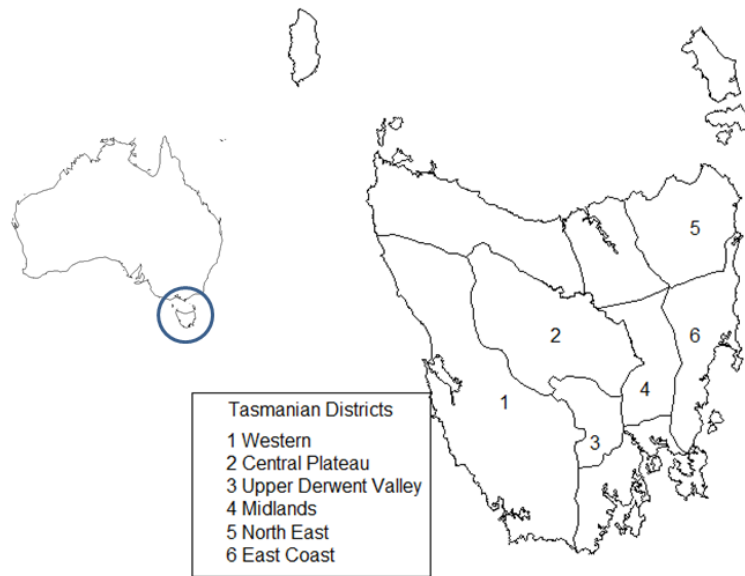


Figure 6.1: Locations of Tasmania relative to the rest of Australia, and of Tasmanian weather forecast districts used in the analysis of changes to fire danger. Un-numbered regions were not considered in the current study.

rately. To better resolve changes at a regional level within Tasmania, we also examined 99th percentile FFDI averaged over one decade periods and over forecast districts. We performed a generalised least squares regression in the same manner as for $\sum\text{FFDI}$.

6.2.5 Synoptic climatology

We examined changes to the frequency of maximum FFDI at four specific locations over time, and identified surface pressure patterns corresponding to the highest FFDI events. This allowed us to verify that the models were behaving in a manner consistent with observed synoptic patterns of elevated fire danger, as discussed above, and identify any projected changes in those patterns associated with dangerous fire weather in the future. Specifically, we identified days on which FFDI exceeded particular thresholds, chosen to reflect the range of fire danger at each site. For the south-east location, for example, FFDI 38 was chosen as the threshold, because it is the level at which the Tasmanian Fire Service usually imposes a Total Fire Ban. With no further filtering, using the surface pressure plots corresponding to days that exceeded the site-specific thresholds of fire danger we constructed multi-model composite surface pressure plots for the start (1961-1980) and end (2081-2100) of the model simulations. We then used a bootstrapping approach (Davison and Hinkley, 1997) to test the significance of the composite plots.

6.3 Results

6.3.1 Validation of modelled FFDI

The plot of multi-model mean annual 99th percentile FFDI, for the period 2002-2012, reflects quite closely the observed pattern of higher and lower FFDI at 16 locations around Tasmania (Figure 6.2). Ideally, we would compare a grid generated from observations with the model grid; however the density of observations is insufficient for any gridded observation product to be reliable. Comparing the point observations with CCAM data does demonstrate that the multi-model mean plot reproduces the distribution of observed FFDI across Tasmania, with highest values of both in south-eastern Tasmania, declining towards the west and more slowly to the north. In addition, elevated values observed in the Derwent Valley, through the Tamar Valley and Tasmanian Midlands and even slightly higher values of FFDI in smaller valleys in the northeast are resolved by the multi-model mean plot. Differences are most evident at some coastal locations and those with sharply varying topography – or both, such as in the northeast, where topography rises quite steeply moving inland from the coast and the observed values differ by a larger than average amount from the model values.

Values of \sum FFDI derived from the multi-model mean simulations match those from observations quite well. Thus, the average values of \sum FFDI for Hobart and Launceston Airport weather stations for the period 1961-2000 are 2248 (2321, range 2299-2371) and 1817 (1412, range 1371-1467), respectively. Corresponding multi-model mean values, over the same period, are bracketed following the observed values, together with the range of individual models.

Cumulative and 99th percentile FFDI values computed from observations are similar to those calculated from CCAM output for corresponding locations, across geographically diverse regions. This increases our confidence that CCAM has captured the behaviour of the weather parameters contributing to FFDI. The alternative possibility, that compensating errors in CCAM weather parameters have resulted in realistic FFDI, is very unlikely given the geographical diversity of the matching observational and CCAM values.

6.3.2 Projected changes to accumulated fire danger

Figure 6.3 shows changes in multi-model mean \sum FFDI, between two-decade averages at (a) the start (1961-1980) and (b) end (2081-2100) of the model simulation, together with (c) the difference between (a) and (b). A large range of values is obvious across Tasmania for both

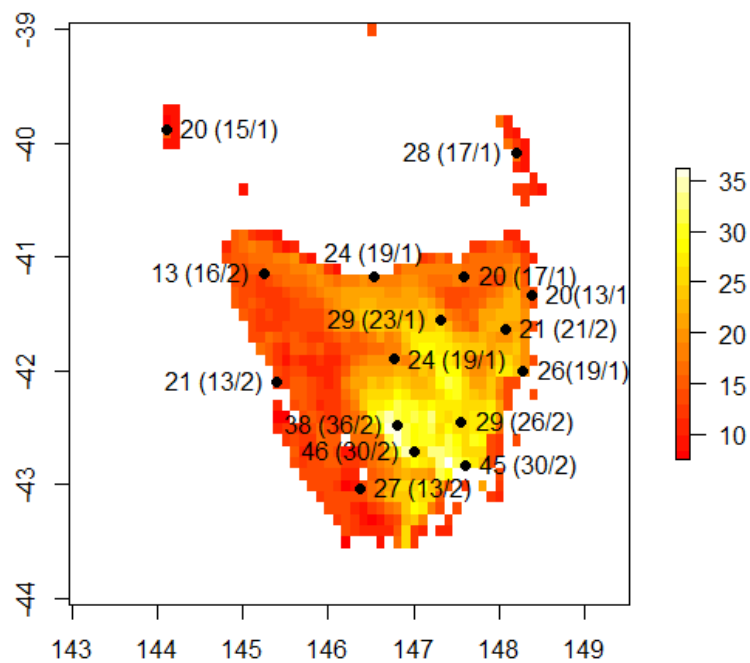


Figure 6.2: Multi-model mean of annual 99th percentile FFDI for each grid point over Tasmania between model times 2002-2012. Corresponding values from AWS observations for the same decade are superimposed for validation, together with bracketed values of the multi-model mean/standard deviation at the observation point).

periods, over relatively short distances, from 500 or below in the west to greater than 2500 in parts of the southeast. A broad increase is apparent in $\sum\text{FFDI}$ from the 1961-1980 average to that of 2081-2100 in all areas of Tasmania. The increase ranges from less than 100 in the west to more than 500 in parts of the east and southern Central Plateau (Figure 6.3(c)). The greatest percentage increase, however, is in the northwest and parts of the northeast, where $\sum\text{FFDI}$ is up to 50% greater by 2081-2100 than during 1961-1980.

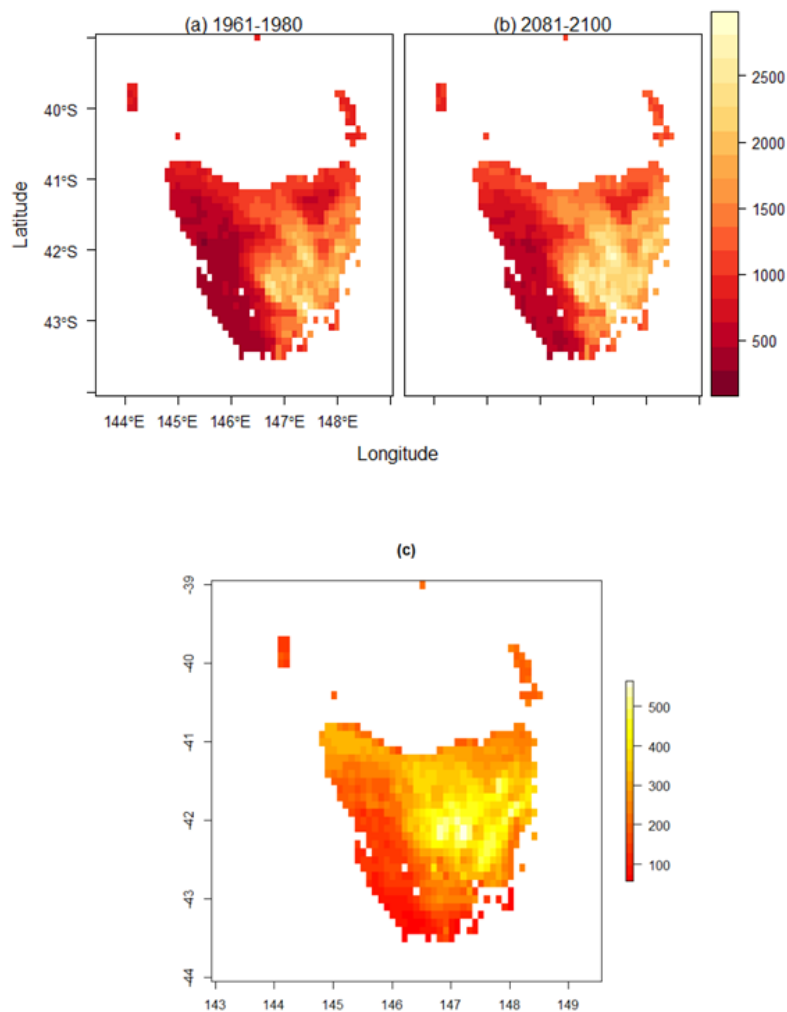


Figure 6.3: Multi-model mean $\sum\text{FFDI}$ across Tasmania, averaged over (a) 1961-1980, (b) 2081-2100 and (c) the difference between (a) and (b). Note the different scale for (c).

We present plots of $\sum\text{FFDI}$ for the six CCAM downscaled models in Figure 6.4, averaged by decade and by weather forecast district, with fitted least squares regression lines. Several questions are addressed with this analysis:

- Are the changes in district $\sum\text{FFDI}$ significant?

- Are these changes significantly different between districts?
- What are the confidence limits to the estimated rates of change?
- Can the variability in $\sum\text{FFDI}$ be quantified by district?

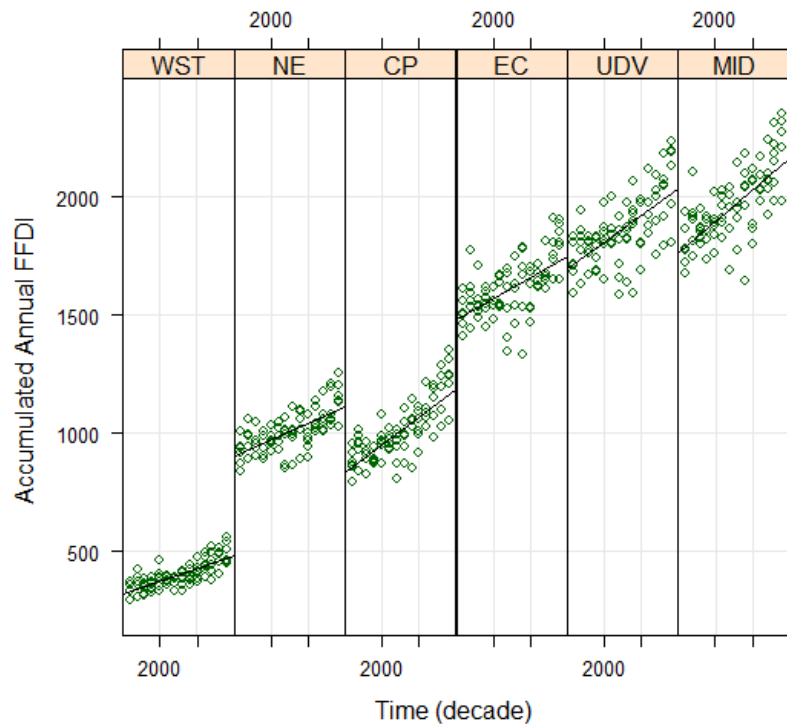


Figure 6.4: $\sum\text{FFDI}$ for the six regional climate models used in this study, averaged by decade 1960-2090 and by BoM weather forecast district (WST=Western, NE=North East, CP=Central Plateau, EC=East Coast, UDV=Upper Derwent Valley, MID=Midlands). Solid black lines are fitted generalised least squares regression lines.

Table 6.1 contains parameter estimates for the least squares regression models for each district, together with 95% confidence limits for the linear estimates. In addition, we obtained an error estimate, ϵ , with zero mean and standard deviation 114. Districts are listed in increasing order of $\sum\text{FFDI}$, and Table 6.1 suggests that this order is unlikely to change during the 21st century, as districts with higher $\sum\text{FFDI}$ have generally higher rates of change. Further, confidence limits for each district are positive. While different CCAM runs produced different magnitudes of change in $\sum\text{FFDI}$, all projected an increase in each forecast district. Finally, the order of variability ratios reflects that of $\sum\text{FFDI}$ itself. The variability ratios are likely then to contribute further to the increase in mean values, amplifying fire danger extremes.

	district	estimate	2.50%	97.50%	β_{i2}
β_{i0}	Western	403.16	395.29	411.03	0.323
	Northeast	1008.26	992.21	1024.31	0.574
	Central Plateau	1014.04	995.73	1032.35	0.678
	East Coast	1618.06	1595.56	1640.56	0.85
	Upper Derwent V	1865.19	1839.57	1890.81	1
	Midlands	1964.5	1938.75	1990.25	1.006
β_{i1}	Western	1.07	0.88	1.27	
	Northeast	1.4	1.05	1.74	
	Central Plateau	2.41	2	2.82	
	East Coast	1.79	1.27	2.3	
	Upper Derwent V	2.27	1.66	2.87	
	Midlands	2.71	2.11	3.32	

Table 6.1: Parameter estimates for linear model representing change in \sum FFDI 1960-2090 by weather forecast district, including endpoints for 95% confidence intervals. Intercept values β_{i0} are expected \sum FFDI values at 2025 (the midpoint of the temporal scale), and β_{i1} are slopes for the linear model. The rightmost column provides point estimates for the variance ratio parameter β_{i2} .

6.3.3 Projected changes to spatial extent and seasonality of fire danger

We examine 95th and 99th percentiles as a means to approach extremes of fire danger. Figure 6.5 displays 95th and 99th percentile plots of FFDI for the fire season (October-March) averaged over 1961-1980, 2041-2060 and 2081-2100. There is a similar pattern of increase through time for both sets of percentiles, with the regions of highest fire danger remaining the southeast, including the Derwent Valley and Lower Midlands, as in Figure 6.4. An increase is clear in both sets of percentile values across each time period, and across Tasmania. Table 6.2 shows the percentage of Tasmania (as represented by the 715 grid cells of the model over land) exceeding four FFDI thresholds at each time slice. The area subject to each threshold increases with each time step, with the increase itself accelerating by the end of the century. For example, 31% of Tasmania is subject to a 99th percentile FFDI greater than 24 during 1961-1980. Bearing in mind 182 days October-March, this means that 31% of Tasmania is likely to experience about two days per year with FFDI > 24 during 1961-1980. The proportion of the island subject to this threshold increases to 36% by 2041-2060 and to 46% by 2081-2100.

We examined seasonal changes to dangerous fire weather by considering 99th percentile FFDI for spring (SON), summer (DJF) and autumn (MAM). Little fire activity occurs during the Tasmanian winter, so results for June-August are not presented. We present 99th percentile FFDI only, as the changes are similar for 95th percentile FFDI. Figure 6.6

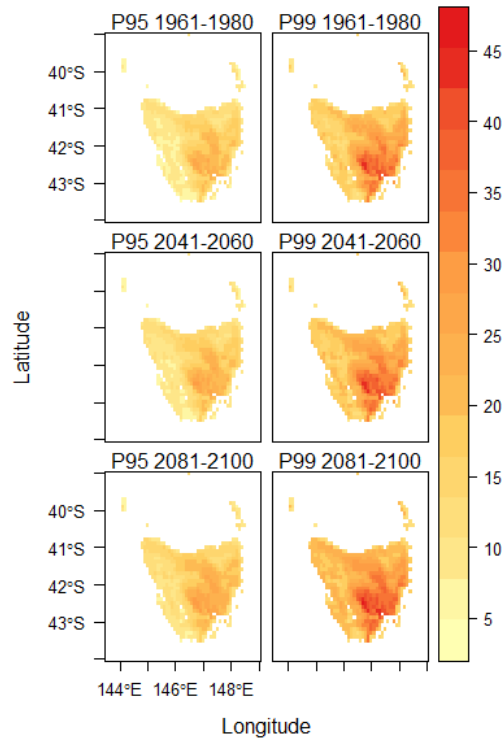


Figure 6.5: Multi-model mean 95th and 99th percentile FFDI during the fire season (October-March) for the periods 1961-1980, 2041-2060 and 2081-2100.

contains plots of 99th percentile FFDI by season for two-decade time periods 1961-1980, 2041-2060 and 2081-2100, as for Figure 6.5. Table 6.3 displays the proportion of Tasmania subject to the same thresholds of 99th percentile FFDI as Table 6.2.

	Percentile	1961-1980	2041-2060	2081-2100
FFDI > 11	95 th	0.56	0.64	0.79
	99 th	0.96	0.97	0.99
FFDI > 18	95 th	0.19	0.24	0.34
	99 th	0.57	0.69	0.83
FFDI > 24	95 th	0.02	0.04	0.09
	99 th	0.31	0.36	0.46
FFDI > 38	95 th	0	0	0
	99 th	0.02	0.03	0.05

Table 6.2: Proportion of Tasmania exceeding FFDI percentile thresholds during the fire season (Oct-Mar). The proportions are averaged over two-decade periods at the start (1961-1980), middle (2041-2060) and end (2081-2100) of the model simulations. FFDI of 11 is the top of “Moderate” McArthur Fire Danger Rating range, while 24 is top of the “High” range. Values of 18 and 38 sit at the centre of the “High” and “Very High” ranges, respectively. The McArthur rating system indicates differing levels of fire behaviour, and is used in fire management and public advice.

In general, Table 6.3 and Figure 6.6 indicate that at the lower thresholds of 99th percentile FFDI that we consider (FFDI greater than 11 and 18), there appears to be a steady increase

across the seasons in the area of Tasmania subject to increased fire danger. At higher thresholds, however, increases occur only in spring and summer, with a larger increase towards the end of the century.

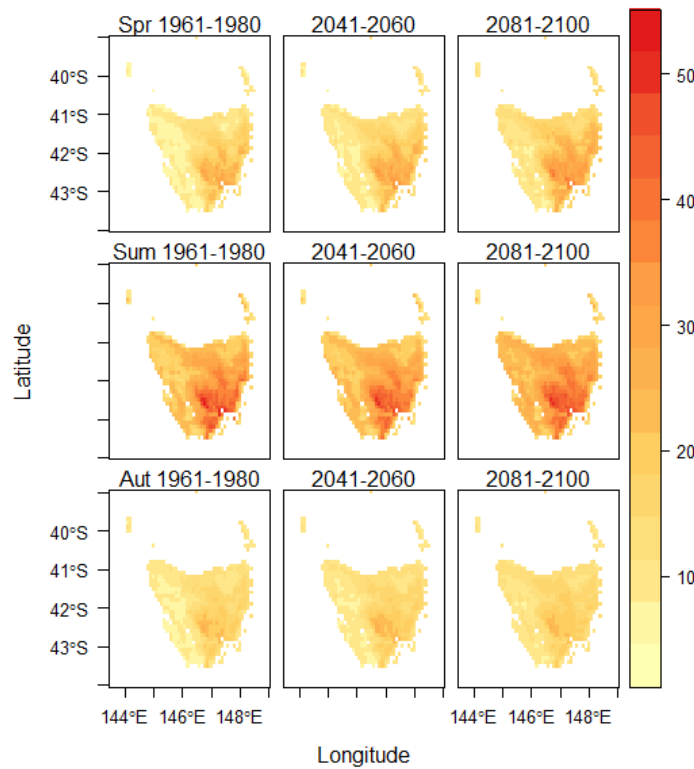


Figure 6.6: Multi-model mean 99th percentile FFBI for spring (SON), summer (DJF) and autumn (MAM), for the periods 1961-1980, 2041-2060 and 2081-2100.

Peak FFBI clearly occurs in summer, affecting all areas of Tasmania across all time periods (i.e. increase in 99th percentile FFBI). Figure 6.6 shows that spring is subject to higher FFBI at each time step than is autumn, a pattern strongest in eastern and south-eastern Tasmania. Table 6.3 affords a more quantitative examination of these differences and changes. As in Table 6.2, increasing 99th percentile FFBI occurs through time for most seasons and FFBI categories. However, in autumn there is effectively no change in the area of Tasmania subject to FFBI above 24. In contrast there is an increase from 6 to 21% of Tasmania during spring, and from 48 to 65% during summer. Little change occurs in the proportion of Tasmania in the highest fire danger category (FFBI>38), in any season.

Figure 6.7 presents 99th percentile FFBI averaged by district and decade, in the same format and with the same district ordering as Figure 6.4. Comparing Figure 6.4 and Figure 6.7 shows a greater variability around the line of best fit of 99th percentile FFBI compared to \sum FFBI. This reflects the fact that 99th percentile FFBI is a measure of extreme fire dan-

	Season	1961-1980	2041-2060	2081-2100
FFDI > 11	Spring	0.51	0.64	0.77
	Summer	0.98	0.98	0.99
	Autumn	0.53	0.61	0.72
FFDI > 18	Spring	0.22	0.29	0.4
	Summer	0.77	0.84	0.9
	Autumn	0.13	0.15	0.16
FFDI > 24	Spring	0.06	0.13	0.21
	Summer	0.43	0.49	0.65
	Autumn	0.01	0.01	0
FFDI > 38	Spring	0	0	0
	Summer	0.08	0.09	0.14
	Autumn	0	0	0

Table 6.3: Proportion of Tasmanian grid cells exceeding thresholds of 99th percentile FFDI by season.

ger, while \sum FFDI is a conservative measure of aggregate fire danger across a fire season, and extremes are more variable than means. Also, districts in Figure 6.4 were ordered by increasing \sum FFDI. The same ordering is apparent for 99th percentile FFDI, except that the Upper Derwent Valley and Midlands are reversed, indicating that the Upper Derwent Valley experiences higher extremes of fire danger compared to the Midlands in the model projections, but lower average fire danger. This is consistent with observations of southeast Tasmania experiencing the highest fire danger in the state.

Table 6.4 presents details of the generalised linear regression applied to 99th percentile FFDI. Estimates of slope and intercept differ between districts, but all slopes and their confidence intervals are positive, pointing to a steady rise in the measure of extreme FFDI. As with \sum FFDI, districts with higher current 99th percentile FFDI were those with higher variability ratios, leading to potentially more extreme fire danger through time.

6.3.4 Surface pressure patterns associated with elevated fire danger

During the baseline period of 1961-1980, there were 101 occasions on which FFDI at grid location (43.0 °S, 147.0 °E), near Hobart, reached at least 38 in one of the six model simulations. By 2081-2100, the number of such events had increased to 169. The composite Mean Sea Level Pressure pattern during these events in southeast Tasmania, and those for three other locations in Tasmania, are shown in Figure 6.8, and the count of events is shown in Table 6.5. In each case, the pressure patterns for 2081-2100 are very similar to those for 1961-1980, with a similar pressure gradient across Tasmania. For most locations, however, the absolute value of pressure is higher for the 2081-2100 composite than for 1961-

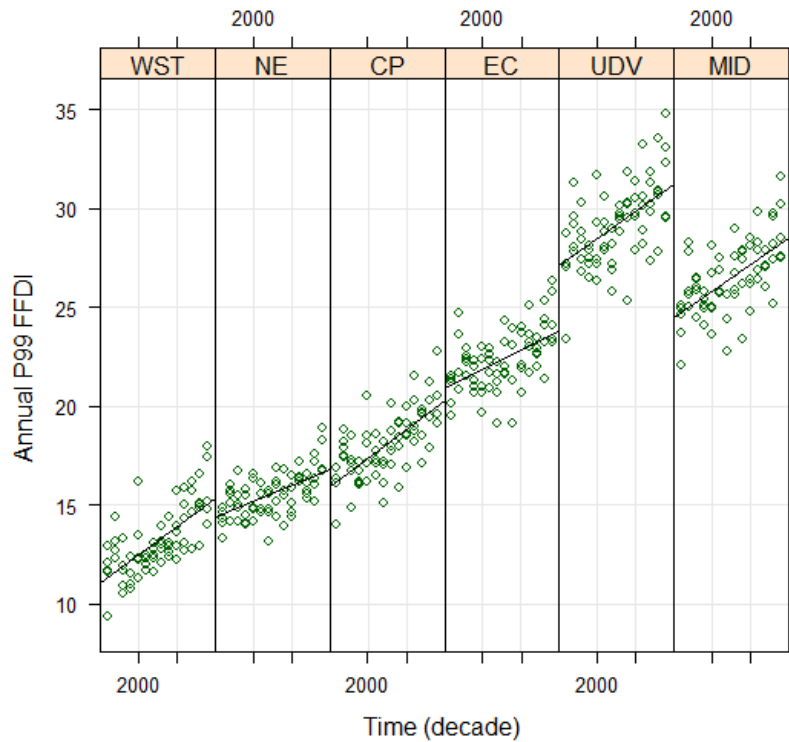


Figure 6.7: 99th percentile FFDI for the six regional climate models used in this study, averaged by decade 1960-2090 and by BoM weather forecast district (WST=Western, NE=North East, CP=Central Plateau, EC=East Coast, UDV=Upper Derwent Valley, MID=Midlands). Solid black lines are fitted generalised least squares regression lines.

	district	estimate	2.50%	97.50%	β_{i2}
β_{i0}	Western	13.2	12.91	13.48	0.718
	Northeast	15.6	15.24	15.95	0.538
	Central Plateau	18.15	17.73	18.57	0.767
	East Coast	22.36	21.96	22.78	0.764
	Upper Derwent V	29.17	28.68	29.66	1
	Midlands	26.48	26.04	26.93	0.854
β_{i1}	Western	0.029	0.022	0.036	
	Northeast	0.017	0.011	0.022	
	Central Plateau	0.029	0.022	0.037	
	East Coast	0.019	0.012	0.027	
	Upper Derwent V	0.028	0.018	0.038	
	Midlands	0.027	0.018	0.035	

Table 6.4: Parameter estimates for linear model representing change in 99th percentile FFDI 1960-2090 by weather forecast district. Intercept values β_{i0} are expected 99th percentile FFDI values at 2025 (the midpoint of the temporal scale). The right-most column provides point estimates for the variance ratio parameter β_{i2} .

1980. An exception is the pair of composites for the west coast, where there is little or no difference between the earlier and later pressure values. In Figure 6.8(a)-(f), stippling shows areas where the quantile for mean SLP on days classified as having high FFDI, calculated against the distribution formed from 2000 replicate means of samples from days classified as having low FFDI, is less than 0.05, indicating that the difference is highly significant. In Figure 6.8(g)-(h), there were insufficient cases of high FFDI for statistical analysis to be applied.

Location in Tasmania	FFDI threshold	1961-1980	2081-2100
Southeast (43.0 °S, 147.0 °E)	38	101	169
West Coast (42.1 °S, 145.4 °E)	24	49	118
Central North (41.4 °S, 147.1 °E)	30	57	129
North Coast (41.2 °S, 146.4 °E)	35	2	10

Table 6.5: Frequency of occurrence of FFDI thresholds at the start (1961-1980) and end (2081-2100) of model simulations. At each location, a specific composite pressure pattern is associated with exceedence of the FFDI threshold.

At each location, there is a substantial increase over time in the frequency of events that reach or surpass the threshold for that location. In the southeast, the increase is approximately 70%, but in the central north (near Launceston) and west coast (near Strahan), the incidence of threshold events more than doubles. On the north coast (near Devonport) a fivefold increase is projected, but with very low numbers of events of this synoptic type.

The composite pressure pattern associated with high FFDI in southeast Tasmania in the model simulations is a mesoscale low pressure system prior to the passage of a cool change, a feature which has been the subject of some study, as it is associated with severe weather (Mills and Pendlebury, 2003, Mills, 2010). Also for each location examined, the composite pattern associated with elevated fire danger corresponds to that expected from a high resolution pressure analysis of airflow around a mountainous area, resolving lee (and in some cases heat) troughs and low pressures regions, again reinforcing the view that the model has captured important fine-scale aspects of the meteorology of the situations being examined. It is particularly significant that the patterns for each location appear naturally as the composite of individual events, without any manipulation or synoptic typing applied, other than selecting for high FFDI, indicating that they are a dominant feature of elevated fire danger in their regions.

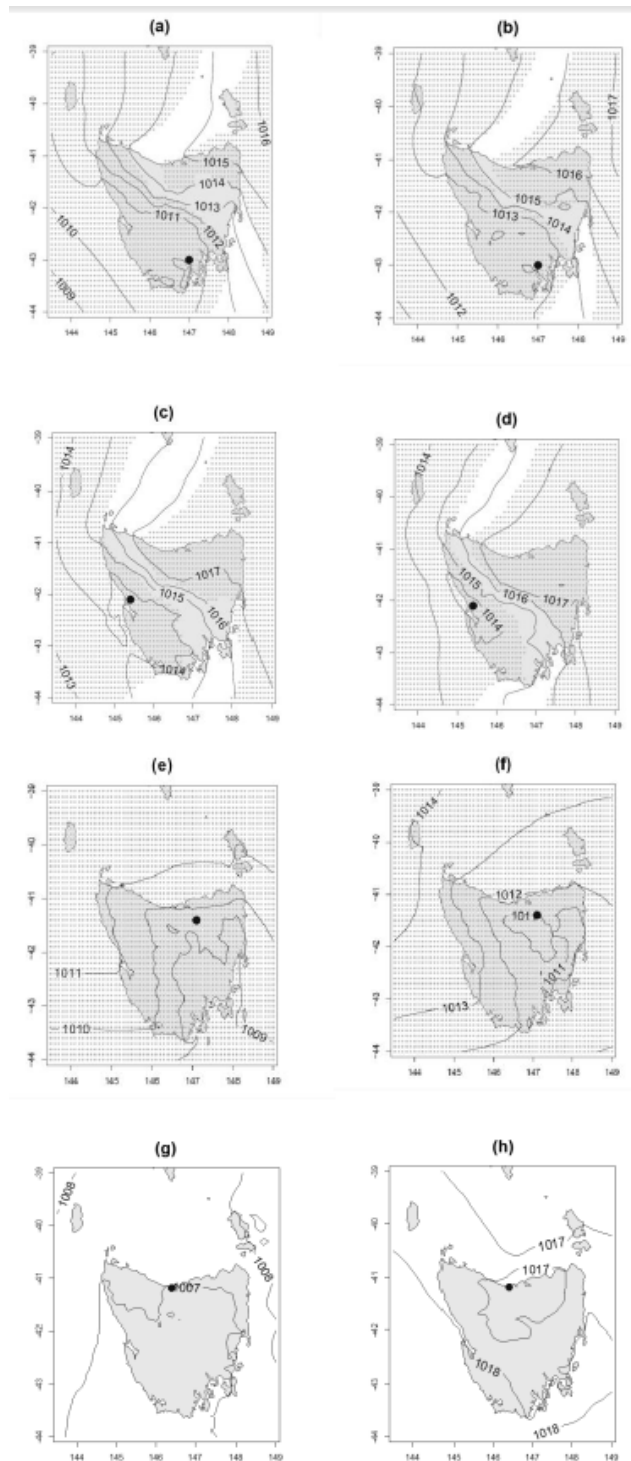


Figure 6.8: High resolution model domain, displaying composite surface pressure patterns for elevated FFDI in southeast (a) and (b), west coast (c) and (d), central north (e) and (f) and north coast Tasmania (g) and (h), for 1961-1980 and 2081-2100 respectively. Isobar spacing is one hectopascal. Dots indicate the location for which pressure pattern is associated with elevated FFDI.

6.4 Discussion and Conclusion

These results show that CCAM captures essential aspects of recently observed Tasmanian fire danger climatology, giving us confidence that the model is a useful tool to characterise changes in fire danger in Tasmania during this century. The CCAM simulations resolve a pressure pattern associated with many of the highest fire dangers across southeast Tasmania, consisting of a lee low pressure system ahead of a cool change. The results presented in this paper, and those in Grose et al. (2014), demonstrate that the CCAM simulations reproduce not only this pattern well, but also simulate distinct synoptic patterns associated with elevated fire danger in several other regions not previously studied in detail (but mentioned in Marsh (1987)). The patterns are found in current observations, the modelled baseline and the future projections, providing confidence in the validity of the model simulations.

Following the close match of the synoptic conditions, values of 99th percentile FFDI match projections quite closely (Figure 6.2), showing that the model represents current Tasmanian fire weather climate well and providing confidence not only in the larger scale features driving fire weather, but the expression of those patterns in the surface variables that determine FFDI. In particular, as noted in Fox-Hughes (2008) and discussed in Grose et al. (2014), FFDI peaks in southeast Tasmania, grading to substantially lower values in the west and about the north coast.

The simulations not only represent the current climate, but also the changes over recent decades that have been observed in Tasmanian fire weather. As Racherla et al. (2012) discuss, accurate representation of changes in recent climate is a more stringent test of the performance of regional climate models than is the successful representation of a static climate. There has been an increase in springtime fire danger, particularly in eastern and south-eastern Tasmania in recent decades (Fox-Hughes, 2008), but little change in autumn fire danger. The seasonal breakdown of the simulations shown in Figure 6.6 and Table 6.3 are highly consistent with this, where increases in spring FFDI can be seen in the southeast of Tasmania but little or no change is apparent during autumn. Indeed, it is only central southern Tasmania, around the Derwent Valley, that appears to experience elevated FFDI (at the 99th percentile level) during autumn throughout the model simulation.

Overall, the simulations provide important information for fire managers and the broader community, including:

- a broad, steady increase in measures of fire danger through the 21st century, as in-

licated in Tables 1-5 and Figs. 3-7. Multi-model mean fire dangers indicate this increase accelerating later this century. This contrasts with earlier results suggesting little future change in Tasmanian fire dangers (Hennessy et al., 2005);

- a continuation of the trend of increasing springtime fire danger, a gradual increase in summer fire danger, but little change in autumn;
- an overall broadening of the fire season;
- an increase in the number of days at the highest range of fire danger at a number of representative locations around Tasmania, associated with synoptic patterns conducive to dangerous fire weather.

There have been recent public discussions in Australia around approaches to wildfire safety and management, including the possibility of increasing fuel reduction burning and its timing relative to the peak fire season. The discussions have also included methods of protecting housing from wildfire, even to the extent of preventing construction in particularly high risk areas. This work can inform such discussions, providing an indication of how critical fire danger thresholds for safety and management may change over the next several decades. In addition, it is hoped that the work will be useful for management of parks, reserves and forest resources, allowing an assessment of likely changes in the timing and extent of opportunities, again, for safe and effective fuel reduction and for regeneration burning.

We have used FFDI as a general index of fire danger, based on a standard 12.5 tonnes/hectare of available fuel, as observations of fuel load are not generally available. A comprehensive calculation of site-specific fire danger also requires information about particular regimes of fuel and other environmental factors, including slope and aspect or variations in atmospheric stability. Projecting future changes in fuel load is not feasible because of the unknowable influence of altered fire regime (frequency, intensity and timing of fire) and plant growth, due to factors such as changing CO₂ levels (Clarke et al., 2013). Fire danger will very likely also be influenced by broader changes to climate modes such as El Nino, the Indian Ocean Dipole and Southern Annular Mode that may occur in future. We have not explicitly considered such changes, but they may contribute to the variability displayed in Figure 6.4 and Figure 6.7. Finally, we note that emissions pathways other than the A2 scenario may result in different fire danger climatologies.

A number of areas of potential future work arise from this study. It would be of interest to ascertain the frequency at which the synoptic patterns noted above actually occur (in

contrast to how often they cause fire weather events). Also, changes such as the relatively greater increase in accumulated FFDI in the southern Central Plateau district (Figure 6.3) may be related to projected decreases in rainfall and a concomitant increase in maximum temperature reported for this area in Grose et al. (2010), but we have not investigated the basis of such changes here. Finally, the variability evident in time series of \sum FFDI and 99th percentile FFDI (Figure 6.4 and Figure 6.7, respectively) may be partly due to forcing by teleconnections to ocean basins. The recognised teleconnections have differing impacts on different areas in Tasmania (see, for example, Risbey et al. (2009), Fig. 15). It would be valuable to confirm that the models are representing such teleconnections realistically. Dynamically downscaled climate models, such as that used here, provide a useful tool for pursuing such questions as their level of detail is sufficient to resolve smaller scale features, while the length of time over which they are run allows consideration of subtle changes and multidecadal cycles.

6.5 Acknowledgements

Graham Mills and Mark Chladil provided helpful comments on drafts of this paper, and the anonymous reviewers suggested useful additions and clarifications. The work was enabled by a National Disaster Resilience Program grant administered through the Tasmanian State Emergency Service, and was supported by the Australian government's Cooperative Research Centres Program through the ACE CRC. The work builds upon the Climate Futures for Tasmania project.

7: Conclusion

7.1 Overview

This thesis has aimed to explore the occurrence of springtime fire danger in Tasmania through a series of papers which have (apart from the most recent) appeared in the peer-reviewed literature. In many parts of the world, springtime fire danger is a common phenomenon, including subtropical Australia (Luke and McArthur, 1978), western North America (Westerling et al., 2006) and boreal Eurasia (Stocks and Lynham, 1996). There is, however, little documentation of significant fire danger during spring in Tasmania. It has long been recognised (Luke and McArthur, 1978, Foley, 1947) that the peak fire danger period in Tasmania is summer-autumn, although there was anecdotal discussion of a “springtime bump” among land managers and forecasters during the 1970’s and 1980’s. Also, Foley (1947) does note the occurrence of “extensive” bushfires during October 1914 and Marsh (1987) documents the extreme fire danger day 6 November 1982. Such events, however, were notable for their rarity.

Eastern and southeastern Tasmania have experienced a rapid increase in the occurrence of particularly dangerous fire weather (defined as those days with a peak FFDI of 40 or more) in the period since the mid-1980’s. Chapter Two of the thesis (Fox-Hughes, 2008) documented this significant finding while establishing the occurrence of an early season peak of “Very High” springtime fire danger in the east and southeast of the state approximately one year in two, thereby confirming the existence of the springtime bump discussed amongst operational staff in the forecasting and land management sectors. In analysing fire dangers computed from Bureau of Meteorology three-hourly (SYNOP) weather station data, it also became clear that there were differences in diurnal patterns of fire danger peak between the west and east of the state, and, particularly between high level and low-lying stations. Strahan, on the west coast, tended to experience an earlier peak of fire danger (most commonly at 1200 Local Time) than stations in the east and southeast, where the peak time of FFDI was during the mid-afternoon. It is likely (but remains to be proven) that this timing difference is a consequence of diurnal forcing, due to land-sea temperature contrast, of the progress of cool changes moving across Tasmania, as described in Mills (2002). Differences in time of maximum fire danger between high and low-lying observation sites had been noted and commented on locally in the Hobart Regional Office of the Bureau of Meteorology, but had not been documented earlier in Tasmania. Chapter Two demonstrated that diurnal peak fire danger at the summit of Mt Wellington, in southeast Tasmania, tended to occur during the early morning. At Hobart however, in close geographical proximity to Mt Wellington

but near to sea-level, peak fire danger was commonly during the afternoon.

The geographical differences in diurnal variability examined in Chapter Two highlighted the need to study fire danger at increased temporal resolution. In Chapter Three (Fox-Hughes, 2011), half-hourly resolution fire danger observations were studied, whereas in Chapter Two, the data used were synoptic, mainly three-hourly, observations. Digitised half-hourly data for Australian observation sites has only become available since the early 1990's with the increasing use of Automatic Weather Stations (AWS), and the Tasmanian data were among the earliest to be stored in a readily accessible format. Such data afford the opportunity to examine rapidly changing fire weather events, which is important for gauging the full range of fire weather variability, to inform forecast and fire management decisions.

Chapter Three examined, in particular, the degree to which more coarsely sampled data – three-hourly, or 1500 Local Time only – miss the peak of fire weather events, or miss the events entirely. In the case of Hobart Airport, for example, it was demonstrated that approximately 50% of days have a fire danger peak around 1500 Local Time. Thus, around half of the fire danger peaks are missed by 1500-only data. This result is important because many climate studies employ 1500-only observations; as such data are available for generally longer periods than three hourly synoptic or more frequent observations, and for a greater number of observation locations than the other data types. Using the above results, one could then estimate the degree to which a correction is required in the assessment of fire event frequency following from such studies. High temporal resolution data examined in this chapter also allowed study of the length of fire weather events, and the relationship between duration and severity of events. This relationship was not always obvious – while it was sometimes the case that longer events were more severe, a number of dangerous fire weather events in southeast Tasmania were found to have been of quite short duration. These latter events are important to document for a number of reasons: their brevity means that they can be overlooked, as noted, in long-term climate studies, and it is possible that they will not be fully resolved by forecasts of fire weather. They are, however, capable of causing death and substantial damage.

Chapters Two and Three examined collective characteristics of Tasmanian fire weather events, but both pointed to the value of close examination of specific events, particularly extreme events. Case studies of two such dangerous springtime fire weather events were examined in Chapter Four (Fox-Hughes, 2012), both involving periods of “Catastrophic” fire danger, i.e. a forest fire danger index in excess of 100. During one event, on 12 October

2006, FFDI was greater than 100 for more than four hours, arguably making the event a more extreme fire weather event (while not a human catastrophe) than the “Black Tuesday” fire weather in southern Tasmania on 7 February 1967. The other event, occurring on 7 November 2002, had a different character, peaking sharply in the early evening after an apparently “normal” diurnal increase in fire danger earlier in the day. Such abrupt increases in fire danger, or “spikes”, have the potential to be particularly dangerous, as they may not be anticipated by fire managers or the community, especially if they occur at unusual times of the day.

Of particular significance in Chapter Four, investigation of the dynamics of the two events revealed that the rapid change in the November 2002 event followed from the descent into the lower troposphere of dry, high-momentum air, while the extreme conditions in the October 2012 event were a consequence of the advection of very dry air from drought-affected areas in inland Australia. Thus, the severity of the two events was a consequence of quite different mechanisms. The structure and location of upper tropospheric features was also quite different, with the “spike” event characterised by a negatively tilting upper tropospheric trough close to Tasmania while the other, more typical, event lacked this feature, having a more common positively tilted trough further to the west of Tasmania during the peak of the fire weather. This observation led to the work in Chapter Five assessing the generality of structural differences between the two types of fire weather event. Both events did, however, show evidence of a foehn influence as their respective airmasses crossed the Tasmanian central highlands.

It was clear from the case study of the November 2002 and October 2006 fire weather events that there was considerable value in examining other events with characteristics common to the two cases. In order to do that, elements of the two previous chapters were combined in Chapter Five (Fox-Hughes, in review). The high temporal resolution dataset of FFDDI created for Chapter Three’s research was used to identify fire weather events involving a rapid increase in fire danger. The marked differences between the two case studies investigated in Chapter Four were shown to be common to classes of fire weather events, with one class –those involving rapid fire danger increases– showing strong evidence of dry air descending through much of the depth of the troposphere, and the other class lacking such evidence. The structural differences evident in the case studies were also shown to occur more generally, with “spike” events typically associated with a negatively tilted upper tropospheric trough near Tasmania and “normal” events lacking this feature.

The most significant finding from Chapter Five was that clear differences in the location

and structure of upper tropospheric features could be identified between the classes of events studied. These differences allow the possibility of forecasting well in advance situations where there is likely to be a rapid increase in fire danger, an important advance given the risk to life and property that such events pose.

The work documented in Chapters Two to Five examined past fire weather in Tasmania. Some of that work highlighted changes that had occurred in recent decades. It was a natural next step then, of substantial strategic and operational significance, to examine how Tasmanian fire weather might change in coming decades. Thus, Chapter Six (Fox-Hughes et al., 2014a) investigated projections of fire danger in Tasmania through the course of the current century, using downscaled climate model data from the Climate Futures for Tasmania project. An important aspect of this Chapter was to validate the model results against observations, and to assess the degree to which the future model results could be trusted. The pattern of modelled fire danger across Tasmania for the decade 2002-12 resembled closely the corresponding pattern of fire dangers derived from automatic weather station observations, with an increase from quite low values in the north and west of the state to substantially higher values in the southeast, and relatively high values in the Tamar and Derwent Valleys.

Of particular significance, both for validation of the models and for the theme of this thesis, the change in seasonality of fire danger observed in Tasmania (and documented in Chapter Two) was resolved, with an increase in the last several decades in spring, but little change in autumn. This seasonal shift was projected to continue through the current century, suggesting that springtime fire weather events will remain a concern in future years. The climate models were forced by increased CO₂ concentrations (using the SRES A2 scenario), suggesting, but not proving, that the seasonal changes observed to date may be a response to circulation changes resulting from changing CO₂ concentrations.

A number of datasets were analysed during the course of this study, each of which had particular strengths and limitations, characteristics common to the data used in other meteorological studies in the literature. Observations at 1500 Local Time are generally the most geographically widely available weather observations (apart from 0900 rainfall reports) with a length of record sometimes in excess of a century. Many post offices in rural and regional Australia conducted such observations in the past, for example. Diurnal development of weather systems is not, however, amenable to study using these data. Three-hourly synoptic weather observations allow some study of diurnal changes while having a more limited geographical extent than 1500-only data. These observations are also generally available for

a number of decades for several locations in Tasmania, and formed the basis of the study in Chapter Two of Tasmanian fire weather climatology which highlighted the existence of the “springtime” bump and dramatic springtime increase in dangerous events in the last 20-30 years. The most geographically restricted dataset used in this study was the half-hourly observation dataset, available (in digital format) only at sites where automatic weather stations were installed in the 1990’s and for which the data was archived in the Bureau of Meteorology’s Australian Digital Archive for Meteorology (ADAM) database. Approximately twenty years’ of data were available in ADAM at three sites in Tasmania of fire weather significance. While the geographical extent of these data was limited, the high temporal resolution allowed a much closer study of diurnal variation of fire danger than was possible with the synoptic, or especially 1500-only, data. In particular, the temporal resolution afforded the opportunity to study abrupt increases in fire danger, and their associated synoptic weather systems. Also important in the study of the synoptic features of abrupt fire danger events was the global NCEP/NCAR reanalysis dataset. While its temporal and spatial resolution is limited, the reanalysis allowed the identification of the atmospheric features associated with abrupt fire danger increases and afforded the opportunity to study important features of negatively tilted troughs.

Greater detail was available from the (at the time) operational Australian numerical weather prediction model, mesoLAPS, used in the case studies of springtime events. MesoLAPS data was available on a relatively fine (12.5 km x 12.5 km x 29 sigma level) three-dimensional grid, at hourly timesteps, permitting a detailed analysis of mesoscale atmospheric processes occurring during the events, and setting the scene for the more broadscale synoptic climatology study in Chapter Five. Both the reanalysis and mesoLAPS datasets were constrained by observations. The future fire danger dataset was derived from Climate Futures for Tasmania data, run with a climate model with daily resolution over 140 years, 1961-2100, and approximately 10 km x 10 km horizontal resolution. It was, however, constrained only by model physics and parameterisation including a specified emissions pathway. Even so, it represented well current features of the Tasmanian fire danger climatology.

Part of the process of employing each dataset was to attempt to maximise the benefit to be gained, while minimising the impact of the limitations of the sets. It is also pertinent to recognise the debt owed to those workers who generated, quality-controlled, archived and made available the data for further use.

7.2 Consideration of initial questions and application of results

The idea for this thesis grew out of a perception, within the context of operational fire weather meteorology, that dangerous springtime fire weather events were becoming increasingly frequent in Tasmania. It was always intended that the insights that might be gained from the work could be readily applied, both by meteorologists and by fire and land managers, so the questions asked at the commencement of the project tended to be ones likely to have immediately applicable answers. Thus, there are a number of directly applicable results, either as tools to interpret weather events or as contextual information to understand what is common in fire weather situations. Most have been noted above but are summarised here. They include:

- confirmation of the existence of secondary (and sometimes primary) springtime fire danger peaks, with an increased awareness that dangerous events have become more common in recent decades;
- identification of synoptic patterns conducive to the descent of dry, high-momentum air from near the tropopause that cause rapid increases in fire danger at the earth's surface, and that have contributed to a proportion of recent springtime fire weather events;
- use of regional climate projections to suggest, under an emissions regime similar to that currently observed, a broad increase in fire danger across Tasmania during the twenty-first century, a steeper increase in the occurrence of more extreme high fire danger days and a continuing increase in the frequency of dangerous springtime fire weather.

Other results have been a serendipitous outcome of the research to resolve the original questions. These include:

- characterising the variability in diurnal peaks of fire danger between western and eastern Tasmania, and between elevated and low-lying areas;
- documenting of the sometimes very different seasonal patterns of fire danger occurrence between different regions in Tasmania;

- highlighting the frequency with which diurnal fire danger peaks occur at times other than mid-afternoon;
- identifying separate types of the fire weather event in Tasmania, with one type (“spike” events, involving rapid fire danger increases) very similar in character to events documented in other areas of Australia and in the Northern Hemisphere.

Both of these sets of results have had a number of applications to date. Fire weather forecasting in Tasmania has benefitted from confirmation of anecdotally observed features including the diurnal and topographic variation in peak time of fire danger. The high proportion of (Tasmanian) fire danger peaks occurring other than mid-afternoon has prompted a similar study at other Australian sites (Kepert et al., 2012). Identification of events likely to result in abrupt spikes in fire danger has occurred well in advance of the events (e.g. Fox-Hughes (2014)). A technical report summarising and explaining the results of the future fire danger study for Tasmania has been distributed to Tasmanian Government agencies, to inform policy decisions such as the amount of resourcing likely to be required for future fire management and how development planning guidelines should be amended to address changes in Tasmania’s climate (Fox-Hughes et al., 2014b).

7.3 Future Work

A number of avenues for further research have become apparent during the course of the current study. It is not entirely clear why there has been a steep increase in the number of days of dangerous springtime fire danger in recent decades. That the Climate Futures for Tasmania modelling analysis also indicates increasing springtime fire danger but, as also observed, no concomitant increase during autumn suggests that the change is a result of anthropogenic greenhouse gas forcing. As noted above however, this remains to be demonstrated conclusively.

Negatively-tilting upper tropospheric troughs have been demonstrated to be associated with abrupt increases in fire danger, and have played a part in a number of dangerous spring fire weather events in Tasmania. It would be of interest to attempt to identify such features from reanalysis data, to assess their frequency, and thereby the proportion of them that result in fire danger spikes. It would also be valuable to identify whether there are notable interannual variations in the occurrence of the features that might link their occurrence to broadscale influences such as ENSO or the Southern Annular Mode or an increasing trend

in their occurrence that could account, in part, for the increase in dangerous springtime fire weather. This could form the basis of very useful outlook guidance aimed at forecasters and emergency managers for these often dangerous events.

There are hints that the atmospheric structures associated with fire danger spikes, negatively tilted troughs, can be linked to prolific lightning events. The ignition date of the Arthur-Pieman (or Franklin-Donaldson) fire in northwest Tasmania which burnt some 100,000 Ha (Thackway et al., 2008) in November 2003 was one of the fire danger spike days at Hobart Airport, for example. While the occurrence of lightning ignition of wildfires is not a specifically springtime occurrence, it does contribute as a meteorological factor to the fire management problem during springtime. Might the increased ascent at the inflection point downstream from the (negatively tilted) trough apex increase the likelihood of thunderstorm occurrence in that region? Other questions pertinent to fire danger apply equally well to lightning: what is the seasonality of lightning occurrence; are lightning ignitions increasing in frequency and, if so, why? Further study of negatively tilted troughs seems well-justified on a number of fronts.

Several of the questions addressed during the course of my PhD have a much wider applicability than Tasmania. For example, diurnal variability of fire danger and its changes with elevation are significant in other parts of Australia and in fire-prone regions globally. Similarly, as highlighted in Chapter Five, negatively tilted upper tropospheric troughs can have a very substantial impact on fire danger levels in numerous locations around the globe for which documentation of rapid increases in fire activity and fire danger exists, and very likely have such an impact in all fire-prone areas.

The topics investigated in this PhD have all shed light on fire danger in Tasmania, and the occurrence of the “springtime bump” in particular. The work has had immediate applicability in operational forecasting and is of use in the practice of fire management. Finally, it has underscored several areas of potentially rewarding further investigation.

Bibliography

- Albertson, K., Ayles, J., Cavan, G., McMorrow, J., et al., 2011. Climate change and the future occurrence of moorland wildfires in the Peak District of the UK. *Climate Research* 45 (1), 105–118.
- Alexander, L. V., Hope, P., Collins, D., Trewin, B., Lynch, A., Nicholls, N., et al., 2007. Trends in Australia's climate means and extremes: a global context. *Australian Meteorological Magazine* 56 (1), 1–18.
- Atallah, E., Bosart, L. F., Aiyyer, A. R., 2007. Precipitation distribution associated with landfalling tropical cyclones over the eastern United States. *Monthly Weather Review* 135 (6), 2185–2206.
- Attorney-General's Department, 2011. <http://www.disasters.ema.gov.au/BrowseDetails/DisasterEventDetails.aspx?DisasterEventID=2008>.
- Beals, E. A., 1914. Value of weather forecasts in the problem of protecting forests from fire. *Monthly Weather Review* 42 (2), 111–119.
- Beck, J., Alexander, M., Harvey, S., Beaver, A., 2002. Forecasting diurnal variations in fire intensity to enhance wildland firefighter safety. *International Journal of Wildland Fire* 11 (4), 173–182.
- Beck, J., Trevitt, A., 1989. Forecasting diurnal variations in meteorological parameters for predicting fire behaviour. *Canadian Journal of Forest Research* 19 (6), 791–797.
- Beer, T., Gill, A., Moore, P., 1988. Australian bushfire danger under changing climatic regimes. *Greenhouse, Planning for Climate Change*, 421–427.
- Beer, T., Williams, A., 1995. Estimating Australian forest fire danger under conditions of doubled carbon dioxide concentrations. *Climatic Change* 29 (2), 169–188.
- Bell, A., 1983. Fire and rainforest in Tasmania. *Ecos* 37, 3–8.

- Black, M. P., Mooney, S. D., 2006. Holocene fire history from the Greater Blue Mountains World Heritage area, New South Wales, Australia: the climate, humans and fire nexus. *Regional Environmental Change* 6 (1-2), 41–51.
- Bluestein, H. B., 1993. Synoptic-dynamic Meteorology in Midlatitudes: Observations and theory of weather systems. Vol. 2. Taylor & Francis, p. 119.
- Bond, H., MacKinnon, K., Noar, P. F., 1967. Report on the meteorological aspects of the catastrophic bushfires in south-eastern Tasmania on 7 February 1967. Bureau of Meteorology.
- Bradstock, R. A., 2010. A biogeographic model of fire regimes in Australia: current and future implications. *Global Ecology and Biogeography* 19 (2), 145–158.
- Brotak, E. A., 1980. A comparison of the meteorological conditions associated with a major wildland fire in the United States and a major bush fire in Australia. *Journal of Applied Meteorology* 19 (4), 474–476.
- Brotak, E. A., Reifsnnyder, W. E., 1977. An investigation of the synoptic situations associated with major wildland fires. *Journal of Applied Meteorology* 16 (9), 867–870.
- Brown, T. J., Hall, B. L., Westerling, A. L., 2004. The impact of twenty-first century climate change on wildland fire danger in the western United States: an applications perspective. *Climatic Change* 62 (1-3), 365–388.
- Bureau of Meteorology, 1985. Report on the meteorological aspects of the Ash Wednesday fires - 16 February 1983. Tech. rep., Bureau of Meteorology, Melbourne, Australia. 143 pp.
- Bureau of Meteorology, 2002. Monthly Weather Review Tasmania for November 2002. Tech. rep., Bureau of Meteorology, Hobart, Australia. 23 pp.
- Bureau of Meteorology, 2003. Meteorological aspects of the eastern Victorian fires January-March 2003. Tech. rep., Bureau of Meteorology, Melbourne, Australia. 82 pp.
- Burgan, R. E., et al., 1988. 1988 revisions to the 1978 national fire-danger rating system. US Department of Agriculture, Forest Service, Southeastern Forest Experiment Station.
- Carmona-Moreno, C., Belward, A., Malingreau, J.-P., Hartley, A., Garcia-Alegre, M., Antonovskiy, M., Buchshtaber, V., Pivovarov, V., 2005. Characterizing interannual vari-

- ations in global fire calendar using data from Earth observing satellites. *Global Change Biology* 11 (9), 1537–1555.
- Carvalho, A., Carvalho, A., Martins, H., Marques, C., Rocha, A., Borrego, C., Viegas, D., Miranda, A., 2011. Fire weather risk assessment under climate change using a dynamical downscaling approach. *Environmental Modelling & Software* 26 (9), 1123–1133.
- Carvalho, A., Flannigan, M. D., Logan, K. A., Gowman, L. M., Miranda, A. I., Borrego, C., 2010. The impact of spatial resolution on area burned and fire occurrence projections in Portugal under climate change. *Climatic Change* 98 (1-2), 177–197.
- Charney, J. J., Keyser, D., 2010. Mesoscale model simulation of the meteorological conditions during the 2 June 2002 Double Trouble State Park wildfire. *International Journal of Wildland Fire* 19 (4), 427–448.
- Clarke, H., Lucas, C., Smith, P., 2013. Changes in Australian fire weather between 1973 and 2010. *International Journal of Climatology* 33 (4), 931–944.
- Corney, S., Grose, M., Bennett, J. C., White, C., Katzfey, J., McGregor, J., Holz, G., Bindoff, N. L., 2013. Performance of downscaled regional climate simulations using a variable-resolution regional climate model: Tasmania as a test case. *Journal of Geophysical Research: Atmospheres* 118 (21), 11–936.
- Corney, S., Katzfey, J., McGregor, J., Grose, M., Bennett, J., White, C., Holz, G., Gaynor, S., Bindoff, N., 2010. Climate Futures for Tasmania: climate modelling technical report. Antarctic Climate and Ecosystems Co-operative Research Centre, Hobart, Australia.
- Crimmins, M. A., 2006. Synoptic climatology of extreme fire-weather conditions across the southwest United States. *International Journal of Climatology* 26 (8), 1001–1016.
- Crimmins, M. A., Comrie, A. C., 2005. Interactions between antecedent climate and wildfire variability across south-eastern Arizona. *International Journal of Wildland Fire* 13 (4), 455–466.
- Dai, A., 2011. Drought under global warming: a review. *Wiley Interdisciplinary Reviews: Climate Change* 2 (1), 45–65.
- Davison, A. C., Hinkley, D. V., 1997. *Bootstrap Methods and their Applications*, Cambridge Series in Statistical and Probabilistic Mathematics. Cambridge University Press, Cambridge.

- Department of Premier and Cabinet, 2013. Tasmanian Bushfire Recovery Taskforce Interim Action Plan February 2013. Tech. rep.
- Dowdy, A. J., Mills, G. A., 2012. Atmospheric and fuel moisture characteristics associated with lightning-attributed fires. *Journal of Applied Meteorology and Climatology* 51 (11), 2025–2037.
- Dowdy, A. J., Mills, G. A., Finkele, K., de Groot, W., 2009. Australian fire weather as represented by the mcarthur forest fire danger index and the canadian forest fire weather index. CAWCR Technical Report 10, Centre for Australian Climate and Weather Research.
- Dowdy, A. J., Mills, G. A., Finkele, K., de Groot, W., 2010. Index sensitivity analysis applied to the Canadian forest fire weather index and the McArthur forest fire danger index. *Meteorological Applications* 17 (3), 298–312.
- Draper, C., Mills, G., 2008. The atmospheric water balance over the semiarid Murray-Darling River basin. *Journal of Hydrometeorology* 9 (3), 521–534.
- Draxler, R. R., Hess, G., 1998. An overview of the HYSPLIT_4 modelling system for trajectories. *Australian Meteorological Magazine* 47 (4), 295–308.
- Drobyshev, I., Niklasson, M., Linderholm, H. W., 2012. Forest fire activity in Sweden: Climatic controls and geographical patterns in 20th century. *Agricultural and Forest Meteorology* 154, 174–186.
- Ellis, R., 1985. The relationships among eucalypt forest, grassland and rainforest in a highland area in north-eastern Tasmania. *Australian Journal of Ecology* 10 (3), 297–314.
- Engel, C. B., Lane, T. P., Reeder, M. J., Rezny, M., 2013. The meteorology of Black Saturday. *Quarterly Journal of the Royal Meteorological Society* 139 (672), 585–599.
- Enright, N. J., Thomas, I., 2008. Pre-European fire regimes in Australian ecosystems. *Geography Compass* 2 (4), 979–1011.
- Flannigan, M., Cantin, A. S., de Groot, W. J., Wotton, M., Newbery, A., Gowman, L. M., 2013. Global wildland fire season severity in the 21st century. *Forest Ecology and Management* 294, 54–61.
- Flannigan, M., Harrington, J., 1988. A study of the relation of meteorological variables to monthly provincial area burned by wildfire in Canada (1953-80). *Journal of Applied Meteorology* 27 (4), 441–452.

- Flannigan, M., Logan, K., Amiro, B., Skinner, W., Stocks, B., 2005. Future area burned in Canada. *Climatic Change* 72 (1-2), 1–16.
- Flannigan, M., Stocks, B. J., Wotton, B., 2000. Climate change and forest fires. *Science of the Total Environment* 262 (3), 221–229.
- Flannigan, M., Wotton, B., 2001. Climate, weather, and area burned. In: *Forest fires: Behavior and Ecological Effects*. Academic Press, New York, pp. 351–373.
- Flannigan, M. D., Krawchuk, M. A., de Groot, W. J., Wotton, B. M., Gowman, L. M., 2009. Implications of changing climate for global wildland fire. *International Journal of Wildland Fire* 18 (5), 483–507.
- Foley, J. C., 1947. A study of meteorological conditions associated with bush and grass fires and fire protection strategy in Australia. JJ Gourley, Government Printer, Melbourne, Australia.
- Fox-Hughes, P., 2008. A fire danger climatology for Tasmania. *Australian Meteorological Magazine* 57 (2), 109–120.
- Fox-Hughes, P., 2011. Impact of more frequent observations on the understanding of Tasmanian fire danger. *Journal of Applied Meteorology and Climatology* 50 (8), 1617–1626.
- Fox-Hughes, P., 2012. Springtime fire weather in Tasmania, Australia: two case studies. *Weather and Forecasting* 27 (2), 379–395.
- Fox-Hughes, P., 2014. Severe winds in south-east Tasmania, 9 february 2014. *Bulletin of the Australian Meteorological and Oceanographic Society* 27 (2), 48–49.
- Fox-Hughes, P., Harris, R., Lee, G., Grose, M., Bindoff, N., 2014a. Future fire danger climatology for Tasmania, Australia, using a dynamically downscaled regional climate model. *International Journal of Wildland Fire* 23 (3), 309–321.
- Fox-Hughes, P., Harris, R. M. B., Lee, G., Jabour, J., Grose, M. R., Remenyi, T. A., Bindoff, N. L., 2014b. *Climate Futures for Tasmania: future fire danger technical report*. Antarctic Climate and Ecosystems Co-operative Research Centre, Hobart, Australia.
- Fried, J. S., Torn, M. S., Mills, E., 2004. The impact of climate change on wildfire severity: a regional forecast for northern California. *Climatic Change* 64 (1-2), 169–191.
- Geldenhuys, C., 1994. Bergwind fires and the location pattern of forest patches in the southern Cape landscape, South Africa. *Journal of Biogeography* 21 (1), 49–62.

- Georgiev, C. G., Martín, F., 2001. Use of potential vorticity fields, Meteosat water vapour imagery and pseudo water vapour images for evaluating numerical model behaviour. *Meteorological Applications* 8 (01), 57–69.
- Gillett, N., Weaver, A., Zwiers, F., Flannigan, M., 2004. Detecting the effect of climate change on Canadian forest fires. *Geophysical Research Letters* 31 (L18211), doi:10.1029/2004GL020876.
- Glickman, T. S., Macdonald, N. J., Sanders, F., 1977. New findings on the apparent relationship between convective activity and the shape of 500 mb troughs. *Monthly Weather Review* 105, 1060.
- Griffiths, D., 1998. Improved formulae for the McArthur forest fire danger meter. *Meteorological Note* 214, Bureau of Meteorology, Melbourne, Australia.
- Griffiths, D., 1999. Improved formula for the drought factor in McArthur's forest fire danger meter. *Australian Forestry* 62 (2), 202–206.
- Grose, M., Barnes-Keoghan, I., Corney, S., White, C., Holz, G., Bennett, J., Gaynor, S., Bindoff, N., 2010. *Climate Futures for Tasmania: general climate impacts technical report*. Antarctic Climate and Ecosystems Co-operative Research Centre, Hobart, Australia.
- Grose, M. R., Fox-Hughes, P., Harris, R. M., Bindoff, N. L., 2014. Changes to the drivers of fire weather with a warming climate—a case study of southeast Tasmania. *Climatic Change* 124 (1-2), 255–269.
- Hanstrum, B., Wilson, K., Barrell, S., 1990. Prefrontal troughs over southern Australia. Part I: A climatology. *Weather and Forecasting* 5 (1), 22–31.
- Hasson, A., Mills, G., Timbal, B., Walsh, K., et al., 2009. Assessing the impact of climate change on extreme fire weather events over southeastern Australia. *Climate Research* 39 (2), 159.
- Hennessy, K., Lucas, C., Nicholls, N., Suppiah, J., Ricketts, J., 2005. *Climate change impacts on fire-weather in south-east Australia*. CSIRO Marine and Atmospheric Research.
- Hessl, A. E., 2011. Pathways for climate change effects on fire: Models, data, and uncertainties. *Progress in Physical Geography* 35 (3), 393–407.
- Hoinka, K. P., Carvalho, A., Miranda, A. I., 2009. Regional-scale weather patterns and wildland fires in central Portugal. *International Journal of Wildland Fire* 18 (1), 36–49.

- Huang, C., Lin, Y., Kaplan, M., Charney, J., 2009. Synoptic-scale and mesoscale environments conducive to forest fires during the October 2003 extreme fire event in southern California. *Journal of Applied Meteorology and Climatology* 48 (3), 553–579.
- Irving, D. B., Whetton, P., Moise, A. F., 2012. Climate projections for Australia: a first glance at CMIP5. *Australian Meteorological and Oceanographic Journal* 62 (4), 211–225.
- Kalnay, E., Kanamitsu, M., Kistler, R., Collins, W., Deaven, D., Gandin, L., Iredell, M., Saha, S., White, G., Woollen, J., et al., 1996. The NCEP/NCAR 40-year reanalysis project. *Bulletin of the American Meteorological Society* 77 (3), 437–471.
- Kaplan, M. L., Huang, C., Lin, Y.-L., Charney, J., 2008. The development of extremely dry surface air due to vertical exchanges under the exit region of a jet streak. *Meteorology and Atmospheric Physics* 102 (1-2), 63–85.
- Karl, T. R., Trenberth, K. E., 2003. Modern global climate change. *Science* 302 (5651), 1719–1723.
- Kepert, J., Fawcett, R., 2013. Meteorological aspects of the Margaret River fires on November 2011. extended abstracts. In: 20th International Congress on Modelling and Simulation, Adelaide, December. pp. 1–6.
- Kepert, J., Wain, A., Tory, K., 2012. A comprehensive, nationally consistent climatology of fire weather parameters. In: Proceedings AFAC Conference, Perth, W.A., August 28-30.
- King, K. J., Cary, G. J., Gill, A. M., Moore, A. D., 2012. Implications of changing climate and atmospheric CO₂ for grassland fire in south-east Australia: insights using the GRAZPLAN grassland simulation model. *International Journal of Wildland Fire* 21 (6), 695–708.
- Kohonen, T., 2001. Self-organizing maps. Vol. 30 of Springer Series in Information Sciences. Springer.
- Kondo, J., Kuwagata, T., 1992. Enhancement of forest fires over northeastern Japan due to atypical strong dry wind. *Journal of Applied Meteorology* 31 (4), 386–396.
- Kraaij, T., Cowling, R. M., van Wilgen, B. W., 2013. Lightning and fire weather in eastern coastal fynbos shrublands: seasonality and long-term trends. *International Journal of Wildland Fire* 22 (3), 288–295.
- Levin, N., Saaroni, H., 1999. Fire weather in Israel - synoptic climatological analysis. *Geo-Journal* 47 (4), 523–538.

- Liu, Y., L Goodrick, S., A Stanturf, J., 2013. Future US wildfire potential trends projected using a dynamically downscaled climate change scenario. *Forest Ecology and Management* 294, 120–135.
- Liu, Y., Stanturf, J., Goodrick, S., 2010. Trends in global wildfire potential in a changing climate. *Forest Ecology and Management* 259 (4), 685–697.
- Long, M., 2006. A climatology of extreme fire weather days in Victoria. *Australian Meteorological Magazine* 55 (1), 3–18.
- Lucas, C., 2010. On developing a historical fire weather data-set for Australia. *Australian Meteorological and Oceanographic Journal* 60 (1), 1–14.
- Lucas, C., et al., 2007. Bushfire weather in Southeast Australia: recent trends and projected climate change impacts. Bushfire Co-operative Research Centre, Melbourne, Australia.
- Luke, R. H., McArthur, A. G., 1978. Bush fires in Australia. Australian Government Publishing Service.
- Lynch, A. H., Beringer, J., Kershaw, P., Marshall, A., Mooney, S., Tapper, N., Turney, C., Van Der Kaars, S., 2007. Using the paleorecord to evaluate climate and fire interactions in Australia. *Annu. Rev. Earth Planet. Sci.* 35, 215–239.
- Lynch, C., Hessel, A., 2010. Climatic controls on historical wildfires in West Virginia, 1939–2008. *Physical Geography* 31 (3), 254–269.
- Macdonald, N. J., 1976. On the apparent relationship between convective activity and the shape of 500 mb troughs. *Monthly Weather Review* 104 (12), 1618–1622.
- Macphail, M., 2010. The burning question: Claims and counter claims on the origin and extent of buttongrass moorland (blanket moor) in southwest Tasmania during the present glacial-interglacial. *terra australis* 32, 323–339.
- Macphail, M., Jordan, G., Hill, R., 1993. Key periods in the evolution of the flora and vegetation in western Tasmania. I. The Early-Middle Pleistocene. *Australian Journal of Botany* 41 (6), 673–707.
- Malevsky-Malevich, S., Molkentin, E., Nadyozhina, E., Shklyarevich, O., 2008. An assessment of potential change in wildfire activity in the Russian boreal forest zone induced by climate warming during the twenty-first century. *Climatic Change* 86 (3-4), 463–474.

- Marlon, J., Bartlein, P., Walsh, M., Harrison, S. P., Brown, K., Edwards, M., Higuera, P., Power, M., Anderson, R., Briles, C., et al., 2009. Wildfire responses to abrupt climate change in North America. *Proceedings of the National Academy of Sciences* 106 (8), 2519–2524.
- Marsden-Smedley, J., Catchpole, W., 1995a. Fire behaviour modelling in Tasmanian buttongrass moorlands. I. Fuel characteristics. *International Journal of Wildland Fire* 5 (4), 203–214.
- Marsden-Smedley, J., Catchpole, W., 1995b. Fire behaviour modelling in Tasmanian buttongrass moorlands. II. Fire behaviour. *International Journal of Wildland Fire* 5 (4), 215–228.
- Marsden-Smedley, J. B., 1998. Changes in southwestern Tasmanian fire regimes since the early 1800s. In: *Papers and Proceedings of the Royal Society of Tasmania*. Vol. 132. pp. 15–29.
- Marsden-Smedley, J. B., Catchpole, W. R., 2001. Fire modelling in Tasmanian buttongrass moorlands. III. Dead fuel moisture. *International Journal of Wildland Fire* 10 (2), 241–253.
- Marsden-Smedley, J. B., Catchpole, W. R., Pyrke, A., 2001. Fire modelling in Tasmanian buttongrass moorlands. IV. Sustaining versus non-sustaining fires. *International Journal of Wildland Fire* 10 (2), 255–262.
- Marsden-Smedley, J. B., Kirkpatrick, J. B., 2000. Fire management in Tasmania's Wilderness World Heritage Area: Ecosystem restoration using indigenous-style fire regimes? *Ecological Management & Restoration* 1 (3), 195–203.
- Marsh, L., 1987. Fire weather forecasting in Tasmania. *Meteorological Note* 171, Bureau of Meteorology, Melbourne, Australia.
- Martin, H., 2006. Cenozoic climatic change and the development of the arid vegetation in Australia. *Journal of Arid Environments* 66 (3), 533–563.
- McArthur, A. G., 1966. Weather and grassland fire behaviour. Leaflet 100, Forestry and Timber Bureau, Canberra. 23 pp.
- McArthur, A. G., 1967. Fire behaviour in eucalypt forests. Leaflet 107, Forestry and Timber Bureau, Canberra. 35 pp.

- McInnes, K. L., Erwin, T. A., Bathols, J. M., 2011. Global climate model projected changes in 10 m wind speed and direction due to anthropogenic climate change. *Atmospheric Science Letters* 12 (4), 325–333.
- McLeod, R., 2003. Inquiry into the operational response to the January 2003 bushfires in the ACT. Tech. rep., Department of Urban Services, ACT, 273 pp.
- Meehl, G. A., Covey, C., Taylor, K. E., Delworth, T., Stouffer, R. J., Latif, M., McAvaney, B., Mitchell, J. F., 2007. The WCRP CMIP3 multimodel dataset: A new era in climate change research. *Bulletin of the American Meteorological Society* 88 (9), 1383–1394.
- Meyn, A., White, P. S., Buhk, C., Jentsch, A., 2007. Environmental drivers of large, infrequent wildfires: the emerging conceptual model. *Progress in Physical Geography* 31 (3), 287–312.
- Millán, M. M., Estrela, M. J., Badenas, C., 1998. Meteorological processes relevant to forest fire dynamics on the Spanish Mediterranean coast. *Journal of Applied Meteorology* 37 (1), 83–100.
- Miller, N. L., Schlegel, N. J., 2006. Climate change projected fire weather sensitivity: California Santa Ana wind occurrence. *Geophysical Research Letters* 33 (L15711), doi:10.1029/2006GL025808.
- Mills, G., 2002. A case of coastal interaction with a cool change. *Australian Meteorological Magazine* 51 (4), 203.
- Mills, G. A., 2005a. On the sub-synoptic scale meteorology of two extreme fire weather days during the Eastern Australian fires of January 2003. *Aust. Met. Mag* 54, 265–290.
- Mills, G. A., 2005b. A re-examination of the synoptic and mesoscale meteorology of Ash Wednesday 1983. *Australian Meteorological Magazine* 54 (1), 35–55.
- Mills, G. A., 2008a. Abrupt surface drying and fire weather Part 1: overview and case study of the South Australian fires of 11 January 2005. *Australian Meteorological Magazine* 57 (4), 299–309.
- Mills, G. A., 2008b. Abrupt surface drying and fire weather Part 2: a preliminary synoptic climatology in the forested areas of southern Australia. *Australian Meteorological Magazine* 57 (4), 311–328.

- Mills, G. A., 2010. A westward propagating roll cloud and cool change on Tasmania's north coast. *Australian Meteorological and Oceanographic Journal* 60 (4), 237–247.
- Mills, G. A., Pendlebury, S., 2003. Processes leading to a severe wind-shear incident at Hobart Airport. *Australian Meteorological Magazine* 52 (3), 171–188.
- Mooney, S., Harrison, S., Bartlein, P., Daniau, A.-L., Stevenson, J., Brownlie, K., Buckman, S., Cupper, M., Luly, J., Black, M., et al., 2011. Late Quaternary fire regimes of Australasia. *Quaternary Science Reviews* 30 (1), 28–46.
- Moore, J. T., Vanknowe, G. E., 1992. The effect of jet-streak curvature on kinematic fields. *Monthly Weather Review* 120 (11), 2429–2441.
- Moriondo, M., Good, P., Durao, R., Bindi, M., Giannakopoulos, C., Corte-Real, J., 2006. Potential impact of climate change on fire risk in the Mediterranean area. *Climate Research* 31 (1), 85–95.
- Moritz, M. A., Moody, T. J., Krawchuk, M. A., Hughes, M., Hall, A., 2010. Spatial variation in extreme winds predicts large wildfire locations in chaparral ecosystems. *Geophysical Research Letters* 37 (L04801), doi:10.1029/2009GL041735.
- Moritz, M. A., Parisien, M.-A., Batllori, E., Krawchuk, M. A., Van Dorn, J., Ganz, D. J., Hayhoe, K., 2012. Climate change and disruptions to global fire activity. *Ecosphere* 3 (6), art49.
- Mount, A., 1972. The derivation and testing of a soil dryness index using run-off data. Forestry Commission, Tasmania.
- Nairn, J., Prideaux, J., Ray, D., Watson, A., 2005. Meteorological report on the Wangary and Black Tuesday fires, Lower Eyre Peninsula, 10-11 January 2005. Tech. rep., Bureau of Meteorology, Melbourne, Australia. 64 pp.
- Nakićenović, N., 2000. Summary for Policymakers: Emission Scenarios: a Special Report of Working Group III of the Intergovernmental Panel on Climate Change. Intergovernmental Panel on Climate Change.
- Newark, M., 1975. The relationship between forest fire occurrence and 500 mb longwave ridging. *Atmosphere* 13 (1), 26–33.

- Nicholls, N., Lucas, C., 2007. Interannual variations of area burnt in Tasmanian bushfires: relationships with climate and predictability. *International Journal of Wildland Fire* 16 (5), 540–546.
- Nimchuk, N., 1983. Wildfire behavior associated with upper ridge breakdown. Tech. rep., Alberta Energy and Natural Resources, Forest Service: Edmonton, Alberta. 45 pp.
- Noble, I., Gill, A., Bary, G., 1980. McArthur's fire-danger meters expressed as equations. *Australian Journal of Ecology* 5 (2), 201–203.
- Papadopoulos, A., Paschalidou, A., Kassomenos, P., McGregor, G., 2013. Investigating the relationship of meteorological/climatological conditions and wildfires in Greece. *Theoretical and Applied Climatology* 112 (1-2), 113–126.
- Pechony, O., Shindell, D., 2009. Fire parameterization on a global scale. *Journal of Geophysical Research: Atmospheres* (1984–2012) 114 (D16).
- Pereira, M. G., Trigo, R. M., da Camara, C. C., Pereira, J., Leite, S. M., 2005. Synoptic patterns associated with large summer forest fires in Portugal. *Agricultural and Forest Meteorology* 129 (1), 11–25.
- Peters, D. P., Pielke, R. A., Bestelmeyer, B. T., Allen, C. D., Munson-McGee, S., Havstad, K. M., 2004. Cross-scale interactions, nonlinearities, and forecasting catastrophic events. *Proceedings of the National Academy of Sciences* 101 (42), 15130–15135.
- Peters, G. P., Andrew, R. M., Boden, T., Canadell, J. G., Ciais, P., Le Quéré, C., Marland, G., Raupach, M. R., Wilson, C., 2013. The challenge to keep global warming below 2 C. *Nature Climate Change* 3 (1), 4–6.
- Pinheiro, J., Bates, D., DebRoy, S., Sarkar, D., R Core Team, 2013. nlme: Linear and Nonlinear Mixed Effects Models. R package version 3.1-108.
- Pinheiro, J. C., Bates, D. M., 2000. *Mixed-effects models in S and S-PLUS*. Springer.
- Piñol, J., Terradas, J., Lloret, F., 1998. Climate warming, wildfire hazard, and wildfire occurrence in coastal eastern Spain. *Climatic Change* 38 (3), 345–357.
- Pitman, A., Narisma, G., McAneney, J., 2007. The impact of climate change on the risk of forest and grassland fires in Australia. *Climatic Change* 84 (3-4), 383–401.
- Podur, J., Wotton, M., 2010. Will climate change overwhelm fire management capacity? *Ecological Modelling* 221 (9), 1301–1309.

- Pollina, J. B., Colle, B. A., Charney, J. J., 2013. Climatology and meteorological evolution of major wildfire events over the northeast United States. *Weather and Forecasting* 28 (1), 175–193.
- Potter, B. E., 2012a. Atmospheric interactions with wildland fire behaviour–I. Basic surface interactions, vertical profiles and synoptic structures. *International Journal of Wildland Fire* 21 (7), 779–801.
- Potter, B. E., 2012b. Atmospheric interactions with wildland fire behaviour–II. Plume and vortex dynamics. *International Journal of Wildland Fire* 21 (7), 802–817.
- Power, M. J., 2013. A 21 000-year history of fire. In: *Fire phenomena and the Earth system: an interdisciplinary guide to fire science*. Wiley Online Library, pp. 207–227.
- Power, S., Haylock, M., Colman, R., Wang, X., 2006. The predictability of interdecadal changes in ENSO activity and ENSO teleconnections. *Journal of Climate* 19 (19), 4755–4771.
- Prins, E. M., Feltz, J. M., Menzel, W. P., Ward, D. E., 1998. An overview of GOES-8 diurnal fire and smoke results for SCAR-B and 1995 fire season in South America. *Journal of Geophysical Research: Atmospheres* (1984–2012) 103 (D24), 31821–31835.
- Puri, K., Dietachmayer, G., Mills, G., Davidson, N., Bowen, R., Logan, L., 1998. The new BMRC limited area prediction system, LAPS. *Australian Meteorological Magazine* 47, 203–223.
- R Development Core Team, 2012. *R: A Language and Environment for Statistical Computing*. R Foundation for Statistical Computing, Vienna, Austria, ISBN 3-900051-07-0.
URL <http://www.R-project.org/>
- Racherla, P., Shindell, D., Faluvegi, G., 2012. The added value to global model projections of climate change by dynamical downscaling: A case study over the continental US using the GISS-ModelE2 and WRF models. *Journal of Geophysical Research: Atmospheres* (1984–2012) 117 (D20).
- Rasilla, D. F., García-Codron, J. C., Carracedo, V., Diego, C., 2010. Circulation patterns, wildfire risk and wildfire occurrence at continental Spain. *Physics and Chemistry of the Earth, Parts A/B/C* 35 (9), 553–560.

- Risbey, J. S., Pook, M. J., McIntosh, P. C., Wheeler, M. C., Hendon, H. H., 2009. On the remote drivers of rainfall variability in Australia. *Monthly Weather Review* 137 (10), 3233–3253.
- Rivas Soriano, L., Tomás, C., de Pablo, F., García, E., 2013. Circulation weather types and wildland forest fires in the western Iberian Peninsula. *International Journal of Climatology* 33 (6), 1401–1408.
- Russell-Smith, J., Yates, C. P., Whitehead, P. J., Smith, R., Craig, R., Allan, G. E., Thackway, R., Frakes, I., Cridland, S., Meyer, M. C., et al., 2007. Bushfires' down under': patterns and implications of contemporary Australian landscape burning. *International Journal of Wildland Fire* 16 (4), 361–377.
- Ryan, B. C., 1977. A mathematical model for diagnosis and prediction of surface winds in mountainous terrain. *Journal of Applied Meteorology* 16 (6), 571–584.
- Salloum, L., Mitri, G., 2014. Assessment of the temporal pattern of fire activity and weather variability in Lebanon. *International Journal of Wildland Fire* 23, 503–509.
- Santos, B., Clegg, P., Courtney, J., Burton, A., 2011. High resolution extreme fire weather climatology in the southwest of Western Australia. Tech. rep., Bureau of Meteorology, Perth, Western Australia.
- Schaefer, V. J., 1957. The relationship of jet streams to forest wildfires. *Journal of Forestry* 55 (6), 419–425.
- Schroeder, M. J., Glovinsky, M., Henricks, V. F., Hood, F. C., Hull, M. K., 1964. Synoptic weather types associated with critical fire weather. Tech. rep., USDA Forest Service, Pacific Southwest Forest and Range Experiment Station.
- Sharples, J. J., Mills, G. A., McRae, R. H., Weber, R. O., 2010. Foehn-like winds and elevated fire danger conditions in southeastern Australia. *Journal of Applied Meteorology and Climatology* 49 (6), 1067–1095.
- Shepherd, D., 1991. The effect of site changes on climatic records: a Tasmanian example. *Meteorological Note* 194, Bureau of Meteorology, Melbourne, Australia.
- Sheridan, S. C., Lee, C. C., 2010. Synoptic climatology and the general circulation model. *Progress in Physical Geography* 34 (1), 101–109.

- Sherwood, S. C., Ingram, W., Tsushima, Y., Satoh, M., Roberts, M., Vidale, P. L., O’Gorman, P. A., 2010. Relative humidity changes in a warmer climate. *Journal of Geophysical Research: Atmospheres* (1984–2012) 115 (D9).
- Shkolnik, I., Molkentin, E., Nadezhina, E., Khlebnikova, E., Sall, I., 2008. Temperature extremes and wildfires in Siberia in the 21st century: the MGO regional climate model simulation. *Russian Meteorology and Hydrology* 33 (3), 135–142.
- Skinner, W., Stocks, B., Martell, D., Bonsal, B., Shabbar, A., 1999. The association between circulation anomalies in the mid-troposphere and area burned by wildland fire in Canada. *Theoretical and Applied Climatology* 63 (1-2), 89–105.
- Smith, D. T., 1998. Mapping the bushfire danger of Hobart. Grad. Dip. Env. Studies, University of Tasmania.
- Smith, I., Chandler, E., 2010. Refining rainfall projections for the Murray Darling Basin of south-east Australia—the effect of sampling model results based on performance. *Climatic Change* 102 (3-4), 377–393.
- Speer, M. S., Leslie, L. M., et al., 2000. A comparison of five flood rain events over the New South Wales north coast and a case study. *International Journal of Climatology* 20 (5), 543–563.
- Stocks, B., Lynham, T., 1996. Fire weather climatology in Canada and Russia. In: *Fire in ecosystems of Boreal Eurasia*. Springer, pp. 481–494.
- Stocks, B., Mason, J., Todd, J., Bosch, E., Wotton, B., Amiro, B., Flannigan, M., Hirsch, K., Logan, K., Martell, D., et al., 2002. Large forest fires in Canada, 1959–1997. *Journal of Geophysical Research: Atmospheres* (1984–2012) 107 (D1), FFR–5.
- Takle, E., Bramer, D., Heilman, W., Thompson, M., 1994. A synoptic climatology for forest-fires in the NE US and future implications from GCM simulations. *International Journal of Wildland Fire* 4 (4), 217–224.
- Taylor, J., Webb, R., 2004. Meteorological aspects of the 2002/2003 bushfire season in NSW. In: *Proc. The 11th Annual AFAC Conference and Inaugural Bushfire CRC Conference*, Perth, Western Australia, 7-9 October 2004. pp. 349–358.
- Thackway, R., Mutendeudzi, M., Kelley, G., 2008. Assessing the extent of Australia’s forest burnt by planned and unplanned fire. Bureau of Rural Sciences, Canberra, ACT, Australia.

- Thatcher, M., McGregor, J. L., 2009. Using a scale-selective filter for dynamical downscaling with the conformal cubic atmospheric model. *Monthly Weather Review* 137 (6), 1742–1752.
- Thurston, W., Fawcett, R., Tory, K., Kepert, J., 2014. Simulating boundary-layer rolls with a numerical weather prediction model. *Quarterly Journal of the Royal Meteorological Society*, accepted.
- Tian, X., Zhao, F., Shu, L., Wang, M., 2014. Changes in forest fire danger for south-western China in the 21st century. *International Journal of Wildland Fire* 23 (2), 185–195.
- Timbal, B., Drosowsky, W., 2013. The relationship between the decline of Southeastern Australian rainfall and the strengthening of the subtropical ridge. *International Journal of Climatology* 33 (4), 1021–1034.
- Tolhurst, K. G., Cheney, N. P., 1999. Synopsis of the knowledge used in prescribed burning in Victoria. Department of Natural Resources and Environment.
- Treloar, A., Stern, H., 1993. A climatology and classification of Victorian severe thunderstorms. In: 4th Int. Conf. On Southern Hemisphere Meteorology and Oceanography, Hobart, Australia.
- Trenberth, K. E., 2011. Changes in precipitation with climate change. *Climate Research* 47 (1), 123.
- Trewin, B., 2006. An exceptionally dry decade in parts of southern and eastern Australia October 1996 - September 2006. Special Climate Statement 9, Bureau of Meteorology, Melbourne, Australia.
- Trouet, V., Taylor, A. H., Carleton, A. M., Skinner, C. N., 2009. Interannual variations in fire weather, fire extent, and synoptic-scale circulation patterns in northern California and Oregon. *Theoretical and Applied Climatology* 95 (3-4), 349–360.
- Valendik, E., Ivanova, G., Chuluunbator, Z., Goldammer, J., 1998. Fire in forest ecosystems of Mongolia. *International Forest Fire News* 19, 58–63.
- Van Vuuren, D. P., Edmonds, J., Kainuma, M., Riahi, K., Thomson, A., Hibbard, K., Hurtt, G. C., Kram, T., Krey, V., Lamarque, J.-F., et al., 2011. The representative concentration pathways: an overview. *Climatic Change* 109, 5–31.

- van Wagner, C., Stocks, B., Lawson, B., Alexander, M., Lynham, T., McAlpine, R., 1992. Development and structure of the Canadian forest fire behaviour prediction system. Information Report ST-X-3, Forestry Canada.
- Van Wilgen, B., Biggs, H., O'Regan, S., Mare, N., 2000. Fire history of the savanna ecosystems in the Kruger National Park, South Africa, between 1941 and 1996. *South African Journal of Science* 96, 167–178.
- Vázquez de la Cueva, A., Quintana, J. R., Cañellas, I., 2012. Fire activity projections in the SRES A2 and B2 climatic scenarios in peninsular Spain. *International Journal of Wildland Fire* 21 (6), 653–665.
- Verdon, D. C., Kiem, A. S., Franks, S. W., 2004. Multi-decadal variability of forest fire risk-eastern Australia. *International Journal of Wildland Fire* 13 (2), 165–171.
- Vines, R., 1974. Weather patterns and bush-fire cycles in southern Australia. Technical Paper 2, CSIRO Division of Chemical Technology, Melbourne, Australia.
- Von Platen, J., Kirkpatrick, J., Allen, K. J., 2011. Fire frequency variation in south-eastern Tasmanian dry eucalypt forest 1740–2004 from fire scars. *Australian Forestry* 74 (3), 180–189.
- Wallace, W., Gloe, H., 1938. Forest fire weather. *Australian Forestry* 3 (1), 28–36.
- Westerling, A. L., Hidalgo, H. G., Cayan, D. R., Swetnam, T. W., 2006. Warming and earlier spring increase western US forest wildfire activity. *Science* 313 (5789), 940–943.
- Whiteman, C. D., 2000. Mountain meteorology: fundamentals and applications. Pacific Northwest National Laboratory, Richland, WA (US).
- Whittingham, H., 1964. Meteorological conditions associated with the Dandenong bushfires of 14-16 January 1962. *Australian Meteorological Magazine* 44, 10–37.
- Whittingham, I., 1961. A review of fire weather investigations in Australia. *Australian Meteorological Magazine* (35), 10–14.
- Williams, A. A., Karoly, D. J., 1999. Extreme fire weather in Australia and the impact of the El Nino-Southern Oscillation. *Australian Meteorological Magazine* 48 (1), 15–22.
- Williams, A. A., Karoly, D. J., Tapper, N., 2001. The sensitivity of Australian fire danger to climate change. *Climatic Change* 49 (1-2), 171–191.

- Wood, S., Hua, Q., Allen, K., Bowman, D., 2010. Age and growth of a fire prone Tasmanian temperate old-growth forest stand dominated by *Eucalyptus regnans*, the world's tallest angiosperm. *Forest Ecology and Management* 260 (4), 438–447.
- Wotton, B. M., Alexander, M. E., Taylor, S. W., 2009. Updates and revisions to the 1992 Canadian forest fire behavior prediction system. Great Lakes Forestry Centre.
- Yarnal, B., 1993. *Synoptic climatology in environmental analysis: a primer*. Belhaven Press London.
- Yarnal, B., Comrie, A. C., Frakes, B., Brown, D. P., 2001. Developments and prospects in synoptic climatology. *International Journal of Climatology* 21 (15), 1923–1950.
- Yue, X., Mickley, L. J., Logan, J. A., 2013. Projection of wildfire activity in southern California in the mid-twenty-first century. *Climate Dynamics*, 1–19.
- Zhang, X., Kondragunta, S., 2008. Temporal and spatial variability in biomass burned areas across the USA derived from the GOES fire product. *Remote Sensing of Environment* 112 (6), 2886–2897.
- Zimet, T., Martin, J. E., Potter, B. E., 2007. The influence of an upper-level frontal zone on the Mack Lake Wildfire environment. *Meteorological Applications* 14 (2), 131–147.